

Synthesis of Diphosphoinositol Polyphosphates

Dissertation

zur

Erlangung der naturwissenschaftlichen Doktorwürde
(Dr. sc. nat.)

vorgelegt der

Mathematisch-naturwissenschaftlichen Fakultät

der

Universität Zürich

von

Samanta Capolicchio

aus

Italien

Promotionskomitee

Prof. Dr. John Robinson (Vorsitz)

Dr. Henning J. Jessen

Prof. Dr. Roland Sigel

Zürich, 2015

AKNOWLEDGMENTS

Dr. Henning J. Jessen
for giving me the opportunity to work on the topics of this PhD thesis, for his constant support, helpful discussions and encouragement over the years

Prof. Dr. John Robinson and Prof. Dr. Roland Sigel
for being part of my PhD committee

Prof. Dr. Jay Siegel and Prof. Dr. Kim Baldridge
for constant support during my PhD

Prof. Dr. Oliver Zerbe, Simon Jurt and team
for support with NMR experiments

PD Dr. Laurent Bigler, Urs Stalder and Rahel Bucher
for the measurement of mass spectra

PD Dr. Anthony Linden and team
for X-ray analysis

Prof. Dr. Stephen Shears and team
for biological assays and elucidation of crystal structures

Dr. Jan Helbing
for support with VCD experiments

All group members past and present

ABSTRACT

Diphosphoinositol polyphosphates (PP-InsP_y) represent a novel group of secondary messengers that regulate diverse important cellular processes, including signal transduction, vesicle trafficking and apoptosis. The concentration of PP-InsP_y in cells is very low which makes their isolation from biological sources difficult. An alternative is the preparation of PP-InsP_y by enzymatic reactions. However, this method does not permit to obtain large amounts of material and it is not suitable for the preparation of non-natural isomers and analogs. Therefore, an efficient method to prepare scalable amounts of different PP-InsP_y is essential for the study of functions of PP-InsP_y. The preparation of PP-InsP_y by chemical synthesis holds promise to access these required amounts. Additionally, such a method can also provide access to several non-natural derivatives that can be used as chemical tools to study the metabolism of PP-InsP_y. In order to achieve such a synthesis, novel efficient synthetic routes and methods are in high demand.

We will report a novel total synthesis of unsymmetric diphosphoinositol polyphosphates. An efficient synthetic route has been developed based on reagent controlled asymmetric phosphorylation using a C₂-symmetric phosphoramidite. This novel phosphorylating reagent enabled us to target all four possible unsymmetric X-PP-InsP₅ (1-PP-InsP₅, 3-PP-InsP₅, 4-PP-InsP₅ and 6-PP-InsP₅). Moreover, we developed an outstanding one-flask procedure for the formation of the pyrophosphate moiety that is characteristic of all PP-InsP_y. Unsymmetric 1,5-(PP)₂-InsP₄ and 3,5-(PP)₂-InsP₄ were prepared for the first time adapting these methods. A novel synthesis of the two symmetric 5-PP-InsP₅ and 5-PPP-InsP₅ (contains a triphosphate) will be also reported. These results are a new approach to obtain PP-InsP_y on multimilligram scale. Additionally, it is the starting point for the development of efficient reagents for asymmetric phosphorylation and pyrophosphorylation. These methods have been applied already in the synthesis of chemical tools that can be used to decipher inositol related cellular signalling pathways.

ZUSAMMENFASSUNG

Diphosphoinositol Polyphosphate (PP-InsP_y) verkörpern eine neue Gruppe von sekundären Botenstoffen, welche diverse wichtige zelluläre Prozesse wie Signalübermittlung, Vesikel-Transport und Apoptose regulieren. Kürzlich wurde berichtet, dass PP-InsP_y Proteine phosphorylieren in einem Prozess bekannt als Pyrophosphorylierung. Diese neue Art der posttranslationalen Modifikation findet *in vitro* statt; jedoch ist immer noch unklar, ob es auch *in vivo* erfolgt. Die Konzentration von PP-InsP_y in Zellen ist sehr tief, was ihre Gewinnung aus biologischen Quellen erschwert. PP-InsP_y wurden enzymatisch hergestellt. Auf diesem Weg kann jedoch nicht genügend Material für biologische Studien gewonnen werden. Zusätzlich ist die Herstellung der nicht-natürlichen Isomere nicht möglich und die Stereochemie der hergestellten Moleküle kann nicht bestimmt werden. Daher ist eine effiziente Methode, um einen skalierbaren Mengen an PP-InsP_y zu erhalten, entscheidend für Studien bezüglich der Struktur und Funktionen der PP-InsP_y. Die Gewinnung von PP-InsP_y mittels chemischer Synthese offeriert die besten Chancen, um eine skalierbare Menge an Material mit bekannter Stereochemie zu produzieren. Diese Methode liefert zusätzlich den Zugang zu einigen unnatürlichen Derivaten, welche als chemische Hilfsmittel in der Analyse des Metabolismus der PP-InsP_y verwendet werden können. Verschiedene Synthesen von enantiomerenreinen Inositol Polyphosphaten wurden publiziert, aber PP-InsP_y sind nicht kommerziell erhältlich und die Qualität der früheren Zubereitungen wurden in Frage gestellt. Asymmetrische Phosphorylierung ist eine ausgezeichnete Art und Weise, um eine Phosphat Gruppe an einer spezifischen Position in der Struktur von *myo*-Inositol einzuführen.

Wir werden eine neue Totalsynthese von unsymmetrischen Diphosphoinositol Polyphosphaten veröffentlichen, in der ein C₂-symmetrisches Phosphoramidit verwendet wird, um verschiedene Inositol Derivate asymmetrisch zu machen. Dieses neue Phosphorylierungsreagenz ermöglichte uns, alle vier möglichen unsymmetrischen X-PP-InsP₅ (1-PP-InsP₅, 3-PP-InsP₅, 4-PP-InsP₅, und 6-PP-InsP₅) herzustellen. Zum ersten Mal wurden zusätzlich 1,5-(PP)₂-InsP₄, und 3,5-(PP)₂-InsP_y mit der selben Methode zubereitet. Eine neue Synthese des symmetrischen 5-PP-InsP₅ und die erste Totalsynthese von *meso* 5-PPP-InsP₅ werden ebenfalls veröffentlicht. Diese Resultate verkörpern einen neuen Ansatz in der geplanten Totalsynthese von PP-InsP_y, sowie einen Ausgangspunkt für die Entwicklung von effizienten Reagenzien für die asymmetrische Phosphorylierung und Pyrophosphorylierung. Sie liefern uns zusätzlich Mittel, um die mit Inositol verwandte zelluläre Signalwege entschlüsseln zu können.

TABLE OF CONTENTS

CHAPTER 1	1
Biological Importance of Inositol Polyphosphates	1
1.1 <i>myo</i> -Inositol	2
1.1.1 Biosynthesis of <i>myo</i> -inositol	3
1.2 Inositol polyphosphates	4
1.3 Diphosphoinositol polyphosphates	6
1.3.1 Initial discoveries	6
1.3.2 Stereochemistry and presence in biological systems	9
1.3.2.1 Inositol pyrophosphates in mammalian cells	9
1.3.2.2 Inositol pyrophosphates in <i>Dictyostelium discoideum</i>	10
1.3.3 Biosynthesis and metabolism of inositol pyrophosphates	11
1.3.3.1 Kinases	12
1.3.3.2 Phosphatases	12
1.3.3.3 Turnover	13
1.3.4 Mechanism of action and functions	13
1.3.4.1 Protein binding	14
1.3.4.2 Protein pyrophosphorylation	16
 CHAPTER 2	 18
Chemical Synthesis of Inositol Polyphosphates	18
2.1 "Why nature chose phosphates"	19
2.2 Phosphoramidite chemistry	19
2.2.1 Introduction	19
2.2.2 Mechanism of the phosphoramidite coupling reaction	20
2.2.3 Activators	21
2.3 Stereoselective synthesis	23
2.4 Desymmetrization of <i>myo</i> -inositol	25
2.5 Synthesis of diphosphoinositol polyphosphates	28
 CHAPTER 3	 33
Goals	33

CHAPTER 4	38
Results and Discussion	38
4.1 Synthesis of symmetric di- and triphosphoinositol polyphosphates	39
4.1.1 Synthesis of <i>meso</i> 5-PP-InsP ₅	39
4.1.2 Synthesis of <i>meso</i> 5-PPP-InsP ₅	47
4.2 Development of a C ₂ -symmetric phosphoramidite and its application to desymmetrize <i>myo</i> -inositol.....	51
4.3 Synthesis of unsymmetric X-PP-InsP ₅ derivatives	60
4.3.1 Synthesis of 1- and 3-PP-InsP ₅	60
4.3.1.1 Assignment of the absolute configuration of 1- and 3-PP-InsP ₅	66
4.3.1.2 Synthesis of a sulfurized analog.....	68
4.3.2 Synthesis of 4- and 6-PP-InsP ₅	69
4.4 Synthesis of unsymmetric X,Y-(PP) ₂ -InsP ₄ derivatives	71
4.4.1 Assignment of the absolute configuration of 1,5- and 3,5-(PP) ₂ -InsP ₄	80
4.5 Biological applications of diphosphoinositol polyphosphates.....	82
 CHAPTER 5	 85
Summary and Outlook	85
 CHAPTER 6	 88
Experimental Part	88
6.1 Experimental procedures	89
6.2 Synthesis of 1-PP-InsP ₅ and 3-PP-InsP ₅	90
6.3 Synthesis of 4-PP-InsP ₅ and 6-PP-InsP ₅	107
6.4 Synthesis of 1,5-(PP) ₂ -InsP ₄ and 3,5-(PP) ₂ -InsP ₄	118
6.5 Synthesis of 5-PP-InsP ₅ and 5-PPP-InsP ₅	130
6.6 General procedures for the desymmetrization of <i>myo</i> -inositol.....	138
 LITERATURE	 140

ABBREVIATIONS

ADP	Adenosine diphosphate
Akt/PKB	Protein kinase B
ATP	Adenosine triphosphate
Bn	Benzyl
BSTFA	N,O-Bis(trimethylsilyl)trifluoroacetamide
<i>t</i> -BuOH	<i>tert</i> -Butyl alcohol
<i>t</i> -BuOOH	<i>tert</i> -Butyl hydroperoxide
β -CE	β -Cyanoethyl
<i>m</i> CPBA	<i>meta</i> -Chloro perbenzoic acid
DAG	Diacylglycerol
DBU	1,8-Diazabicyclo[5.4.0]undec-7-ene
DCI	4,5-Dicyanoimidazole
DCM	Dichloromethane
DIBAL-H	Diisobutylaluminium hydride
DIPP	Diphosphoinositol polyphosphate phosphatase
DMF	Dimethylformamide
DMSO	Dimethyl sulfoxide
DNA	Deoxyribonucleic acid
ESI	Electrospray ionization
FC	Flash chromatography
Fm	Fluorenylmethyl
HPLC	High-performance liquid chromatography
HRMS	High-resolution mass spectrometry
InsP ₅	Inositol pentakisphosphate
InsP ₆	Inositol hexakisphosphate
IP6K	Inositol hexakisphosphate kinase
IPMK	Inositol phosphate multikinase
IPPK	Inositol 1,3,4,5,6-pentakisphosphate 2-kinase
IR	Infrared
KD	Kinase domain
MeCN	Acetonitrile
MeOH	Methanol
m.p.	Melting point
NMR	Nuclear magnetic resonance

PAGE.....	Polyacrylamide gel electrophoresis
PH.....	Pleckstrin homology domain
PLC.....	Phospholipase C
PMB.....	<i>para</i> -Methoxybenzyl
PP-InsP _y	Diphosphoinositol polyphosphates
PP-InsP ₅	Diphosphoinositol pentakisphosphate
(PP) ₂ -InsP ₄	Bisdiphosphoinositol tetrakisphosphate
PPIPK.....	Diphosphoinositol pentakisphosphate kinase
ppm.....	Parts per million
R _f	Retention factor
RNA.....	Ribonucleic acid
RP.....	Reversed phase
TBAI.....	Tetrabutylammonium iodide
TBME.....	<i>tert</i> -Butyl methyl ether
TBS.....	<i>tert</i> -Butyldimethylsilyl
TEA.....	Triethylamine
TES.....	Triethylsilyl
TFA.....	Trifluoroacetic acid
TMS.....	Trimethylsilyl
TH.....	1 <i>H</i> -Tetrazole
THF.....	Tetrahydrofuran
TLC.....	Thin-layer chromatography
<i>p</i> -TsOH.....	<i>para</i> -Toluenesulfonic acid
v/v.....	Volume/Volume

CHAPTER 1

BIOLOGICAL IMPORTANCE OF INOSITOL POLYPHOSPHATES

1.1 MYO-INOSITOL

Inositols are a family of cyclohexanehexols (cyclitols) that include nine stereoisomers prefixed: *myo*-, *neo*-, *D-chiro*(+)-, *L-chiro*(-)-, *scyllo*-, *cis*-, *epi*-, *allo*- and *muco*- (Figure 1.1).^{1,2} The first five forms are naturally occurring, while the others are synthetic isomers.^{3,4} The building block of several biologically relevant molecules is the isomer *myo*-inositol⁵ that has been isolated by the German scientist Johann Joseph Scherer in 1850 from muscle tissue and designated “Inosit”.⁶ Subsequently, the suffix –ol was added to describe all the other stereoisomers.

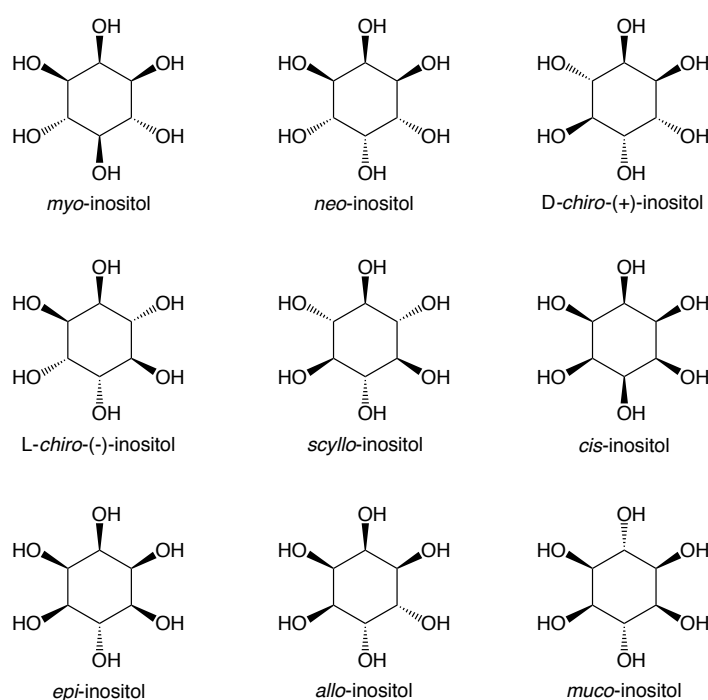


Figure 1.1. Structures of the nine possible stereoisomers of inositol.

myo-Inositol is an optically inactive (meso) molecule due to a plane of symmetry that dissects the 2- and 5-position of the ring. Therefore, substitutions on the 1- or 3-position and on the 4- or 6-position form enantiomers. The thermodynamically most stable conformation of *myo*-inositol is its chair structure⁷ that has been associated with the shape of a turtle by Bernard W. Agranoff in 1978.⁸ The Haworth projection of the molecule can cause confusion in numbering of the six hydroxyl groups,⁹ therefore the turtle is used as a mnemonic to avoid such confusion. The axial hydroxyl group in 2-position represents the head, the four equatorial groups in 1-, 3-, 4- and 6-position the

limbs and the equatorial hydroxyl group in 5-position the tail of the turtle (Figure 1.2). In natural systems, *myo*-inositol is linked to a lipid backbone through one of the equatorial hydroxyl groups and by convention the number 1 in the *myo*-inositol molecule is assigned to this position. The numbering of the other hydroxyl groups proceeds counterclockwise using the D numbering convention.

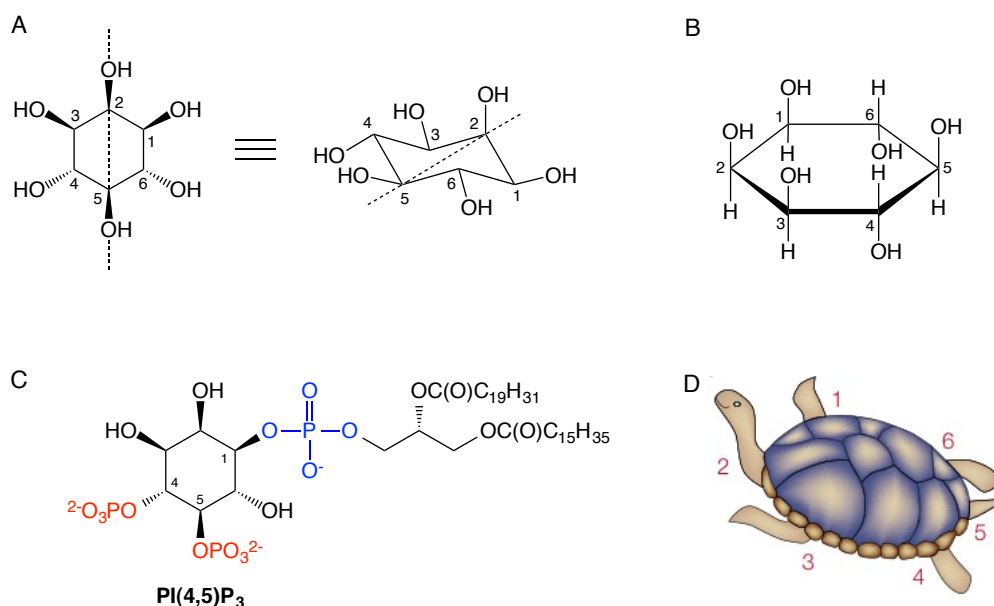


Figure 1.2. A) Plane of symmetry through the 2- and 5-position of *myo*-inositol; B) Haworth projection of *myo*-inositol; C) Structure of phosphatidylinositol 4,5-bisphosphate; D) Agranoff's turtle⁷ (Adapted by permission from Macmillan Publishers Ltd: Nat. Rev. Mol. Cell Biol. **2001**, 2, 327-338, Copyright © 2001).

1.1.1 BIOSYNTHESIS OF MYO-INOSITOL

myo-Inositol is very abundant in plants and most of the amount present in mammals is obtained from the diet.¹ However, it can be also synthesized from D-glucose 6-phosphate by the enzymes L-*myo*-inositol 1-phosphate synthase and *myo*-inositol 1-phosphatase (Figure 1.3). The latter enzyme is of special importance, as it is supposed to be the target of lithium cations in the treatment of bipolar disorders.¹⁰ *myo*-Inositol that is taken up from food is not able to cross the blood brain barrier, therefore the levels of the molecule in the brain depend on its biosynthesis from D-glucose 6-phosphate. Rats that were treated with lithium showed a lower concentration of *myo*-inositol in the brain, which can be related to the inhibition of *myo*-inositol 1-phosphatase by the cation.¹⁰ In

absence of *myo*-inositol, phosphoinositides cannot be biosynthesized, therefore the signaling pathways that are regulated by these lipid derivatives and that are associated to the origin of manic depression are blocked.¹¹

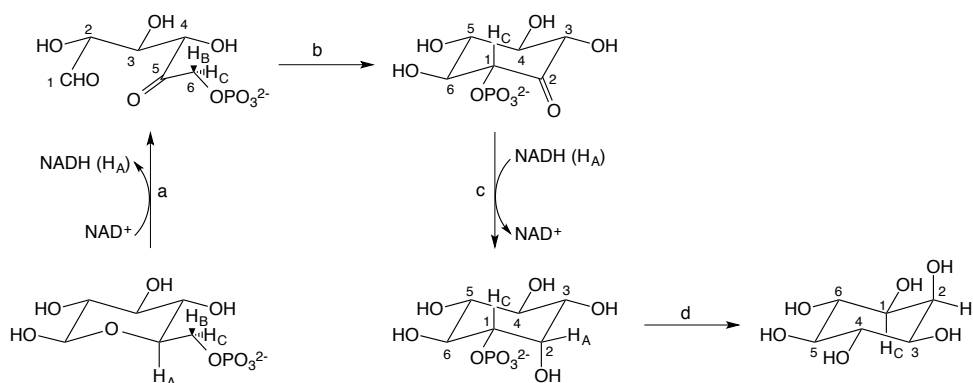


Figure 1.3. a) Oxidation of *D*-glucose 6-phosphate to 5-keto-glucose 6-phosphate by *L*-*myo*-inositol 1-phosphate (oxidoreductase activity); b) Conversion to *L*-*myo*-inosose-2-1-phosphate (aldolase activity); c) Formation of *D*-*myo*-inositol 3-phosphate by hydrogen transfer from NADH; d) Phosphate hydrolysis to *myo*-inositol by *myo*-inositol 1-phosphatase. (Scheme reproduced from Ref.¹)

1.1 INOSITOL POLYPHOSPHATES

Inositol polyphosphates are a class of second messengers that regulate several cellular signaling processes.^{7,12–14} Due to the special stereochemistry of *myo*-inositol, phosphorylation of the molecule allows the construction of 63 phosphate esters, from the mono- to the hexakisphosphate (6 x InsP₁, 6 x InsP₅, 15 x InsP₂, 15 x InsP₄, 20 x InsP₃ and InsP₆).¹⁵ At least half of these isomers exist in biological systems, although cellular functions have not been attributed to all of them.^{7,16,17}

The best characterized inositol polyphosphate is inositol 1,4,5-trisphosphate (InsP₃ or IP₃), a second messenger discovered in 1983 that stimulates calcium release from intracellular reservoirs.¹⁸ Phosphatidylinositol 4,5-bisphosphate [PI(4,5)P₂] is hydrolyzed by phospholipase C (PLC) to diacylglycerol,¹⁹ which is hydrophobic and remains in the membrane after cleavage, and InsP₃, which is soluble in the cytosol and able to bind the inositol trisphosphate receptor (InsP₃R) present on membranes of cellular compartments, especially in the endoplasmic reticulum (ER) (Figure 1.4).²⁰ After binding to its receptor, InsP₃ stimulates the release of calcium ions from the intracellular stores to the cytosol. The increase of calcium concentration in the cytoplasm is important

in muscular contraction, secretion, cell growth and transformation, sensory perception and others.²¹

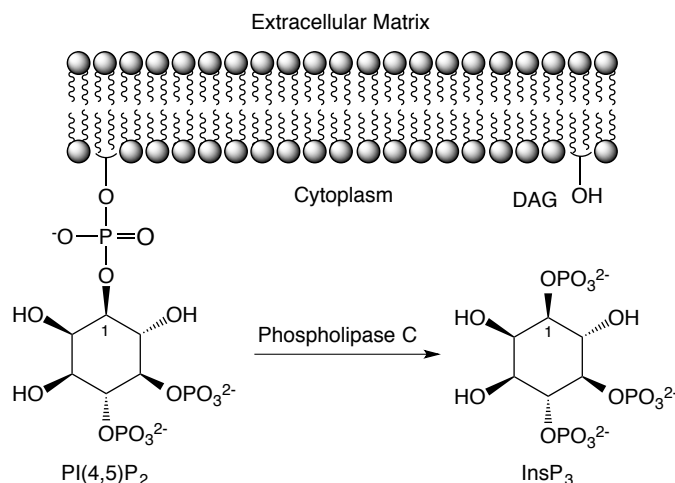


Figure 1.4. Hydrolysis of PI(4,5)P₂ by phospholipase C to form diacylglycerol (DAG) and InsP₃ (Picture reproduced from Ref.²²).

The enzyme Ins(1,4,5)P₃ 3-kinase catalyzes the conversion of Ins(1,4,5)P₃ to inositol-1,3,4,5-tetrakisphosphate [Ins(1,3,4,5)P₄] that is able to activate Ca²⁺ channels in the plasma membrane of endothelial cells and neurons (Figure 1.5).^{23,24} Additionally, it interacts with InsP₃ receptors on the membrane of the endoplasmic reticulum inhibiting or enhancing the action of Ins(1,4,5)P₃, depending on the receptor isoform.⁷ Finally, it is dephosphorylated by the enzyme 5-phosphatase, the same enzyme that hydrolyzes Ins(1,4,5)P₃, but with higher affinity, thus protecting InsP₃ from hydrolysis.²⁵ The role of inositol-3,4,5,6-tetrakisphosphate [Ins(3,4,5,6)P₄] is correlated to the secretion of Cl⁻ as it inhibits Cl⁻ channels that are stimulated by calcium ions.²⁶ This process is especially important in cystic fibrosis, as this is the only Cl⁻ channel that is active in patients affected by the disease. Therefore, generation of Ins(1,4,5)P₃ in these patients can be both beneficial as it leads to an increased concentration of calcium cations in the cell and consequently to Cl⁻ secretion, but also harmful as the metabolite Ins(3,4,5,6)P₄ is produced and inhibits Cl⁻ secretion.

Inositol-1,3,4,5,6-pentakisphosphate (InsP₅) is abundant in mammalian cells (Figure 1.5).²⁷ Among the roles that have been attributed to it, it has been shown that it interacts with proteins competing for their binding to phosphoinositides. For example, it

binds Akt (protein kinase B), inhibiting its activation and therefore stimulating apoptosis in cancer cells.⁷

The most abundant InsP is *myo*-inositol (1,2,3,4,5,6)-hexakisphosphate (InsP₆ or phytic acid) with a concentration of 10-60 μ M in mammalian cells and 0.7 mM in *Dictyostelium discoideum* (Figure 1.5).²⁸ It is the first inositol phosphate that has been discovered²⁹ and it is the main phosphate storage molecule in plants – “look at a field of wheat and you are gazing at tons of InsP₆” (quote from Irvine and Schell, Ref.⁷). InsP₆ is a highly negatively charged molecule able to interact with positively charged groups on proteins that are mainly involved in secretion and vesicular trafficking.⁷

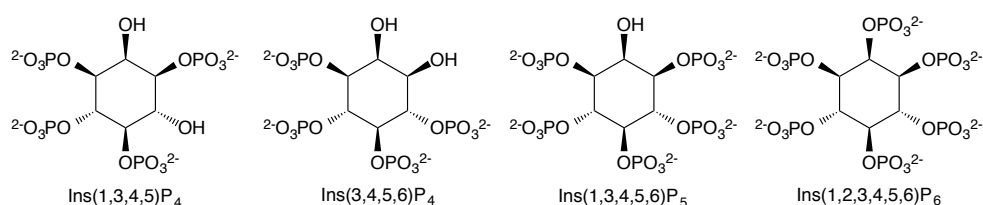


Figure 1.5. Structures of some *myo*-inositol polyphosphates present in organisms.

1.3 DIPHOSPHOINOSITOL POLYPHOSPHATES

1.3.1 INITIAL DISCOVERIES

The structural diversity of inositol polyphosphates can be expanded by introducing one or two diphosphate groups onto the fully phosphorylated InsP₆, generating InsP₇ and InsP₈, that contain seven or eight phosphate groups (Figure 1.6). These molecules are commonly known as inositol *pyrophosphates*, a designation that has been introduced by Steven Shears and subsequently used by others. However, it is important to mention that this is not the correct IUPAC nomenclature since the term “pyrophosphate” describes an inorganic phosphoanhydride.¹⁴ Therefore the correct prefix for this particular moiety is diphospho- and the appropriate name for these molecules would be “diphosphoinositol polyphosphates”. They have been discovered in 1993 independently by two distinct research groups: by the group of Shears that was studying pancreaticoma cells and by the group of Mayr that was studying the amoeba *Dictyostelium discoideum*.^{30,31} These molecules have been identified by strong ion-exchange HPLC column and characterized by ³¹P-NMR and subsequently they have been found to be present in all eukaryotic cells (Figure 1.6). A higher level of phosphorylation was

attributed to them as they were retained in the column more than InsP_6 and therefore they had to be more polar than the fully phosphorylated InsP_6 . Subsequently, in a chromatography analysis of the yeast *Saccharomyces cerevisiae*, lower inositol pyrophosphates have been identified and considered to be PP-InsP_3 , PP-InsP_4 , $(\text{PP})_2\text{-InsP}_2$ and $(\text{PP})_2\text{-InsP}_3$.³²

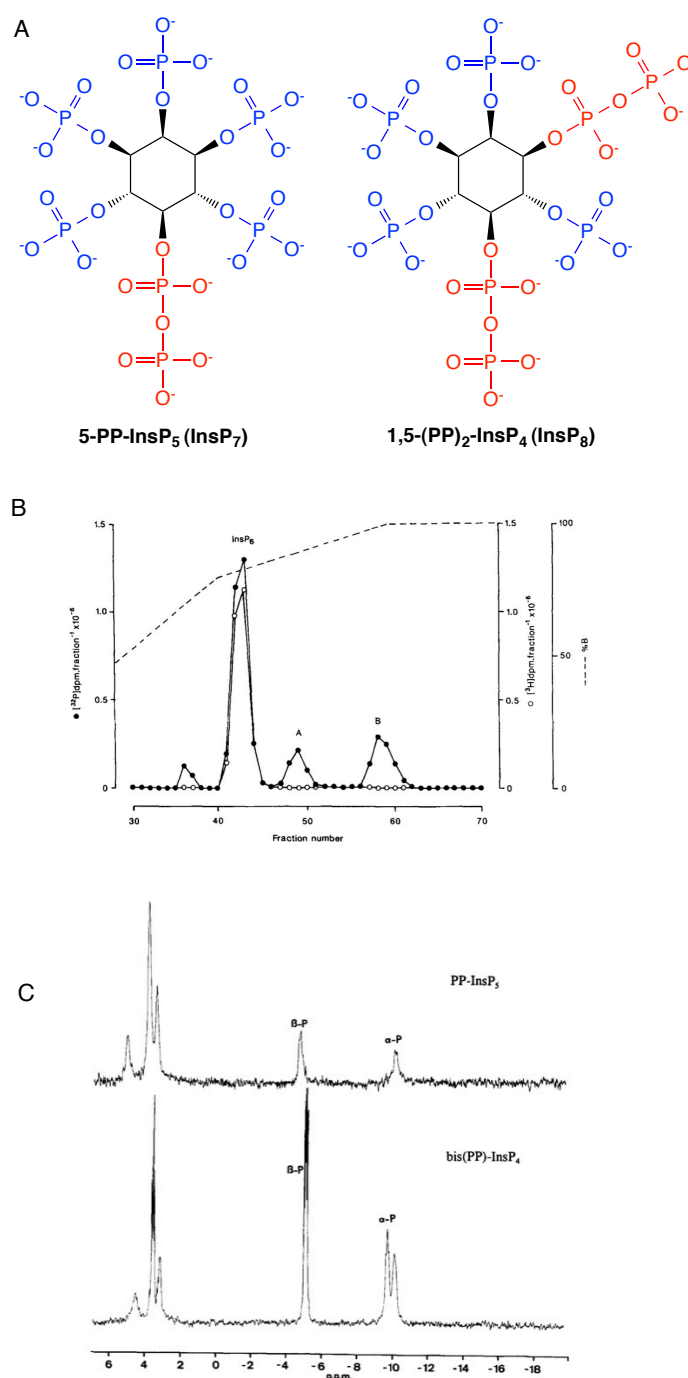


Figure 1.6. A) Two exemplary structures of diphosphoinositol polyphosphates; B) HPLC separation of inositol polyphosphates; C) ^{31}P -NMR spectra of PP-InsP₅ (top spectrum) and bis(PP)-InsP₄ (bottom spectrum) separated by HPLC.³¹ (Pictures B and C were originally published in the *Journal of Biological Chemistry*. Stephens, L.; Radenberg, T.; Thiel, U.; Vogel, G.; Khoo, K. H.; Dell, a; Jackson, T. R.; Hawkins, P. T.; Mayr, G. W. The detection, purification, structural characterization, and metabolism of diphosphoinositol pentakisphosphate(s) and bisdiphosphoinositol tetrakisphosphate(s). *J. Biol. Chem.* 1993, 268, 4009–4015. © the American Society for Biochemistry and Molecular Biology)

1.3.2 STEREOCHEMISTRY AND PRESENCE IN BIOLOGICAL SYSTEMS

The assignment of the correct stereochemistry of diphosphoinositol polyphosphate isomers that are present in the cell has been under discussion for years. This question is of high importance to understand which isomers mediate cellular signaling pathways and has recently been solved (see below). In general, a specific isomer is recognized by the catalytic site of an enzyme, thus the determination of the correct stereochemistry would provide a better understanding of the mechanism that is responsible for the metabolism of PP-InsPs. Similarly, receptors can distinguish between different isomers, thus providing information about their structure-function relationships.³³

1.3.2.1 INOSITOL PYROPHOSPHATES IN MAMMALIAN CELLS

The most abundant inositol pyrophosphate in mammalian cells is 5-diphosphoinositol pentakisphosphate (5-PP-InsP₅ or 5-InsP₇) as demonstrated by Shears and coworkers in 1997 (Figure 1.7).³³ The minor inositol pyrophosphate isomer found in mammalian cells is 1-PP-InsP₅, while the most abundant (PP)₂-InsP₄ contains pyrophosphate moieties in the 1 and 5 positions.³⁴ As mentioned above, the determination of the correct stereochemistry of the naturally occurring isomers has not been straightforward.³⁵ In 2007, the O'Shea and York laboratories identified an InsP₇ isomer produced by Vip1 and involved in phosphate starvation and they wrongly believed that it contained a diphosphate moiety in the 4 or 6 position.^{36,37} In 2009 Mayr and coworkers showed that the product of Vip1 is pyrophosphorylated in the 1 or 3 position³⁸ and only in 2011 the Shears laboratory obtained crystal structures of the kinase domain of human PIP5K2 complexed with various substrates demonstrating that the naturally occurring isomers are 1-InsP₇ and 1,5-InsP₈.³⁴

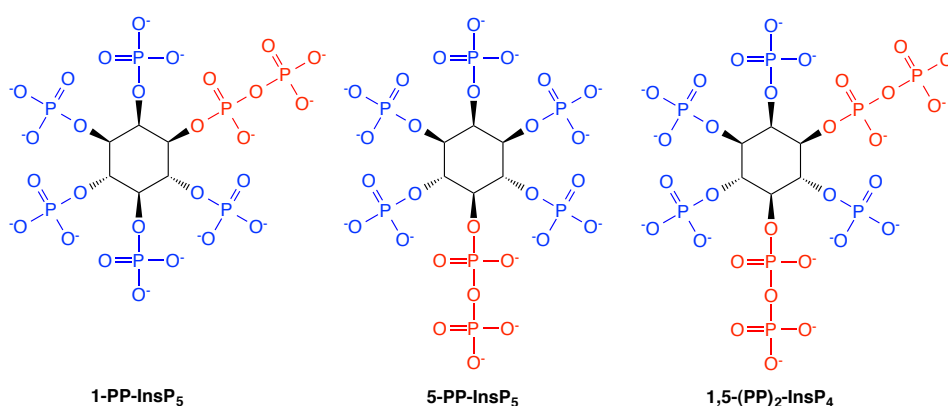


Figure 1.7. Structures of diphosphoinositol polyphosphates present in mammalian cells.

1.3.2.2 INOSITOL PYROPHOSPHATES IN *Dictyostelium discoideum*

The investigation of the functions of $PP_x\text{-InsP}_y$ in mammalian cells is difficult due to the low intracellular concentration of these molecules (less than 1 μM). Therefore, the slime mold *Dictyostelium discoideum* has been investigated, as in this organism the intracellular levels of PP-InsPs are about 300-fold higher (0.05-0.25 mM).³¹ However, the slime mold is not a representative model to study inositol pyrophosphate related signaling pathways in mammalian cells, as the isomers present in the two organisms are different. Vogel and coworkers determined in 1996 by two-dimensional $^1\text{H}/^{31}\text{P}$ NMR analysis that the diphosphoinositol pentakisphosphate present in *Dictyostelium discoideum* was the 4- and/or the 6-PP-InsP₅ and that the bisdiphosphoinositol tetrakisphosphate was the 4,5- and/or 5,6-(PP)₂-InsP₄.³⁹ However, using NMR spectroscopy only, it was not possible to differentiate the enantiomers and determine which isomers were present in the slime mold. The following year, the same group reported that the naturally occurring isomers in *Dictyostelium* are 6-PP-InsP₅ and 5,6-(PP)₂-InsP₄ using a PP-InsP₅ kinase isolated from the mold, which phosphorylates only the naturally occurring PP-InsP₅. Synthetic PP-InsP₅ (1-, 3-, 4- and 6-PP-InsP₅) were used as substrates for the enzyme, showing that only the 6-PP-InsP₅ was converted, thus producing 5,6-(PP)₂-InsP₄ (Figure 1.8).⁴⁰ However, low purity of the synthetic compounds might have biased these results.

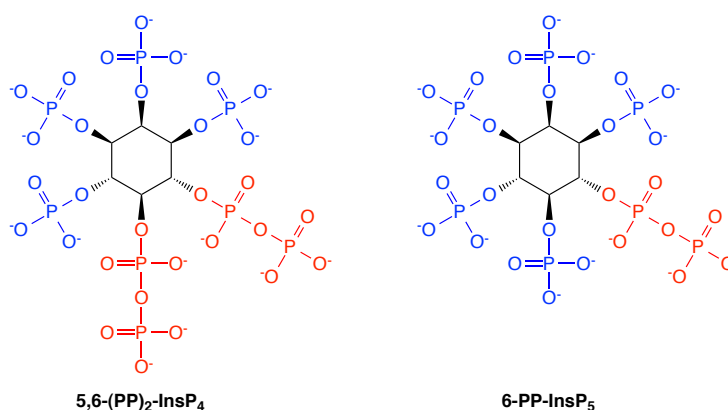


Figure 1.8. Structures of diphosphoinositol polyphosphates present in *Dictyostelium discoideum*.

1.3.3 BIOSYNTHESIS AND METABOLISM OF INOSITOL PYROPHOSPHATES

Phosphatidylinositol 4,5-bisphosphate (PIP₂) anchors *myo*-inositol to the plasma membrane in biological systems and it is the precursor of the various inositol phosphate derivatives that are present in the cell. Phospholipase-C (PLC) is the enzyme that hydrolyzes the phospholipid generating the membrane-bound diacylglycerol (DAG) and the cytosol-soluble inositol 1,4,5-trisphosphate (InsP₃). InsP₃ is then converted to the various phosphorylated forms of inositol by a series of kinases and phosphatases starting the IP signaling (Figure 1.9).^{12,13,41}

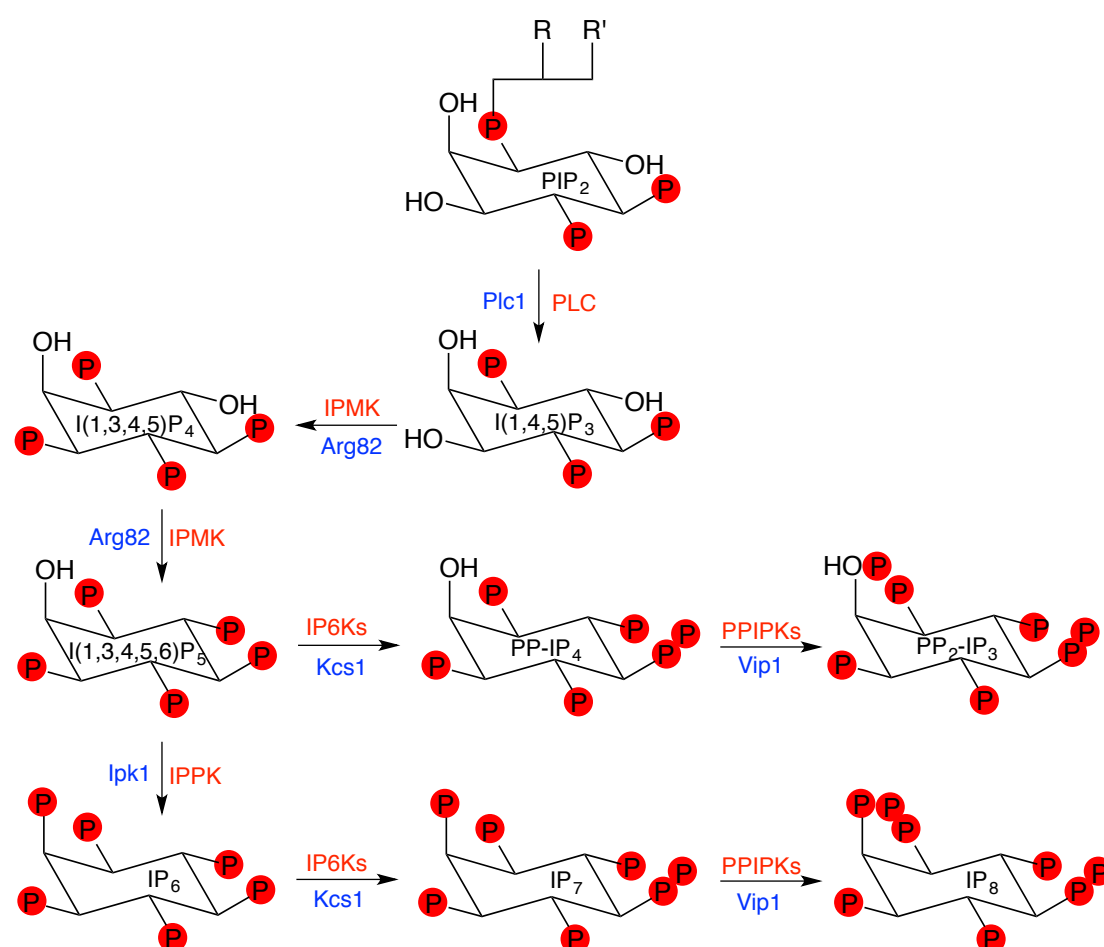


Figure 1.9. Possible routes of inositol pyrophosphates synthesis in mammalian (red) and *S. cerevisiae* (blue). PLC/Plc1 = Phospholipase C; IPMK/Arg82 = Inositol phosphate multikinase; IPPK/lpk1 = Inositol 1,3,4,5,6-pentakisphosphate 2-kinase; IP6Ks/Kcs1 = Inositol hexakisphosphate kinase; PPIP2Ks/Vip1 = Diphosphoinositol pentakisphosphate kinase. (Picture reproduced from Ref.¹³)

1.3.3.1 KINASES

InsP₆ is the precursor of 5-PP-InsP₅ and inositol hexakisphosphate kinases (IP6Ks) are the enzymes responsible for this transformation using ATP as a phosphate donor. Three different isoforms of the kinase exist in mammalian cells: IP6K1, IP6K2 and IP6K3. IP6K1 and IP6K3 phosphorylate InsP₅ and InsP₆, with a slight preference for InsP₆, while the selectivity of IP6K2 for InsP₆ is 20-fold higher than for InsP₅.^{42,43} In a study of the three different isoforms, it has been suggested that IP6K2 is also able to synthesize a higher phosphorylated inositol derivative with a triphosphate in position 5 known as 5-PPP-InsP₅ (InsP₈), although in lower concentration as compared to InsP₇.^{43–45} Incubation of IP6K2 with InsP₆ for a longer period of time (12 h) leads to the formation of a more polar molecule, presumably an InsP₉ isomer.⁴⁵ Another precursor of inositol pyrophosphates is Ins(1,3,4,5,6)P₅ that can be phosphorylated by IP6K at positions 1 or 3 generating 1/3-PP-InsP₄.⁴³ This substrate that contains one unphosphorylated hydroxyl group can be then phosphorylated again by the same enzyme to generate (PP)₂-InsP₃.⁴⁶

Besides the IP6K family, PPIP5K or PP-InsP₅ kinases are another class of enzymes responsible for the biosynthesis of inositol pyrophosphates in mammalian cells.^{47,48} They phosphorylate both InsP₆ and 5-PP-InsP₅, introducing a phosphate specifically in position 1 and generating 1-PP-InsP₅ and 1,5-(PP)₂-InsP₄ respectively.^{34,38} However, PPIP5K contains also a phosphatase domain that might antagonize the action of the kinase domain by dephosphorylating 1-PP-InsP₅, suggesting that the main target of the enzyme is InsP₇.¹³

The kinases found in yeast *S. cerevisiae* are Kcs1 (IP6K homolog) and Vip1 (PPIP5K homolog) and phosphorylate the 5 and 1 position of InsP₆ and 5-PP-InsP₅, respectively.^{13,37,42}

1.3.3.2 PHOSPHATASES

Diphosphoinositol-polyphosphate phosphatases (DIPPs) are phosphatases that belong to the nudix (nucleoside diphosphate attached-moiety X) family and catalyze the hydrolysis of diphosphate bonds in inositol pyrophosphates, diadenosine polyphosphates and inorganic polyphosphate.^{46,49} In mammalian cells, 4 DIPP genes have been identified that encode for 5 proteins: (DIPP1, DIPP2 α , DIPP2 β , DIPP3 α and DIPP3 β), while in yeast *S. cerevisiae* only the protein Ddp1 has been found.⁵⁰ DIPP1 is the most active in hydrolyzing inositol pyrophosphates, followed by the two isoforms of DIPP2 and finally

DIPP3, which is the least active.⁵¹ This class of enzymes dephosphorylates mainly the β -phosphate in position 1 of inositol pyrophosphate, followed by dephosphorylation at position 5.⁵¹

Multiple inositol polyphosphate phosphatase (MIPP) is another enzyme that catalyzes the hydrolysis of the pyrophosphate bond in position 5 of diphosphoinositol polyphosphates *in vitro*, but not *in vivo*.^{52,53}

1.3.3.3 TURNOVER

The proposal that inositol pyrophosphates have significant biological functions was inspired by their rapid metabolic turnover caused by the action of kinases and phosphatases. Intracellular concentrations of InsP₅ and InsP₆ are high as compared to the concentration of inositol pyrophosphates, however every 60-90 min 20% of InsP₅ and 50% of InsP₆ are converted to PP-InsP₄ and PP-InsP₅. Therefore the low concentration of inositol pyrophosphates can be associated with their rapid turnover, suggesting that these molecules have a role in cellular signaling.³⁰ Shears and coworkers also demonstrated that in primary cultured hepatocytes inositol pyrophosphate pools turn over ten times every 40 minutes, while only the 10% of the InsP₆ pool turns over in the same time.⁵⁴

1.3.4 MECHANISM OF ACTION AND FUNCTIONS

Many functions have been attributed to inositol pyrophosphates since their discovery and it has been proposed that they act in the cell mainly by two mechanisms of action: by binding to a particular protein and by donating the β -phosphate of the pyrophosphate moiety to a specific protein target (Figure 1.10).^{14,55-57}

The intracellular concentrations of inositol pyrophosphates increase in response to stimuli generated inside cells, related to the maintenance of energy balance, therefore a description of them as “metabolic messengers” has been proposed.^{14,35} However, InsP₈ levels increase on extracellular stimulus in line with a functional second messenger.⁵⁸⁻⁶⁰ An example that supports the definition as metabolic messengers comes from a recent study by Saiardi and coworkers that demonstrates that inositol pyrophosphates regulate intracellular ATP concentration.⁶¹ They showed that in yeast *Saccharomices cerevisiae* ATP concentration increased in the absence of inositol pyrophosphates, while when IP6K

was overexpressed, and therefore the levels of inositol pyrophosphates were presumably higher, the intracellular concentration of ATP dropped. The hypothesis that arises is that inositol pyrophosphates are “biosensors that detect variations in energy balance”.¹⁴ If they are not synthesized, then ATP is not consumed and the energy of the cell is conserved, which is especially important when the cell is in an energetically challenging condition.

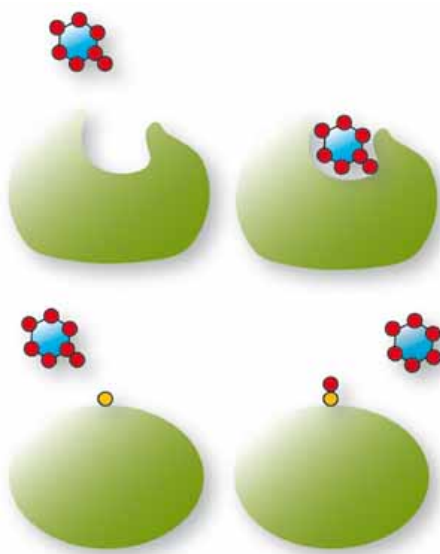


Figure 1.10. “Possible mechanisms of signal transduction by inositol pyrophosphates. The upper panel depicts the direct binding mechanism in which a protein target possesses a specific pocket able to recognise InsP₇. The lower panel shows the pyrophosphorylation modification of a protein carried out by InsP₇. A pre-phosphorylated serine (yellow circle) is the recipient of the b-phosphate (red circle) of the pyrophosphate moiety of InsP₇.”⁵⁷ (Burton, A.; Hu, X.; Saiardi, A. Are inositol pyrophosphates signalling molecules? *J. Cell. Physiol.* 2009, 220, 8-15. Copyright © 2009 Wiley-Liss, Inc.)

1.3.4.1 PROTEIN BINDING

Similarly to InsP_y, X-PP-InsP_y can modulate cellular signaling pathways by binding proteins, especially those involved in vesicular trafficking.^{62–67} The first suggestion that inositol pyrophosphates might have this role emerged from a study on pancreatic β cells where InsP₇ was produced after overexpression of IP6K stimulating exocytosis of insulin, while RNA silencing of IP6K1 inhibited exocytosis.⁶⁸

Pleckstrin homology (PH) domains are responsible for protein-protein and protein-phospholipid interactions.³⁵ Proteins that contain PH domains are recruited to the plasma membrane and bind phosphoinositides in response to certain cellular stimuli, but

they are able to bind also soluble inositol phosphates.⁶⁹ Therefore, InsP_y can compete with the polar head groups of phosphoinositides for binding PH domains, thus inhibiting the migration of certain proteins to the cell membrane.^{70–72} The Snyder laboratory was the first to demonstrate that also inositol pyrophosphates can bind PH domains of proteins. They showed that in *Dictyostelium* 5-InsP₇ competes with PtdIns(3,4,5)P₃ by binding PH domain containing proteins and ultimately decreasing the chemotactic response that is regulated by these proteins in the mold.⁷³ The PH domain of Akt is another binding site of InsP₇. Akt is a kinase that is activated by binding PIP₃ at the plasma membrane and InsP₇ competes with this binding. The kinase regulates various cellular processes, such as growth factor signaling, glucose uptake, glycogen synthesis and protein synthesis.⁷⁴ Therefore, an abnormal activity of the kinase can lead to diseases such as cancer or diabetes.^{74,75} It has been shown that IP6K1 knockout (KO) mice are characterized by a reduced fat accumulation and consequently by a reduced body weight in comparison to wild type (WT) mice. When IP6K1 KO mice were on high-fat diet (HFD) they showed resistance to obesity, suggesting that inhibition of IP6K1 could represent a strategy to treat obesity and diabetes.⁷⁴

In mammalian cells, inositol pyrophosphates seem to have a role in the regulation of apoptosis through inositol hexakisphosphate kinase (IP6K), the enzyme responsible for the conversion of InsP₆ to 5-PP-InsP₅. In the absence of this enzyme there is no increment of the intracellular levels of 5-PP-InsP₅ and cell death is also decreased, suggesting that 5-PP-InsP₅ promotes apoptosis.⁷⁶

Inositol pyrophosphate levels, and especially the levels of 1/3,5-(PP)₂-InsP₄, increases as a consequence of hyperosmotic stress, thus representing a sensor for this stimulus.^{59,60}

Another function that has been attributed to inositol pyrophosphate is the regulation of telomere length in yeast. Telomeres are DNA sequences situated at the end of chromosomes with the function of preventing their degradation. Their shortening is associated with cellular aging.⁷⁷ When Kcs1 (yeast homologue of IP6K) was overexpressed and high levels of inositol pyrophosphates were produced, telomere shortening was observed, while longer telomeres were a consequence of reduced levels of inositol pyrophosphates. This function is specific for PP-InsP₄, the inositol pyrophosphate that is produced by phosphorylation of InsP₅.^{78,79}

1.3.4.2 PROTEIN PYROPHOSPHORYLATION

Diphosphoinositol polyphosphates are especially interesting for their role as phosphate donors. Diphosphoinositol polyphosphates phosphorylate proteins in a process called protein pyrophosphorylation or transphosphorylation. This new kind of post-translational modification has been described to take place *in vitro* in 2004, but it is not clear if it takes place also *in vivo*.^{80,81} The high amount of energy released upon hydrolysis of the diphosphate bond of InsP₇ (6.6 kcal/mol) and InsP₈ (7.3 kcal/mol) is comparable to the energy released upon hydrolysis of ADP and ATP.³¹ This is due to the release of electrostatic and steric constraints.³⁹ Therefore these molecules are able to transfer their β -phosphate to proteins. Strikingly, these processes occur in a kinase independent mechanism. This transfer seems to target prephosphorylated serine residues surrounded by acidic aminoacids in the presence of Mg²⁺ cations (Figure 1.11).⁸²

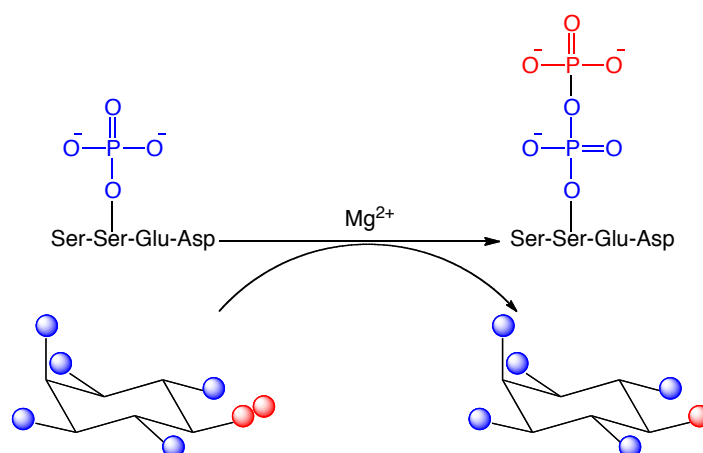


Figure 1.11. Mechanism of protein pyrophosphorylation mediated by diphosphoinositol polyphosphates. (Picture reproduced from Ref.⁸³)

Proteins that are targets of pyrophosphorylation belong to the family of nucleolar proteins, which are involved in the synthesis of ribosomal RNA (rRNA) and the best characterized are the yeast proteins Srp40p and Nsr1p and the mammalian proteins nucleolin, Nopp140 and TCOF1.⁸⁰ This is another example that suggests that inositol pyrophosphates might be metabolic messengers involved in the maintenance of energy balance, as ribosomal synthesis consumes 80% of the energy of the proliferating cell.¹⁴

Pyrophosphorylation as well as regular protein phosphorylation induce changes in protein conformation, influencing their activity and localization. The difference between the two modifications is evidenced by the special properties conferred to the pyrophosphorylated proteins. They are more acid labile and more resistant to phosphatases and pyrophosphatases than proteins modified by regular phosphorylation.⁸² This means that they are able to transduce the signal over a longer period of time in the presence of a phosphatase.⁵⁷ However, it is not known if the opposite process occurs, that is the dephosphorylation of pyrophosphorylated proteins, as no phosphatase able to mediate such activity has been identified.¹⁴

CHAPTER 2

CHEMICAL SYNTHESIS OF INOSITOL POLYPHOSPHATES

2.1 “WHY NATURE CHOSE PHOSPHATES”

In 1987 Westheimer stated that “phosphate esters and anhydrides dominate the living world”. Phosphates are found, for example, in DNA and RNA, coenzymes, ATP and many metabolic intermediates demonstrating the importance of this functional group in biological systems.⁸⁴ Phosphates are ionized in living systems due to the pH (6.8 to 7.3) of the environment and the negative charges have mainly two functions: 1) to prevent hydrolysis of phosphodiester, since it is not likely that a hydroxide ion attacks a negatively charged species such as a phosphate; 2) to retain phosphorylated molecules inside cells by inhibiting their diffusion across lipid membranes. However, phosphorylated compounds are not the only ionized species that could exist in biological systems and examples include citric acid, arsenic acid and silicic acid. Although all these compounds bear negative charges, they can be hydrolyzed much faster than phosphates. Thus, biomolecules (e.g. genetic material) that would contain them would not be protected from hydrolysis. Therefore, these negatively charged molecules are not appropriate to substitute phosphates in living systems, as biomolecules would not be stable enough over longer periods of time, which is fundamental for the life of organisms.

Westheimer also stated that the phosphate group is rarely used by organic chemists due to its poor reactivity and therefore groups that can be activated more easily (e.g. chlorides, tosylates) are preferred in synthetic organic chemistry. However, this statement is not correct anymore due to the enormous advances that have been made in phosphorus chemistry in the past decades.

2.1 PHOSPHORAMIDITE CHEMISTRY

2.2.1 INTRODUCTION

Phosphoramidites are amides of trivalent phosphorous acid H_3PO_3 characterized by one P-N and two P-O bonds (Figure 2.1).⁸⁵ Over the past decades, phosphoramidites have been used to introduce phosphate moieties on hydroxyl groups of a variety of molecules.^{86,87} Phosphoramidites are phosphitylating reagents involved in a nucleophilic substitution reaction by an alcohol on a trivalent phosphorus centre.⁸⁸ Initially P(III) chloridite reagents have been employed in the coupling reaction with alcohols. A drawback of these highly reactive compounds is that they are not stable, therefore they have been replaced with phosphoramidites (P-amidites) by Caruthers. P-amidites are less reactive and therefore prior activation by an acidic promoter is required.⁸⁹ The acidic

promoter protonates the nitrogen atom and the amino group is displaced, favoring the subsequent coupling to an alcohol (Figure 2.1).

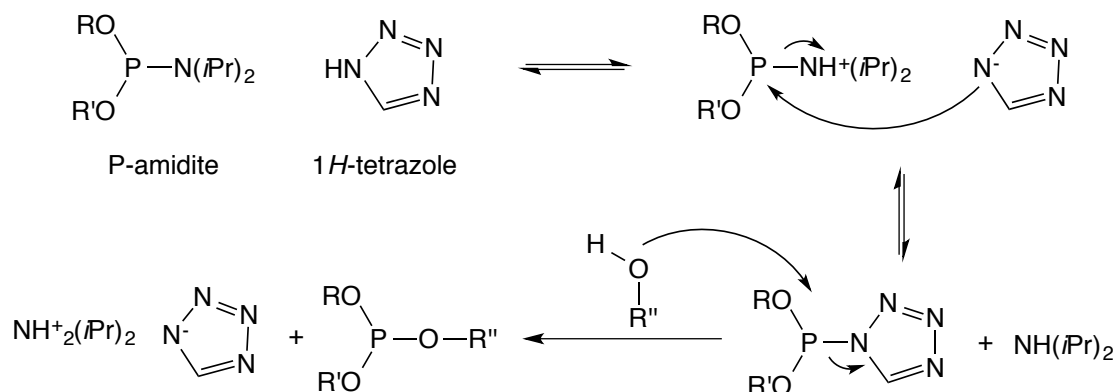


Figure 2.1. Phosphitylation mechanism. Phosphoramidites are activated by acidic promoters, which favors the coupling to an alcohol to form the phosphitylation product and a salt. (Scheme reproduced from Ref. ⁹⁰)

Many P(III) amidites are moisture sensitive in the presence of acid, as these species react with water generating hydrogen phosphonates. Therefore, dry aprotic solvents are employed in phosphoramidite chemistry, such as dichloromethane or, more commonly, acetonitrile. Pentavalent (P(V)) reagents are also employed as phosphorylating reagents, however their P(III) analogs are preferred by many groups due to their higher reactivity. Moreover, phosphitylated (P(III)) compounds can be converted into their P(V) analogs by oxidation, also facilitating sulfurizations and selenizations.

2.2.2 MECHANISM OF THE PHOSPHORAMIDITE COUPLING REACTION

The phosphoramidite coupling reaction or phosphitylation (often confused with phosphorylation) can be defined as a nucleophilic substitution reaction and classified in three sub-categories depending on the attack of the nucleophile and the displacement of the amino group: 1) dissociative S_N1 -type reaction; 2) concerted S_N2 -type reaction; 3) associative mechanism (Figure 2.2).^{88,91} The dissociative S_N1 -type mechanism is characterized by the departure of the amino group after protonation and the subsequent formation of a phosphonium cation that reacts with a nucleophile. In the S_N2 -type mechanism the nucleophilic attack and the departure of the amino group occur

simultaneously, while the associative mechanism occurs through the formation of a pentacoordinated intermediate. However, also the formation of a four-membered ring has been proposed to be involved in the substitution of phosphoramidites.

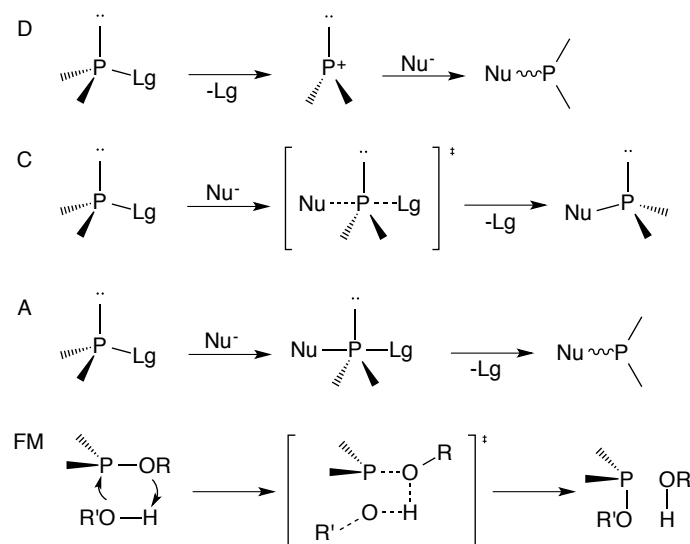


Figure 2.2. Dissociative (D), concerted (C) and associative mechanism (A) for P(III) substitution. Four-membered (FM) ring transition state involved in the mechanism of the phosphoramidite coupling reaction. Lg = leaving group. (Schemes reproduced from Ref.⁸⁸)

Protonation of the phosphorus atom shortens and strengthens the P-N bond and it promotes the phosphoramidite coupling via pentacoordination, while protonation of the nitrogen atom lengthens and weakens the P-N bond favoring a dissociative or concerted mechanism.⁸⁸ However, nitrogen protonation is required for the phosphoramidite coupling reaction to occur.⁹²

2.2.3 ACTIVATORS

Activators used in phosphoramidite chemistry have a pK_a in the range of 12.5-18.5 in acetonitrile, while the pK_a of the same activators is different in other solvents. Promoters with a pK_a in this range protonate the nitrogen of phosphoramidites weakening the P-N bond and favoring a dissociative mechanism, while weaker acids ($pK_a > 18.5$) are not able to activate phosphoramidites. More acidic activators ($pK_a < 10$) promote the

protonation of the phosphorus atom, strengthening the P-N bond and slowing down the alcoholysis (Figure 2.3).⁹²

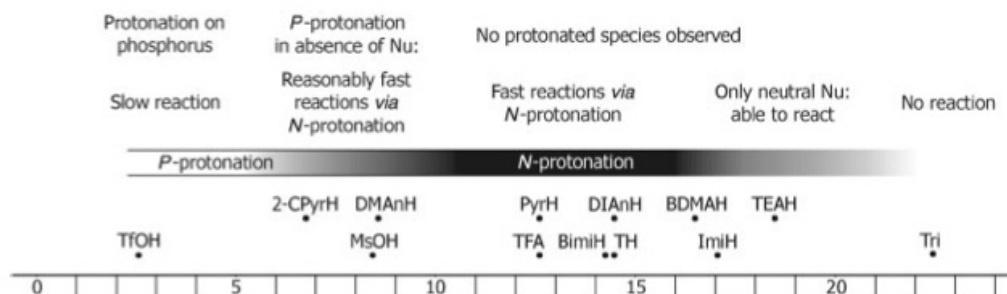


Figure 2.3. "Effect of acids on phosphoramidites as a function of the acid strength."⁸⁸ 2-CPyrH = 2-chloropyridinium ion; DManH = N,N-dimethylanilinium ion; PyrH = pyridinium ion; DIAnH = diisopropylanilinium ion; BDMAH = N,N-dimethylbenzylammonium ion; BImiH = benzimidazolium ion; ImiH = imidazolium ion; Tri = triazole; TH = 1H-Tetrazole; TFA = Trifluoroacetic acid. (Nurminen, E.; Lönnberg, H. *Mechanisms of the substitution reactions of phosphoramidites and their congeners*. *J. Phys. Org. Chem.* 2004, 17, 1–17. Copyright © 2003 John Wiley & Sons, Ltd.)

The first reported and most common activator of phosphoramidites is 1H-tetrazole⁸⁹ (for structure see Figure 2.1) and it can be modified with electron-withdrawing groups at the C-5 position to obtain more acidic and therefore more potent activators (e.g. 5-nitrophenyl-1H-tetrazole, 5-ethylthio-1H-tetrazole, 5-benzylthio-1H-tetrazole, 5-methylthio-1H-tetrazole, 5-mercapto-tetrazole).⁹³ 1H-Tetrazole is usually used as a 0.45 M solution in acetonitrile, as higher concentrations cause its precipitation (> 0.5 M). 1H-Tetrazole has a dual role in the activation of phosphoramidites and promotion of phosphitylation, as it acts as a proton donor and subsequently as a nucleophile.⁹⁴ The mechanism of phosphitylation by 1H-tetrazole can be divided into three steps: 1) 1H-tetrazole protonates the nitrogen of the phosphoramidite; 2) it acts as a nucleophile displacing the amino group and forming a tetrazolide intermediate; 3) a nucleophilic attack by the alcohol on the tetrazolide intermediate generates the phosphite triester (Figure 2.1).⁹⁰ However, due to its cost, hygroscopy, poor solubility, toxicity and instability (explosive), alternative activators are also employed, such as acidic azoles, azolium salts, pyridinium salts, anilinium salts, ammonium salts, carboxylic acids and phenols.^{88,93} Besides increasing the acidity of activators, the phosphitylation reaction can be improved by accelerating the displacement of the amino group, which is the rate determining step.

For example, 4,5-dicyanoimidazole (DCI) is less acidic but more nucleophilic than 1*H*-tetrazole and it has been shown that it can improve phosphoramidite couplings.⁹⁵

Activator	p <i>K</i> _a
1 <i>H</i> -Tetrazole	14.5
5-(Ethylthio)-1 <i>H</i> -tetrazole	12.9
Benzimidazolium salts (triflate, fluoroborate)	14.3
Imidazolium salts (triflate, fluoroborate, perchlorate, chloride)	17.1
<i>N</i> -Methylimidazolium salts (triflate, chloride, trifluoroacetate)	17.1
<i>N</i> -Phenylimidazolium salts (triflate, perchlorate, fluoroborate)	16.0
Pyridinium salts (chloride, bromide, fluoroborate, tosylate, triflate)	12.6
4-Chloropyridinium chloride	10.9
2,4-Dinitrophenol	16.0

Table 2.1. List of activators and p*K*_a values in acetonitrile. (Ref.⁸⁸)

2.3 STEREOSELECTIVE SYNTHESIS

“One of the most active current areas of chemical research is centered on how to synthesize handed (chiral) compounds in a selective manner, rather than as mixtures of mirror-image forms (enantiomers) with different three-dimensional structures (stereochemistries). Nature points the way in this endeavor: different enantiomers of a given biomolecule can exhibit dramatically different biological activities, and enzymes have therefore evolved to catalyze reactions with exquisite selectivity for the

formation of one enantiomeric form over the other. Drawing inspiration from these natural catalysts, chemists have developed a variety of synthetic small- molecule catalysts that can achieve levels of selectivity approaching, and in some cases matching, those observed in enzymatic reactions.”

T. P. Yoon and E. N. Jacobsen, *Science*, **2003**, 299, 1691.

The success of stereoselective synthesis has been made possible by the design of chiral ligands to control regio-, diastereo-, and enantioselectivity of chemical transformations.⁸⁵ High levels of stereocontrol have been achieved with the development of asymmetric catalysts that permit the preferential generation of an enantiomer starting from achiral compounds. The so called “privileged chiral catalysts” are applicable to a broad range of different reactions resulting in high enantioselectivity of the chemical transformation (Figure 2.4).⁹⁶ They also facilitate the discovery of new enantioselective reactions after screening and optimization of privileged catalyst structures. Some examples include BINAP, BINOL, TADDOLs, bis(oxazoline) and salen complexes.

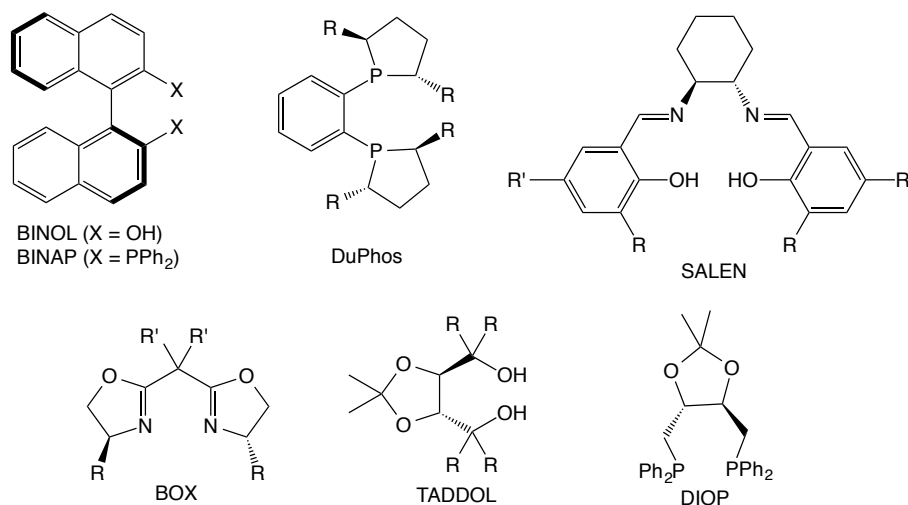


Figure 2.4. Privileged ligand structures (Structures reproduced from Ref.⁹⁷)

A common characteristic of these structures is that they possess C_2 -symmetry. Dang and Kagan developed the C_2 -symmetric ligand DIOP in 1971.⁹⁸ This symmetry was chosen as the ligand resulted in two equivalent P atoms, thus reducing the number of possible isomeric metal complexes, substrate-catalyst arrangements and reaction

pathways.⁹⁷ It was assumed that C_2 -symmetry could be responsible for the high enantioselectivity generated by this class of catalysts and the next decades were characterized by an intensive development of C_2 -symmetric catalysts.

Phosphoramidites are a class of privileged chiral ligands that have shown to enable high levels of stereocontrol (Figure 2.5).⁸⁵ These ligands have been used in combination with metals to form complexes that are used in catalysis of a wide range of metal-mediated reactions such as arylations, cycloadditions, hydrosilylations, hydrogenations and cross-coupling reactions.⁸⁵ Some examples include the application of monodentate phosphoramidites to the asymmetric synthesis of α - and β -amino acids, diacid and esters, heterocycles and amines, all prepared in excellent *ee* values.⁸⁵ However, phosphoramidites possessing C_2 -symmetry have never been employed as reagents in direct phosphorylations of the achiral *meso*-compound *myo*-inositol, leading to its desymmetrization.

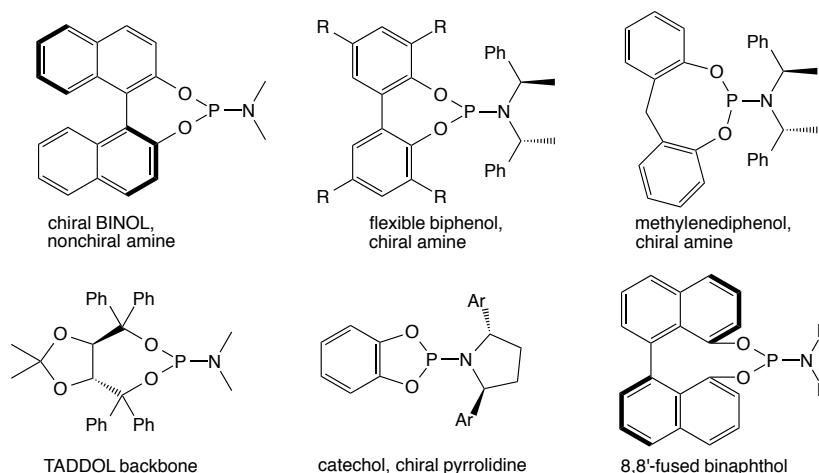


Figure 2.5. Examples of chiral phosphoramidites (Structures reproduced from Ref.⁸⁵)

2.4 DESYMMETRIZATION OF *MYO*-INOSITOL

The chemical synthesis of InsP_y and X-PP-InsP_y is challenging due to numerous factors, one of the most important being the requirement of a selective phosphorylation of a specific hydroxyl group of the inositol ring. Different strategies have been employed to achieve this goal and they include numerous protective group manipulations and the use of chiral auxiliaries, the use of precursors of inositol (e.g. glucose) and, more recently,

101

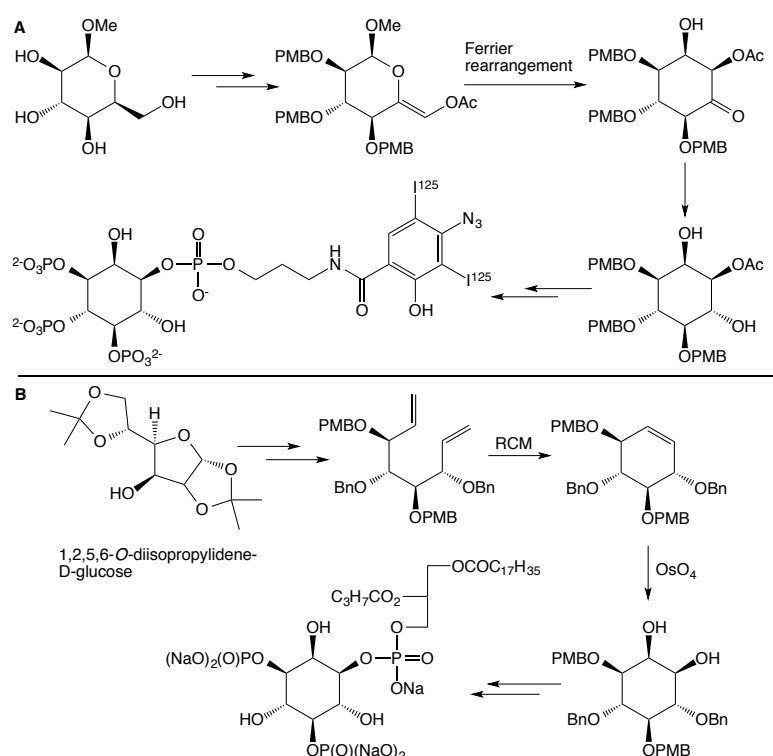


Figure 2.6. Synthesis of enantiomerically pure InsP_y via a Ferrier rearrangement (A) and ring closing methathesis (B). Ac = acetyl; Bn = benzyl; Me = methyl; PMB = *p*-methoxybenzyl; RCM = ring closing methathesis. (Schemes reproduced from Ref.⁹⁹ and Ref.¹⁰¹)

Numerous protective group manipulations and chiral auxiliary approaches have been employed towards the same goal. The first total synthesis of Ins(1,4,5)P₃ has been reported three years after the discovery of this second messenger and was achieved by appropriate protection of the OH groups of *myo*-inositol with acetal groups, followed by optical resolution and phosphorylation of specific positions.¹⁰² However, this approach resulted in a large number of steps to obtain enantiomerically pure InsP₃. Therefore, a new methodology that used chiral acetals was developed, thus avoiding the additional

optical resolution step.^{103,104} This approach consisted in the use of D- and L-camphor acetals to obtain various enantiomerically pure inositol derivatives. Protective groups like orthoesters (orthoformates, orthoacetates or orthobenzoates) allow the selective protection of the hydroxyl groups in 1-, 3- and 5-position of *myo*-inositol leaving the other hydroxyl groups free for further functionalizations (Figure 2.7),^{105–108} while the regioselective protection of hydroxyl groups of *myo*-inositol with reagents like bis-dihydropyran, disiloxane and butanedione permits to have the OH in 2-position free.^{3,109–111} However, these approaches require multiple protecting group manipulations leading to a low synthetic efficiency.

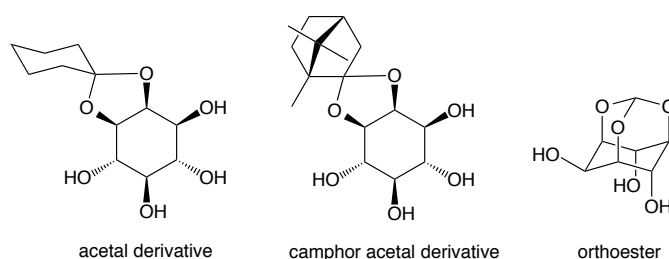


Figure 2.7. Protection of *myo*-inositol with acetal groups, chiral camphor acetals and orthoesters.

The desymmetrization of *myo*-inositol by phosphorylation is a very attractive approach for the synthesis of enantiomerically pure InsP_y. The group of Scott Miller made impressive achievements in the asymmetric phosphorylation of *myo*-inositol using peptides as catalysts that enabled the introduction of a phosphate group in a specific position of *myo*-inositol. In 2001 the group reported the asymmetric synthesis of enantiomerically pure Ins-(1)-P catalyzed by a small peptide¹¹² and subsequently also the synthesis of other unsymmetric isomers was reported using the same catalytic approach.^{113–115} However, this approach had important limitations: only P(V) reagents could be employed, which are much less reactive than their P(III) analogues; exclusively phenyl substituents could be used as protecting groups of the phosphate moiety, which required harsh conditions for their cleavage in later stages of the synthesis and additional protective group manipulations were required; Ins(1)P and Ins(3)P could be obtained in high enantiomeric excess, but the enantioselectivity was low in case of the 4- and 6-InsP derivatives (Figure 2.8). To overcome these drawbacks, the group developed a tetrazole-

based chiral peptide that allowed the enantioselective synthesis of Ins(6)P using P(III) reagents protected with benzyl groups.¹¹⁶

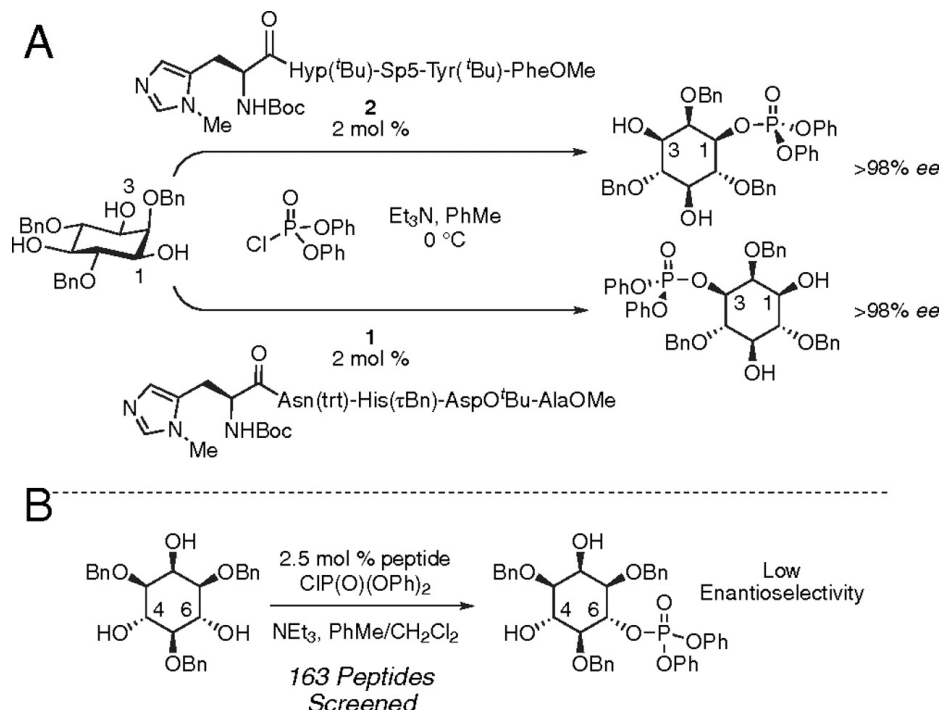


Figure 2.8. Desymmetrization of *myo*-inositol using peptides as catalysts. Selective phosphorylation of (A) 1,3 and (B) 4,6 hydroxyls.¹¹⁶ (Jordan, P. a; Kayser-Bricker, K. J.; Miller, S. J. Asymmetric phosphorylation through catalytic P(III) phosphoramidite transfer: enantioselective synthesis of *D*-*myo*-inositol-6-phosphate. *Proc. Natl. Acad. Sci. U. S. A.* 2010, 107, 20620–20624. Copyright © 2010 National Academy of Sciences, USA)

2.5 SYNTHESIS OF DIPHOSPHOINOSITOL POLYPHOSPHATES

The first total synthesis of 1-PP-InsP₅ and 3-PP-InsP₅ was reported by the group of Falck in 1995 (Figure 2.8).¹¹⁷ The reported synthesis started from an enantiopure cyclohexylidene *myo*-inositol derivative or its enantiomer that had been obtained using the camphor acetal approach, followed by phosphorylation of the hydroxyl group in 1- or 3-position with benzyl methyl *N,N*-diisopropylphosphoramidite. Demethylation with LiCN and coupling with dibenzyl chlorophosphate facilitated the formation of the pyrophosphate moiety. However, the ³¹P-NMR and ¹H-NMR spectra were published only for the 1-PP-InsP₅ isomer and the integrations were not reported. Poorly resolved spectra were obtained (see Figure 2.9 B and C).

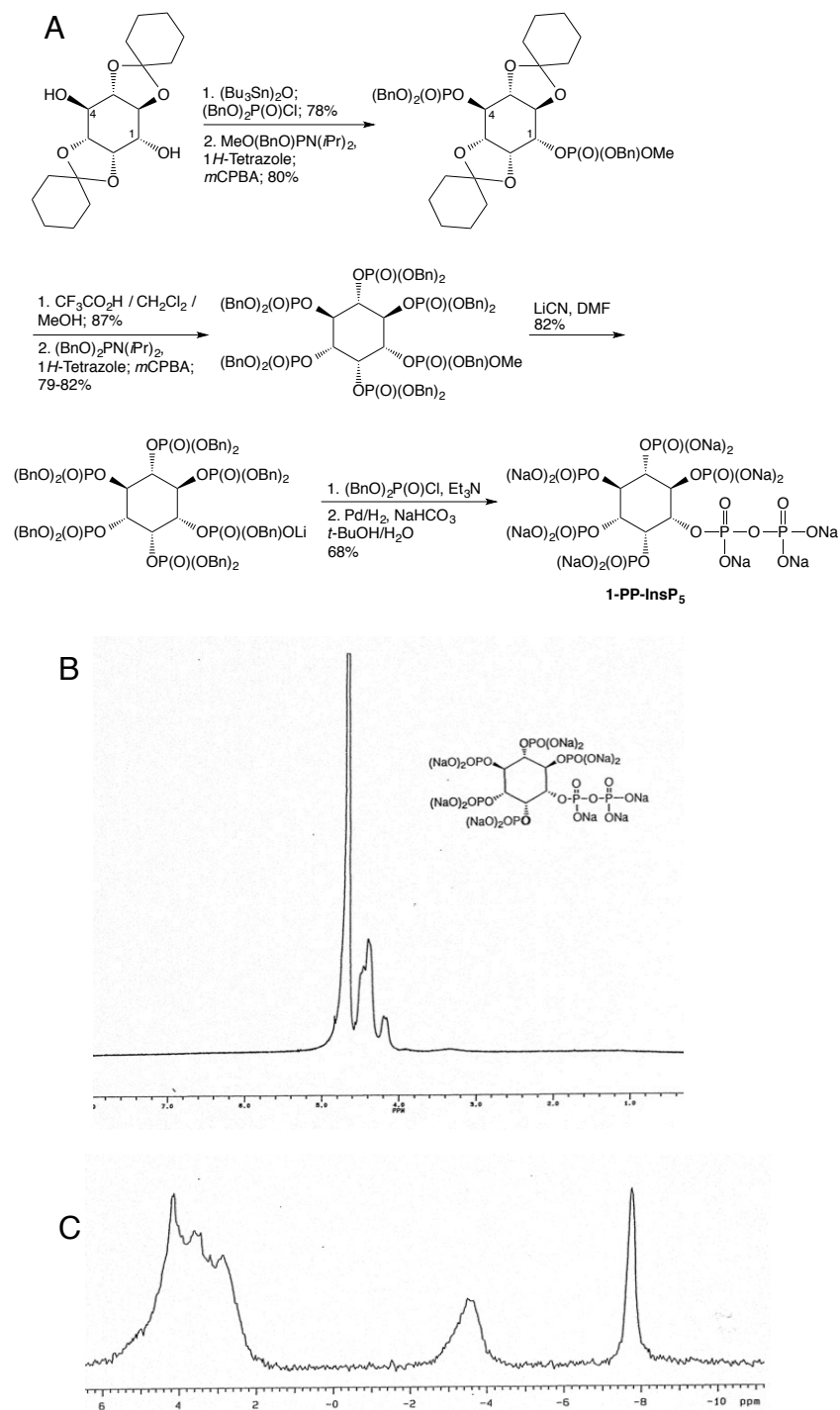


Figure 2.9. A) First synthesis of 1/3-PP-InsP₅; B) ¹H-NMR of 1-PP-InsP₅; C) ³¹P-NMR of 1-PP-InsP₅. (Scheme reproduced from Ref. ¹¹⁷; Figures B and C adapted with permission from Falck, J. R.; Reddy, K. K.; Ye, J.; Saady, M.; Mioskowski, C.; Shears, S. B.; Tan, Z.; Safranyg, S. Synthesis and structure of cellular mediators: inositol polyphosphate diphosphates. *J. Am. Chem. Soc.* 1995, 117, 12172–12175. Copyright © 1995 American Chemical Society)

This procedure was then adapted for the preparation of the isomers pyrophosphorylated in 4- and 6-position (Figure 2.10).³³ The same group reported also the first total synthesis of the *meso* compounds 2- and 5-PP-InsP₅.¹¹⁸ Their approach consisted in the use of symmetric bis-disiloxane derivative of *myo*-inositol that was prepared employing a procedure developed by Ozaki¹¹⁹ and subsequently phosphorylated in 2- or 5-position with benzyl methyl N,N-diisopropylphosphoramidite. Desilylation and phosphorylation of the remaining hydroxyl groups, followed by demethylation with LiCN and coupling with dibenzyl chlorophosphate yielded the corresponding inositol pyrophosphates (Figure 2.10).

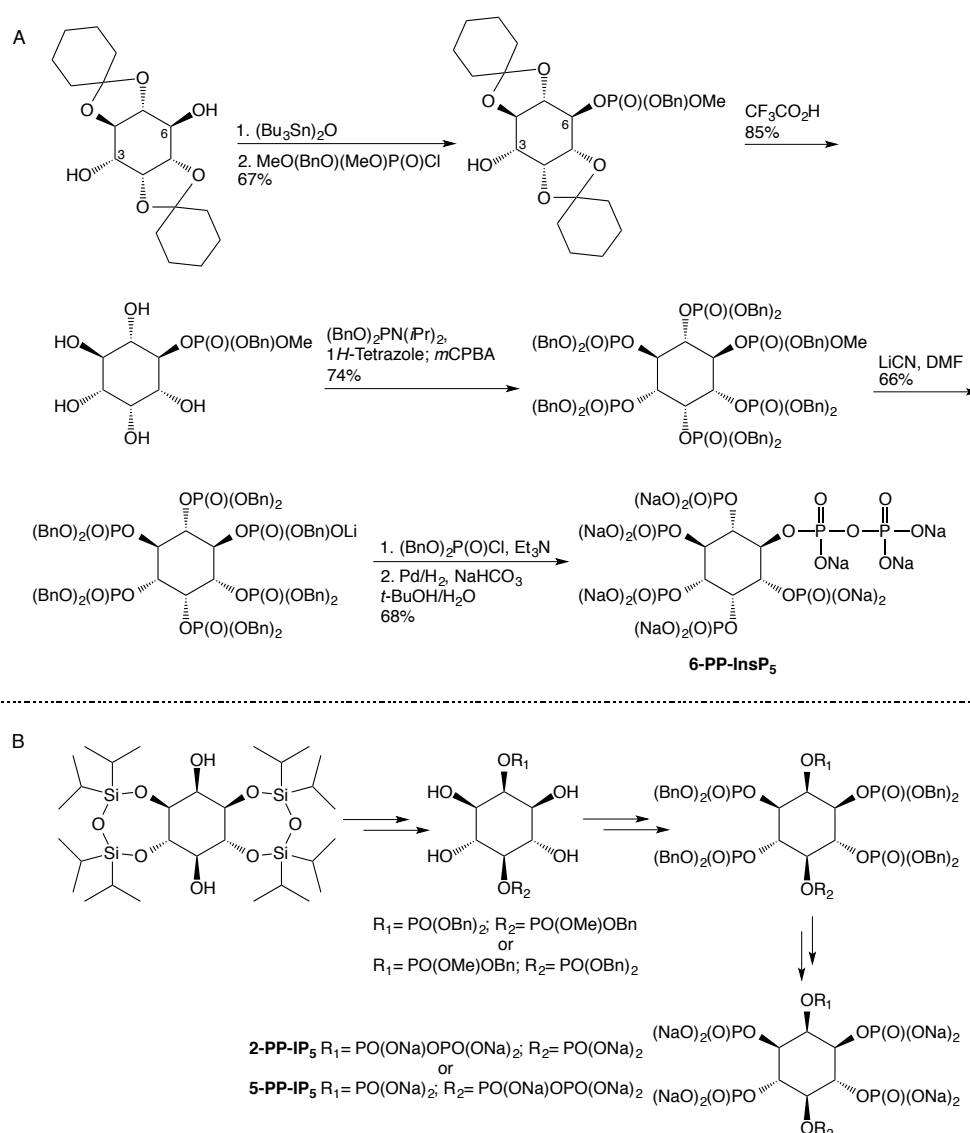


Figure 2.10. A) Synthesis of 6-PP-InsP₅; B) Synthesis of 2-PP-InsP₅ and 5-PP-InsP₅. (Schemes reproduced from Ref.³³ and Ref.¹¹⁸)

The synthesis of 5-PP-InsP₅ has been reported also by the group of Prestwich in 2009.¹²⁰ After appropriate protection and deprotection of the *myo*-inositol ring via an orthoformate intermediate, the pyrophosphate moiety was introduced in position 5. To this aim, a β -cyanoethyl phosphoramidite was used, since the protecting group of this phosphoramidite can be easily cleaved under mild basic conditions, thus allowing the formation of a diphosphate in position 5. Final hydrogenation yielded 5-PP-InsP₅ that was obtained after 13 steps in 5% overall yield. However, the ³¹P-NMR and ¹H-NMR spectra of the final product were complex, which was justified by attributing its complexity to a “distribution of sodium salt and protonated species each with characteristic chemical shifts” (Figure 2.11).¹²⁰ PAGE analysis of these compounds has now clearly shown that they are impure.¹²¹ After this analysis, the commercialized 5-PP-InsP₅ has been withdrawn from the market.

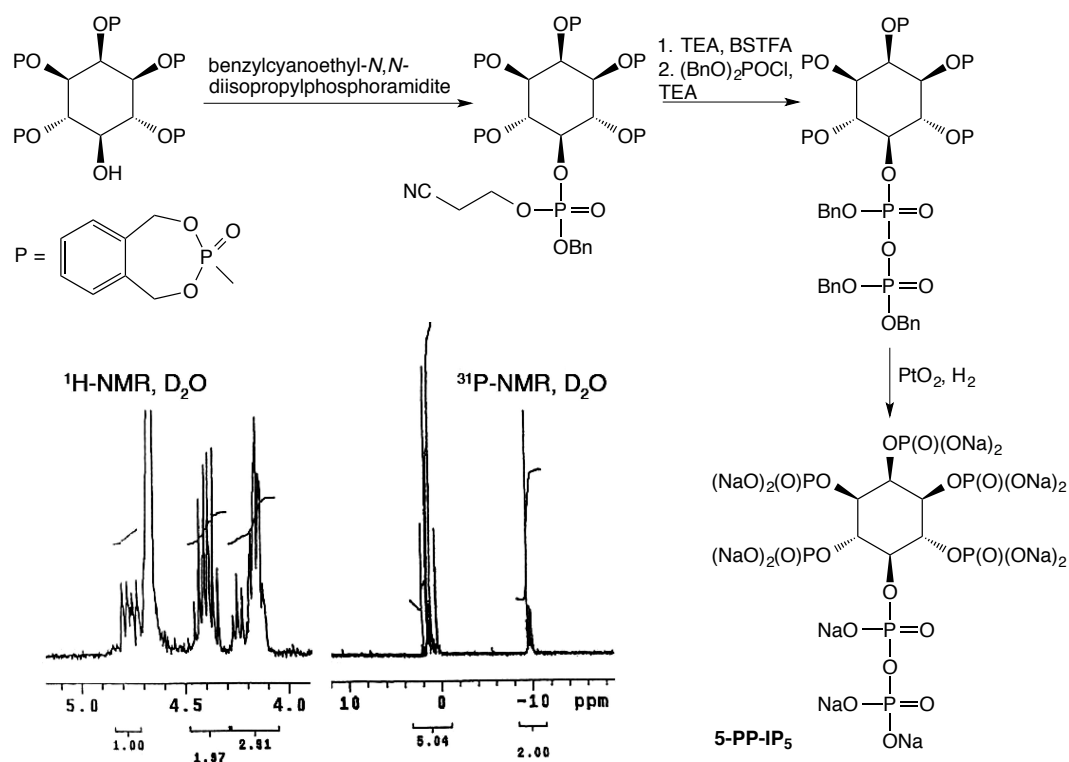


Figure 2.11. Synthesis, ¹H-NMR and ³¹P-NMR of 5-PP-InsP₅. (Scheme reproduced from Ref.¹²⁰; NMR spectra adapted with permission from Zhang, H.; Thompson, J.; Prestwich, G. A scalable synthesis of the IP₇ isomer, 5-PP-Ins(1,2,3,4,6)P₅. *Org. Lett.* 2009, 11, 1551–1554. Copyright © 2009 American Chemical Society)

The synthesis of the *meso* compound 2,5-(PP)₂-IP₄ is the only literature-known preparation of a bis-diphosphoinositol polyphosphate. However, this is not a naturally occurring isomer and the only proof that it has been synthesized is shown in an HPL chromatogram where the compound is highly impure (Figure 2.12-C, purity < 10%).³⁸ Additionally, the procedure for its preparation and the NMR spectra have never been reported, although the authors claimed that they prepared it by chemical synthesis.

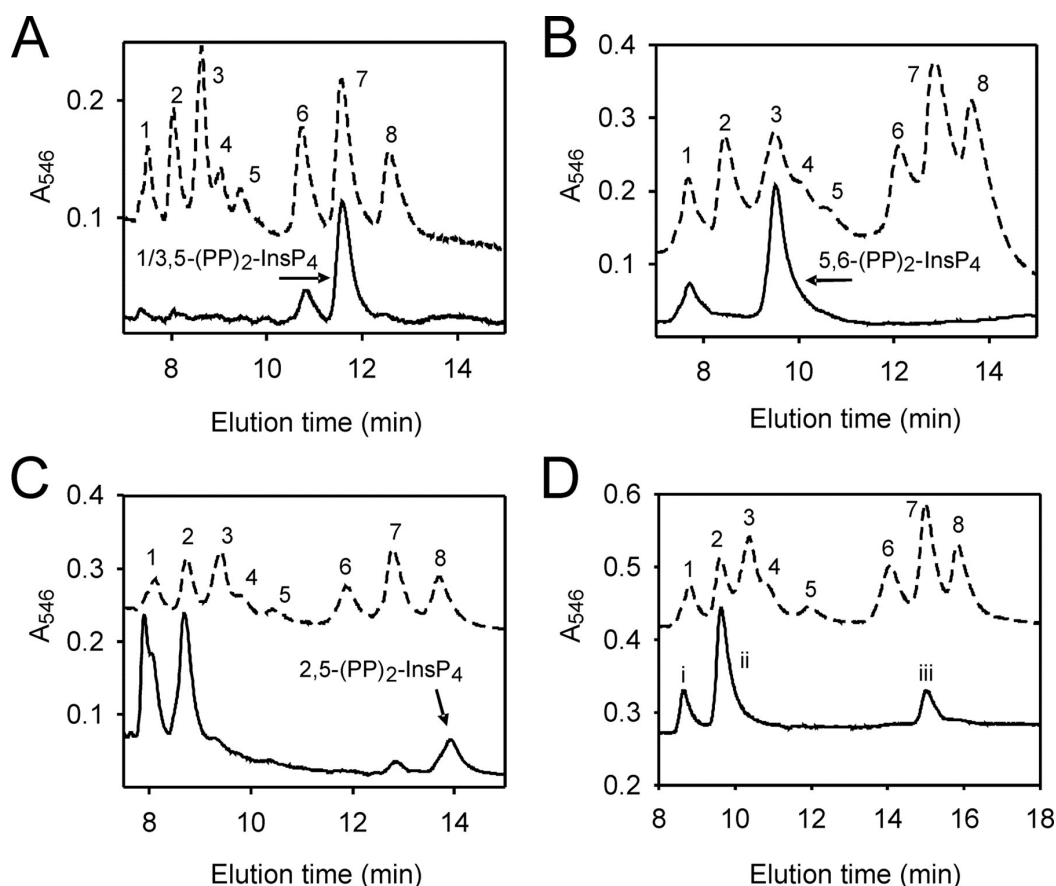


Figure 2.12. HPLC analysis of eight different (PP)₂-IP₄ isomers. 1/3,5-(PP)₂-InsP₄ (A) and 5,6-(PP)₂-InsP₄ are enzymatic preparations and derive from *Polysphondylium* and *Dictyostelium*, respectively. 2,5-(PP)₂-InsP₄ (C) has been prepared chemically, however the purity is low. Panel D shows PP-InsP₅ and (PP)₂-InsP₄ prepared enzymatically by human GST-IP6K1 and GST-ScVip1 from InsP₆. The broken line in each panel represents the HPLC separation of a standard mixture containing PP-InsP₅ (peaks 1-2) and (PP)₂-InsP₄ isomers (peaks 3-8).³⁸ (This figure was originally published in the *Journal of Biological Chemistry*. Lin, H.; Fridy, P. C.; Ribeiro, A. a; Choi, J. H.; Barma, D. K.; Vogel, G.; Falck, J. R.; Shears, S. B.; York, J. D.; Mayr, G. W. Structural analysis and detection of biological inositol pyrophosphates reveal that the family of VIP/diphosphoinositol pentakisphosphate kinases are 1/3-kinases. *J. Biol. Chem.* 2009, 284, 1863–1872. Copyright © the American Society for Biochemistry and Molecular Biology)

CHAPTER 3

GOALS

Second messengers are important for the maintenance of life as they carry information within cells. Disphosphoinositol polyphosphates (PP-InsP_y, Figure 3.1 and Figure 3.2) are a novel class of second messengers that are involved in several cellular processes (Chapter 1). It has been suggested that they act in the cell with two different mechanisms: by binding a particular receptor and by transferring a phosphate group to proteins, giving rise to a new type of posttranslational modification called protein pyrophosphorylation. This process occurs *in vitro* but it is still unclear if it occurs also *in vivo*. The identification of PP-InsP_y in nature is relatively recent and the elucidation of their roles in living systems requires further investigation. However, the detailed understanding of their structure and functions is complicated by the scarce amount of material that is available for biological studies. The concentration of PP-InsP_y in mammalian cells is low, which complicates the isolation and purification of these molecules. A higher amount of PP-InsP_y is present in the amoeba *Dictyostelium discoideum* and this organism is often taken into account for the study of PP-InsP_y. However, PP-InsP_y isomers differ from one species to another and therefore *D. discoideum* cannot be considered a general model. Moreover, the isolated enantiomers cannot be distinguished by NMR or by HPLC but only enzymatically, and this complicates the assignment of the correct stereochemistry of the isomers that are found in nature. Enzymatic preparations of PP-InsP_y are possible but failed to produce an amount of material that is suitable for biological studies. Additionally, this technique does not give access to functionalized isomers that could be used as chemical probes to study the cellular pathways regulated by diphosphoinositol polyphosphates.

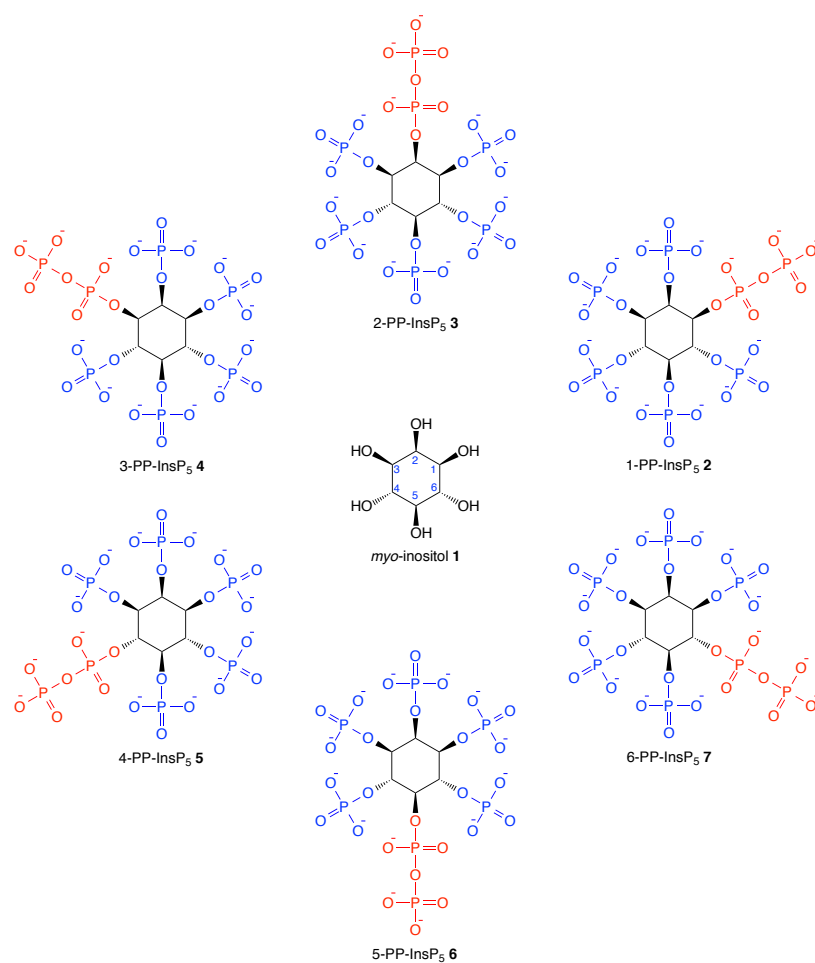


Figure 3.1. Structures of all *X*-PP-InsP₅. The backbone of all isomers is *myo*-inositol **1**.

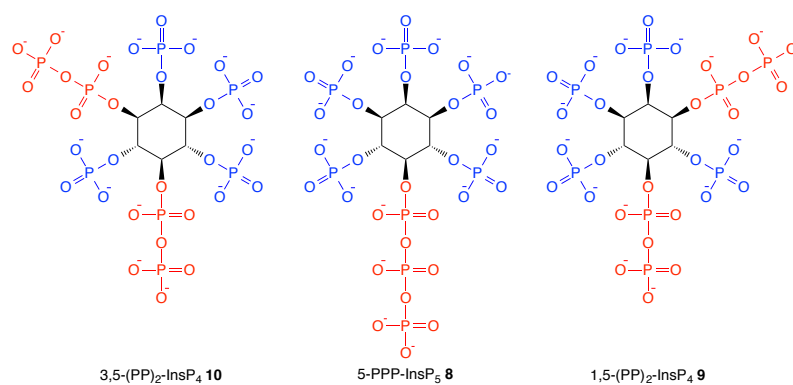


Figure 3.2. Structures of two unsymmetric *X,Y*-(PP)₂-InsP₄ and meso 5-PPP-InsP₅.

Chemical synthesis is the only method that guarantees to obtain large amounts of PP-InsP_y with known stereochemistry. The chemical routes could be then also adapted for the generation of differently modified natural and unnatural isomers, giving access to a set of tools that could be useful to elucidate the chemical biology of PP-InsP_y. The synthesis of PP-InsP_y has already been reported by other groups. However, the natural products were obtained in low purity after a large number of synthetic steps due to multiple protecting group manipulations. This fact underscores the interest and the challenges related to the total synthesis of PP-InsP_y. Diphosphoinositol polyphosphates are highly charged molecules and the high hydrophilicity makes their synthesis and purification difficult. These molecules contain up to thirteen (X-PP-InsP₅) or fourteen (X,Y-(PP)₂-InsP₄) negative charges distributed on the rim of the *myo*-inositol ring (Figure 3.1 and Figure 3.2). Another problem is represented by phosphate migration that can occur when adjacent hydroxyl groups are not protected. This event may lead to the formation of polar mixture of compounds that are phosphorylated in different positions and difficult to separate. Another complication is the instability of the phosphoanhydride bond and its potential hydrolysis, especially in the protected state during synthesis.

A novel synthesis of the most abundant diphosphoinositol polyphosphate in nature (5-PP-InsP₅) will be reported (Chapter 4.1.1). The choice of protecting groups allowed us to introduce specifically a pyrophosphate moiety in position 5. For this key step, we developed an efficient one-flask procedure that combined eight transformations. This procedure was then adapted for the generation of a triphosphate moiety that enabled us to achieve the first total synthesis of 5-PPP-InsP₅ (Chapter 4.1.2). It has been shown that this isomer can be synthesized enzymatically *in vitro*. This finding suggested that it might be present also in nature and a chemical synthesis will help us to elucidate its biological role.

Unsymmetric diphosphoinositol polyphosphates require a stereoselective synthetic approach. Different methods have been employed for the desymmetrization of *myo*-inositol. However, a desymmetrization by phosphorylation permits the direct introduction of a phosphate in a specific position of the *myo*-inositol ring, thus avoiding multiple protecting group manipulations and reducing the number of synthetic steps necessary for the synthesis.

The development of a novel C₂-symmetric phosphoramidite will be reported (Figure 3.3 and Chapter 4.2). This reagent allowed the desymmetrization of *myo*-inositol

giving access to all four X-PP-InsP₅ (Figure 3.1 and Chapter 4.3) and two possible X,Y-(PP)₂-InsP₄ (Figure 3.2 and Chapter 4.4). At the same time the chiral auxiliary served as an orthogonal protecting group, as it can be cleaved without affecting the other protecting groups in the molecule. The structure of this reagent resembles β -cyanoethyl phosphoramidites (Figure 3.3) used in DNA chemistry and it can be cleaved under mild basic conditions. This feature will be exploited in a one-flask synthesis of the phosphoanhydride bond characteristic of diphosphoinositol polyphosphates. This procedure is also useful to introduce modifications in the pyrophosphate moiety, thus allowing the construction of biological probes. The synthesis of a sulfurized analog of 3-PP-InsP₅ will be reported as an example (Chapter 4.3.1.2).

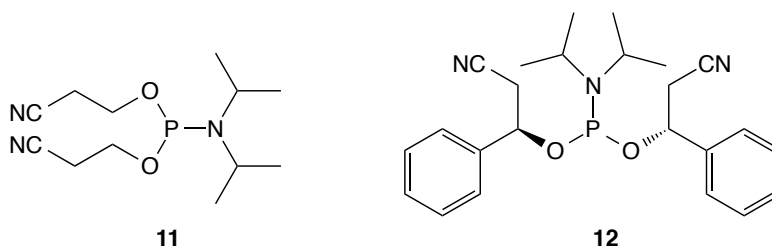


Figure 3.3 Structures of β -cyanoethyl phosphoramidite **11** and C_2 -symmetric phosphoramidite **12**. **12** can be understood as a chiral version of **11**.

CHAPTER 4

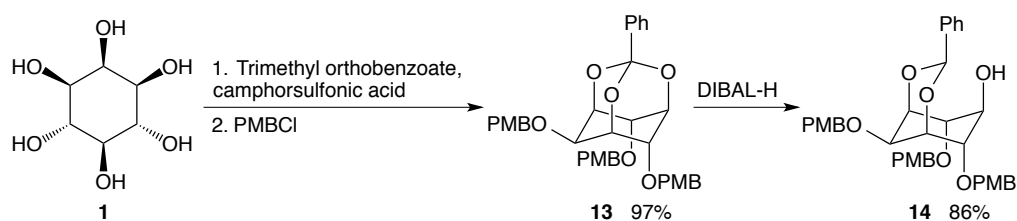
RESULTS AND DISCUSSION

4.1 SYNTHESIS OF SYMMETRIC DI- AND TRI-PHOSPHOINOSITOL POLYPHOSPHATES

4.1.1 SYNTHESIS OF *MESO* 5-PP-InsP₅

The most abundant diphosphoinositol polyphosphate in cells is 5-PP-InsP₅. This molecule is a *meso* compound and therefore its preparation does not require an asymmetric synthetic approach. The total synthesis of 5-PP-InsP₅ has been reported by the group of Falck in 1997, by the group of Prestwich in 2009 and by the Fiedler group in 2012.^{118,120,122} However, the syntheses reported by these groups required multiple protecting group manipulations resulting in low yields and the purity of the final compounds was questionable. Therefore, we developed a novel synthetic approach for the total synthesis of 5-PP-InsP₅ that resulted in a lower number of steps required for the preparation of the compound, higher overall yield and higher purity of the final natural product.

The first step of the synthesis was the regioselective protection of commercially available *myo*-inositol **1**. Following a reported procedure, the hydroxyl groups in positions 1, 3 and 5 of the molecule were protected employing trimethyl orthobenzoate as protecting group.³ The remaining free hydroxyl groups in positions 2, 4 and 6 were now protected with three *p*-methoxybenzyl (PMB) groups. Next, diisobutylaluminium hydride (DIBAL-H) was used for the selective reductive cleavage of the cyclic acetal **13** to release the hydroxyl group in position 5 (Scheme 4.1).



Scheme 4.1. Regioselective protection of *myo*-inositol with trimethyl orthobenzoate and *p*-methoxybenzyl (PMB) groups, followed by selective reductive cleavage with diisobutylaluminium hydride (DIBAL-H).

It has already been reported on a benzyl (Bn) protected substrate (**13**, replace PMB with Bn) that reduction with DIBAL-H is highly selective and allows the release of the bicyclic 1,3-acetal at room temperature in DCM.¹²³ However, using the reported

reaction conditions we observed also the formation of the 1,5-acetal and only when we performed the reaction at -78 °C we could observe high selectivity for the formation of the 1,3-acetal **14**. The two products can be distinguished by ¹H-NMR analysis, since the pattern of signals that appear in the ¹H-NMR of the two molecules is different due to the different substitution of the *myo*-inositol ring. The 1,3-acetal is a *meso* compound while the 1,5-acetal is unsymmetric, therefore the higher symmetry of the 1,3-acetal enables its unambiguous identification by NMR spectroscopy.

Two equivalents of DIBAL-H are necessary for the completion of the reaction. One equivalent acts as a Lewis acid coordinating the oxygen in position 5 of *myo*-inositol and subsequently cleaves the bond, forming an oxocarbenium ion. The second equivalent of DIBAL-H reduces the oxocarbenium ion forming the 1,3-acetal. Therefore, the side product 1,5-acetal is formed when the oxygen in position 3 is coordinated by DIBAL-H. The opposite happens when the substrate is treated with trimethylaluminium. In this case the oxygen in position 3 of *myo*-inositol is coordinated by the reducing agent and the preferred product is the 1,5-acetal (Figure 4.1).^{124,125} The difference in the selectivity of the reduction depends on steric effects related to the two reducing reagents. DIBAL-H is a bulky reagent and the oxygen in position 5 of *myo*-inositol is the most accessible one of the ring. Consequently, this oxygen is coordinated preferentially and the related bond cleaved. Additionally, when the hydroxyl group in position 5 is released, the *myo*-inositol ring can flip into a boat conformation relieving steric crowding, which would not be possible in case of cleavage in position 1 or 3.¹²⁴ Trimethylaluminium is less bulky than DIBAL-H and it has been suggested that it coordinates first to the oxygen in C-2 and then to one of the two equivalent oxygens in C-1 or C-3, cleaving one of the two bonds.¹²⁴

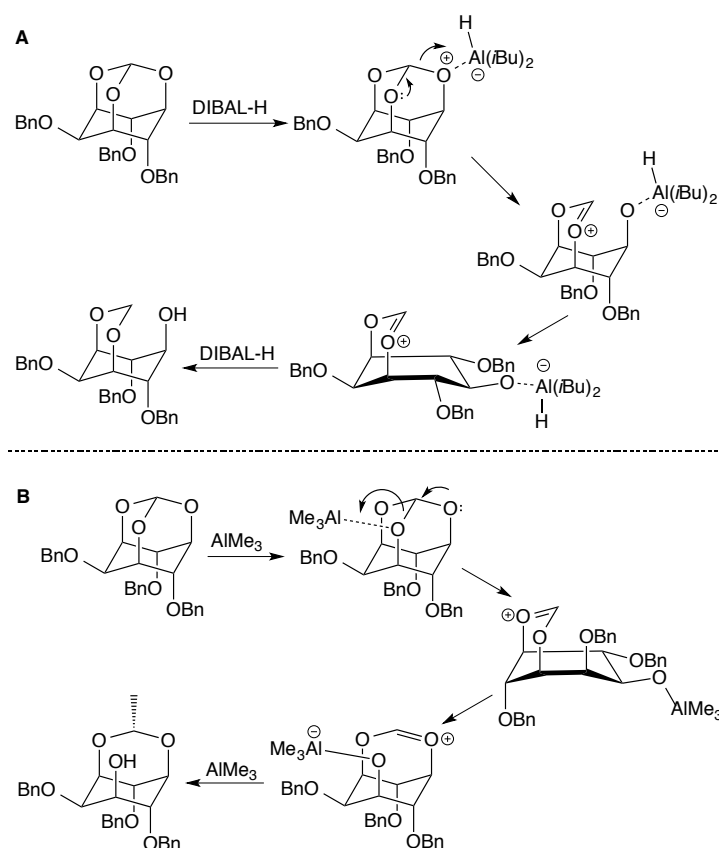
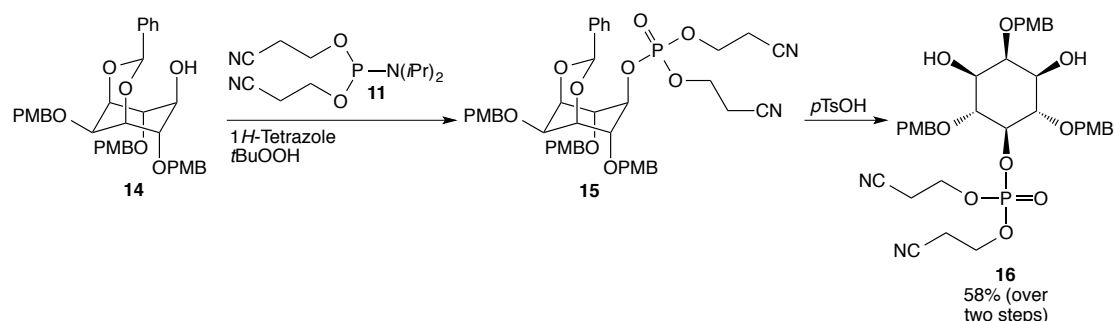


Figure 4.1. Proposed mechanism of the (A) DIBAL-H and (B) AlMe₃ reduction. (Schemes reproduced from Ref.¹²⁶)

We observed that the obtained 1,3-benzylidene acetal **14** is very sensitive towards acids. Therefore, it was necessary to avoid acidic conditions during the preparation and purification of the molecule. For example, NMR spectra were recorded only in DMSO-d₆, as the addition of the acidic CDCl₃ cleaved the acetal group. Purification of the final compound was achieved by column chromatography, after neutralizing acidic protons on the silica gel with triethylamine, which was necessary to avoid deprotection at the 1 and 3 position of *myo*-inositol. Finally, compound **14** was obtained in high purity on a 10 g scale with only the hydroxyl at position 5 free for further functionalization.

Position 5 was subsequently phosphorylated with bis-cyanoethyl-*N,N*-diisopropyl phosphoramidite **11** (Scheme 4.2). The special feature of this molecule is that the protecting groups can be cleaved under mild basic conditions. This property was later

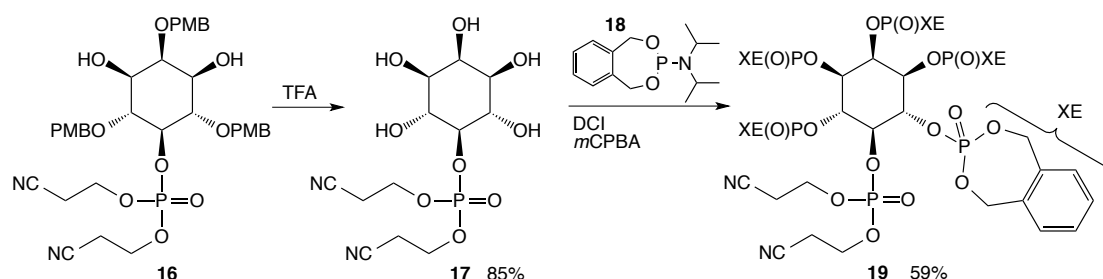
exploited in the formation of the pyrophosphate bond in position 5 (Scheme 4.4 and Scheme 4.5). The acetal group that is blocking positions 1 and 3 is very sensitive under acidic conditions, while the protecting groups on the phosphate are cleaved under basic conditions. Therefore special considerations had to be made. First, oxidation after phosphitylation with bis-cyanoethyl phosphoramidite **11** has been achieved using *tert*-butyl hydroperoxide (*t*BuOOH), as it is less acidic than *meta*-chloroperbenzoic acid (*m*CPBA) that is commonly used as an oxidizing reagent in phosphoramidite chemistry (pK_a *t*BuOOH = 12.69; pK_a *m*CPBA = 7.57 (water)). Again, it was not possible to record NMR spectra in CDCl₃ but only in DMSO due to the sensitivity of the 1,3-acetal. Purification of the crude material was not possible by flash column chromatography, as the acetal group would have been cleaved by the acidity of the silica gel. In this case, it was not an option to neutralize the silica gel with triethylamine as previously described, because basic treatment would have cleaved the protecting groups on the phosphate in position 5. Therefore, the crude mixture was used directly without purification in the selective deprotection of the benzylidene acetal (Scheme 4.2). The usefulness of intermediate **16** will be described further in section 4.3 for the preparation of unsymmetric X,Y-(PP)₂-InsP₄ derivatives.



Scheme 4.2. Selective phosphorylation of position 5 of *myo*-inositol and cleavage of the 1,3-benzylidene acetal. *t*BuOOH = *tert*-butyl hydroperoxide; PMB = *para*-methoxybenzyl; *p*TsOH = *para*-toluenesulfonic acid.

In contrast, treatment of **15** with trifluoroacetic acid (TFA) cleaved all PMB protecting groups and pentaol **17** was obtained after crystallization (Scheme 4.3). Hexakisphosphate **19** was obtained after phosphorylation of the five free hydroxyl group of intermediate **17** with *o*-xylene *N,N*-diisopropylamino phosphoramidite **18** (XEP-amidite). Phosphoramidite **18** is widely used as a phosphitylating reagent in inositol

chemistry. It is characterized by “benzyl-like” protecting groups that can be cleaved by hydrogenation, which is orthogonal to the β -cyanoethyl protecting group. This property was exploited in the next step for the formation of the pyrophosphate bond in position 5.

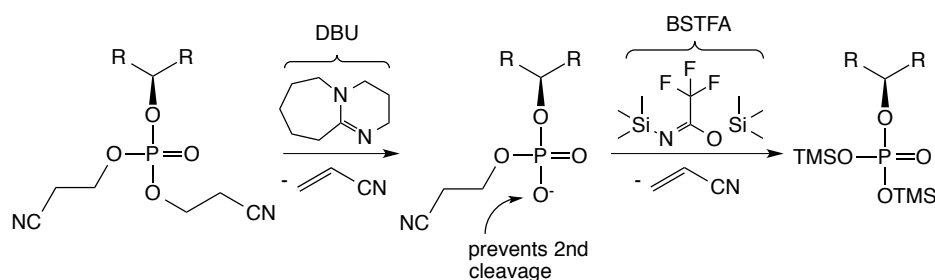


Scheme 4.3. Cleavage of PMB protecting groups and generation of hexakisphosphate **9**. mCPBA = meta-chloroperbenzoic acid; DCI = 4,5-dicyanoimidazole; PMB = para-methoxybenzyl; TFA = trifluoroacetic acid.

Next, a novel one-flask procedure was developed for the synthesis of the phosphoanhydride moiety. The first step toward this goal was to remove efficiently the two β -cyanoethyl protecting groups in order to enable the introduction of a second phosphate in position 5 to form a phosphoanhydride. The β -cyanoethyl protecting group is commonly used in nucleotide synthesis and it is known that it can be cleaved under basic conditions. The protecting groups at the remaining five hydroxyl groups cannot be cleaved using this methodology. Therefore, this property can be exploited for the selective release of only the 5 phosphate in the molecule. It has been previously reported that treatment with 1,8-diazabicyclo[5.4.0]undec-7-ene (DBU) permits the cleavage of only one of the two β -cyanoethyl protecting groups, but addition of chlorotrimethylsilane (TMS-Cl) completes the deprotection.^{127,128}

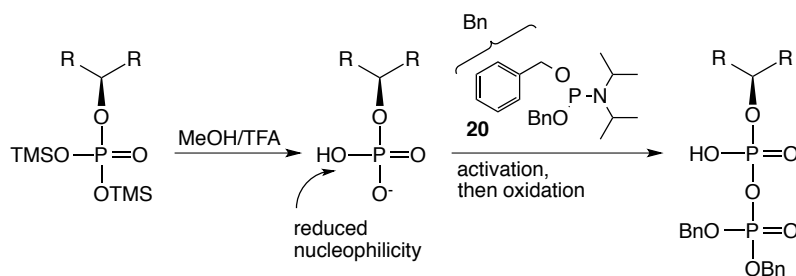
We exploited this knowledge to develop an appropriate methodology to cleave the protecting groups of the phosphate in position 5 of *myo*-inositol. Also in our case, we observed that addition of DBU cleaves only one of the two β -cyanoethyl protecting groups, even when an excess of the base was added. The cleavage of the first protecting group leads to the formation of a negative charge on the phosphate diester. Presumably this negative charge prevents the removal of the second β -cyanoethyl group due to repulsive coulombic interactions, as a second negative charge would be formed on the same phosphate group upon deprotection. Therefore, it was necessary to mask these

negative charges with groups that would be easier to cleave than the β -cyanoethyl protecting groups, in order to complete the deprotection. We decided to use a trimethylsilyl (TMS) group to transiently mask the charges on the phosphate and N,O-bis(trimethylsilyl)trifluoroacetamide (BSTFA) as a silyl donor. Treatment with TMS-Cl as described above led to decomposition. Treatment of hexakisphosphate **9** with DBU and BSTFA led to complete deprotection of the β -cyanoethyl group on the phosphate in position 5 and their replacement with TMS groups (Scheme 4.4).



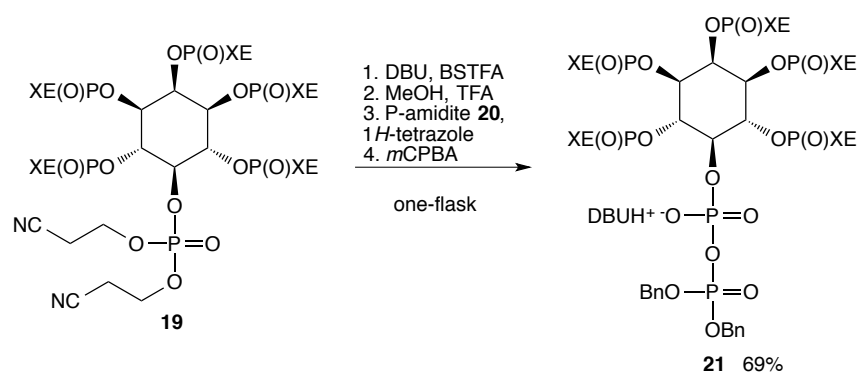
Scheme 4.4. Mechanism of the generation of the phosphoanhydride bond in a one-pot procedure. Part A: cleavage of the β -cyanoethyl protecting groups.

TMS groups are easier to cleave as compared to β -cyanoethyl groups and the removal occurs quickly in MeOH. However, when both the TMS groups are removed, negative charges are generated on the dibasic phosphate and the neighboring phosphotriesters at positions 4 and 6 are electrophilic, so that a nucleophilic attack occurs. This cleaves the xylene protecting group and a cyclic diphosphate is formed between positions 4-5 or positions 5-6 as evidenced by phosphoanhydride resonances in ^{31}P -NMR. Therefore, it was necessary to protonate one of the oxygens of the phosphate after removal of the TMS group in order to avoid this side reaction by adding trifluoroacetic acid (TFA) simultaneously with MeOH (Scheme 4.5).



Scheme 4.5. Mechanism of the generation of the phosphoanhydride bond in a one-pot procedure. Part B: deprotection of the TMS groups and phosphoramidite coupling.

Next, after mild deprotection, the phosphoanhydride was introduced in position 5: coupling with *bis*-benzyl *N,N*-diisopropylamino phosphoramidite **20** and oxidation with *m*CPBA afforded the pyrophosphate derivative **21** (Scheme 4.6). It is remarkable to mention that the compound was purified by simple crystallization and that the generated pyrophosphate derivative was pure enough to be used in the final step. With the described protocol, eight transformations were conducted in a one-flask procedure to form the pyrophosphate bond. This is the first example for the application of P^{III} - P^V chemistry in the synthesis of inositol pyrophosphates. A feature of this one-flask procedure is that it allows to introduce other functionalities in the β -phosphate. This property will be described in detail in section 4.1.3.2 where the synthesis of a sulfurized analog is illustrated. This procedure has already been adapted by other groups.¹²⁹



Scheme 4.6. One-pot synthesis of protected inositol pyrophosphate **21**.

Analysis of the ^{31}P -NMR spectrum of **21** showed characteristic signals at -10 and -12 ppm that correspond to the phosphoanhydride moiety. The signals that correspond to the other five phosphates in the *myo*-inositol ring are visible in the range between -1 and -3 ppm, in a ratio of 2:1:2 since it is a *meso* compound (Figure 4.2).

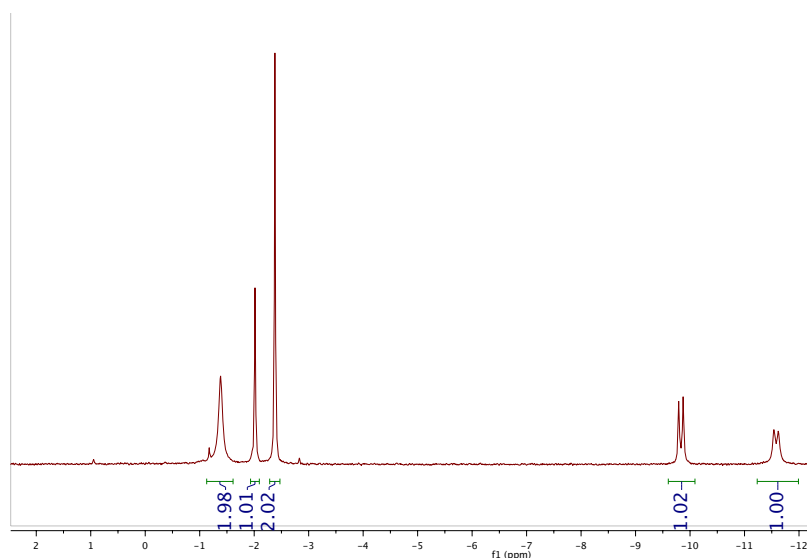
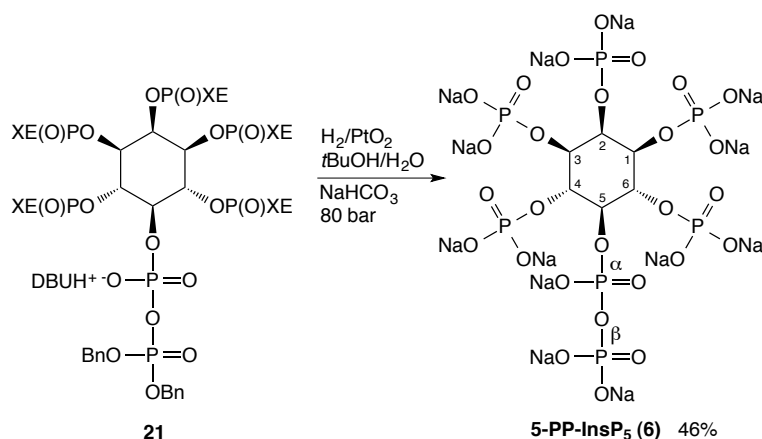


Figure 4.2. ^{31}P -NMR (decoupled) of pyrophosphate **21**.

Final high pressure hydrogenation was applied to cleave all protecting groups in the molecule yielding 5-PP-InsP₅ (Scheme 4.7). The final compound was purified by simple crystallization from water-acetone. ^{31}P -NMR analysis and polyacrylamide gel electrophoresis (PAGE) showed that the synthesized material was highly pure and no signals were present in the aromatic region of ^1H -NMR spectrum, confirming that all the protecting groups were successfully cleaved by hydrogenation. The assignment of each peak to the α or β phosphate was possible after evaluation of the proton coupled ^{31}P -NMR spectrum where the coupling with neighboring protons were visible (Figure 4.3).



Scheme 4.7. High pressure hydrogenation of intermediate **21** to generate 5-PP-InsP₅.

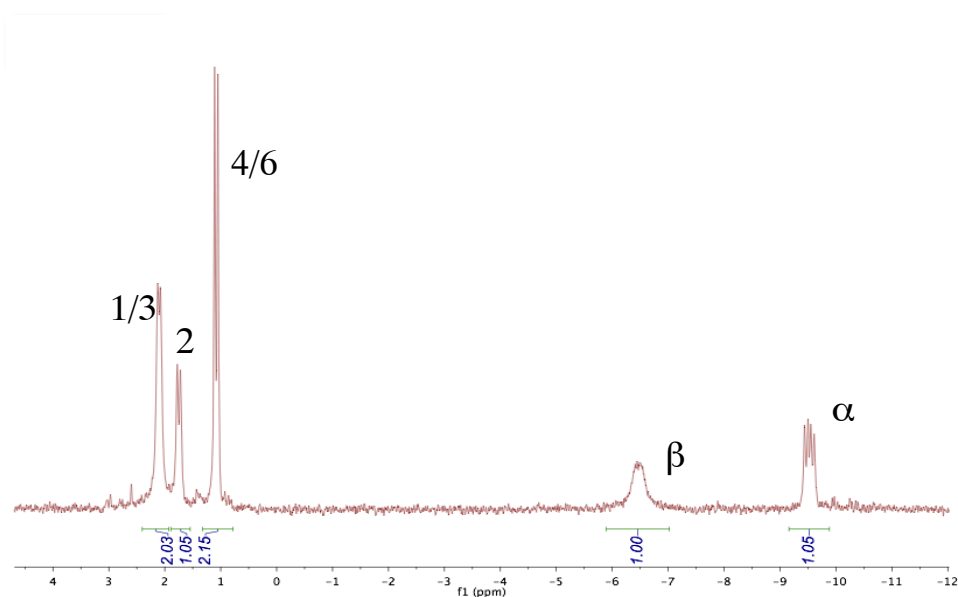


Figure 4.3. ^{31}P -NMR (coupled) of 5-PP-InsP₅ and assignment of the signals to each phosphate in the molecule. The coupling of the signals (doublets) in range between 3 and 1 ppm indicates that all protecting groups in the molecule have been removed. The signal at -9.5 ppm has been attributed to the α -phosphate (doublet of doublets, indicates P-P and P-H couplings).

4.1.2 SYNTHESIS OF MESO 5-PPP-InsP₅

It has been reported that the enzyme IP6K synthesizes not only diphosphate but also triphosphate groups on the inositol ring, generating 5-PPP-InsP₅ (for structure see Figure 4.4) from InsP₅ or InsP₆ in vitro.⁴⁵ The compound has been purified by HPLC and characterized by ^{31}P -NMR spectroscopy that revealed two doublets at -4.3 ppm and -10.2 ppm, and a multiplet at -20 ppm. These signals were assigned to γP5 , αP5 and βP5 , respectively (Figure 4.4).⁴⁵

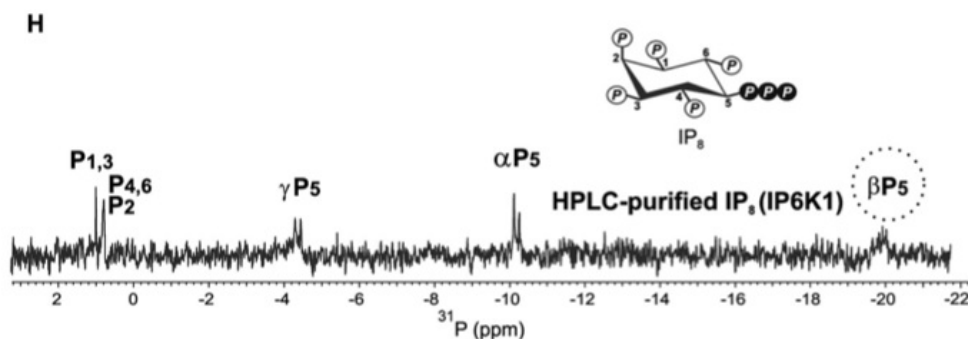
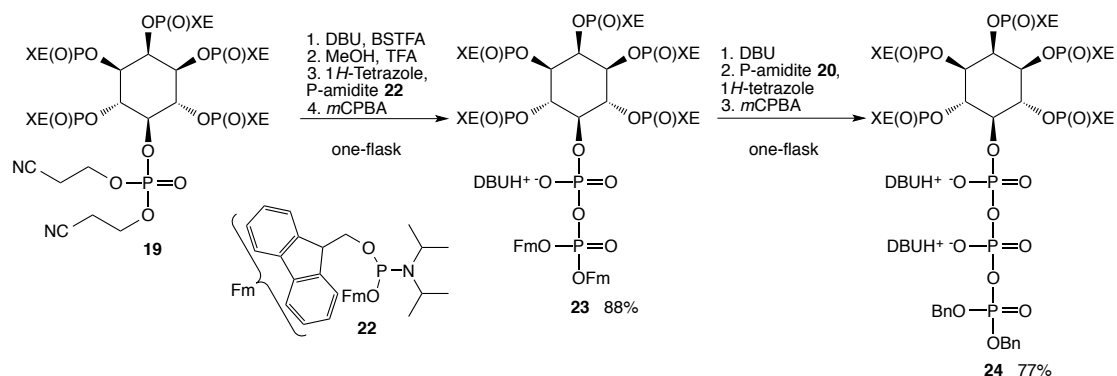


Figure 4.4. ^1H -decoupled ^{31}P -NMR spectrum of HPLC-purified IP₈ synthesized by IP6K1 in vitro (Picture taken from Ref.⁴⁵).

The synthesis of 5-PPP-InsP₅ (Figure 4.4) in vitro by mammalian enzymes indicates that this compound might be present in biological systems, although its importance is not known. The enzymatic preparation could provide the material in sufficient amount for NMR analysis, however a chemical synthesis of 5-PPP-InsP₅ has never been reported.

A modified version of the synthetic procedure developed for the preparation of 5-PP-InsP₅ can in principle be applied for the synthesis of 5-PPP-InsP₅. The installation of the diphosphate moiety in position 5 of the inositol ring previously described was achievable due to the possibility to cleave selectively the protecting groups of that particular phosphate without affecting other functional groups in the molecule. Therefore, we envisaged that the same strategy could be used for the introduction of a third phosphate in position 5. The β -phosphate of the pyrophosphate moiety of derivative **21** is protected with a benzyl group that can be cleaved by hydrogenation, thus cleaving also the remaining phosphate protecting groups. Therefore, the benzyl group had to be replaced with a group that could be cleaved under, for example, basic conditions. To this aim, instead of *bis*-benzyl *N,N*-diisopropylamino phosphoramidite **20**, fluorenylmethyl (Fm) protected phosphoramidite **22** has been chosen to pyrophosphorylate derivative **19** in the one-flask procedure described above. The Fm protecting group can be cleaved under basic condition like the β -cyanoethyl group and this property can be exploited in the next step for the formation of the triphosphate in position 5. A similar strategy has recently been described for nucleoside oligophosphate synthesis.¹³⁰

Diphosphorylation of hexakisphosphate derivative **19** with (FmO)₂PN(*i*Pr)₂ **22** required a special precaution. The removal of the β -cyanoethyl group is performed with an excess of DBU that remains in the reaction mixture during the formation of the pyrophosphate moiety. This is not an issue when reagents like *bis*-benzyl *N,N*-diisopropylamino phosphoramidite **20** are used, as the benzyl groups are stable under basic conditions. However, when the Fm-P-amidite **22** is added to such a mixture, the excess of base can cleave the Fm protecting groups. Therefore, an excess of 1*H*-tetrazole has to be added before the Fm-P-amidite **22** to neutralize the DBU present in the flask. This creates mild acidic conditions and thus favors activation of the phosphoramidite. Oxidation with *m*CPBA and crystallization afforded pyrophosphate derivative **23** that was subsequently transformed into the triphosphate **24** employing a modified version of the one-flask procedure applied before (Scheme 4.8).



Scheme 4.8. One-pot syntheses of diphosphate **23** and triphosphate **24**.

Treatment of pyrophosphate derivative **23** with DBU in DMF was sufficient to cleave both the Fm protecting groups on the β -phosphate without the requirement of a silylating reagent to complete the cleavage. Therefore, the use of the Fm-P-amidite **22** rather than the β -cyanoethyl-P-amidite **11** permitted a faster cleavage of the protecting groups. Coupling with *bis*-benzyl *N,N*-diisopropylamino phosphoramidite **20** afforded the protected triphosphate derivative **24** (Scheme 4.8). The compound was purified by simple crystallization and obtained in a purity that was sufficient to use the material in the next step without further purification. ³¹P-NMR analysis showed the characteristic signals of the triphosphate moiety at -10.9 ppm, -11.2 ppm and -21.2 ppm that can be attributed to the γ P5, α P5 and β P5, respectively (Figure 4.5).

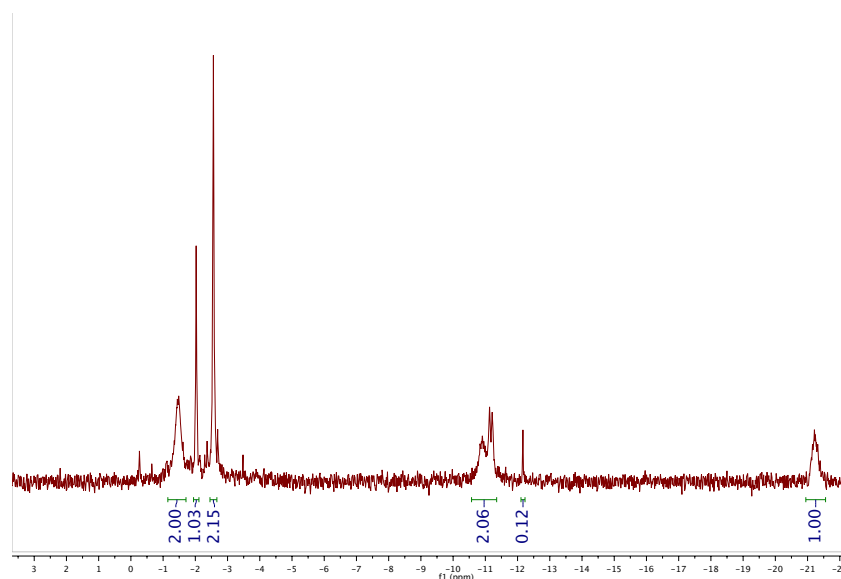
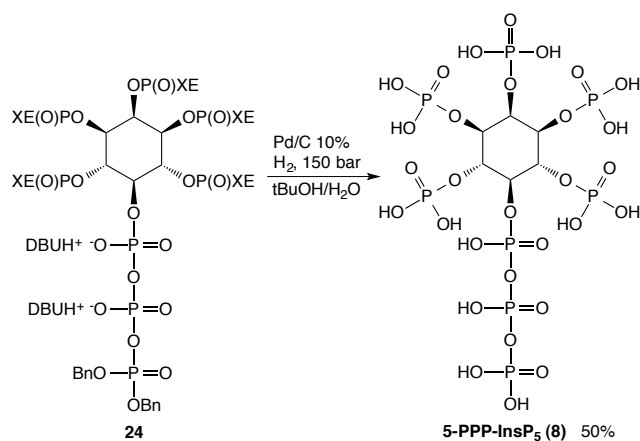


Figure 4.5. ^{31}P -NMR (proton decoupled) of crude triphosphate **24**.

Cleavage of all protecting groups in the molecule was achieved by final high pressure hydrogenation (Scheme 4.9). However, the standard hydrogenation procedure that employs NaHCO_3 lead to partial decomposition of the triphosphate moiety. When the hydrogenation was performed without the addition of base, 5-PPP-InsP₅ was obtained in good quality, although partial decomposition to 5-PP-InsP₅ could not be avoided (Figure 4.6).



Scheme 4.9. Hydrogenation of protected triphosphate **24** to form **5-PPP-InsP₅**.

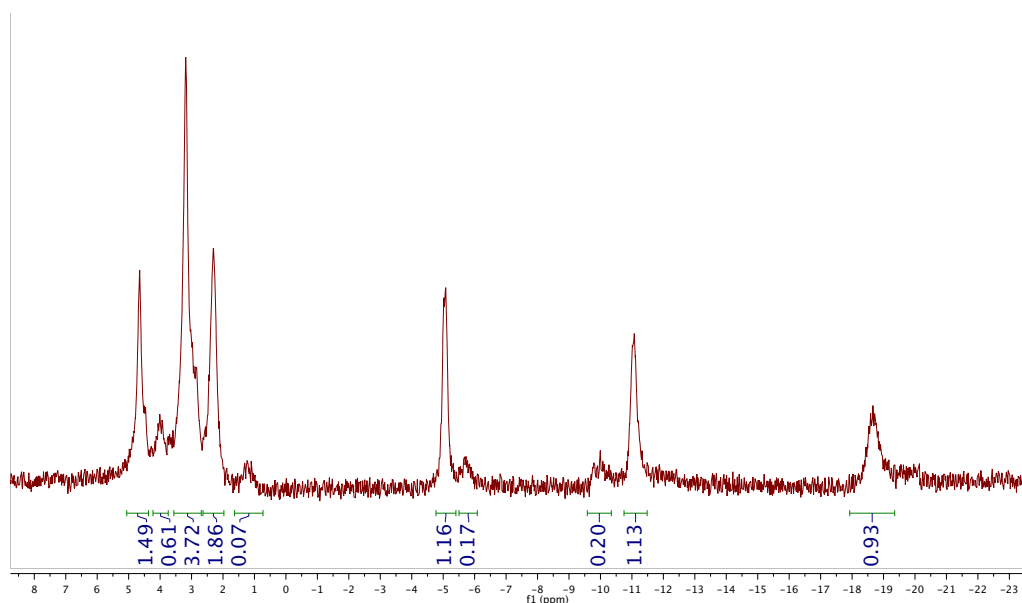


Figure 4.6. ^{31}P -NMR (decoupled) of 5-PPP-InsP₅.

4.2 DEVELOPMENT OF A C_2 -SYMMETRIC PHOSPHORAMIDITE AND ITS APPLICATION TO DESYMMETRIZE *MYO*-INOSITOL

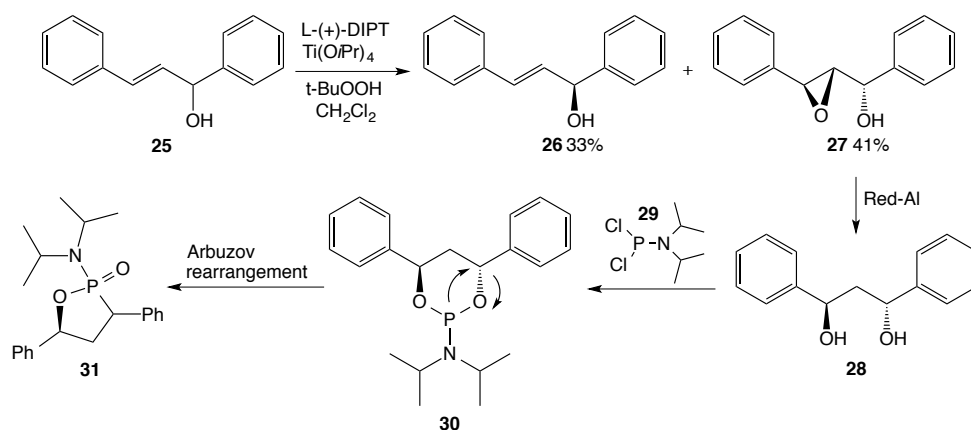
The synthesis of *meso* diphospho- and triphospho- derivatives of *myo*-inositol was complicated due to several factors previously described in Chapter 3 and in Chapter 4.1. The preparation of unsymmetric diphosphorylated derivatives such as 1-PP-InsP₅, 3-PP-InsP₅, 4-PP-InsP₅ and 6-PP-InsP₅ adds one more challenge to the synthesis of these molecules, as the introduction of a diphosphate moiety in a position different from 2 or 5 of the *myo*-inositol ring requires the development of a stereoselective synthetic approach.

Many methods have been described for the desymmetrization of *myo*-inositol (Chapter 2.4). However, a desymmetrization by phosphorylation represents a more efficient and elegant approach, as many protecting group manipulations can be avoided. Scott Miller's strategy made use of peptides as catalysts to phosphorylate or phosphitylate a specific position of the *myo*-inositol ring. This method allowed the preparation of unsymmetric inositol phosphates with high enantioselectivity (>98% ee).¹¹⁶ However, only phenol and benzyl protecting groups can be introduced in the molecule using this approach, which have to be cleaved using harsh conditions or conditions that require hydrogenation.

Although all these techniques proved to be efficient in the desymmetrization of *myo*-inositol, we did not find them appropriate for our aims. We wanted to develop a method to desymmetrize efficiently *myo*-inositol that would allow the synthesis of all four unsymmetric X-PP-InsP₅. We wanted to obtain our target molecules in few synthetic steps using mild conditions in order to avoid the decomposition of the delicate phosphoanhydride bond and other protecting groups in the molecule. Therefore, we envisaged that a desymmetrization by phosphorylation would represent the most advantageous strategy toward this goal.

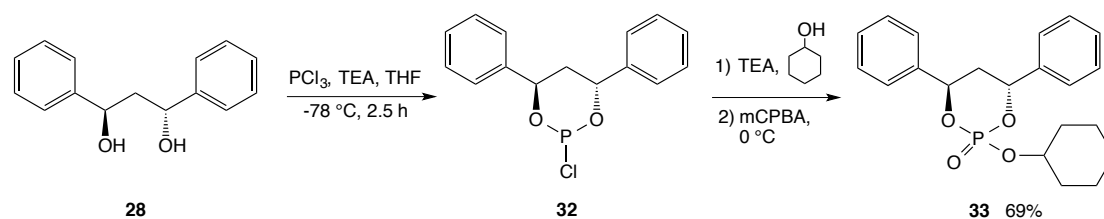
*C*₂-symmetric phosphoramidites have never been applied in the desymmetrization of *myo*-inositol. Given the ability of *C*₂-symmetric ligands to achieve high stereocontrol in chemical transformations, we envisaged the possibility to exploit this property for the desymmetrization of *myo*-inositol. Additionally, *C*₂-symmetry would avoid chirality at the phosphorus atom, thus facilitating the interpretation of ³¹P-NMR spectra. One advantage compared to enantioselective phosphorylation is that using a *C*₂-symmetric phosphoramidite reagent one obtains diastereomers that can be separated. Consequently, no high selectivity is required for this approach to be synthetically useful.

The first phosphitylating reagent that we designed for our studies was a cyclic *C*₂-symmetric phosphoramidite that contained benzyl like protecting groups (Scheme 4.10). Hydroxyalkene **25** was subjected to Sharpless epoxidation conditions to obtain a mixture of the enantiomerically enriched hydroxyalkene **26** and the epoxyalcohol **27** using a previously reported procedure.¹³¹ After separation, the enantiomerically pure epoxide was treated with Red-Al to generate the *C*₂-symmetric 1,3-diol **28** that was subsequently converted into the phosphoramidite **30** by treatment with dichloro *N,N*-diisopropylphosphoramidite **29**. However, the resulting phosphoramidite was not stable and a considerable amount of material was converted into a P(V) side product, probably derived from an Arbuzov ring contraction rearrangement to phosphonate **31**.



Scheme 4.10. Synthesis of phosphoramidite **30** and proposed mechanism for its decomposition through an Arbuzov ring contraction rearrangement. $t\text{BuOOH}$ = *tert*-butyl hydroperoxide; L-(+)-DIPT = L-(+)-diisopropyl tartrate; Red-Al = sodium bis(2-methoxyethoxy)aluminum dihydride; $\text{Ti}(\text{OiPr})_4$ = titanium isopropoxide.

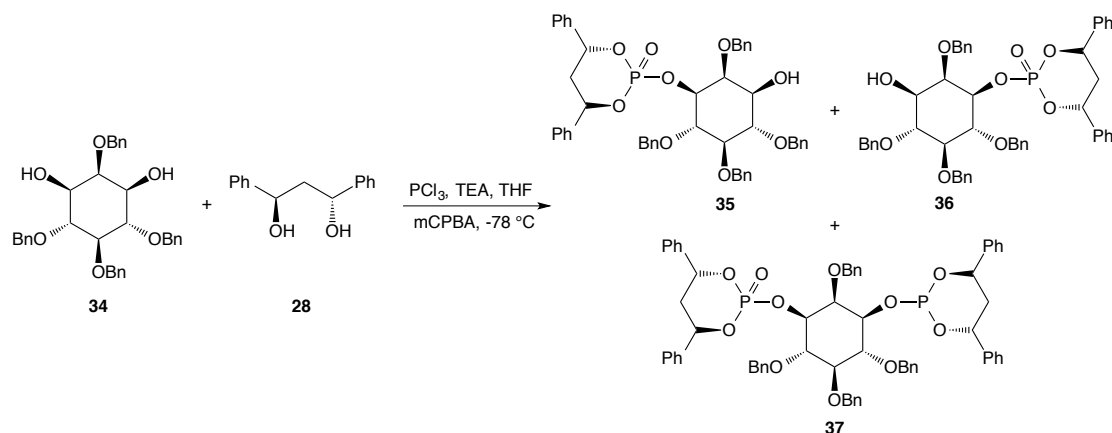
Treatment of the 1,3-diol **28** with PCl_3 lead to the formation of the phosphochloridite analog **32**. Due to the high reactivity of P(III) chloridites, isolation of this compound was not possible. Therefore, to test the phosphitylating properties of the reagent, it was generated in situ and used directly to phosphitylate cyclohexanol or phenol. After oxidation with *m*CPBA it was possible to isolate the phosphorylated alcohol **33** (Scheme 4.11).



Scheme 4.11. Phosphitylation of cyclohexanol with phosphochloridite **32**.

Next, we investigated the ability of the phosphochloridite derivative to desymmetrize benzyl protected *meso* diol **34** with free hydroxyls at positions 1 and 3. In situ generation of **32** followed by addition of the diol **34** (1 eq.) to the reaction mixture at -78°C resulted in the formation of the two diastereomers **35** and **36** and the double phosphorylated side product **37**. ^{31}P -NMR analysis showed three signals in ratio 1:1.6:0.7.

With further experiments we noticed that we could decrease the amount of side product **37** by using an excess of the *meso* diol **34** (1.5 eq.) (Scheme 4.12). The ratio of signals from ^{31}P -NMR analysis was 1.0:1.4:0.3 (Figure 4.7).



Scheme 4.12. Desymmetrization of benzyl protected *myo*-inositol **34**.

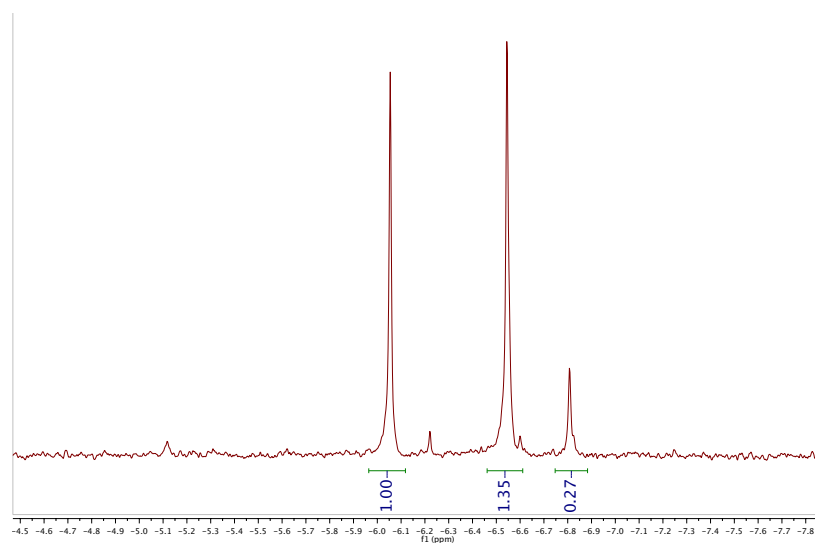


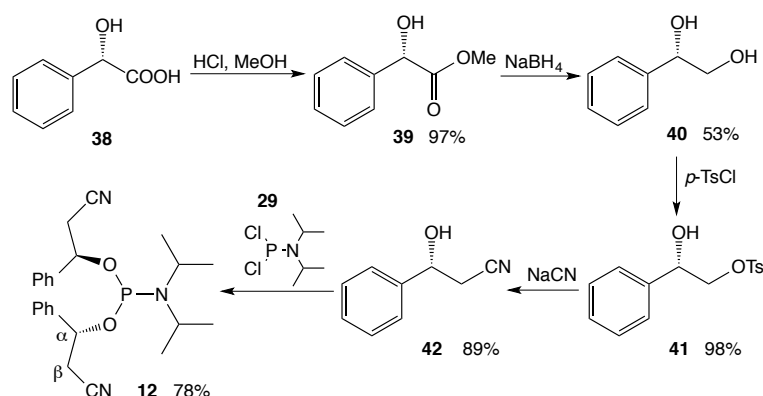
Figure 4.7. ^{31}P -NMR of the reaction mixture containing **35**, **36** and **37** using 1.5 eq. of diol **34**. Signals at -6.0 ppm and -6.5 ppm correspond to compounds **35** and **36**. The double phosphorylated side product **37** appears in the spectrum at -6.8 ppm and -6.5 ppm, overlapping with the signal of one of the two diastereomers.

However, the benzyl like protecting groups of this reagent were not orthogonal to the rest of the groups in the molecule. Hydrogenation was necessary to remove them and these reaction conditions would have affected also the other protecting groups in the

molecule. Additionally, due to the high reactivity of the phosphochloridite, we could not isolate or store the reagent. Therefore, it had to be prepared every time and used immediately in a phosphorylation reaction.

The next goal was the development of a phosphorylating reagent that could be easily prepared on scale and that would be stable enough to be stored and used over a long period of time. Another important feature was the orthogonality with other protecting groups that would allow in a successive step its selective cleavage without affecting other protecting groups in the molecule.

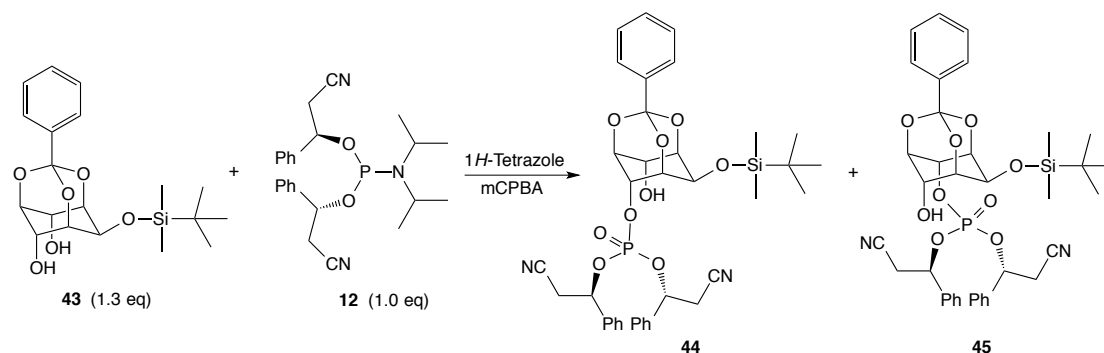
Analyzing the structure of phosphoramidite **11**, we realized that it was possible to create a C_2 -symmetric reagent by introducing a phenyl group in position C- α of the cyanoethyl protecting group. The synthesis of the compound that we wanted to use as a protecting group has been already reported. We employed a chiral pool synthesis starting from mandelic acid.^{132,133} Briefly, S-(+)-mandelic acid **38** was converted to the methyl ester **39** by treatment with HCl in MeOH and subsequently reduced to the diol **40** using NaBH₄. Selective tosylation of the primary alcohol, followed by treatment with NaCN yielded nitrile **42**. Finally, coupling of nitrile **42** with dichloro N,N-diisopropylphosphoramidite **29** afforded C_2 -symmetric phosphoramidite **12** as a white solid on a 10 gram scale (Scheme 4.13). The phosphoramidite was highly pure (> 95%) after column chromatography and stable for over one year when stored at -18 °C without additional special handling.



Scheme 4.13. Synthesis of C_2 -symmetric phosphoramidite **12**.

The C_2 -symmetric reagent **12** was used in the desymmetrization of silylated *myo*-inositol derivative **43** with free OH groups in position C-4 and C-6. The activation of the phosphoramidite **12** was performed in DCM at room temperature employing 1*H*-tetrazole

as activator. After complete activation, a cooled solution of *meso* diol **43** was added to the mixture at -78 °C and the desymmetrization was analyzed by ^{31}P -NMR. The two diastereomers were now formed in 2.3:1 ratio when using 1*H*-tetrazole as activator due to the lower temperature. This finding set the foundation for further studies on the asymmetric phosphorylation of *myo*-inositol using C_2 -symmetric phosphoramidite **12**.



Scheme 4.14. Desymmetrization of diol **43** with the C_2 -symmetric phosphoramidite **12**.

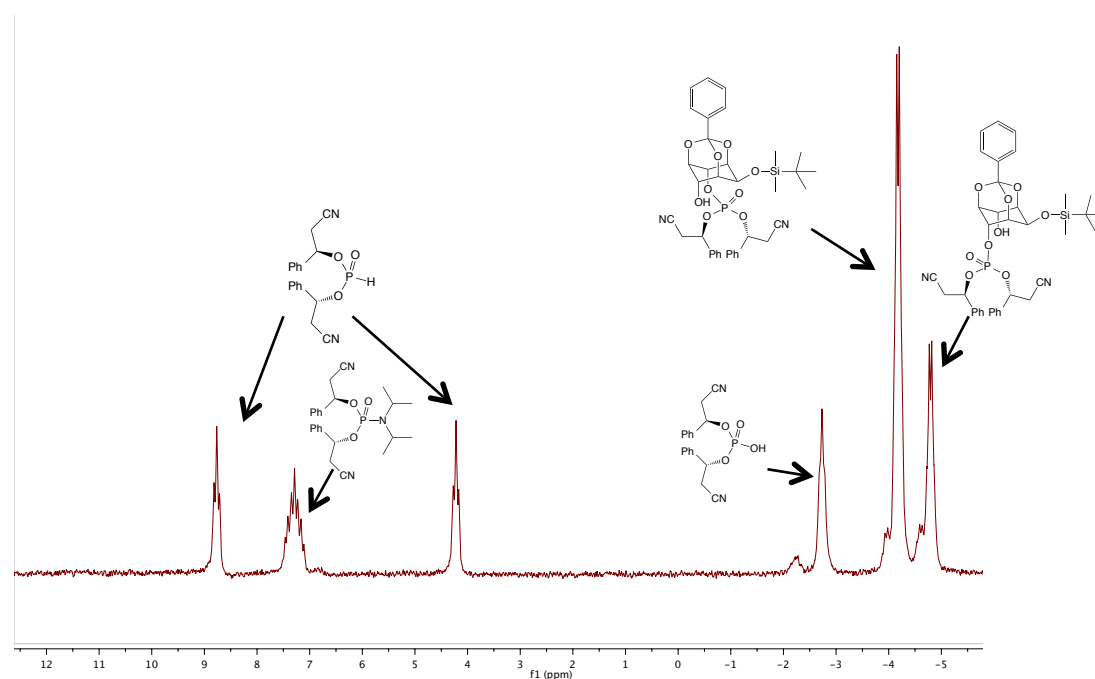
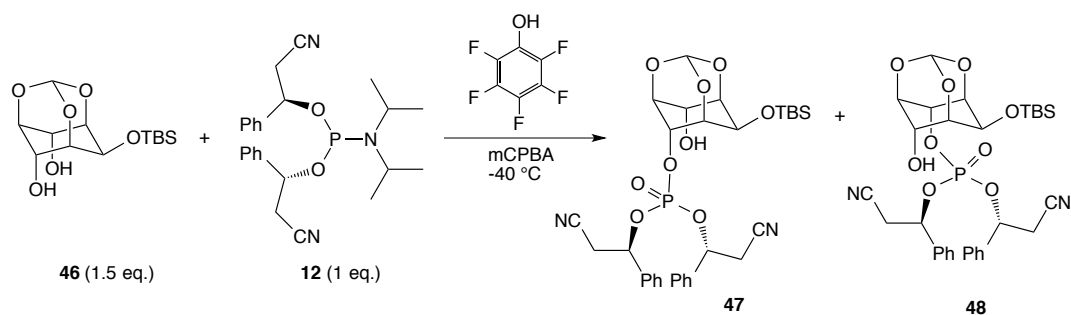


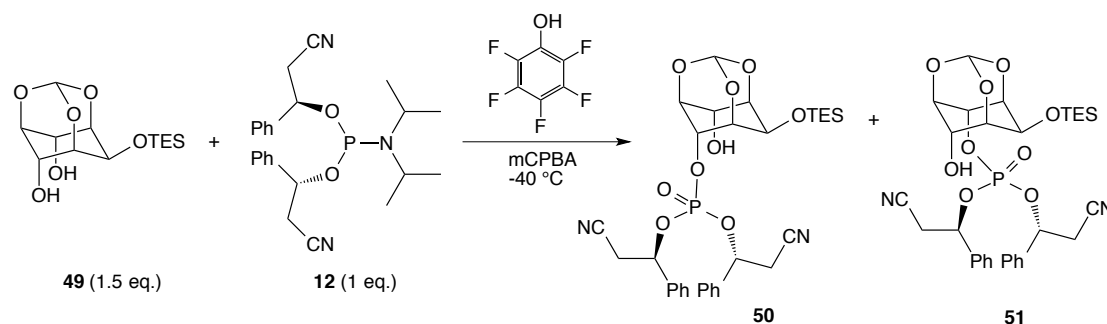
Figure 4.8. ^{31}P -NMR (coupled) of the mixture derived from desymmetrization of diol **43** with phosphoramidite **12**. The stereochemistry of diastereomers **44** and **45** was not assigned. However, in section 4.3.2 the crystal structure of a similar derivative is reported. This enables us to suggest tentatively that diastereomer **45** is formed preferentially after desymmetrization.

We assumed that a higher selectivity in the desymmetrization would be achievable by decreasing the rate of phosphorylation at low temperatures. The first step in the activation of phosphoramidites by acidic promoters is the protonation of the amino group. Subsequently, the promoter acts as a nucleophile displacing the protonated amino group (Figure 2.1, page 20). The phosphoramidite in this form is active and can phosphitylate hydroxyl groups. The reaction rate of phosphitylation depends on the ability of the hydroxyl group to displace the acidic promoter, in other words it depends on how good the promoter is as a leaving group. Phosphoramidite chemistry has been well developed in the field of oligonucleotide synthesis, where a fast phosphorylation is preferred. Therefore, all known activators are easily displaced by the hydroxyl group and theoretically are thus not ideal for a selective phosphitylation. Our goal was to find an acidic promoter that would activate quickly the C_2 -symmetric phosphoramidite, without being displaced easily by the OH group at the same time. A screening of possible activators led to the identification of pentafluorophenol as a good candidate for our aims.¹³⁴ The activation of C_2 -symmetric phosphoramidite with this phenol derivative at rt was fast (30 - 40 min) and led to the formation of a more stable phosphite triester that could be tracked by ^{31}P -NMR. This is usually not possible with conventional activators. As expected, a slower phosphitylation reaction resulted at low temperatures. Consequently, also a higher selectivity in the phosphitylation of derivative **46** with free hydroxyls at positions 4- and 6- was observed, leading to the formation of the two diastereomers in 1:2.7 ratio at $-40\text{ }^\circ\text{C}$ (Scheme 4.15).¹³⁴ However, at lower temperatures the reaction became very slow and was not synthetically useful anymore.¹³⁴



Scheme 4.15. Desymmetrization of TBS protected myo-inositol **46** with phosphoramidite **12** in the presence of pentafluorophenol.

A similar result was obtained when using pentafluorophenol as activator for the desymmetrization of TES derivative **49** with C_2 -symmetric phosphoramidite **12** (Scheme 4.16). According to ^{31}P -NMR diastereomers **50** and **51** were obtained in 2.7:1 ratio (Figure 4.9). Diastereomer **50** phosphorylated in position 6 was formed preferentially as confirmed by crystal structure reported in section 4.3.2.



Scheme 4.16. Desymmetrization of TES protected myo-inositol **49** with phosphoramidite **12** in the presence of pentafluorophenol. Diastereomers **50** and **51** were obtained in 2.7:1 ratio as confirmed by ^{31}P -NMR.

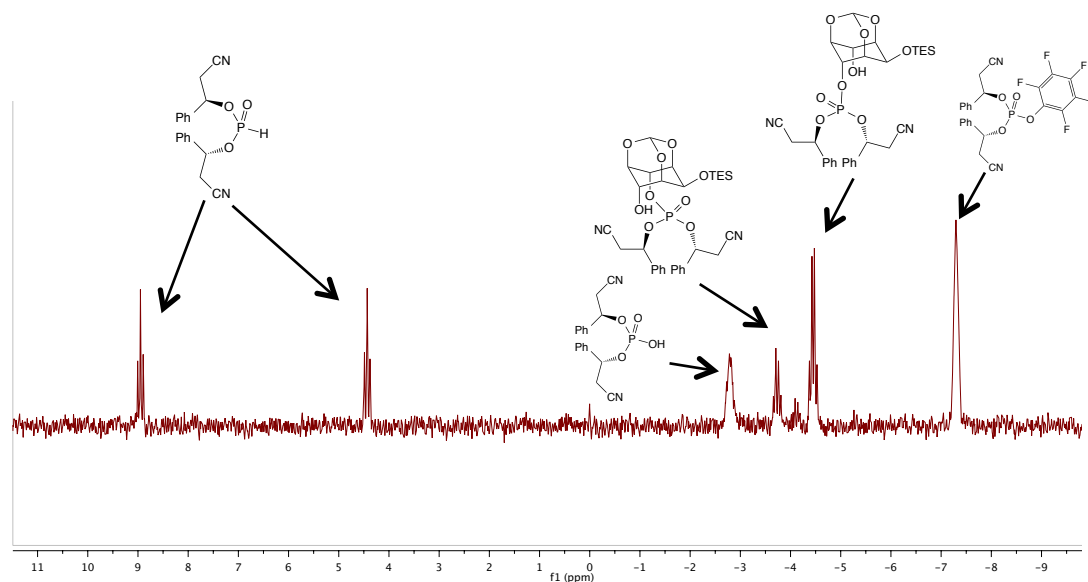
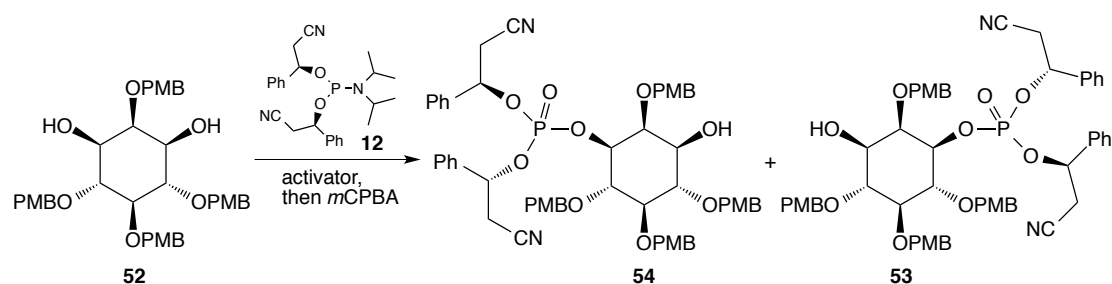


Figure 4.9. ^{31}P -NMR (coupled) of the mixture derived from reaction illustrated in Scheme 4.16. The diastereomer that is formed preferentially is phosphorylated in position 6 as confirmed by crystal structure reported in section 4.3.2.

Meso diol **52** with free hydroxyls at position 1- and 3- was also desymmetrized with C_2 -symmetric phosphoramidite **12** using different activators (Scheme 4.17). However, the degree of selectivity was much lower as compared to phosphitylation of 4,6-diols, presumably due to lower steric hindrance of the molecule. The desymmetrization was performed using 1*H*-tetrazole as activator in acetonitrile at room temperature. A ratio of 1.2:1 was observed in the formation of the two diastereomers **53** and **54** and it was important to use an excess of the *meso* substrate (3.5 eq.) to avoid the formation of the double phosphitylated side product. The absolute configuration was assigned by comparison of optical rotations after cleavage of all protecting groups (Chapter 4.3.1.1). When pentafluorophenol was used as activator at room temperature, the two diastereomers phosphitylated at positions 1- or 3- were obtained in 1:1.8 ratio and using only 2 eq. of the achiral substrate **52**.¹³⁴



Scheme 4.17. Desymmetrization of *meso* diol **52** with phosphoramidite **34**.

In summary, we developed a novel phosphoramidite that is easy to prepare, stable and additionally equipped with protecting groups that are easily cleaved under mild basic conditions. This property will be described in the next section, where the generation of a pyrophosphate moiety was possible exploiting this feature. This feature facilitated the application of the phosphoanhydride synthesis reported for symmetric 5-PP-InsP₅ (Chapter 4.1.1). Additionally, the C_2 -symmetry avoided chirality at phosphorus and offered a starting point for the investigation of a method to phosphorylate selectively any non-symmetric position of the *myo*-inositol ring.

4.3 SYNTHESIS OF UNSYMMETRIC X-PP-InsP₅ DERIVATIVES

The features of the novel phosphoramidite **12** were exploited for the installation of a pyrophosphate moiety in a specific position of *myo*-inositol, thus providing access to all four unsymmetric X-PP-InsP₅.

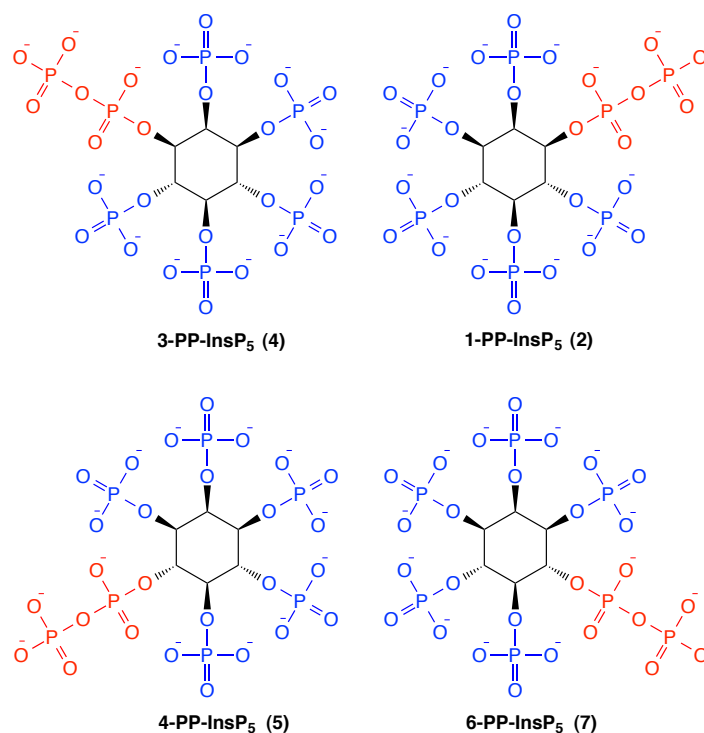
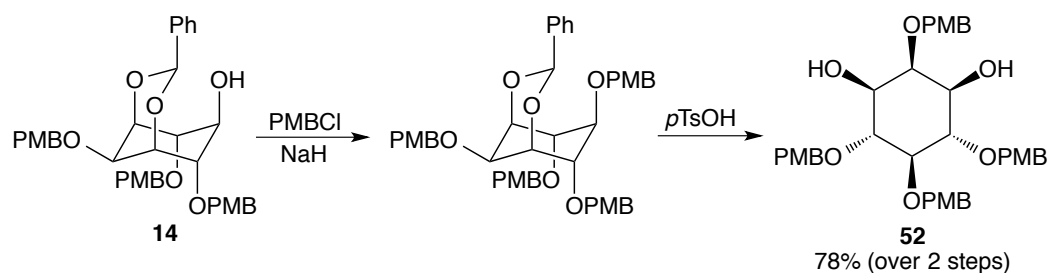


Figure 4.10. Structures of the four unsymmetric X-PP-InsP₅.

4.3.1 SYNTHESIS OF 1- AND 3-PP-InsP₅

The preparation of 1- and 3-PP-InsP₅ was achieved by modifying the procedure developed for the preparation of *meso* derivative 5-PP-InsP₅. A different pattern of protecting groups was required, as we now wanted to introduce selectively a pyrophosphate moiety in 1- or 3- position. Achiral 1,3-benzylidene acetal **14** obtained by selective DIBAL-H reduction was protected at position 5 with a PMB group. Selective acid-catalyzed cleavage of the acetal yielded PMB-protected diol **52** with positions 1- and 3- free for desymmetrization (Scheme 4.18).



Scheme 4.18. Preparation of meso derivative **52**.

Phosphitylated diastereomers **53** and **54** were obtained in 1.2:1 ratio as shown by ^{31}P -NMR analysis (Scheme 4.17 and Figure 4.11). 1*H*-tetrazole was used as an activator and the resulting P(III) intermediate was oxidized with *m*CPBA. Both of the diastereomers were required in successive steps of the synthesis and it was possible to separate them efficiently by flash chromatography or crystallization on gram scale. However, it was necessary to use an excess of the meso substrate **52** (3.5 eq.) to avoid the formation of a side product phosphorylated in both 1- and 3-position that was difficult to separate from the reaction mixture. After separation of the excess of starting material by flash column chromatography, diastereomer **54** was isolated by simple crystallization and obtained as a white solid in a diastereomeric ratio of >99:1. The other diastereomer **53** was purified by column chromatography and obtained as a colorless oil in a diastereomeric ratio of 98:2. The excess of starting material was then subjected to additional desymmetrizations using the same conditions.

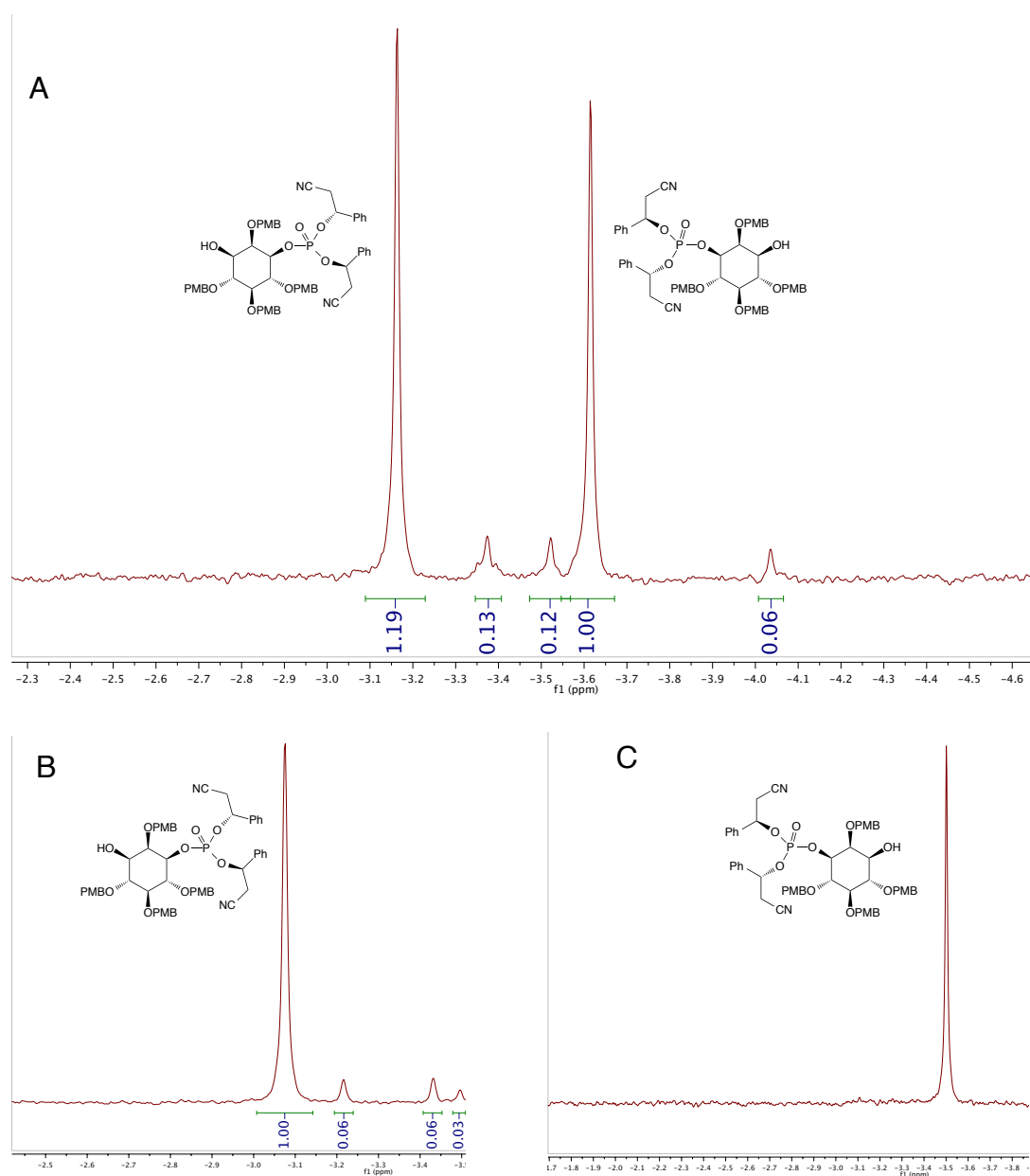
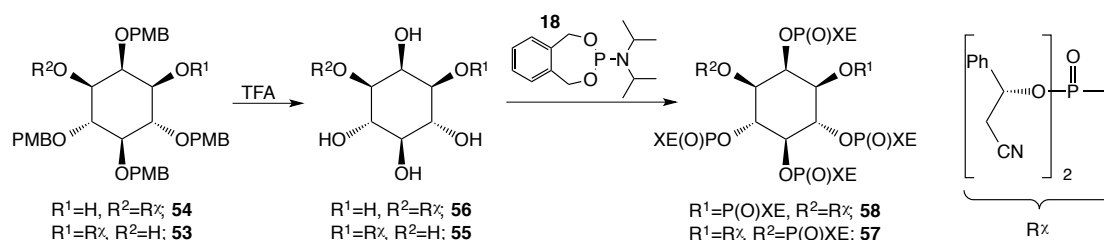


Figure 4.11. ^{31}P -NMR (decoupled) of reaction illustrated in Scheme 4.16. A) ^{31}P -NMR of diastereomeric mixture containing diastereomers **53** and **54** (ratio 1.2:1) and double substituted side product before separation; B) ^{31}P -NMR of diastereomer **53** after flash column chromatography; C) ^{31}P -NMR of diastereomer **54** after crystallization. The assignment of the absolute configuration of **53** and **54** will be explained in section 4.3.1.1.

After separation of diastereomers **53** and **54**, the same synthetic procedures were used for the preparation of natural compounds 1-PP-InsP₅ and 3-PP-InsP₅. PMB groups in **53** and **54** were removed by treatment with TFA to yield the pentaols **55** or **56** that

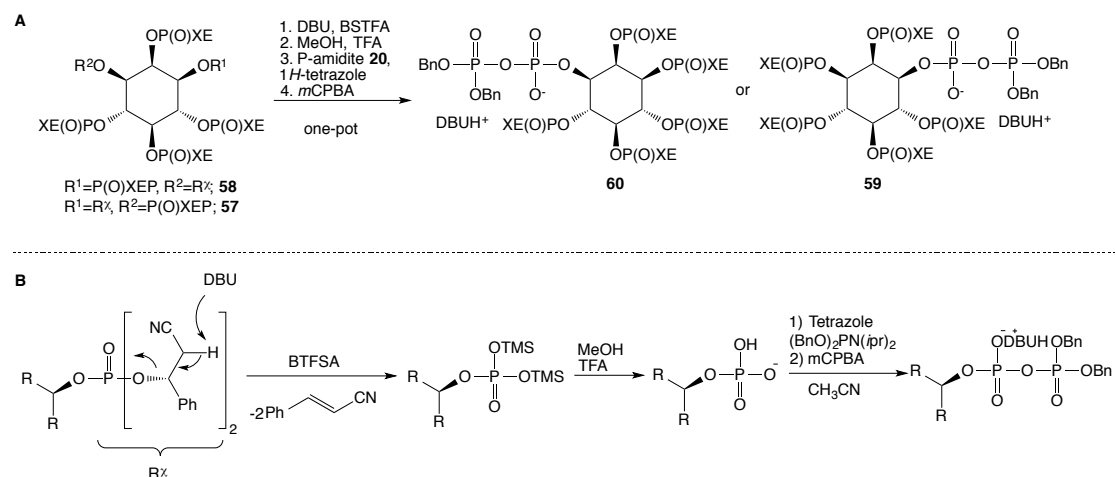
were purified by crystallization from diethyl ether. The compounds were obtained in good quality and no further purification was necessary. **55** and **56** were then phosphitylated with XEP-amidite **18** and oxidized in situ with *m*CPBA. The excess of non reacted XEP-amidite **18** was removed by crystallization and filtration over a plug of silica gel. This procedure yielded hexakisphosphates **57** or **58** in high purity. Purification of these compounds by longer flash column chromatography led to a significant loss of material and crystallization should thus be preferred (Scheme 4.19).



Scheme 4.19. Acidic removal of PMB protecting groups and phosphorylation to hexakisphosphates **57** and **58**.

With these protected derivatives in hand, the generation of the pyrophosphate moiety in position 1- or 3- was possible under the same one-pot reaction conditions described previously for the formation of 5-PP-InsP₅. Addition of DBU and BSTFA cleaved the two chiral auxiliaries on the phosphate eliminating cinnamionitrile. Therefore, the chiral auxiliary that we developed proved to be equivalent to the β-cyanoethyl protecting group when the method of cleavage is considered, but additionally enabled desymmetrization of a *myo*-inositol derivative. The bis-TMS protected phosphate was then subjected to methanolysis. TFA was added simultaneously with MeOH to reduce the risk of nucleophilic attack of the negatively charged phosphate to the neighboring XEP-protected phosphates. Coupling with dibenzyl-N,N-diisopropyl phosphoramidite in the presence of 1*H*-tetrazole, followed by oxidation and crystallization yielded protected pyrophosphates **59** and **60** in high yield. The purity was good enough to use the compounds in the next step without further purification, although better results are achieved also after purification by reversed column chromatography (Scheme 4.20 and Figure 4.12).

RESULTS AND DISCUSSION



Scheme 4.20. A) One-pot synthesis of diphosphates **59** and **60**; B) Mechanism: 1. DBU permits the cleavage of one of the chiral phenyl modified beta-cyanoethyl protecting groups; 2. BTfSA transfers a TMS group facilitating the cleavage of the second protecting group by DBU, followed by a second silylation; 3. MeOH removes the TMS groups and TFA protonates one of the two negatively charged oxygens; 4. Tetrazole promotes the phosphitylation, followed by oxidation with mCPBA.

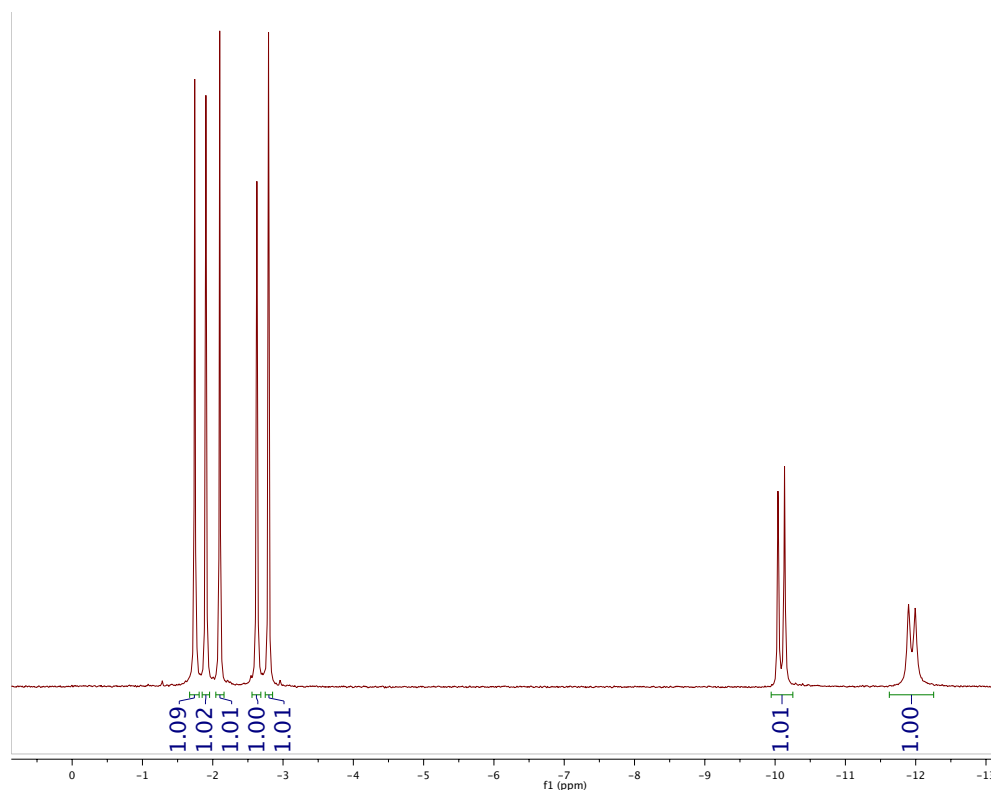
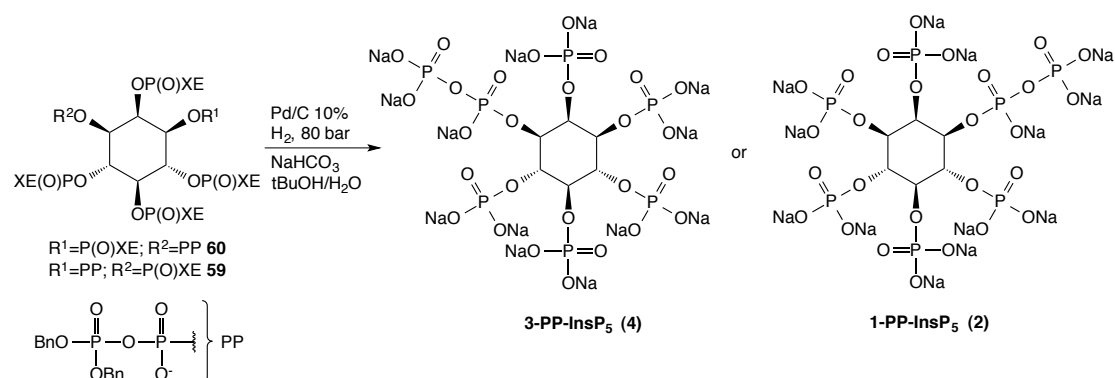


Figure 4.12. ³¹P-NMR (decoupled) of inositol diphosphate **59** after reversed phase column chromatography.

High pressure hydrogenation of pyrophosphates **59** and **60** led to global cleavage of all protecting groups giving natural products 1-PP-InsP₅ and 3-PP-InsP₅. The catalyst was removed by centrifugation and compounds were purified by simple crystallization from water/acetone and no further purification was needed. According to ³¹P-NMR and ¹H-NMR analysis, compounds were completely deprotected and obtained in high purity. These molecules tend to show broad signals in the recorded NMR spectra. However, the quality can often be improved with ion exchange resin (Dowex Na⁺) in order to obtain well-resolved peaks, thus identifying impurities that would go otherwise unnoticed (Scheme 4.21 and Figure 4.13).



Scheme 4.21. Hydrogenation of inositol pyrophosphates **59** and **60** and generation of 1-PP-InsP₅ (**2**) and 3-PP-InsP₅ (**4**).

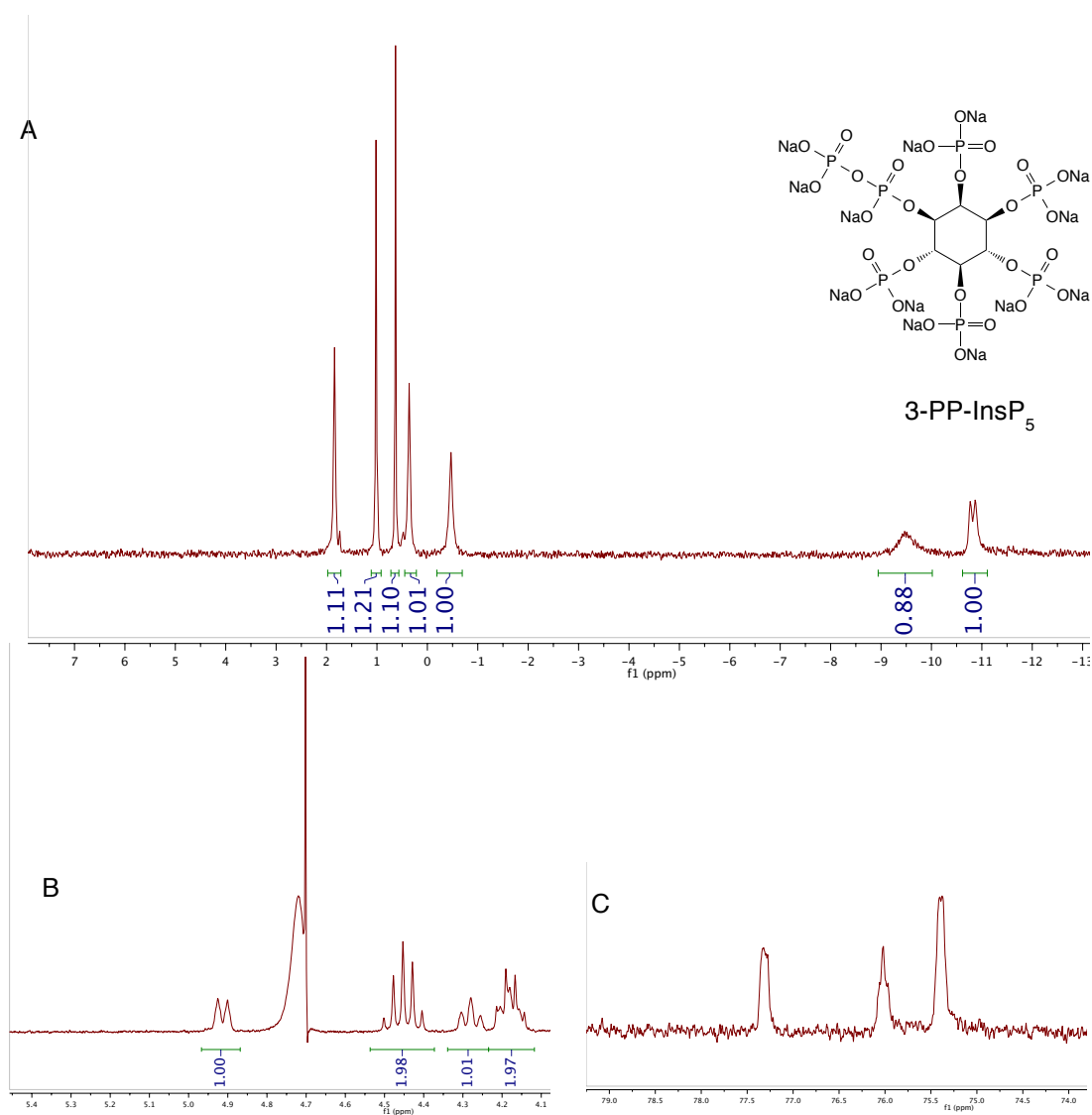


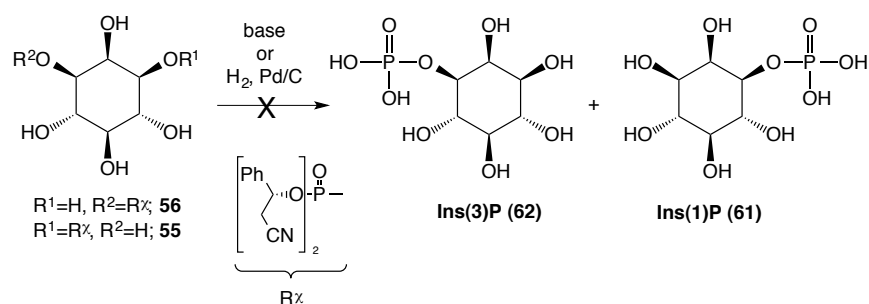
Figure 4.13. A) ^{31}P -NMR (decoupled), B) ^1H -NMR (water suppression) and C) ^{13}C -NMR in D_2O of **3-PP-InsP₅**.

4.3.1.1 ASSIGNMENT OF THE ABSOLUTE CONFIGURATION OF 1-PP-InsP₅ AND 3-PP-InsP₅

After synthesizing the two natural products 1-PP-InsP₅ and 3-PP-InsP₅, we needed to find a method to assign their absolute configuration since optical rotations are very low and have not been reported reliably. As they are enantiomers, ^{31}P -NMR and ^1H -NMR spectra showed the same pattern of signals. Therefore, NMR spectroscopy was not a suitable method to distinguish one isomer from the other. The best solution would have

been the examination of a crystal structure. However, it was not possible to obtain crystals of the two molecules, nor crystals of the intermediates produced in the different steps of the synthesis after several attempts.

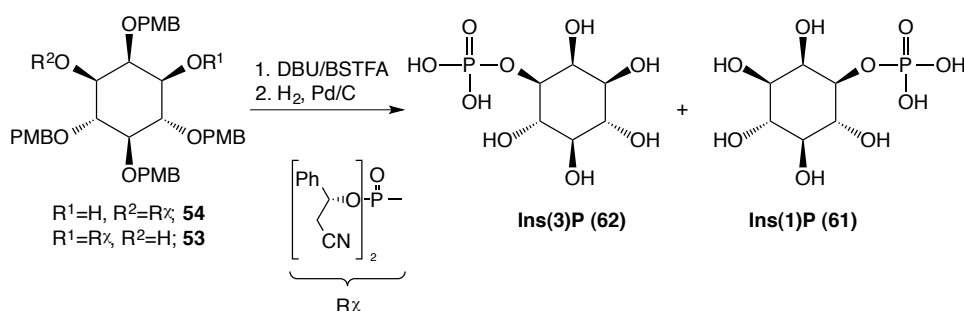
The synthesis of inositol-1-phosphate (Ins(1)P, **61**) and inositol-3-phosphate (Ins(3)P, **62**) has been reported and these compounds have been already fully characterized.¹³⁵ This paper also reported the $[\alpha]_D^{20}$ values in a pH dependent manner and was thus more reliable. As **61** and **62** are enantiomers, they are characterized by opposite optical rotation values and we exploited this property to assign the absolute configuration of 1-PP-InsP₅ and 3-PP-InsP₅. We envisaged that cleavage of all protecting groups of the precursors **55** and **56** would give us access to 1-InsP and 3-InsP. Therefore, we tried to cleave the chiral auxiliaries of pentaols **55** and **56** thinking that this would be the most straightforward way to obtain Ins(1)P and Ins(3)P (Scheme 4.22). However, treatment with bases or hydrogenation of **55** and **56** did not lead to the expected result. ³¹P-NMR analysis showed several signals, indicating that not only Ins(1)P or Ins(3)P was formed. We attributed those peaks to phosphorylated side products that were formed probably due to phosphate migration generating a mixture of polar compounds.



Scheme 4.22. Attempted preparation of Ins(1)P (**61**) and Ins(3)P (**62**).

The hydroxy groups of diastereomers **53** and **54** are protected with PMB groups and we envisaged that this protection could prevent phosphate migration. When the chiral auxiliaries of **53** and **54** were cleaved in the presence of DBU followed by hydrogenation of the PMB protecting groups Ins(1)P **61** and Ins(3)P **62** were obtained in good quality for analytical studies (Scheme 4.23). We measured the optical rotations of the two molecules in water at different pH values and observed the same $[\alpha]_D^{20}$ values

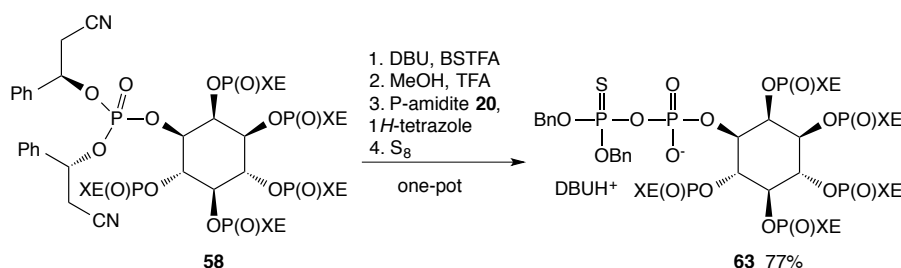
for the two enantiomers, except for opposite signs as expected. Finally, we compared the values that we obtained from these measurements with the data that are already reported in literature to assign the correct stereochemistry of compounds **61** and **62** and indeed also observed an inversion of $[\alpha]_D^{20}$ in a pH dependent manner (See Experimental Part, page 96 for data).¹³⁵



Scheme 4.23. Synthesis of *Ins(1)P* (**61**) and *Ins(3)P* (**62**).

4.3.1.2 SYNTHESIS OF A SULFURIZED ANALOG

The one-pot procedure that we developed allowed not only the efficient generation of a pyrophosphate moiety in the *myo*-inositol structure, but it also enabled us to introduce non-natural modifications on the β -phosphate of the phosphoanhydride. For example, with this strategy we were able to form a thiopyrophosphate in position 3 of *myo*-inositol (**63**) (Scheme 4.24). The synthesis of this moiety was possible following a modified version of the one-flask procedure described above. Briefly, the chiral auxiliaries were removed with DBU and BSTFA, followed by methanolysis in the presence of TFA. Coupling with dibenzyl-*N,N*-diisopropyl phosphoramidite **20** led to the formation of a P(V)-P(III) intermediate. Sulfurization of phosphorus (III) atom in position β was achieved by addition of elemental sulfur, instead of *m*CPBA.



Scheme 4.24. Synthesis of thiopyrophosphate **63**.

^{31}P -NMR analysis revealed a characteristic peak at 60 ppm typical of the thiophosphate moiety (Figure 4.14). This technique enabled us to introduce a different modification in the molecule and it is promising for the development of chemical probes to study inositol metabolism. It furthermore highlights the flexibility provided by P(III) chemistry as opposed to P(V) chemistry.

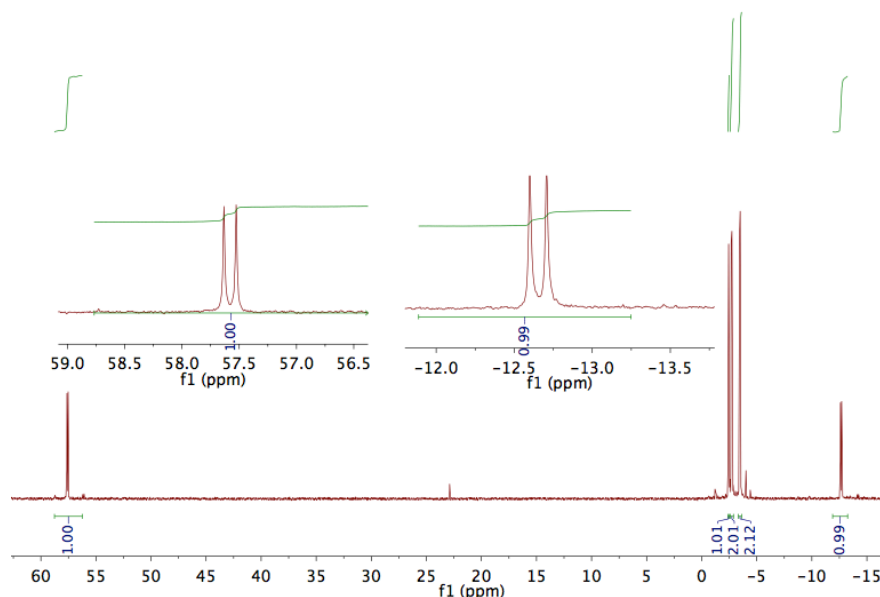
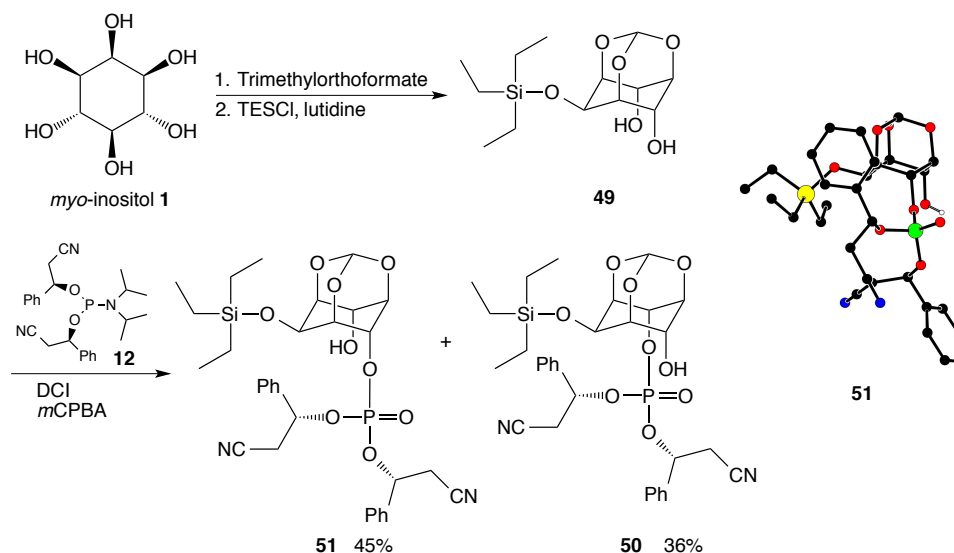


Figure 4.14. ^{31}P -NMR of thiopyrophosphate **63**.

4.3.2 SYNTHESIS OF 4- AND 6-PP-InsP₅

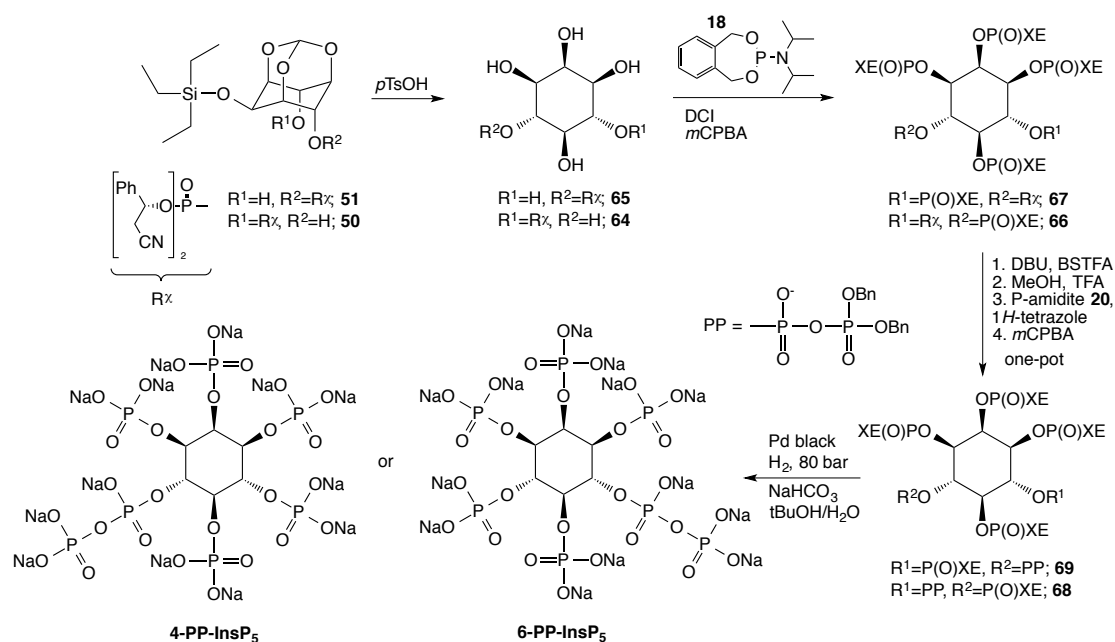
The synthesis of 4- and 6-PP-InsP₅ was achieved by applying the same chemistry developed for the synthesis of 1- and 3-PP-InsP₅. The main difference was the choice of protecting group strategy to have hydroxy groups in positions 4 and 6 available for desymmetrization. This would allow the generation of the pyrophosphate moiety in position 4 or 6 in the following steps. Protection of positions 1, 3 and 5 of *myo*-inositol with an *ortho*-formate protecting group and selective silylation of the equatorial position 2 enabled the generation of the desired substrate **49** (Scheme 4.25). Desymmetrization of compound **49** with C₂-symmetric phosphoramidite **12** yielded diastereomers **50** and **51** in a 0.8:1.0 ratio (Scheme 4.25). After separation by flash column chromatography, diastereomeric ratios of >99:1 were obtained for both the compounds on gram scale. The absolute configuration was determined by analysis of the crystal structure of compound

51 revealing its phosphorylation in position 4 (Scheme 4.25). With this result, the other diastereomer **50** was necessarily phosphorylated at position 6.



Scheme 4.25. Selective protection of *myo*-inositol, desymmetrization of meso compound **49** and crystal structure of **51**. Diastereomers **51** and **50** were obtained in a 1.0:0.8 ratio.

Treatment with catalytic amount of *p*TsOH cleaved first the TES group at position 2 and it is known that this hydroxyl group enables the acid-catalyzed cleavage of *ortho*-esters of *myo*-inositol.^{106,136,137} Consequently, after cleavage of the TES group, the *ortho*-ester was cleaved through a 2-formyl intermediate releasing pentaols **64** and **65** that were purified by crystallization. The same chemistry described above for the synthesis of 1-PP-InsP₅ and 3-PP-InsP₅ was applied in the following steps to yield 4-PP-InsP₅ and 6-PP-InsP₅. Briefly, phosphitylation of pentaols **64** and **65** with XEP-amidite **18** followed by oxidation with *m*CPBA produced hexakisphosphates **66** and **67** that were converted into derivatives **68** and **69** with a pyrophosphate moiety in 4 or 6 position using the one-flask procedure for phosphoanhydride formation described previously (Scheme 4.20, page 64). Global deprotection by high pressure hydrogenation finally yielded natural products 4-PP-InsP₅ and 6-PP-InsP₅ (Scheme 4.26).



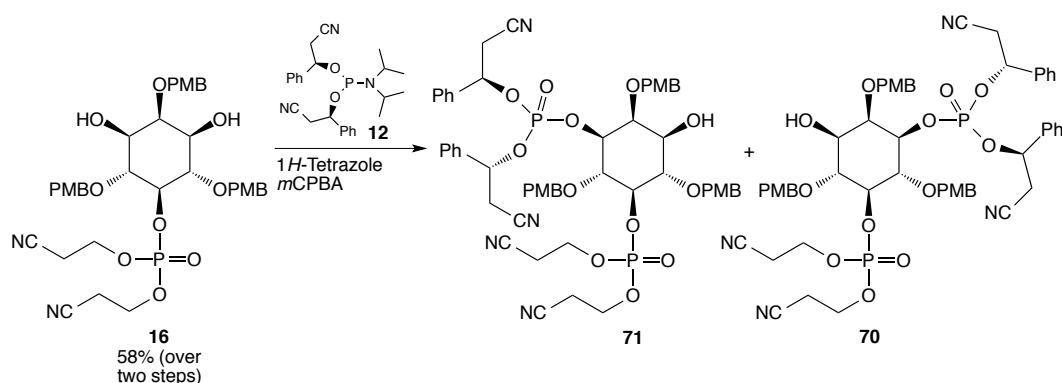
Scheme 4.26. Synthesis of 4-PP-InsP₅ and 6-PP-InsP₅.

4.4 SYNTHESIS OF UNSYMMETRIC X,Y-(PP)₂-InsP₄ DERIVATIVES

Unsymmetric X,Y-(PP)₂-IP₄ derivatives harbor eight phosphate groups and up to fourteen negative charges, thus representing the most densely phosphorylated natural products. The high polarity that characterizes these compounds makes their synthesis and purification difficult. Only symmetric 2,5-(PP)₂-InsP₄ has been prepared chemically.³⁸ However, analysis by HPLC showed that the compound was not pure (Figure 2.12, page 32). We were able to achieve the first preparation of both 1,5-(PP)₂-InsP₄ and 3,5-(PP)₂-InsP₄ in high quality by adapting the synthetic procedures developed for the synthesis of unsymmetric X-PP-InsP₅ further showcasing their broad applicability.¹³⁸ The two key steps that enabled us to synthesize these compounds are: 1) desymmetrization and phosphorylation of *myo*-inositol with C₂-symmetric phosphoramidite **12** and 2) simultaneous generation of two pyrophosphate moiety in a one-flask procedure where sixteen transformations were combined.

Our goal was the introduction of a pyrophosphate moiety in position 5 and another pyrophosphate moiety in position 1 or 3 of *myo*-inositol. We already demonstrated that it is possible to introduce such a group in all these positions, when they are protected with groups that can be cleaved under mild basic conditions. Therefore we selected a

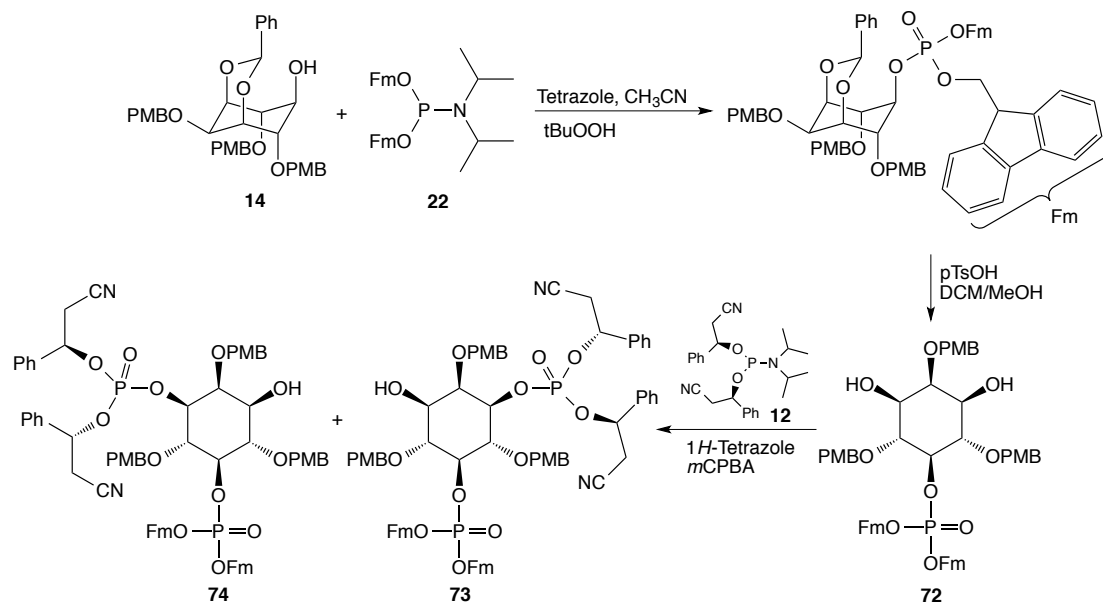
protecting group strategy that would potentially allow us to form two pyrophosphate moieties simultaneously using the one-pot procedure that we developed for the preparation of X-PP-InsP₅. We envisaged that *meso* PMB protected derivative **16** bearing β -cyanoethyl protecting groups on phosphate in position 5 could have been a good starting material for the preparation of 1,5-(PP)₂-InsP₄ and 3,5-(PP)₂-InsP₄. We envisaged that desymmetrization with *C*₂-symmetric phosphoramidite **12** would enable us to generate the substrates with the characteristics that we needed to form the two pyrophosphate moieties in later stages of the synthesis. However, desymmetrization of **16** with *C*₂-symmetric phosphoramidite **12** led to a mixture of diastereomers **70** and **71** that we could not separate by flash column chromatography or crystallization (Scheme 4.27).



Scheme 4.27. Desymmetrization of **16** with phosphoramidite **12** led to a diastereomeric mixture that we could not separate.

Therefore, we decided to introduce a different base-labile protecting group in position 5 that might facilitate separation of the diastereomers after desymmetrization. The fluorenyl protecting group seemed to be a good candidate as it can be cleaved under the same conditions as the β -cyanoethyl protecting group, thus representing another orthogonal group that could potentially allow the generation of the pyrophosphate moiety. Position 5 of 1,3-acetal **14** was phosphorylated with phosphoramidite **22** and acidic treatment led to diol **72** with positions 1 and 3 free for desymmetrization (Scheme 4.28). Phosphorylation of 1,3-diol **72** with *C*₂-symmetric phosphoramidite **12** produced a mixture of diastereomers in a 1.0:1.0 ratio (Figure 4.15). After separation of the excess starting material, repeated flash column chromatography enabled us to obtain diastereomers **73**

and **74** in 90% to 95% purity. More than 1 g of each diastereomer was obtained in this purity starting from 2.7 g of diastereomeric mixture (Scheme 4.28).



Scheme 4.28. Desymmetrization of meso diol **72** with phosphoramidite **12**. Diastereomers **73** and **74** were separated by column chromatography.

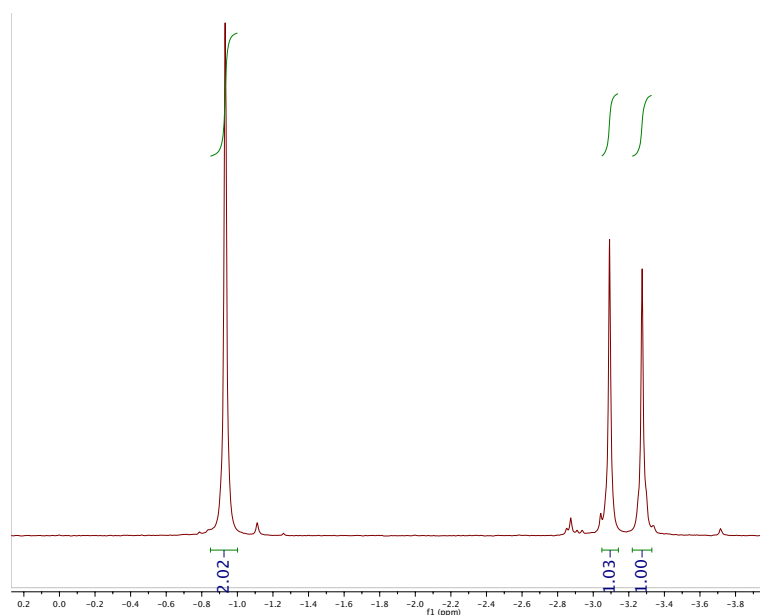
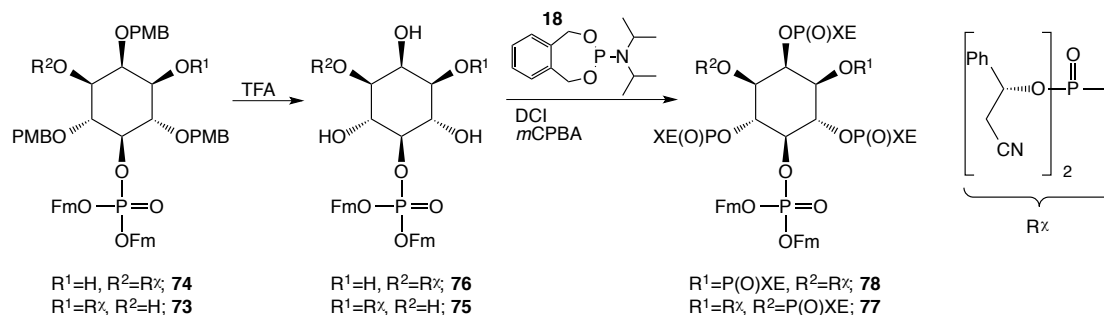


Figure 4.15. ³¹P-NMR of diastereomers **73** and **74** before separation.

Cleavage of the PMB protecting groups under acidic conditions and crystallization led to tetraols **75** and **76** (Scheme 4.29). In this step, essentially diastereopure material was obtained due to enrichment by crystallization. Mixing experiments monitored by ^{31}P -NMR analysis confirmed that the two molecules were obtained in diastereomerically pure form (d.r. >98:2) (Figure 4.16). Phosphitylation of tetraols **75** and **76** with XEP-amidite **18** followed by oxidation with *m*CPBA, generated hexakisphosphates **77** and **78** (Scheme 4.29). Crystallization and filtration over a short plug of silica were necessary for their purification. A >98:2 diastereomeric ratio was confirmed by mixing the two compounds and the diastereomeric purity was again analyzed by ^{31}P -NMR (Figure 4.17).



Scheme 4.29. Cleavage of PMB groups of diastereomers **73** and **74** and generation of hexakisphosphates **77** and **78**.

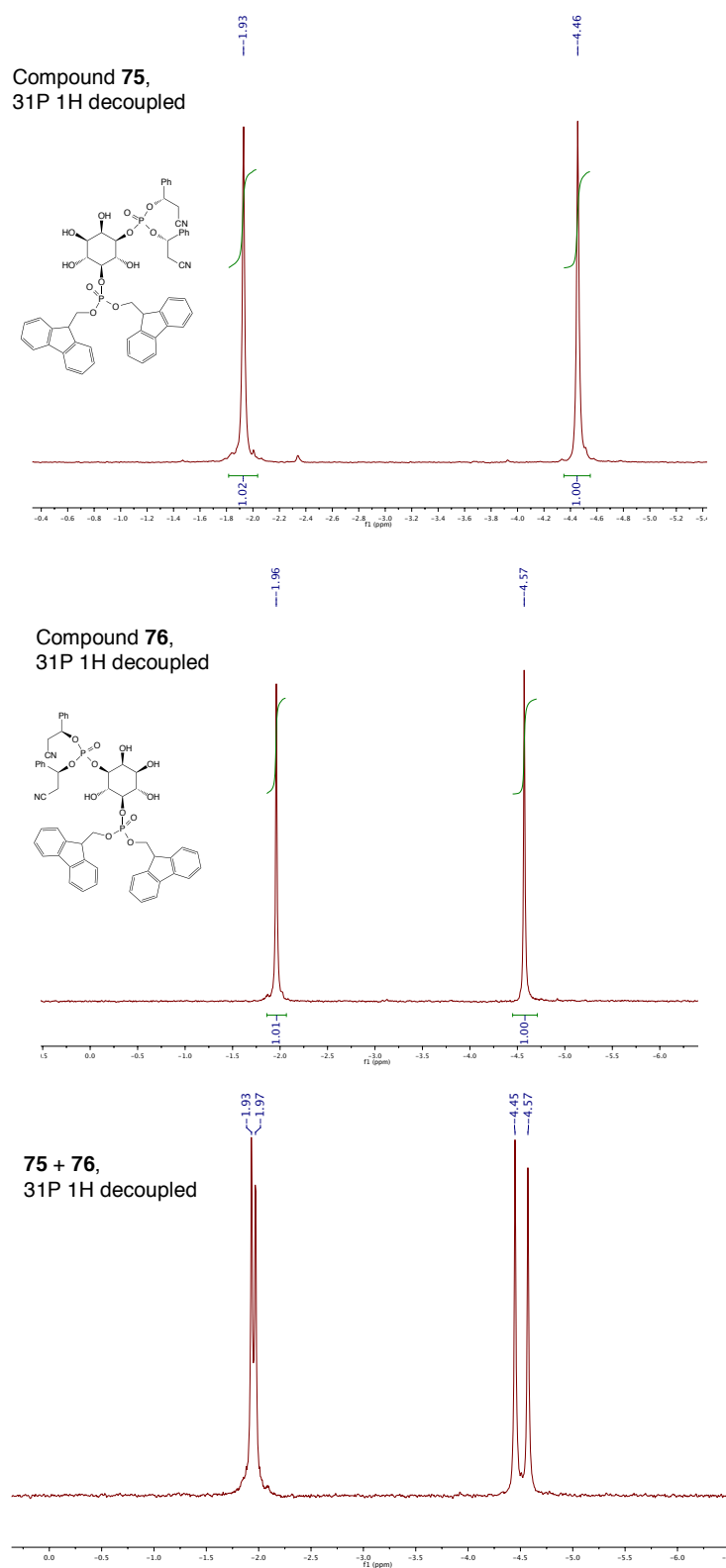


Figure 4.16. Mixing experiments to check the diastereopurity of tetraols **75** and **76**.

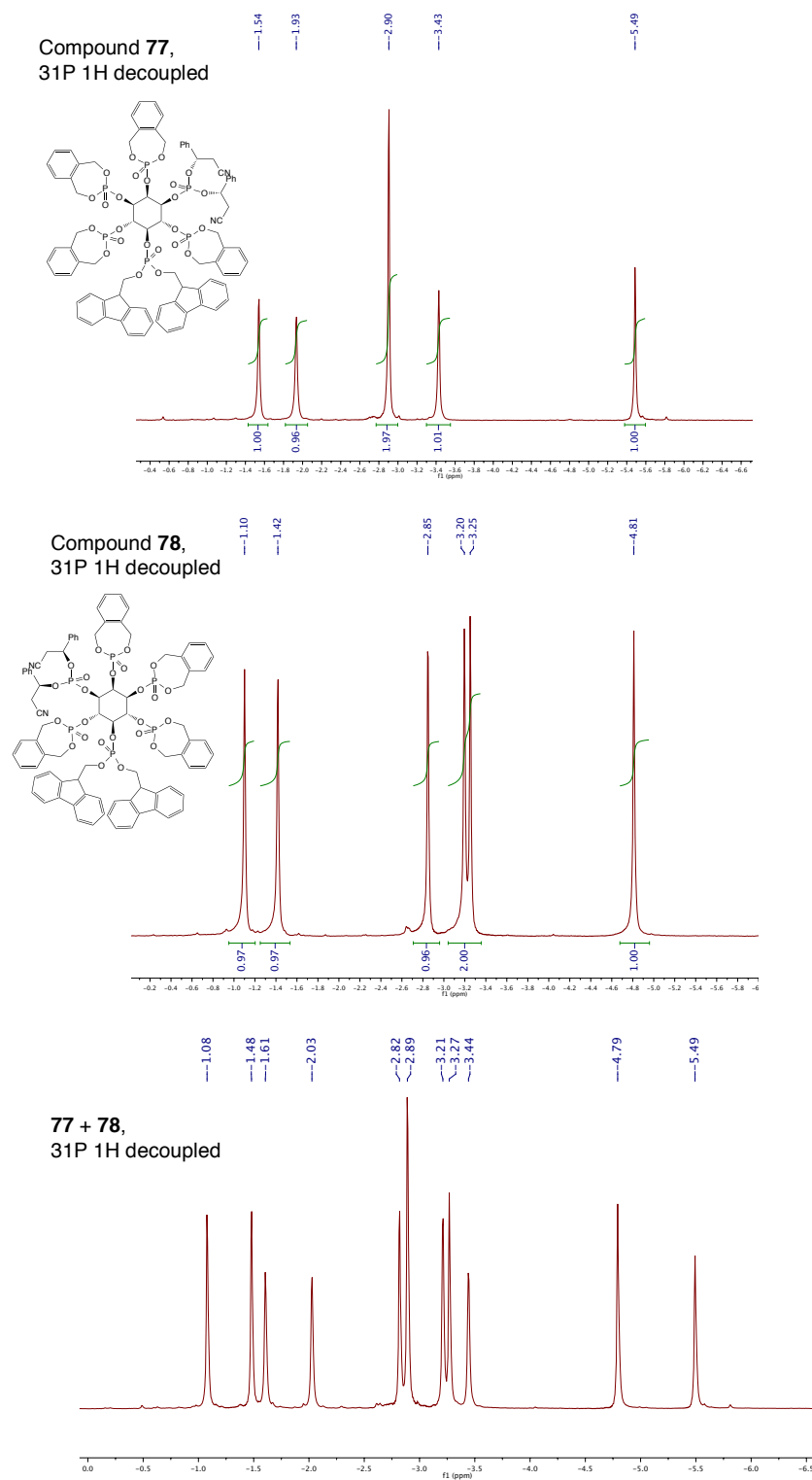
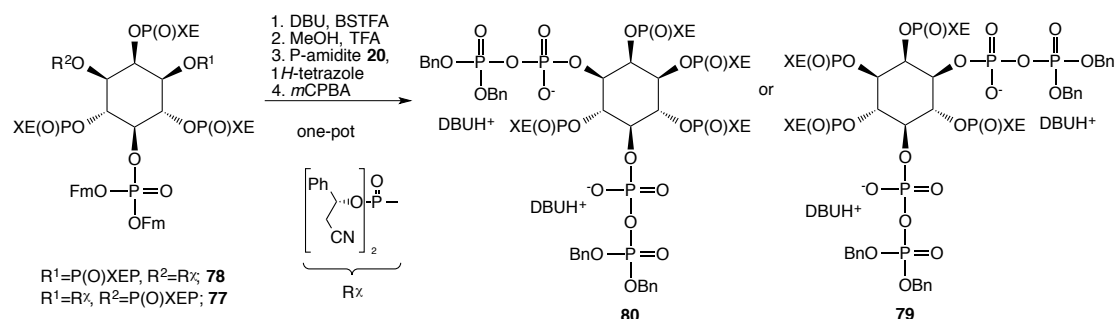


Figure 4.17. Mixing experiments to check the diastereopurity of hexakisphosphates **77** and **78**.

At this point, hexakisphosphates **77** and **78** were used as substrates for the generation of protected 1,5-(PP)₂-InsP₄ (**79**) or 3,5-(PP)₂-InsP₄ (**80**) (Scheme 4.30). The base labile protecting groups at 1 or 3 and 5 positions allowed the simultaneous formation of two pyrophosphate moieties in a one-flask procedure. The reaction conditions developed for the formation of a single phosphoanhydride as for 1/3-PP-InsP₅ (see Scheme 4.20, page 64) were adapted for this step, now combining sixteen transformations. Therefore, the number of equivalents of each reagent was doubled. Briefly, the Fm protecting groups in position 5 and the chiral auxiliaries in position 1 or 3 were cleaved with DBU and silylated with BSTFA. Methanolysis removed the four TMS groups and simultaneous addition of TFA stabilized the molecule by monoprotection of the two phosphates. Twofold phosphitylation with bis-benzyl P-amidite **20** followed by oxidation with *m*CPBA generated finally two pyrophosphate moieties in the 1 or 3 and 5 position (Scheme 4.30). The protected (PP)₂-InsP₄ derivatives were purified by crystallization and obtained in good quality. Additional purifications by column chromatography led to decomposition of the material. The compounds were not stable enough to be stored for a longer period, therefore it was necessary to use them in the next step as soon as they were available.



Scheme 4.30. One-flask synthesis of two diphosphate moieties simultaneously to form **79** and **80**.

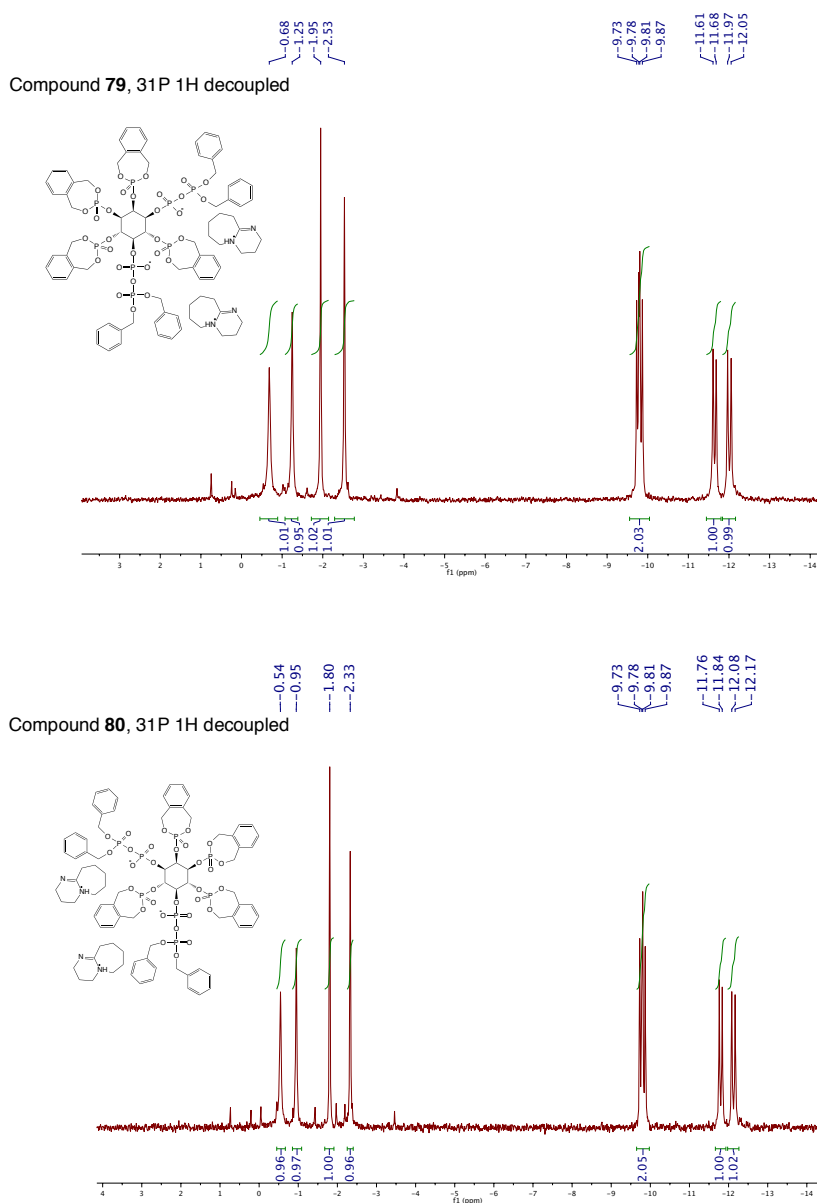
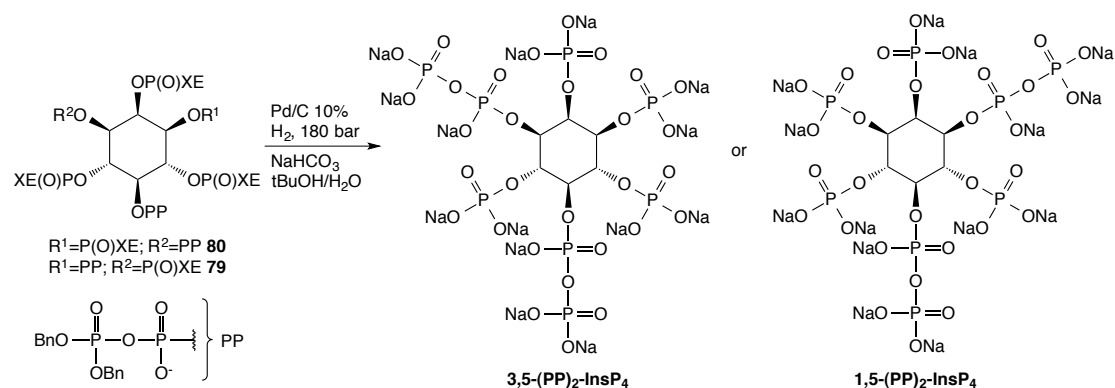


Figure 4.18. ^{31}P -NMR (proton decoupled) of compounds **79** and **80**. This is the result of 16 steps in one-flask after crystallization without additional purification.

Global deprotection was achieved by high pressure hydrogenation (150-180 bar) to obtain 1,5-(PP) $_2$ -InsP $_4$ and 3,5-(PP) $_2$ -InsP $_4$ in high quality after crystallization from water/acetone (Scheme 4.31). The quality of the ^{31}P -NMR spectra was highly dependent on the pH value of the D $_2$ O solution in which the spectra were recorded. Acidic pH led to very broad ^{31}P -NMR signals. However, a strong improvement was observed after

addition of NH_4OH to the same NMR tube until pH values of 9 or 10 were obtained (Figure 4.19). The deprotected compounds were much more stable as compared to their protected precursors **79** and **80**. The resulting quality of the material is suitable for biological assays as shown in Chapter 4.5.



Scheme 4.31. High pressure hydrogenation of **79** and **80** to form **1,5-(PP)₂-InsP₄** and **3,5-(PP)₂-InsP₄**.

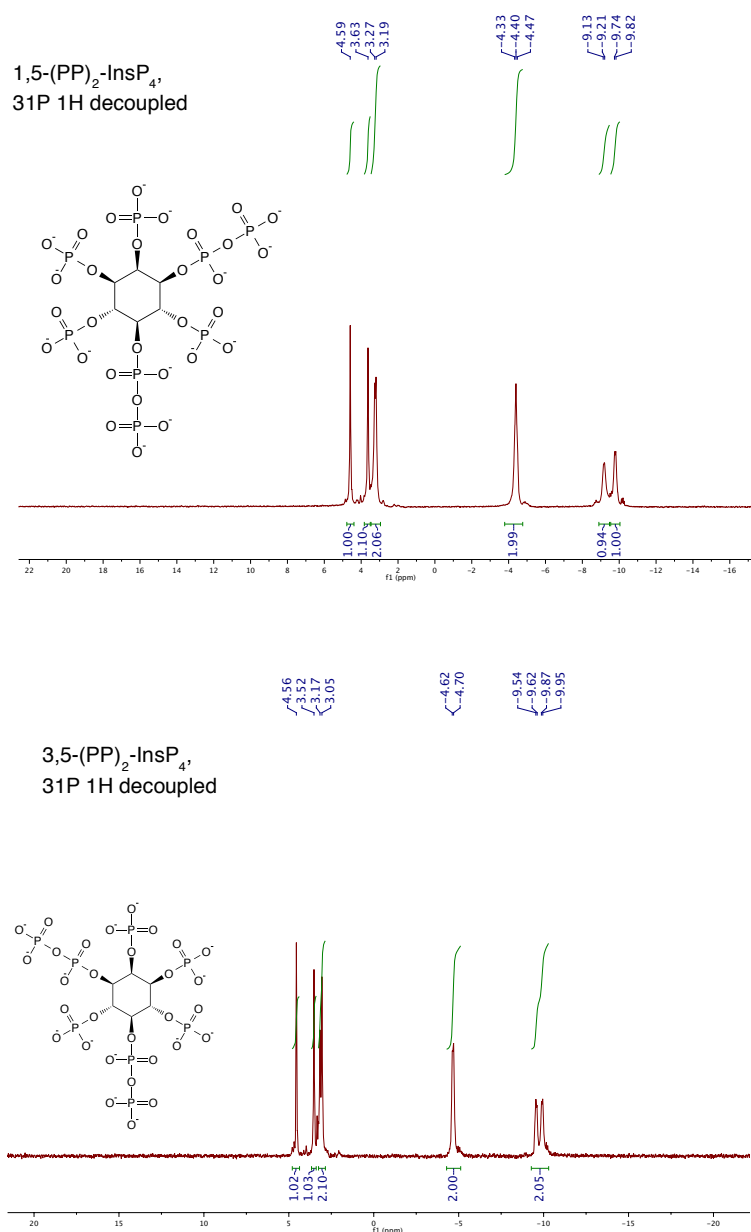


Figure 4.19. ³¹P-NMR (decoupled) of 1,5-(PP)₂-InsP₄ and 3,5-(PP)₂-InsP₄ in D₂O at pH 9 after addition of NH₄OH. The compounds were obtained after crystallization from water-acetone without additional purification.

4.4.1 ASSIGNMENT OF THE ABSOLUTE CONFIGURATION OF 1,5-(PP)₂-InsP₄ AND 3,5-(PP)₂-InsP₄

The determination of the absolute configuration was a challenge since we could not obtain crystals of the final compounds or their precursors after several attempts. We excluded to possibility to assign the absolute configuration of the synthesized compounds

based exclusively on the evaluation of optical rotations, as they tend to be small and change considerably depending on pH values at which the measurement is done.¹¹⁶ In this case, no reliable data were available that facilitated the analysis of the synthesis of 1/3,5-(PP)₂-InsP₄. In collaboration with the group of Steven Shears (National Institutes of Health, NIH, USA) we found a solution to this problem. Both synthetic enantiomers 1,5-(PP)₂-IP₄ and 3,5-(PP)₂-IP₄ were soaked separately into crystals of the kinase domain of human PPIP5K2, the enzyme responsible for the biosynthesis of inositol pyrophosphates in mammalian cells.^{47,48} As the naturally occurring isomer has been recently identified in such complex (PPIP5K2^{KD}),³⁴ the obtained electron-density maps allowed the assignment of the absolute configuration of each isomer. The naturally occurring 1,5-(PP)₂-InsP₄ was accommodated in the catalytic site of the enzyme as expected but surprisingly also the unnatural isomer 3,5-(PP)₂-InsP₄ was found in separate crystals, although in a different orientation.

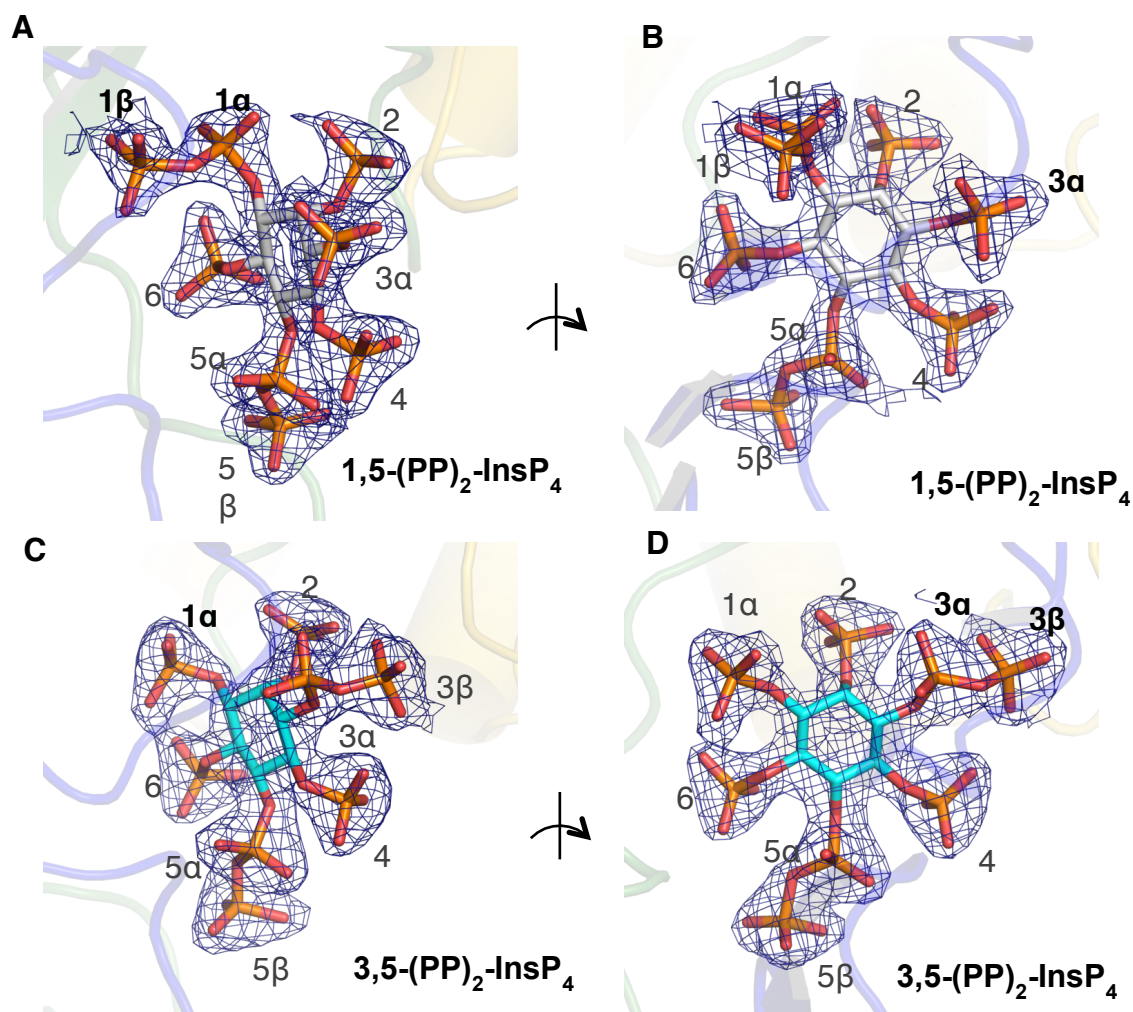


Figure 4.20. Assignment of the absolute configuration of 1,5-(PP)₂-InsP₄ and 3,5-(PP)₂-InsP₄. Refined 2F_o-F_c maps contoured at 2.0 or 1.0 σ are shown in blue mesh. InsP₈ molecules are shown in a stick model. The catalytic domain of PPIP5K2 is shown in a transparent cartoon. The phosphate groups around the inositol ring are numbered. Panels **A** and **B** are PPIP5K2^{KD}/ADP in complex with 1,5-(PP)₂-InsP₄, showing two orientations. Panels **C** and **D** are PPIP5K2^{KD}/AMP-PNP in complex with 3,5-(PP)₂-InsP₄.¹³⁸ (Capolicchio, S.; Wang, H.; Thakor, D. T.; Shears, S. B.; Jessen, H. J. Synthesis of densely phosphorylated bis-1,5-diphospho-myo-inositol tetrakisphosphate and its enantiomer by bidirectional P-anhydride formation. *Angew. Chem. Int. Ed. Engl.* 2014, 53, 9508–9511. Copyright © 2014 Wiley-VCH Verlag GmbH & Co. KGaA, Weinheim)

4.5 BIOLOGICAL APPLICATIONS OF DIPHOSPHOINOSITOL POLYPHOSPHATES

We were able to synthesize several diphosphoinositol polyphosphate derivatives in high purity suitable for biological studies. With all natural and unnatural isomers in

hand, we started to perform evaluations of their biological properties. Moreover, we started to support groups worldwide that are studying the metabolism of diphosphoinositol polyphosphates in biological systems.

The first biological application of our synthetic X-PP-IP₅ derivatives involved the assignment of the regioisomeric preference of diphosphoinositol polyphosphates phosphatase 1 (Ddp1) from yeast. Ddp1 is an enzyme that belongs to a particular class of phosphatases able to cleave the β -phosphate of the pyrophosphate moiety of X-PP-IP₅. 1-PP-InsP₅, 2-PP-InsP₅, 3-PP-InsP₅, 4-PP-InsP₅, 5-PP-InsP₅ and 6-PP-IP₅ were incubated with Ddp1 and the ability of the enzyme to cleave the pyrophosphate of one specific isomer was tested employing a malachite green assay (Figure 4.21).¹³⁹ Analysis of the obtained data showed that Ddp1 dephosphorylates specifically 1-PP-InsP₅ and this outcome is in accordance with documented results.⁵¹ Additionally, this is a further proof of the absolute configuration of synthetic 1-PP-InsP₅. (For more information about enzymes involved in diphosphoinositol polyphosphate metabolism see Chapter 1.3.3).

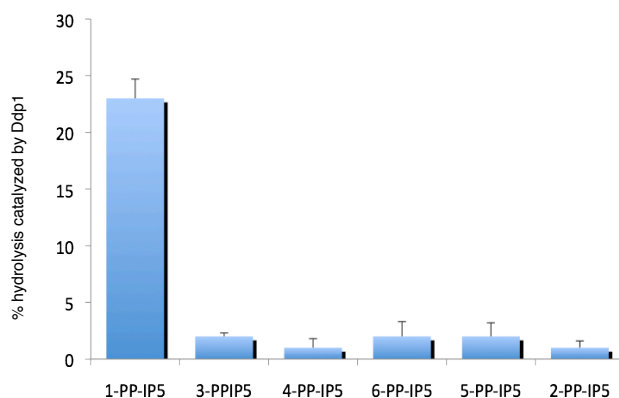


Figure 4.21. Phosphate release from X-PP-InsP₅ upon phosphatase treatment was quantified with a modified malachite green assay. The values on the left of the graph represent the percentage of hydrolysis catalyzed by Ddp1. The obtained data shows that Ddp1 is a selective 1-PP-InsP₅ phosphatase.

In the group of Steven Shears, the activity of the phosphatase DIPPI against the natural 1,5-(PP)₂-IP₄ and unnatural 3,5-(PP)₂-IP₄ enantiomers was tested. The release of the inorganic phosphate was measured using a malachite green assay as previously described by the group,¹⁴⁰ and the obtained data showed that both isomers are substrates for the enzyme.¹³⁸

In the Fiedler group (Princeton University) our synthetic 1-PP-InsP₅ was used as a control in the evaluation of PP-InsP_y ability to inhibit protein kinase Akt.¹⁴¹ It has been shown that binding of X-PP-InsP₅ to the PH domain of Akt inhibits its phosphorylation by 3-phosphoinositide-dependent protein kinase (PDK1), thus preventing the activation of Akt.^{74,141} The group developed a non-hydrolyzable analog of 1-PP-InsP₅ (1-PCP-InsP₅) and its ability to inhibit Akt was evaluated. Our synthetic 1-PP-InsP₅ was used in this study as a reference to compare the activity of the non-hydrolyzable analog toward Akt. Both compounds resulted to be good inhibitors of protein Akt and the activities were comparable (Figure 4.22).

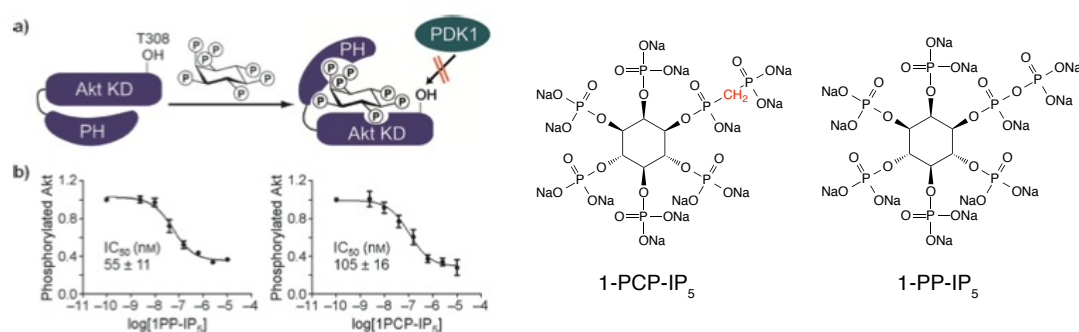


Figure 4.22. A) Binding of X-PP-InsP₅ inhibits Akt phosphorylation by PDK1 (PH = pleckstrin homology domain; KD = kinase domain; T308 = threonine 308; PDK1 = 3-phosphoinositide-dependent protein kinase; B) Inhibition of Akt phosphorylation by 1-PP-InsP₅ and 1-PCP-IP₅ in vitro.¹⁴¹ (Wu, M.; Chong, L. S.; Capolicchio, S.; Jessen, H. J.; Resnick, A. C.; Fiedler, D. Elucidating diphosphoinositol polyphosphate function with nonhydrolyzable analogues. *Angew. Chem. Int. Ed. Engl.* 2014, 53, 7192–7197. Copyright © 2014 Wiley-VCH Verlag GmbH & Co. KGaA, Weinheim)

CHAPTER 5

CONCLUSION AND OUTLOOK

In summary, we developed a novel synthetic strategy for the synthesis of several natural and unnatural diphosphoinositol polyphosphates. The key step in the preparations of both symmetric and unsymmetric isomers was a one-flask generation of the diphosphate moiety characteristic of these natural products. This transformation was possible due to the use of orthogonal phosphate protecting groups that were cleaved under mild basic conditions enabling the introduction of an additional phosphate. This feature facilitated the installation of a diphosphate group in specific positions of the *myo*-inositol ring.

The synthesis of *meso* 5-PP-InsP₅ has been reported previously by other groups. However, multiple protecting group manipulations were required in all the preparations and the final compound was never obtained in good quality. With our approach, we could reduce the number of steps required for its synthesis and the material was pure enough for biological assays. The one-flask procedure has been subsequently adapted for the generation of a triphosphate moiety in position 5 of *myo*-inositol, completing the first total synthesis of 5-PPP-InsP₅. We could therefore gain access to the first chemical tool that can help the elucidation of the biological function of 5-PPP-InsP₅.

We developed a novel *C*₂-symmetric phosphoramidite that was stable, easy to prepare, and the chiral auxiliary served also as an orthogonal protecting group. The double function of the new reagent enabled us to desymmetrize *myo*-inositol and to generate a diphosphate moiety in a one-flask procedure, as the chiral auxiliary could be cleaved under mild basic conditions. These features enabled us to prepare all four possible unsymmetric X-PP-InsP₅ in unprecedented purity and high enantiomeric excess. Moreover, we were able to introduce chemical modifications generating thiopyrophosphates. The desymmetrization of *myo*-inositol by phosphorylation allowed us to introduce directly a phosphate group in a specific position of the molecule, thus reducing the number of steps necessary for the syntheses of unsymmetric X-PP-InsP₅. As all the isomers were required, no high regioselectivity was required in the desymmetrization step. However, we observed the preferential formation of a specific isomer when using different reaction conditions. This finding set the basis for the further development of a methodology based on phosphoramidite chemistry that allows the selective phosphorylation of a specific position in the *myo*-inositol ring.

The same chemistry was then adapted to achieve the first total synthesis of the natural 1,5-(PP)₂-InsP₄ and the unnatural 3,5-(PP)₂-InsP₄. In the key step of their

preparation, sixteen transformations occurred in a one-flask procedure to generate two phosphoanhydride bonds simultaneously.

With all these isomers in hand, we gained access to a set of natural and unnatural chemical tools that will help to elucidate the structure and functions of diphosphoinositol polyphosphates in nature. Moreover, the synthesis can be adapted for the generation of functionalized chemical probes to study the inositol related cellular signalling pathways.

CHAPTER 6

EXPERIMENTAL PART

6.1 EXPERIMENTAL PROCEDURES

Reactions were carried out using oven-dried glassware under an atmosphere of dry Ar or N₂ and magnetically stirred, unless noted otherwise. Air- and moisture-sensitive liquids and solutions were transferred via syringe or stainless steel canula.

Reagents were purchased from commercial suppliers (Acros, Aldrich, Fluka, Lancaster) and used without further purification, unless noted otherwise.

Solvents (methylene chloride, diethyl ether, tetrahydrofuran, acetonitrile, toluene) for reactions were purified by filtration and dried by passage over activated anhydrous neutral A-2 alumina (MBraun solvent purification system) under an atmosphere of dry nitrogen. Chloroform (analytical grade) was filtered over Alox-N. Methanol (analytical grade) was used as received. Ethyl acetate (Fluka, 99.5%), n-hexane (Fluka, 99.5%), *N,N*-dimethylformamide (Fluka, 99.5%) and 1,4-dioxane (Acros, 99.5%) were stored over molecular sieves. Analytical grade solvents were used as received for extractions and chromatographic purifications. Deuterated solvents were obtained from Armar Chemicals, Switzerland, in the indicated purity grade.

Methods. Triethylamine, *N,N*-diisopropylamine and pyridine were distilled from calcium hydride under an atmosphere of dry nitrogen.

Thin Layer Chromatography were used for monitoring reactions and carried out using Merck silica gel 60 F254 plates, visualized with UV light or developed either with aqueous cerium ammonium molybdate (CAM) stain followed by heating or with potassium permanganate solution.

Flash Chromatography was performed using Fluka silica gel 60 (230-400 Mesh) at a pressure of ca. 0.3 bar. Eluents and R_f are indicated.

Lyophilizations were performed on a Christ Freeze Dryer Alpha 1-2 LD+.

Optical rotations were measured at 589 nm (Na-D line) on a Jasco P-2000 polarimeter (1 dm cylindrical cell).

¹H-NMR spectra were recorded on Bruker 400 MHz spectrometers or Bruker 500 MHz spectrometers (equipped with a cryo platform) at 298K in the indicated deuterated solvent. Data are reported as follow: chemical shift (δ , ppm), multiplicity (s, singlet; d, doublet; t, triplet; q, quartet; m, multiplet or not resolved signal; br, broad signal), coupling constant(s) (*J*, Hz), integration. All signals were referenced to the internal solvent signal as standard (CDCl₃, δ 7.26; D₂O, δ 4.79; CD₃OD, δ 3.31; DMSO-*d*₆, δ 2.50).

¹³C-NMR spectra were recorded with ¹H-decoupling on Bruker 101 MHz or Bruker 125 MHz spectrometers (equipped with a cryo platform) at 298K in the indicated deuterated

solvent. All signals were referenced to the internal solvent signal as standard (CDCl_3 , δ 77.0; CD_3OD , δ 49.0; DMSO-d_6 , δ 39.5).

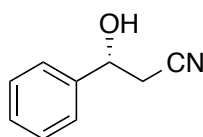
^{31}P -NMR spectra were recorded with proton coupling and ^1H -decoupling on Bruker 162 MHz or Bruker 202 MHz spectrometers (equipped with a cryo platform) at 298K in the indicated deuterated solvent. All signals were referenced to an internal standard (PPP)

IR spectra were recorded on a JASCO FT-IR-4100 spectrometer and data are reported in terms of frequency of absorption (cm^{-1}).

Mass spectra were recorded by the Mass spectroscopy Service of UZH on Finnigan MAT95 MS, Bruker EsquireLC MS, Bruker maXis QToF HR MS and Finnigan TSQ700 MS machines.

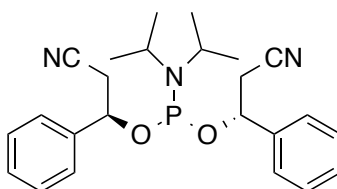
6.2 SYNTHESIS OF 1-PP-InsP₅ AND 3-PP-InsP₅

Synthesis of (*R*)-3-Hydroxy-3-phenylpropanenitrile **42**



Nitrile **42** was synthesized as described before on a 10 g scale starting from (*S*)-(+)-mandelic acid. Analytical data were identical with the values reported in the literature.¹⁴²

Synthesis of bis((*R*)-2-cyano-1-phenylethyl) diisopropylphosphoramidite **12**

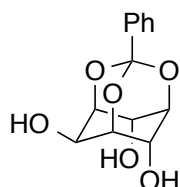


6.25 g (42.5 mmol, 2.0 eq.) nitrile **42**, 4.30 g (21.3 mmol, 1.0 eq.) (dichlorophosphanyl)bis(propan-2-yl)amine and 4.96 g (49.0 mmol, 2.3 eq.) triethylamine were stirred for 3 days at room temperature under an inert atmosphere in dry THF (50

mL). The precipitate was filtered off, rinsed with Et₂O and the solution concentrated *in vacuo*. The product was purified by gradient chromatography (hexane/EtOAc 9:1-1:1). Yield: 7.01 g **11** as colorless crystals (16.6 mmol, 78%)

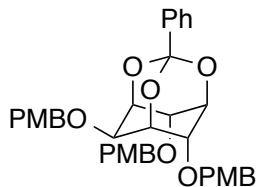
¹H-NMR (500 MHz, 298 K, CDCl₃, δ/ppm): = 7.47 - 7.35 (m, 5H), 7.31 - 7.24 (m, 3H), 7.19 - 7.13 (m, 2H), 5.13 (dt, *J*=9.0, 5.9, 1H), 4.78 (dt, *J*=10.2, 6.0, 1H), 3.61 (dhept, *J*=10.5, 6.8, 2H), 2.88 - 2.77 (m, 2H), 2.58 - 2.47 (m, 2H), 1.24 (d, *J*=6.8, 6H), 0.97 (d, *J*=6.8, 6H); **¹³C-NMR** (126 MHz, 298 K, CDCl₃, δ/ppm): 140.5 (d, *J*=1.6), 140.0 (d, *J*=2.0), 128.9, 128.8, 128.7, 128.7, 126.4, 126.1, 117.0, 116.9, 72.2 (d, *J*=19.5), 71.2 (d, *J*=18.8), 43.7 (d, *J* = 12.6 Hz), 28.5 (d, *J*=5.4), 28.2 (d, *J*=4.0), 24.8 (d, *J*=7.8), 24.3 (d, *J*=7.0); **³¹P{¹H}-NMR** (162 MHz, 298 K, CDCl₃, δ/ppm): 150.76; **³¹P-NMR** (162 MHz, 298 K, CDCl₃, δ/ppm): 150.76 (dddd, *J*=10.2, *J*=10.2, *J*=10.2, *J*=10.2); **m.p.** 66 - 69 °C; **IR** (neat, cm⁻¹) 2967.0, 1455.0, 1180.2, 1027.9, 978.7, 760.8, 700.0, 423.3; **R_f** (SiO₂, hexane/ethylacetate 8:2) 0.38; **HRMS** (ESI) calcd for 446.1973 (M+Na), found 446.1970; **[α]_D²⁰** = - 15.8 (C 1.2, CHCl₃).

Synthesis of (1*R*,3*s*,5*r*,6*R*,7*S*,8*s*,9*S*)-3-phenyl-2,4,10-trioxaadamantane-6,8,9-triol **1a**



The compound was synthesized as described before on a 50 g scale starting from *myo*-inositol. Analytical data were identical with the values reported in the literature.¹⁰⁷

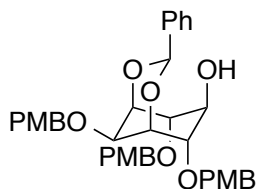
Synthesis of (1*R*,3*s*,5*r*,6*R*,7*S*,8*s*,9*S*)-6,8,9-tris((4-methoxybenzyl)oxy)-3-phenyl-2,4,10-trioxaadamantane **13**



26.6 g (0.100 mol, 1.0 eq.) **1a** were dissolved in dry DMF (150 mL). 14.0 g (0.350 mol, 3.5 eq.) NaH (60% dispersion in oil) were added at 0 °C, followed by careful addition of 51.7 g (0.330 mol, 44.9 mL, 3.3 eq.) PMB-Chloride. The reaction was stirred overnight at room temperature with a catalytic amount of TBAI. The reaction was stopped by addition of water (250 mL), the precipitate was filtered off, rinsed with water and the crystals dried *in vacuo* overnight. Yield: 60.5 g **13** as colorless crystals (0.097 mol, 97%).

¹H-NMR (500 MHz, 298 K, CDCl₃, δ/ppm): 7.69 - 7.64 (m, 2H), 7.36 - 7.27 (m, 5H), 7.17 - 7.11 (m, 4H), 6.87 - 6.80 (m, 6H), 4.64 - 4.61 (m, 2H), 4.59 - 4.57 (m, 1H), 4.57 - 4.54 (m, 1H), 4.53 - 4.50 (m, 1H), 4.48 - 4.40 (m, 6H), 4.08 (t, *J*=1.6, 1H), 3.81 (s, 6H), 3.78 (s, 3H); **¹³C-NMR** (126 MHz, 298 K, CDCl₃, δ/ppm): 159.9, 159.9, 137.9, 130.8, 130.4, 130.2, 129.9, 129.9, 128.5, 126.0, 114.4, 114.4, 108.5, 74.4, 72.6, 71.9, 71.3, 69.8, 66.3, 55.9, 55.8; **m.p.** 145-147 °C; **IR** (neat, cm⁻¹) 1611.2, 1511.9, 1453.1, 1336.4, 1245.8, 1106.0, 978.7, 761.7, 991.1, 514.9; **R_f** (SiO₂, solvent hexane/ethylacetate 7:3) 0.36; **HRMS** (ESI) calcd for 649.2414 (M+Na), found 649.2405.

Synthesis of (1*R*,3*r*,5*S*,6*R*,7*s*,8*S*,9*s*)-6,8,9-tris((4-methoxybenzyl)oxy)-3-phenyl-2,4-dioxabicyclo[3.3.1]nonan-7-ol **14**

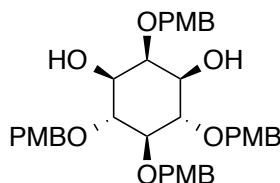


To a cooled solution (-78 °C) of 12 g (19.2 mmol, 1.0 eq.) *ortho*-benzoate **13** in dry DCM (50 mL) were slowly added 51.8 mL (51.8 mmol, 2.7 eq.) DIBAL-H (1.0 M in DCM). The

solution was stirred 1h at -78 °C and then warmed to -20 °C. After another 20 minutes, the reaction was stopped by careful addition of methanol. The solution was diluted with diethylether and saturated aqueous *Rochelle's* salt. The biphasic mixture was stirred vigorously for 45 min. The layers were separated and the organic phase washed twice with water and once with brine. The organic layer was dried over magnesium sulfate, filtered and evaporated *in vacuo*. Purification was achieved by column chromatography (pentane/Et₂O/EtOAc 1:1:0.5). Yield: 10.3 g **14** as a colorless oil (16.5 mmol, 86%).

¹H-NMR (400 MHz, 298 K, MeOD, δ /ppm): 7.55 - 7.44 (m, 2H), 7.41 - 7.24 (m, 9H), 6.93 - 6.85 (m, 6H), 5.79 (s, 1H), 4.82 (s, 4H), 4.67 - 4.54 (m, 6H), 4.24 (d, $J=2.4$, 2H), 3.91 (d, $J=7.6$, 2H), 3.82 - 3.71 (m, 9H), 3.67 (t, $J=7.6$, 1H), 3.56 (t, $J=2.4$, 1H); **¹³C-NMR** (126 MHz, 298 K, DMSO-d₆, δ /ppm): 158.7, 138.8, 130.2, 130.2, 129.3, 129.2, 128.8, 127.9, 126.4, 113.5, 91.8, 82.5, 73.0, 72.9, 70.5, 69.1, 67.5, 55.0, 55.0; **IR** (neat, cm⁻¹) 3500, 1612.2, 1512.9, 1245.8, 819.6; **R_f** (SiO₂, solvent hexanes/ethylacetate 6:4) 0.33; **HRMS** (ESI) calcd for 651.2570 (M+Na), found 651.2561.

Synthesis of (1*R*,2*r*,3*S*,4*R*,5*r*,6*S*)-2,4,5,6-tetrakis((4-methoxybenzyl)oxy) cyclohexane-1,3-diol **52**



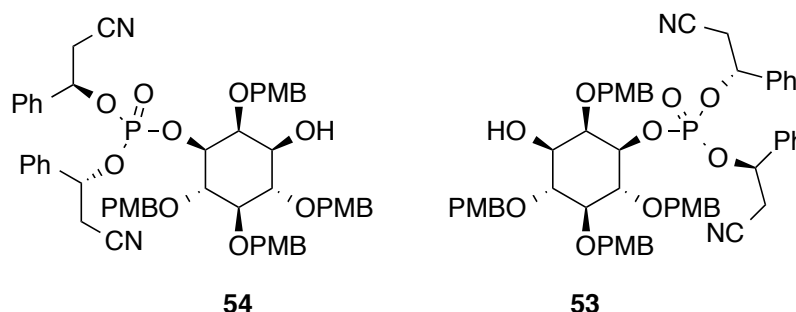
A) 4.40 g (7.00 mmol, 1.0 eq.) **14** were dissolved in dry DMF (15 mL). 336 mg (8.40 mmol, 1.2 eq.) NaH (60% dispersion in oil) were added at 0°C, followed by careful addition of 1.32 g (8.40 mmol, 1.14 mL, 1.2 eq.) PMB-Chloride. The reaction was stirred overnight at room temperature with a catalytic amount of TBAI. The reaction was stopped by addition of saturated ammonium chloride solution (3 mL). The resulting mixture was diluted with Et₂O and washed twice with water and once with brine. The organic layer was dried over magnesium sulfate, filtered and evaporated *in vacuo*. The obtained oil was directly used in the next step.

B) The intermediate was dissolved in 20 mL MeOH and 8 mL DCM. 560 mg (2.94 mmol, 0.42 eq.) *p*TsOH were added and the solution heated to reflux for 5 minutes. After mixing

with saturated aqueous NaHCO_3 (30 mL) and Et_2O (150 mL) and separation, the organic layer was washed once with water and once with brine. The organic layer was dried over MgSO_4 , filtered and concentrated *in vacuo*. Purification was achieved by gradient column chromatography (hexanes/TBME, 0.1% TEA 1:3 until pure TBME, 0.1% TEA). Yield: 3.61 g **52** as a colorless solid (5.44 mmol, 78%, over 2 steps).

$^1\text{H-NMR}$ (400 MHz, 298 K, CDCl_3 , δ/ppm): 7.34 - 7.15 (m, 8H), 6.91 - 6.85 (m, 8H), 4.84 (d, $J=10.9$, 2H), 4.81 (s, 2H), 4.71 (s, 2H), 4.70 (d, $J=11.3$, 2H), 3.96 (t, $J=2.8$, 1H), 3.82 (s, 3H), 3.80 (s, 9H), 3.84 - 3.83 (m, 1H), 3.74 (t, $J=9.5$, 2H), 3.55 - 3.47 (m, 2H), 3.43 (t, $J=9.2$, 1H); **$^{13}\text{C-NMR}$** (101 MHz, 298 K, DMSO-d_6 , δ/ppm): 158.4, 158.4, 158.4, 131.6, 131.3, 131.0, 129.1, 128.9, 128.8, 113.4, 113.3, 113.3, 82.7, 82.2, 81.8, 74.1, 73.9, 73.7, 71.7, 55.0, 55.0, 55.0; **m.p.** 92-93 °C; **IR** (neat, cm^{-1}) 3542.6, 3034.4, 2999.7, 1611.2, 1511.9, 1243.9, 1060.7, 1029.8, 817.7, 733.8, 517.8; **R_f** (SiO_2 , solvent Et_2O) 0.3; **HRMS** (ESI) calcd for 683.2832 ($\text{M}+\text{Na}$), found 683.2831.

Synthesis of bis((*R*)-2-cyano-1-phenylethyl) ((1*R*,2*R*,3*R*,4*R*,5*S*,6*R*)-3-hydroxy-2,4,5,6-tetrakis((4-methoxybenzyl)oxy)cyclohexyl) phosphate **53** and **54**



1.84 g (2.78 mmol, 3.5 eq.) PMB-protected diol **52** and 335 mg (0.79 mmol, 1.0 eq.) phosphoramidite **12** were evaporated twice with dry MeCN (2 mL) and then dissolved in dry MeCN (5 mL). After addition of 195 mg (1.19 mmol, 1.5 eq.) 5-(*para*-F-phenyl)1*H*-tetrazole (dried by twofold evaporation with MeCN) the reaction mixture was stirred at room temperature for 4.5 h. The mixture was cooled down (0 °C) and 164 mg (0.95 mmol, 1.2 eq.) *m*CPBA (70% with water) were added. The mixture was stirred at this temperature for 20 min. The solution was diluted with ethyl acetate, washed with brine (2x), dried over Na_2SO_4 and the solvents were removed *in vacuo*. The excess of starting

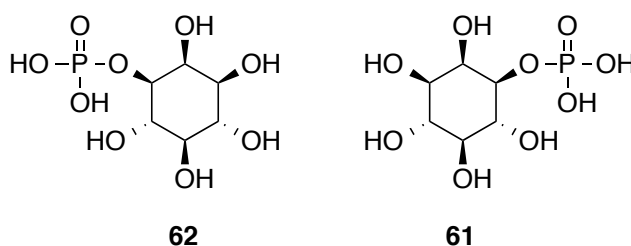
material was recovered by flash column chromatography (diethyl ether/isopropanol 40:1). Crystallization of the mixture at 0 °C from diethyl ether/isopropanol with seeding crystals yielded diastereoisomer **54** (316 mg, 0.32 mmol, 40 %, based on **12**) as a white solid. Diastereoisomer **53** was purified by flash chromatography (dichloromethane/ethyl acetate 1.5:1 v/v) and isolated as a colorless oil (318 mg, 0.32 mmol, 40 %, based on **12**).

Analytical data for **53**: **¹H-NMR** (400 MHz, 298 K, CDCl₃, δ/ppm): 7.43 - 7.14 (m, 16H), 7.12 - 7.04 (m, 2H), 6.91 - 6.79 (m, 8H), 5.55 (ddd, *J*=6.1, *J*=6.1, *J*=6.1, 1H), 5.33 (ddd, *J*=8.0, *J*=8.0, *J*=8.0, 1H), 4.83 - 4.70 (m, 4H), 4.68 - 4.49 (m, 4H), 4.29 - 4.99 (m, 1H), 4.02 - 3.98 (m, 1H), 3.88 (dd, *J*=9.6, *J*=9.6, 1H), 3.83 - 3.77 (m, 12H), 3.67 (dd, *J*=9.6, *J*=9.6, 1H), 3.38 - 3.25 (m, 2H), 2.75 (d, *J*=6.0, 2H), 2.59 - 2.46 (m, 2H); **¹³C-NMR** (126 MHz, 298 K, CDCl₃, δ/ppm): 159.5, 159.4, 136.9 (d, *J*=3.1), 136.7 (d, *J*=4.5), 130.8, 130.8, 130.7, 129.9, 129.8, 129.7, 129.6, 129.4, 129.2, 129.0, 126.4, 126.0, 115.9, 115.5, 114.1, 114.0, 113.9, 113.9, 82.8, 81.3, 80.0 (d, *J*=6.1), 79.4 (d, *J*=6.7), 78.2, 75.6, 75.5, 75.2, 75.2, 75.1 (d, *J* = 4.7 Hz), 75.0, 55.4, 55.4, 27.1 (d, *J*=7.9), 26.8 (d, *J*=6.2); **³¹P{¹H}-NMR** (162 MHz, 298 K, CDCl₃, δ/ppm): -4.12; **³¹P-NMR** (162 MHz, 298 K, CDCl₃, δ/ppm): -4.12 (ddd, *J*=8.0, *J*=8.0, *J*=8.0); **IR** (neat, cm⁻¹): 2933.2, 2835.8, 1612.2, 1512.9, 1246.8, 1028.8, 820.6, 700.0; **R_f** (SiO₂, dichloromethane/ethyl acetate 1:1) 0.45; **HRMS** (ESI) calcd for C₅₆H₅₉N₂O₁₃P [(M+Na)⁺] 1021.3647, found 1021.3651; **[α]_D²⁰** = + 23.3 (*C* 0.5, CHCl₃).

Analytical data for **54**: **¹H-NMR** (500 MHz, 298 K, CDCl₃, δ/ppm): 7.42 - 7.25 (m, 5H), 7.25 - 7.13 (m, 11H), 7.09 - 7.02 (m, 2H), 6.91 - 6.75 (m, 8H), 5.42 (ddd, *J*=7.3, *J*=7.3, *J*=5.7, 1H), 5.26 (ddd, *J*=8.2, *J*=8.2, *J*=5.8, 1H), 4.81 - 4.73 (m, 3H), 4.69 (d, *J*=10.5, 1H), 4.62 (s, 2H), 4.60 (d, *J*=10.9, 1H), 4.46 (d, *J*=10.5, 1H), 4.19 - 4.11 (m, 2H), 3.86 (dd, *J*=9.4, *J*=9.4, 1H), 3.81 - 3.72 (m, 12H), 3.68 (dd, *J*=9.5, *J*=9.5, 1H), 3.44 - 3.32 (m, 2H), 2.84 (ddd, *J*=16.9, *J*=5.5, *J*=1.2, 1H), 2.58 (dd, *J*=16.9, *J*=5.9, 1H), 2.45 (ddd, *J*=16.7, *J*=5.7, *J*=0.9, 1H), 2.37 (dd, *J*=16.8, *J*=5.9, 1H), 2.05 (d, *J*=5.2, 1H); **¹³C-NMR** (126 MHz, 298 K, CDCl₃, δ/ppm): 159.4, 159.2, 136.8 - 136.66 (m), 130.7, 130.7, 130.6, 130.5, 129.7, 129.6, 129.5, 129.4, 129.3, 129.2, 129.0, 128.8, 115.7, 115.6, 114.0, 113.9, 113.8, 113.8, 82.8 (d, *J*=1.9), 81.1, 80.0 (d, *J*=6.4), 78.7 (d, *J*=6.5), 78.0, 75.4, 75.2 (d, *J*=6.0), 75.2, 75.1, 75.1, 75.1, 74.9, 71.8, 55.4 - 55.24 (m), 27.0 (d, *J*=7.7), 27.0 (d, *J*=8.0); **³¹P{¹H}-NMR** (202 MHz, 298 K, CDCl₃, δ/ppm): -4.53; **³¹P-NMR** (202 MHz, 298 K, CDCl₃, δ/ppm): -4.53 (ddd, *J*=7.9, *J*=7.9, *J*=7.9); **m.p.** 141 - 142 °C; **IR** (neat, cm⁻¹): 2933.2, 2836.8, 1612.2, 1513.9, 1247.7, 1029.8, 821.5, 700.0; **R_f** (SiO₂, dichloromethane/ethyl

acetate 1:1) 0.52; **HRMS** (ESI) calcd for $C_{56}H_{59}N_2O_{13}P$ $[(M+Na)^+]$ 1021.3647, found 1021.3641; $[\alpha]_D^{20} = +18.8$ (C 1, $CHCl_3$).

Synthesis of inositol-3-phosphate **61**, **62** for assignment of the absolute configuration of **53**, **54**



70 mg (70 μ mol, 1 eq.) P-triester **54** were dissolved in dry dichloromethane (4 mL) under an inert atmosphere and the solution was cooled to 0 °C. 90 mg (0.35 mmol, 94 μ L, 5 eq.) BSTFA was added and the mixture was stirred for 2 min. 53 mg (5 eq.) DBU were added to the mixture at the same temperature. After stirring for 20 min at 0 °C, MeOH (1.5 mL) was added and the mixture was stirred for another 15 min. The solvents were removed in *vacuo*. The excess of DBU was removed on a dowex column using water/methanol as eluent. The product was collected directly in a flask containing ammonia to form the ammonium salt. Lyophilization yielded 80 mg of product that was dissolved in a mixture of methanol/water (2:1, 10 mL). To this mixture 220 mg Pd/C (10%) were added and the slurry hydrogenated 4 days at 4 bar (Parr apparatus, addition of 10 mL water after 1 day). The catalyst was removed on a celite pad and washed with water. The aqueous phase was extracted twice with DCM and freeze-dried. Crystallization from water/dioxane and passing over a dowex column (H^+ form) yielded compound **62** (15 mg, 58 μ mol, 83%). Half of the product was transferred into a flask containing cyclohexylamine. Lyophilization yielded compound **62** as the *bis*-cyclohexylammonium salt in quantitative yield. Analytical data were identical with those published before.^{113,135} The optical rotation at pH = 9 revealed compound **62** as the 3-phosphate. Thus, compound **54** is modified in the 3-position and an analogous analysis with compound **53** as starting material revealed modification of **61** in the 1-position. This assignment was further verified by converting the compounds into the free phosphoric acids. Optical rotation was measured at pH = 2 and then the solution was adjusted to pH

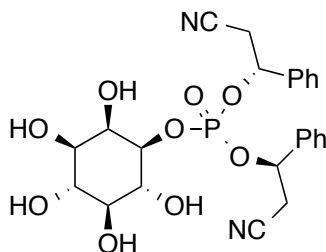
= 9 with NH_4OH . A typical inversion in the sign of optical rotation occurred as described previously at $\text{pH} = 6.3$. This behavior was observed for both enantiomers with inverted values. The NMR spectra obtained for compound **62** showed broad resonances in both the ammonium and acidic form. A titration with 0.5 eq. of cyclohexylamine greatly increased the quality of the obtained spectra.

61 as bis-cyclohexylammonium salt: $^1\text{H-NMR}$ (400 MHz, 298 K, D_2O , δ/ppm): 4.12 - 4.02 (m, 1H), 3.76 (ddd, $J=11.4$, $J=6.2$, $J=2.7$, 1H), 3.61 (dd, $J=10.5$, $J=8.4$, 1H), 3.55 - 3.38 (m, 2H), 3.24 - 3.14 (m, 1H), 3.07 - 2.92 (m, 2H), 1.90 - 1.75 (m, 4H), 1.70 - 1.60 (m, 4H), 1.55-1.45 (m, 2H), 1.34 - 1.11 (m, 8H), 1.09 - 0.91 (m, 2H); $^{13}\text{C NMR}$ (101 MHz, D_2O , δ/ppm): 74.9, 74.8 (d, $J=5.1$), 72.8, 72.8 (d, $J=3.9$), 72.2, 71.4, 50.9, 30.9, 24.8, 24.3; $^{31}\text{P}\{^1\text{H}\}\text{-NMR}$ (202 MHz, 298 K, D_2O , δ/ppm): 5.05; **HRMS** (ESI) calcd for $\text{C}_6\text{H}_{12}\text{O}_9\text{P}^-$ [M^-] 259.0222, found 259.0222; as bis-cyclohexylammonium salt: $[\alpha]_{\text{D}}^{20} = +3.6$ (C 0.5, H_2O , $\text{pH} = 9$), Lit.: $[\alpha]_{\text{D}}^{20} = +3.4$; as free acid: $[\alpha]_{\text{D}}^{20} = -10.7$ (C 0.5, H_2O , $\text{pH} = 2$), Lit.: $[\alpha]_{\text{D}}^{20} = -9.8$; as ammonium salt (free acid solution adjusted to $\text{pH} = 9$ with NH_4OH): $[\alpha]_{\text{D}}^{20} = +3.9$ (C 0.5, H_2O , $\text{pH} = 9$), Lit.: $[\alpha]_{\text{D}}^{20} = +4.4$.

62 all NMR/MS data obtained were identical with its enantiomer **61** despite the amount of counterions for obtaining well-resolved spectra. Optical rotation measurements were conducted as described above.

As bis-cyclohexylammonium salt: $[\alpha]_{\text{D}}^{20} = -3.7$ (C 0.5, H_2O , $\text{pH} = 9$), Lit.: $[\alpha]_{\text{D}}^{20} = -4.5$; as free acid: $[\alpha]_{\text{D}}^{20} = +9.3$ (C 0.5, H_2O , $\text{pH} = 2$), Lit.: $[\alpha]_{\text{D}}^{20} = \text{not available}$; Lit.: $[\alpha]_{\text{D}}^{20} = +3.4$ ($\text{pH} = 6$); as ammonium salt (free acid solution adjusted to $\text{pH} = 9$ with NH_4OH): $[\alpha]_{\text{D}}^{20} = -4.0$ (C 0.5, H_2O , $\text{pH} = 9$), Lit.: $[\alpha]_{\text{D}}^{20} = -4.5$.

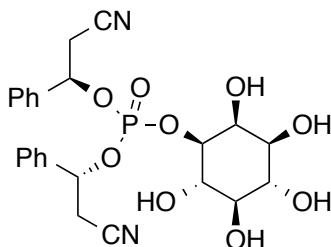
Synthesis of bis((*R*)-2-cyano-1-phenylethyl) ((1*S*,2*R*,3*R*,4*S*,5*S*,6*R*)-2,3,4,5,6-pentahydroxycyclohexyl) phosphate **55**



600 mg (0.60 mmol) P-triester **53** were dissolved in chloroform (37 mL) and trifluoroacetic acid (0.9 mL, 2.5%) was added to the solution. After stirring for 2.5 h at room temperature, hexane (10 mL) was added and the solvents were removed *in vacuo*. Crystallization from TBME yielded compound **55** as a colorless solid (264 mg, 0.51 mmol, 85 %).

¹H-NMR (500 MHz, 298 K, CD₃OD, δ /ppm): 7.44 - 7.27 (m, 10H), 5.75 (ddd, $J=8.1$, $J=8.1$, $J=5.7$, 1H), 5.64 (ddd, $J=8.1$, $J=8.1$, $J=5.7$, 1H), 4.24 (ddd, $J=10.3$, $J=7.9$, $J=2.8$, 1H), 4.14 (dd, $J=2.7$, $J=2.7$, 1H), 3.86 (dd, $J=9.6$, $J=9.6$, 1H), 3.63 (dd, $J=9.5$, $J=9.5$, 1H), 3.35 - 3.32 (m, 1H), 3.22 - 3.05 (m, 5H); **¹³C-NMR** (126 MHz, 298 K, MeOD, δ /ppm): 138.7 (d, $J=2.5$), 138.6 (d, $J=2.2$), 130.3, 130.3, 129.8, 129.8, 127.3, 117.7, 117.4, 81.7 (d, $J=6.7$), 77.0 (d, $J=6.0$), 76.8 (d, $J=4.9$), 76.2 (d, $J=1.7$), 73.9, 72.7, 72.7, 72.7, 72.6 (d, $J=5.8$), 27.4 (d, $J=3.7$), 27.3 (d, $J=4.0$); **³¹P{¹H}-NMR** (162 MHz, 298 K, CDCl₃, δ /ppm): -5.54; **³¹P-NMR** (162 MHz, 298 K, CDCl₃, δ /ppm): -5.54 (ddd, $J=8.0$, $J=8.0$, $J=8.0$); **m.p.** 148.7 - 151.2 °C; **IR** (methanol, cm⁻¹) 3387.4, 1261.2, 1008.6, 700.0, 423.3; **R_f** (SiO₂, DCM/MeOH 14:3) 0.38; **HRMS** (ESI) calcd for C₂₄H₂₇N₂O₉P [(M+Na)⁺] 541.1352, found 541.1357; **[α]_D²⁰** = +29.0 (C 1, methanol).

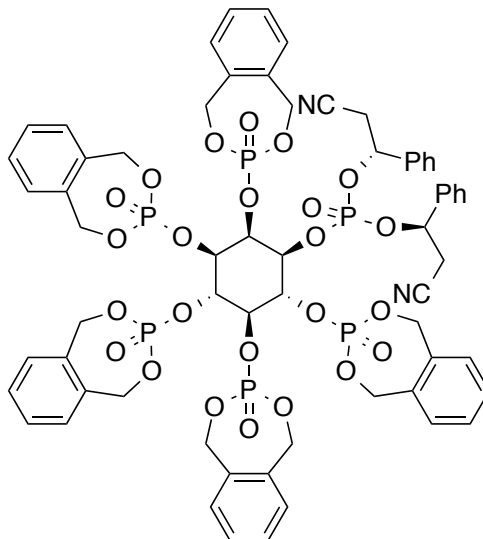
Synthesis of bis((*R*)-2-cyano-1-phenylethyl) ((1*R*,2*S*,3*R*,4*R*,5*S*,6*S*)-2,3,4,5,6-pentahydroxycyclohexyl) phosphate **56**



Compound **54** (488 mg, 0.49 mmol) was dissolved in chloroform (30 mL) and trifluoroacetic acid (0.8 mL, 2.5%) was added to the solution. After stirring for 3 h at room temperature, hexane was added and the solvents were removed *in vacuo*. Crystallization from diethyl ether yielded compound **56** (252 mg, 0.49 mmol, 100%).

¹H-NMR (400 MHz, 298 K, DMSO-*d*₆, δ /ppm): 7.46 - 7.20 (m, 10H), 5.72 - 5.59 (m, 2H), 5.26 (d, *J*=5.2, 1H), 5.06 (d, *J*=4.2, 1H), 4.87 (d, *J*=4.6, 1H), 4.69 - 4.59 (m, 2H), 4.12 - 3.94 (m, 2H), 3.63 (ddd, *J*=9.4, *J*=9.4, *J*=5.2, 1H), 3.40 (d, *J*=7.0, 1H), 3.30 - 3.11 (m, 5H), 3.00 (ddd, *J*=9.1, *J*=9.1, *J*=4.7, 1H); **¹³C-NMR** (126 MHz, 298 K, DMSO-*d*₆, δ /ppm): 137.8 - 137.5 (m), 128.7, 128.6, 128.4, 128.3, 126.2, 125.9, 117.0, 116.9, 79.9 (d, *J*=6.2), 74.7, 74.3 (d, *J*=6.0), 73.6 (d, *J*=4.3), 72.2, 71.0, 70.9, 70.8 (d, *J*=6.1), 26.2 (d, *J*=5.4), 26.0 (d, *J*=6.0); **³¹P{¹H}-NMR** (162 MHz, 298 K, DMSO-*d*₆, δ /ppm): -3.57; **m.p.** 146 - 154 °C; **IR** (methanol, cm⁻¹): 3377.7, 1250.6, 1008.6, 700.0, 417.5; **R_f** (SiO₂, DCM/MeOH 14:3) 0.34; **HRMS** (ESI) calcd for C₂₄H₂₇N₂O₉P [(M+Na)⁺] 541.1352, found 541.1348; **[α]_D²⁰** = +50.6 (*C* 0.5, methanol).

Synthesis of bis((*R*)-2-cyano-1-phenylethyl) ((1*S*,2*R*,3*R*,4*S*,5*S*,6*R*)-2,3,4,5,6-pentakis((3-oxido-1,5- dihydrobenzo[*e*][1,3,2]dioxaphosphepin-3-yl)oxy)cyclohexyl) phosphate **57**

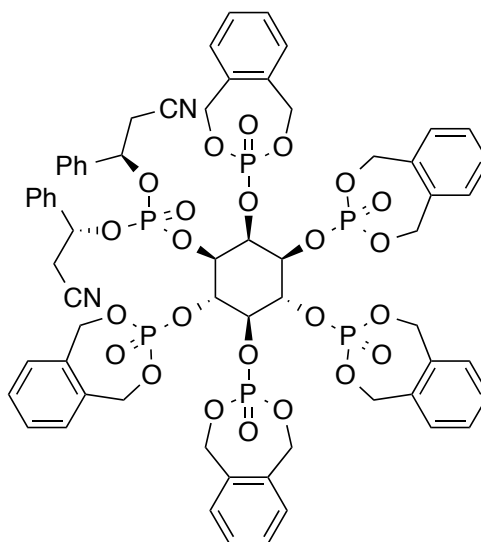


50.0 mg (0.096 mmol, 1.0 eq.) P-triester **55** and 231 mg (0.86 mmol, 9 eq.) *o*-xylylene *N,N*- diisopropylamino phosphoramidite were evaporated twice with dry acetonitrile (2 mL). The residue was dissolved in dry MeCN (3 mL) and cooled down (0 °C). To this solution 3.84 mL (1.73 mmol, 18 eq.) tetrazole (0.45 M in MeCN) were added. Progress of the reaction was monitored by ^{31}P -NMR. After completion of the reaction (2.5 h), oxidation was achieved by slow (!) addition of 133 mg (0.77 mmol, 8 eq.) *m*CPBA (70% moistened with water). The reaction mixture was diluted with EtOAc (40 mL) and washed twice with brine. The organic layer was dried over sodium sulfate, filtered and concentrated *in vacuo*. The product was purified by FC (ethyl acetate/methanol 200:1) yielding 90.0 mg **57** as a colorless solid (0.063 mmol, 65%). The yield of this procedure can be optimized according to the preparation of **58** procedure B.

$^1\text{H-NMR}$ (500 MHz, 298 K, CDCl_3 , δ/ppm): 7.40 - 7.05 (m, 30H), 5.95 - 4.75 (m, 28H), 3.29 (dd, $J = 17.1, 6.4$ Hz, 1H), 3.07 - 2.89 (m, 3H); $^{13}\text{C-NMR}$ (126 MHz, 298 K, CDCl_3 , δ/ppm): 150.6, 148.8, 137.0 (d, $J=3.4$), 136.9 (d, $J=3.8$), 135.7, 135.6, 135.5, 135.4, 135.4 - 135.31 (m), 131.3, 130.1 - 128.7 (m), 127.4, 126.5 - 126.0 (m), 116.5, 116.2, 77.8 - 77.5 (m), 76.6 (d, $J=4.8$), 76.4 (d, $J=4.9$), 76.2 (d, $J=5.7$), 76.0 (d, $J=5.1$), 74.0 - 73.8 (m), 73.8 - 73.6 (m), 69.8 (d, $J=7.5$), 69.7 - 68.9 (m), 27.1 (d, $J=4.6$), 27.0 (d, $J=3.5$); $^{31}\text{P}\{^1\text{H}\}$ -NMR (162 MHz, 298 K, CDCl_3 , δ/ppm): -1.20, -2.20, -2.59, -3.11, -3.63, -4.51; **m.p.** decomposition at 190 °C; **IR** (neat, cm^{-1}): 1292.1, 1050.1, 1022.1, 860.1, 733.8; **R_f**

(SiO₂, ethyl acetate) 0.45; **HRMS** (ESI) calcd for C₆₄H₆₂N₂O₂₄P₆ [(M+Na)⁺] 1451.2016, found 1451.2007; [α]**D**20 = +25.2 (C 1, CHCl₃).

Synthesis of bis((*R*)-2-cyano-1-phenylethyl) ((1*R*,2*S*,3*R*,4*R*,5*S*,6*S*)-2,3,4,5,6-pentakis((3-oxido-1,5-dihydrobenzo[*e*][1,3,2]dioxaphosphepin-3-yl)oxy)cyclohexyl) phosphate **58**



Procedure A: high purity 58 but low yield

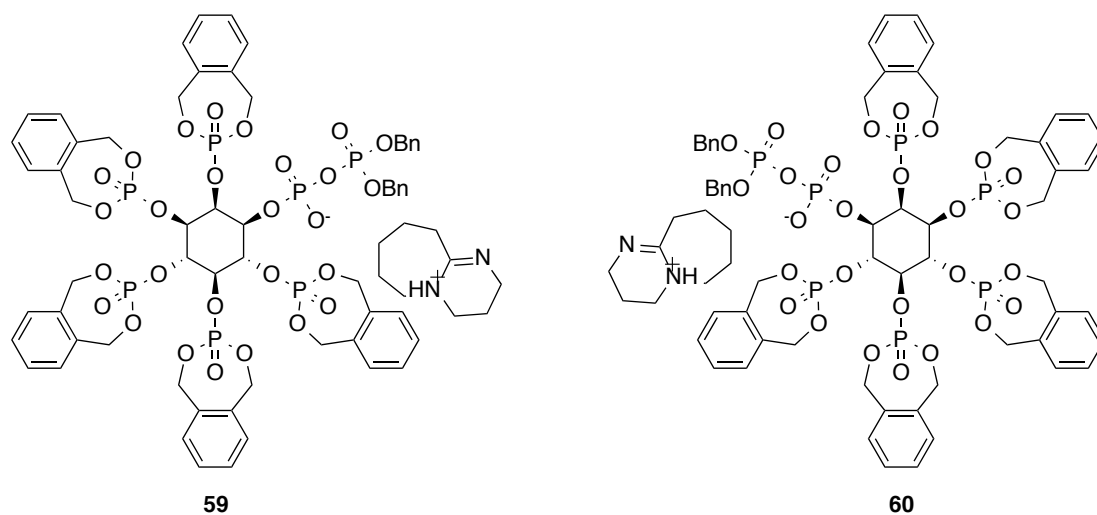
145 mg (0.28 mmol, 1.0 eq.) P-triester **56** and 674 mg (2.52 mmol, 9.0 eq.) *o*-xylylene *N,N*-diisopropylamino phosphoramidite were evaporated twice with dry acetonitrile (2 mL). The residue was dissolved in dry MeCN (9 mL) and cooled down (0 °C). To this solution 11.2 mL (5.04 mmol, 18 eq.) tetrazole (0.45 M in MeCN) were added. Progress of the reaction was monitored by ³¹P-NMR. After completion of the reaction (2.5 h), oxidation was achieved by slow (!) addition of 387 mg (2.24 mmol, 8.0 eq.) *m*CPBA (70% moistened with water). The reaction mixture was diluted with EtOAc (100 mL) and washed twice with brine. The organic layer was dried over sodium sulfate, filtered and concentrated *in vacuo*. The product was purified by FC (ethyl acetate/methanol 200:1) yielding 100 mg **58** as a colorless solid (0.07 mmol, 25%).

Procedure B: slightly impure 58 with quantitative yield

100 mg (0.19 mmol, 1.0 eq.) P-triester **56** and 470 mg (1.74 mmol, 9.0 eq.) *o*-xylylene *N,N*-diisopropylamino phosphoramidite were evaporated twice with dry acetonitrile (2 mL). The residue was dissolved in dry MeCN (15 mL) and cooled down (-5 °C to -10 °C). To this solution 410 mg (3.47 mmol, 18 eq.) 4,5-dicyanoimidazole (DCI) were added. Progress of the reaction was monitored by ³¹P-NMR. After completion of the reaction (1 h), oxidation was achieved by slow (!) addition of 300 mg (1.74 mmol, 9.0 eq.) *m*CPBA (70% moistened with water). The reaction mixture was diluted with DCM (150 mL) and washed twice with brine, dried over MgSO₄ and the solvents were removed *in vacuo*. Crystallization from dichloromethane/diethyl ether yielded compound **58** (300 mg, 0.21 mmol, quant.). ³¹P-NMR showed that the hydrolyzed P-amidite was not completely removed (20% from ³¹P-NMR). This impurity was unproblematic in the next step.

¹H-NMR (400 MHz, 298 K, CDCl₃, δ/ppm): 7.33 - 7.02 (m, 30H), 5.98 - 5.90 (m, 1H), 5.81 - 5.72 (m, 1H), 5.70 - 5.29 (m, 11H), 5.25 - 4.89 (m, 15H), 3.25 (dd, *J*=16.9, *J*=8.6, 1H), 3.08 (dd, *J*=16.7, *J*=3.9, 1H), 2.98 (dd, *J*=16.7, *J*=8.0, 1H), 2.85 (ddd, *J*=16.9, *J*=4.7, *J*=1.6, 1H); **¹³C-NMR** (126 MHz, 298 K, CDCl₃, δ/ppm): 136.7 - 136.5 (m), 136.1 (d, *J* = 2.6 Hz), 135.8, 135.9 - 135.6 (m), 135.6, 135.6, 135.5, 134.9, 134.7, 130.1 - 128.4 (m), 126.3, 126.1, 117.4, 116.0, 77.4 - 77.3 (m), 76.2 (d, *J* = 5.3 Hz), 76.0 (d, *J* = 7.4 Hz), 73.8 - 73.5 (m), 70.0 (d), 69.9 - 69.1 (m), 27.6 (d, *J* = 7.6 Hz), 27.2 (d, *J* = 4.4 Hz); **³¹P{¹H}-NMR** (162 MHz, 298 K, CDCl₃, δ/ppm): -1.69, -1.74, -2.42, -2.87, -3.33, -3.99; **m.p.** 159 - 163 °C; **IR** (neat, cm⁻¹): 1292.1, 1050.1, 1021.1, 860.1, 733.8, 463.8; **R_f** (SiO₂, ethyl acetate) 0.48; **HRMS** (ESI) calcd for C₆₄H₆₂N₂O₂₄P₆ [(M+Na)⁺] 1451.2016, found 1451.2019; **[α]_D²⁰** = +2.4 (C 0.5, CHCl₃).

Synthesis of 3,4,5,6,7,8,9,10-octahydro-2*H*-pyrimido[1,2-*a*]azepin-5-ium dibenzyl ((1*S*,2*R*,3*R*,4*S*,5*S*,6*R*)-2,3,4,5,6-pentakis((3-oxido-1,5-dihydrobenzo[*e*][1,3,2]dioxaphosphepin-3-yl)oxy)cyclohexyl)diphosphate **59** and its enantiomer 3,4,5,6,7,8,9,10-octahydro-2*H*-pyrimido[1,2-*a*]azepin-5-ium dibenzyl ((1*R*,2*S*,3*R*,4*R*,5*S*,6*S*)-2,3,4,5,6-pentakis((3-oxido-1,5-dihydrobenzo[*e*][1,3,2]dioxaphosphepin-3-yl)oxy)cyclohexyl) diphosphate **60**

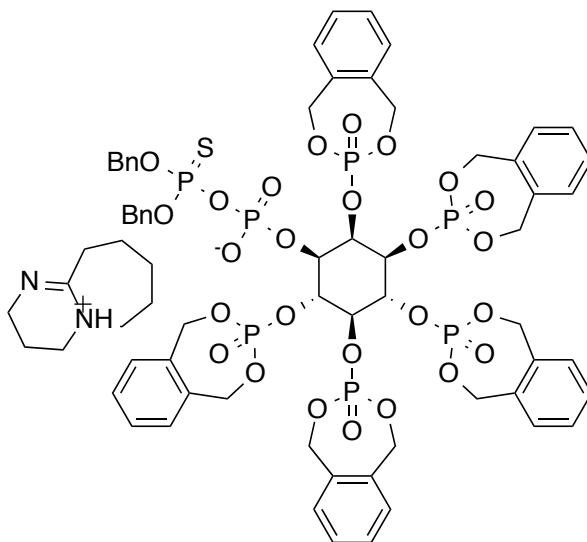


80 mg (56 μmol , 1.0 eq.) hexaphosphate **57** were dissolved in dry MeCN (2 mL). 33 μL (84 mg, 0.22 mmol, 4.0 eq.) DBU were added followed by addition of 60 μL (58 mg, 0.22 mmol, 4.0 eq.) BSTFA. The solution was stirred 10 minutes at room temperature. After completion of the deprotection (check by ^{31}P -NMR), a mixture of 60 μL MeOH and 18 μL (0.22 mmol, 26 mg, 4.0 eq.) TFA were added to the solution. The mixture was stirred for 10 min and then evaporated to dryness. The residue was taken up in dry MeCN (2 mL) and 39 mg (0.11 mmol, 2.0 eq.) *bis*-benzyl *N,N*-diisopropylamino phosphoramidite and 250 μL (0.11 mmol, 2.0 eq.) 1*H*-tetrazole (0.45 M in MeCN) were added. The solution was stirred for 15 minutes at room temperature and then cooled down (0 $^{\circ}\text{C}$). Progress of the reaction was monitored by ^{31}P -NMR. After completion of the reaction, oxidation was achieved by slow (!) addition of 19.0 mg (0.11 mmol, 2.0 eq.) *m*CPBA (70% moistened with water). The reaction mixture was diluted with Et₂O (20 mL) and cooled to 0 $^{\circ}\text{C}$. The precipitate was filtered and washed with cold Et₂O and then dried *in vacuo*. The precipitate was purified by RP-18 chromatography (water/MeOH 3:1 – 1:2 v/v) and isolated by lyophilization. Yield: 58 mg **59** as a colorless solid (37 μmol , 65%). The same

procedure yielded the corresponding enantiomer **60** starting from **58** in comparable yield (73%) and purity. Both compounds contained variable amounts of DBUH⁺ as counterion.

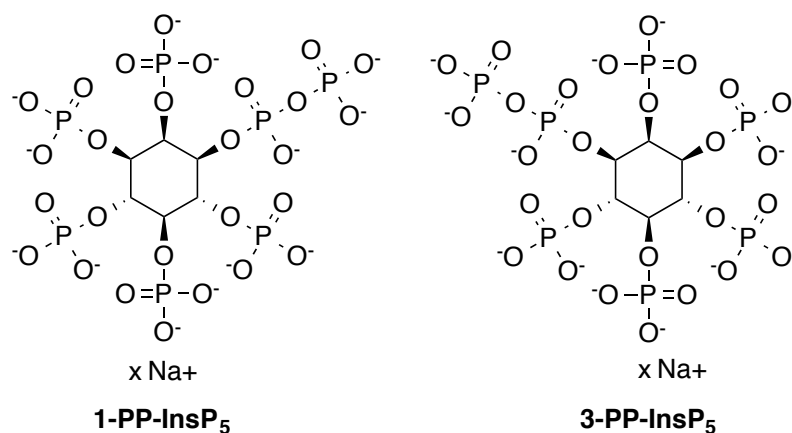
¹H-NMR (500 MHz, 298 K, CDCl₃, δ /ppm): 11.10 (s, DBU), 7.60-6.50 (m, 30H), 6.00 - 4.40 (m, 30H), 3.42 – 3.30 (m, DBU), 3.30 - 3.15 (m, DBU), 2.80 - 2.72 (m, DBU), 1.90 - 1.75 (m, DBU), 1.65 - 1.45 (m, DBU); **¹³C-NMR** (126 MHz, 298 K, CDCl₃, δ /ppm): 166.5, 137.3 - 134.6 (m), 130.2 - 127.3 (m), 74.6 - 73.8 (m), 72.0 - 71.2 (m), 70.6 - 70.2 (m), 70.2 - 67.9 (m), 54.3, 48.7, 38.3, 32.6, 29.8, 29.2, 27.0, 24.1, 19.6; **³¹P{¹H}-NMR** (162 MHz, 298 K, MeOD, δ /ppm): -1.74 , -1.90 , -2.10 , -2.63 , -2.79 , -10.09 (d, $J=15.0$), -11.95 (d, $J=15.2$); **m.p.** decomposition at 170 °C; **IR** (neat, cm⁻¹): 1291.1, 1051.0, 1020.2, 861.1, 733.8, 478.3, 416.6; **R_f** (SiO₂, dichloromethane/methanol 8:1) 0.5; **HRMS** (ESI) calcd for C₆₀H₆₀O₂₇P₇ 1429.1491, found 1429.1497; **[α]_D²⁰** = +10.9 (**59**, C 1, CHCl₃). **[α]_D²⁰** = -9.9 (**60**, C 0.5, CHCl₃). The analytical data obtained for **59**, **60** were identical in all respects (besides minor concentration dependent shifts in the NMR spectra), except for the inverted optical rotations.

Synthesis of 3,4,5,6,7,8,9,10-octahydro-2*H*-pyrimido[1,2-*a*]azepin-5-ium dibenzyl ((1*R*,2*S*,3*R*,4*R*,5*S*,6*S*)-2,3,4,5,6-pentakis((3-oxido-1,5-dihydrobenzo[*e*][1,3,2]dioxaphosphepin-3-yl)oxy)cyclohexyl) diphosphothioate **63**, a sulfurized analog



15 mg (11 μ mol, 1.0 eq.) hexaphosphate **58** were subjected to the same procedure as described above (for **60**). The only difference was that the 2 equivalents of *m*CPBA in the oxidation step were replaced with 2 equivalents of elemental, powdered sulfur. The product was isolated by crystallization yielding 13 mg **63** as a sticky off-white solid (8 μ mol, 77%). Thus, it was proven, that the sequence is amenable to introduce non-natural modifications in the anhydride part of the molecule.

$^1\text{H-NMR}$ (400 MHz, 298 K, CDCl_3 , δ/ppm): 11.07 (s, DBU), 7.52-7.00 (m, 30H), 6.05 - 4.50 (m, 30H), 3.42 - 3.25 (m, DBU), 3.30 - 3.15 (m, DBU), 2.80 - 2.71 (m, DBU), 1.92 - 1.76 (m, DBU), 1.65 - 1.46 (m, DBU); **$^{13}\text{C-NMR}$** (126 MHz, 298 K, CDCl_3 , δ/ppm): 166.4, 136.3 - 135.0 (m), 129.6 - 128.1 (m), 77.8- 77.6 (m), 74.5 - 73.8 (m), 72.0 - 71.2 (m), 70.5 - 70.2 (m), 70.0 - 69.1 (m), 54.3, 48.6, 38.2, 32.5, 29.0, 28.8, 23.9, 19.5; **$^{31}\text{P}\{^1\text{H}\}\text{-NMR}$** (162 MHz, 298 K, CDCl_3 , δ/ppm): 57.58 (d, $J=17.3$), -2.45, -2.68, -2.74, -3.45, -3.49, -12.65 (d, $J=17.4$); **R_f** (SiO_2 , dichloromethane/methanol 8:1) 0.5; **HRMS** (ESI) calcd for $\text{C}_{60}\text{H}_{60}\text{O}_{26}\text{P}_7\text{S}$ 1445.126, found 1445.125.

Synthesis of **1-PP-InsP₅** and **3-PP-InsP₅**

The reactions were either conducted in a stainless steel autoclave with a Teflon inlet at 80 bar H₂ (2-3 hours) or in a Parr apparatus at 4 bar H₂ (6 hours). The reaction is given as an example for compound **59** but was conducted the same way for compound **60**. 15 mg (9.5 μmol, 1.0 eq.) P-anhydride **59** were dissolved in a mixture of *t*BuOH and water (4:1, 1 mL) and 10.4 mg (124 μmol, 13 eq.) NaHCO₃ and PtO₂ (15 eq., 32.5 mg, 143 μmol) were added to the solution. The reaction mixture was then stirred for 2 h under H₂ (80 bar) and then water (1mL) was added. The hydrogenation was continued for 1 more hour. The catalyst was removed by centrifugation, washed with water and the combined aqueous layers were freeze dried. Crystallization of the residue from water/acetone yielded 1-PP-InsP₅ as a colorless solid in the sodium form (6.0 mg, 8.1 μmol, < 85%, sodium salt with unknown amount of counter ions. Maximal yield was calculated for completely protonated species M = 740.01; Minimal yield > 61% (5.8 μmol) for 13 Na⁺; M = 1025.78).

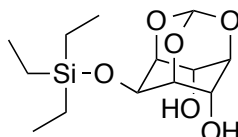
Analytical data for **1-PP-InsP₅**: ¹H-NMR (500 MHz, 298 K, deuterium oxide, δ/ppm): 5.07 - 4.97 (m, 1H), 4.48 (ddd, *J* = 9.9, *J* = 9.9, *J* = 9.9, 1H), 4.56 (ddd, *J* = 9.8, *J* = 9.8, *J* = 9.8, 1H), 4.32 - 4.21 (m, 1H), 4.21 - 4.12 (m, 2H); ¹³C-NMR (126 MHz, 298 K, deuterium oxide, δ/ppm): 77.5 - 77.0 (m), 76.5 - 75.8 (m), 75.2 - 74.7 (m, 2C), 73.7 - 73.4 (m), 73.4 - 73.1 (m); ³¹P{¹H}-NMR (202 MHz, 298 K, deuterium oxide, δ/ppm): 2.30 , 1.25 , 1.06 , 0.90 , 0.45 , -6.61 - (-)8.40 (m), -9.90 (d, *J*=20.1); ³¹P-NMR (202 MHz, 298 K, deuterium oxide, δ/ppm): 2.29 (d, *J*=9.6), 1.25 (d, *J*=9.7), 1.06 (d, *J*=7.9), 0.90 (d, *J*=9.6), 0.44 (d, *J*=7.9), -6.42 - (-)8.36 (m), -9.90 (dd, *J*=21.5, *J*=10.2); **HRMS** (ESI) calcd for 245.6019 (M³⁻, C₆H₁₆O₂₇P₇³⁻), found 245.6022. [α]_D²⁰ = -1.2 (C 0.1, H₂O, adjusted to pH = 9 with

NH₄OH)

Analytical data for **3-PP-InsP₅**: **¹H-NMR** (500 MHz, 298 K, deuterium oxide, δ /ppm): 5.06 - 4.95 (m, 1H), 4.55 (ddd, $J = 9.8$, $J = 9.8$, $J = 9.8$, 1H), 4.54 (ddd, $J = 9.8$, $J = 9.8$, $J = 9.8$, 1H), 4.41 - 4.33 (m, 1H), 4.31 - 4.22 (m, 2H); **¹³C-NMR** (126 MHz, 298 K, deuterium oxide, δ /ppm): 77.6 - 77.0 (m), 76.2 - 75.8 (m), 75.7 - 75.1 (m, 2C), 73.9 - 73.4 (m), 73.4 - 73.0 (m); **³¹P{¹H}-NMR** (202 MHz, 298 K, deuterium oxide, δ /ppm): 1.83, 1.01, 0.62, 0.35, -0.47, -8.84 - -10.28 (m), -10.83 (d, $J=20.4$); **³¹P-NMR** (202 MHz, 298 K, deuterium oxide, δ /ppm): 1.83 (d, $J=9.9$), 1.02 (d, $J=9.2$), 0.63 (d, $J=9.7$), 0.36 (d, $J=9.3$), -0.48 (d, $J=10.9$), -9.21 - (-)9.97 (m), -10.51 - (-)11.28 (m); **HRMS** (ESI) calcd for 245.6019 (M³⁻, C₆H₁₆O₂₇P₇³⁻), found 245.6024; [α]_D²⁰ = +0.5 (C 0.1, H₂O, adjusted to pH = 9 with NH₄OH)

6.3 SYNTHESIS OF 4-PP-InsP₅ AND 6-PP-InsP₅

Synthesis of (1*R*,3*s*,5*S*,6*R*,7*s*,8*S*,9*s*)-9-((triethylsilyl)oxy)-2,4,10-trioxaadamantane-6,8-diol **49**

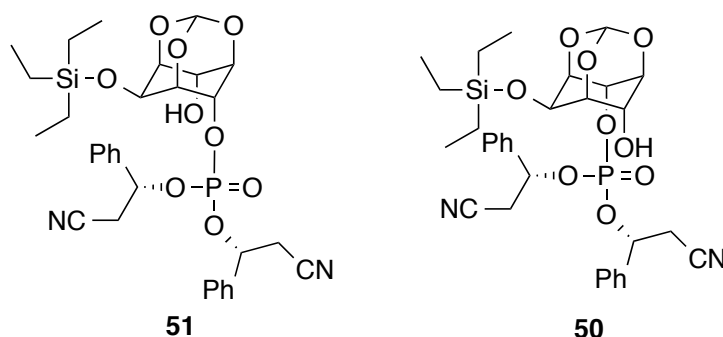


To a cooled solution (0 °C) of 3.65 g (19.2 mmol, 1.0 eq.) D-*myo*-inositol *ortho*-formate in dry DMF (20 mL) were added 3.20 mL (2.87 g, 19.1 mmol, 1.0 eq.) TES-chloride. 3.46 mL (38.4 mmol, 2.0 eq.) Lutidine were added. The solution was stirred 3h at 0 °C. The precipitate was removed by filtration and washed with Et₂O (150 mL). The organic phase was washed three times with water, dried over magnesium sulfate, filtered and evaporated *in vacuo*. Purification was achieved by recrystallization from Et₂O/pentane. Yield: 4.72 g **49** as colorless crystals (15.5 mmol, 81%).

¹H-NMR (500 MHz, 298 K, DMSO-d₆, δ /ppm): 5.53 (s, 2H), 5.47 (s, 1H), 4.28 (dd, $J=3.9$, 3.9, 2H), 4.23 - 4.20 (m, 1H), 4.10 - 4.04 (m, 1H), 3.94 - 3.88 (m, 2H), 0.94 (t, $J=7.9$, 9H), 0.60 (q, $J=8.0$, 6H); **¹³C-NMR** (126 MHz, 298 K, DMSO-d₆, δ /ppm): 101.8, 74.6, 69.4,

67.5, 60.4, 6.7, 4.3; **m.p.** 102-103 °C; **IR** (neat, cm^{-1}) 3445.2, 2956.3, 1427.1, 1162.9, 1060.7, 1017.3, 982.6, 965.2, 745.4, 518.6; **HRMS** (ESI) calcd for 327.1240 ($\text{M}+\text{Na}$), found 327.1237.

Synthesis of bis((*R*)-2-cyano-1-phenylethyl) ((1*S*,3*R*,5*S*,6*S*,7*R*,8*S*,9*S*)-8-hydroxy-9-((triethylsilyl)oxy)-2,4,10-trioxaadamantan-6-yl) phosphate **51** and bis((*R*)-2-cyano-1-phenylethyl) ((1*R*,3*S*,5*R*,6*R*,7*S*,8*R*,9*R*)-8-hydroxy-9-((triethylsilyl)oxy)-2,4,10-trioxaadamantan-6-yl) phosphate **50**



2.30 g (7.56 mmol, 2.8 eq.) *ortho*-formate **49** and 1.14 g (2.69 mmol, 1.0 eq.) P-amidite **7** were evaporated twice with dry MeCN (3 mL), dissolved in 10 mL dry MeCN and cooled down with an ice bath (0 °C). Molecular sieves (3Å) were added. 351 mg (2.97 mmol, 1.1 eq.) 4,5-dicyanoimidazole (previously dried by twofold evaporation with MeCN) were added. The solution was stirred 45 min at 0 °C. After completion of the phosphitylation (checked by ^{31}P -NMR), 1.00 mL (5.50 mmol, 2.0 eq.) *tert*-butylhydroperoxide (5.50 M in nonane) were added. The reaction was allowed to warm to room temperature and was stirred for 20 more minutes. Half of the acetonitrile was removed *in vacuo*, and then ethyl acetate was added (50 mL). The organic phase was washed once with water and twice with brine, dried over magnesium sulfate, filtered and evaporated *in vacuo*. Purification was achieved by flash column chromatography (TBME/hexanes 9:1 v/v to 100% TBME). Yield: 1.31 g **49** (recovered starting material) as colorless crystals (4.31 mmol). 778 mg **51** as colorless crystals (1.21 mmol, 45%). 622 mg **50** as a colorless oil (0.97 mmol, 36%).

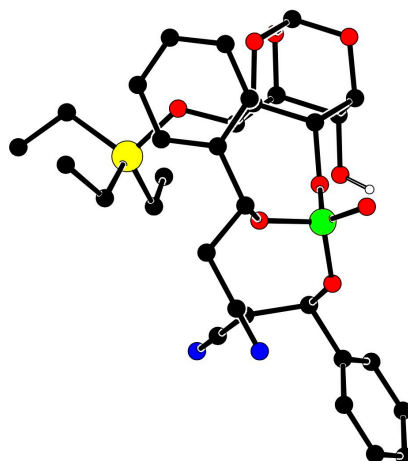
Analytical data for **51**: ^1H -NMR (500 MHz, 298 K, CDCl_3 , δ/ppm): 7.49 - 7.37 (m, 8H), 7.32 - 7.27 (m, 2H), 5.67 (ddd, $J=6.6$, $J=6.6$, $J=6.6$, 1H), 5.44 (s, 1H), 5.45 - 5.39 (m, 2H),

4.93 - 4.84 (m, 1H), 4.54 - 4.41 (m, 1H), 4.20 - 4.11 (m, 1H), 4.10 - 4.02 (m, 2H), 4.01 - 3.96 (m, 1H), 3.00 (d, $J=5.8$, 2H), 2.79 - 2.56 (m, 3H), 0.98 (t, $J=7.8$, 9H), 0.64 (q, $J=7.8$, 6H); $^{13}\text{C-NMR}$ (126 MHz, 298 K, CDCl_3 , δ/ppm): 136.3 (2xd, $J=2.6$), 130.3, 130.2, 129.5, 129.4, 126.3, 126.0, 116.0, 115.6, 102.7, 76.2 (d, $J=4.8$), 76.1 (d, $J=4.9$), 74.3, 72.9 (d, $J=5.5$), 72.6 (d, $J=7.5$), 68.8 (d, $J=3.4$), 67.5, 60.1, 27.4 (d, $J=7.6$), 26.9 (d, $J=8.0$), 6.9, 4.8; $^{31}\text{P}\{^1\text{H}\}\text{-NMR}$ (202 MHz, 298 K, CDCl_3 , δ/ppm): -4.84; **m.p.** 127-129 °C; **IR** (neat, cm^{-1}) 2957.3, 2876.3, 1720.2, 1457.0, 1274.7, 1164.8, 1082.8, 999.0, 836.0, 746.3, 700.0; **R_f** (SiO_2 , solvent DCM/EtOAc 1:1) 0.6; **HRMS** (ESI) calcd for 665.2060 ($\text{M}+\text{Na}$), found 665.2050; $[\alpha]_{\text{D}}^{20} = +35.5$ (C 2.0, CHCl_3).

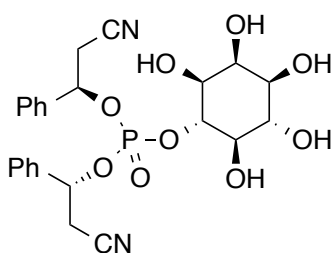
Analytical data for **50**: $^1\text{H-NMR}$ (400 MHz, 298 K, CDCl_3 , δ/ppm): 7.44 - 7.31 (m, 8H), 7.29 - 7.22 (m, 2H), 5.59 (ddd, $J=6.6$, $J=6.6$, $J=6.6$, 1H), 5.50 (ddd, $J=6.1$, $J=6.1$, $J=6.1$, 1H), 5.45 (s, 1H), 4.98 - 4.81 (m, 1H), 4.50 - 4.45 (m, 1H), 4.45-4.41 (m, 1H), 4.05 - 3.92 (m, 2H), 3.79 - 3.64 (m, 1H), 3.38 (d, $J=5.1$, 1H), 2.98 (d, $J=6.1$, 2H), 2.82 - 2.60 (m, 2H), 0.92 (t, $J=8.0$, 9H), 0.57 (q, $J=7.9$, 6H); $^{13}\text{C-NMR}$ (101 MHz, 298 K, CDCl_3 , δ/ppm): 136.3 (2xd, $J=4.3$), 130.0, 129.7, 129.2, 129.0, 126.1, 125.8, 115.9, 115.7, 102.5, 76.1 (d, $J=5.4$), 75.5 (d, $J=5.0$), 74.3, 72.6 (d, $J=6.0$), 72.5 (d, $J=7.6$), 68.9 (d, $J=2.4$), 67.1, 60.0, 27.2 (d, $J=8.0$), 26.8 (d, $J=6.5$), 6.7, 4.6; $^{31}\text{P}\{^1\text{H}\}\text{-NMR}$ (162 MHz, 298 K, CDCl_3 , δ/ppm): -5.45; **IR** (neat, cm^{-1}) 2958.3, 2877.3, 1720.2, 1457.0, 1274.7, 1164.8, 1082.8, 999.9, 835.0, 748.3, 700.0; **R_f** (SiO_2 , solvent DCM/EtOAc 1:1) 0.5; **HRMS** (ESI) calcd for 665.2060 ($\text{M}+\text{Na}$), found 665.2057; $[\alpha]_{\text{D}}^{20} = +25.0$ (C 1.0, CHCl_3).

X-ray crystal Structure of **51**:

CCDC-915304 contains the supplementary crystallographic data for compound **51**. These data can be obtained free of charge from The Cambridge Crystallographic Data Centre via www.ccdc.cam.ac.uk/data_request/cif.



Synthesis of bis((*R*)-2-cyano-1-phenylethyl) ((1*S*,2*R*,3*S*,4*S*,5*S*,6*S*)-2,3,4,5,6-pentahydroxycyclohexyl) phosphate **65**

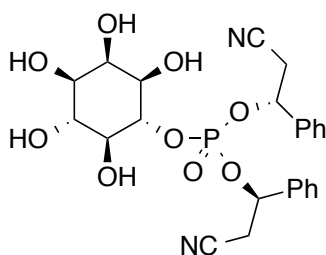


400 mg (0.62 mmol, 1.0 eq.) P-triester **51** and 47 mg (0.25 mmol, 0.4 eq.) *para*-toluene sulfonic acid were dissolved in MeOH (10 mL) and stirred for 6 h. Progress of the reaction was monitored by ^{31}P -NMR. After completion of the reaction, the product was precipitated by addition Et₂O (180 mL) and hexanes (20 mL) at 0 °C. This provoked organogel formation. The gel was filtered and washed with Et₂O/hexanes (9:1) and dried for several hours *in vacuo*. Yield: 305 mg **65** as a colorless solid (0.59 mmol, 95%).

^1H -NMR (400 MHz, 298 K, MeOD, δ /ppm): 7.46 - 7.35 (m, 5H), 7.35 - 7.30 (m, 3H), 7.30 - 7.25 (m, 2H), 5.87 - 5.70 (m, 2H), 4.55 (ddd, $J=9.6$, $J=9.6$, $J=9.6$, 1H), 3.99 (dd, $J=2.9$, $J=2.9$, 1H), 3.67 (dd, $J=9.5$, $J=9.5$, 1H), 3.61 (dd, $J=9.8$, 2.9, 1H), 3.46 - 3.37 (m, 2H), 3.25 - 2.99 (m, 4H); ^{13}C -NMR (126 MHz, 298 K, DMSO-*d*₆, δ /ppm): 138.3 (d, $J=3.8$), 137.9 (d, $J=5.7$), 128.6, 128.4, 128.4, 128.3, 126.3, 125.9, 117.1, 117.0, 82.9 (d, $J=6.9$), 73.6 (d, $J=5.4$), 73.4 (d, $J=4.6$), 73.4 (d, $J=2.7$), 72.9, 72.8, 7.3, 70.25 (d, $J=2.9$), 26.12 (d, $J=6.3$), 25.97 (d, $J=5.1$); $^{31}\text{P}\{^1\text{H}\}$ -NMR (202 MHz, 298 K, MeOD, δ /ppm): -4.57; **m.p.** 117-

120 °C; **IR** (neat, cm^{-1}) 3365.2, 1258.3, 1119.5, 1045.2, 1008.6, 936.3, 754.0, 700.0, 512.0; **R_f** (SiO_2 , solvent DCM:MeOH 8:1) 0.4; **HRMS** (ESI) calcd for 541.1352 ($\text{M}+\text{Na}$), found 541.1355; $[\alpha]_{\text{D}}^{20} = +40.9$ (C 1.0, MeOH).

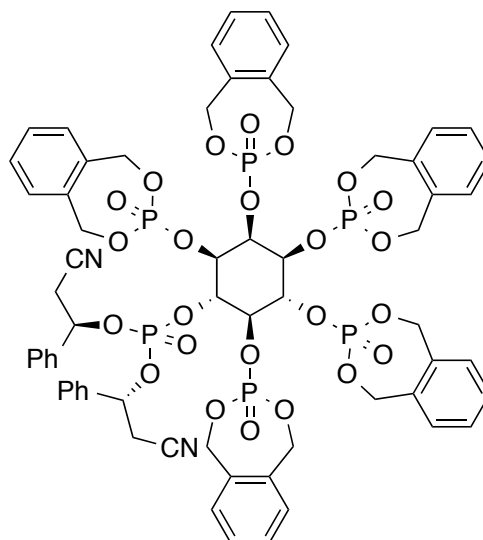
Synthesis of bis((*R*)-2-cyano-1-phenylethyl) ((1*R*,2*R*,3*R*,4*R*,5*R*,6*S*)-2,3,4,5,6-pentahydroxycyclohexyl) phosphate **64**



200 mg (0.31 mmol, 1.0 eq.) P-triester **50** and 23 mg (0.13 mmol, 0.4 eq.) *para*-toluene sulfonic acid were dissolved in MeOH (5 mL) and stirred for 8 h. Progress of the reaction was monitored by ^{31}P -NMR. After completion of the reaction, the product was precipitated by addition Et_2O (50 mL) and hexanes (5 mL) at 0 °C. The precipitate was filtered and washed with Et_2O /hexanes (9:1) and dried for several hours *in vacuo*. Yield: 146 mg **64** as a colorless solid (0.28 mmol, 91%).

^1H -NMR (500 MHz, 298 K, MeOD, δ/ppm): 7.53 - 7.39 (m, 5H), 7.39 - 7.31 (m, 3H), 7.31-7.23 (m, 2H), 5.88 - 5.73 (m, 2H), 4.57 (ddd, $J=9.1$, $J=9.1$, $J=9.1$, 1H), 4.01 (dd, $J=2.8$, $J=2.8$, 1H), 3.72 - 3.63 (m, 2H), 3.45 - 3.39 (m, 2H), 3.27 - 3.00 (m, 4H); **^{13}C -NMR** (126 MHz, 298 K, MeOD, δ/ppm): 139.0 (2xd, $J=3.8$), 130.1, 130.1, 129.7, 129.7, 127.5, 127.2, 117.5, 117.4, 84.6 (d, $J=7.2$), 76.6 (d, $J=6.1$), 76.3 (d, $J=4.8$), 74.8 (d, $J=3.2$), 74.3, 74.2, 73.1, 72.2 (d, $J=3.4$), 27.5 (d, $J=6.6$), 27.4 (d, $J=6.9$); **$^{31}\text{P}\{^1\text{H}\}$ -NMR** (202 MHz, 298 K, MeOD, δ/ppm): -4.47; **m.p.** 112-115 °C; **IR** (neat, cm^{-1}) 3395.1, 1257.4, 1110.8, 1044.3, 1009.6, 700.0, 517.8; **R_f** (SiO_2 , solvent DCM:MeOH 8:1) 0.4; **HRMS** (ESI) calcd for 541.1352 ($\text{M}+\text{Na}$), found 541.1352; $[\alpha]_{\text{D}}^{20} = +35.5$ (C 0.5, MeOH).

Synthesis of bis((*R*)-2-cyano-1-phenylethyl) ((1*S*,2*R*,3*S*,4*S*,5*S*,6*S*)-2,3,4,5,6-pentakis((3-oxido-1,5-dihydrobenzo[*e*][1,3,2]dioxaphosphepin-3-yl)oxy)cyclohexyl) phosphate **67**

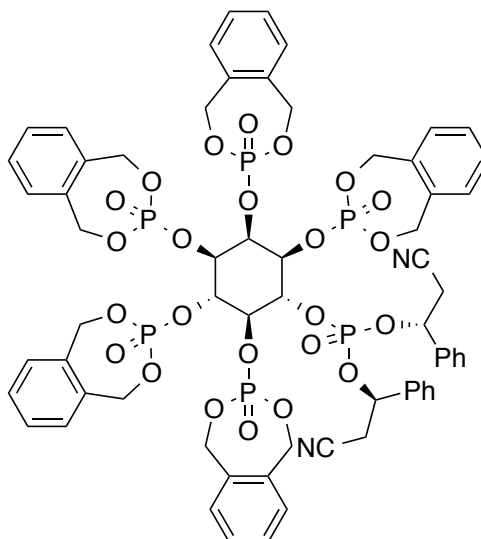


130 mg (0.25 mmol, 1.0 eq.) P-triester **65** and 738 mg (2.75 mmol, 11 eq.) *o*-xylylene *N,N*-diisopropylamino phosphoramidite were evaporated twice with dry acetonitrile (2 mL). The residue was dissolved in 10 mL dry MeCN and cooled down (-10 °C to -15 °C). To this solution 531 mg (4.5 mmol, 18 eq.) 4,5-dicyanoimidazole (DCI) were added. Progress of the reaction was monitored by ³¹P-NMR. After completion of the reaction (20 min), the mixture was warmed to 0 °C. Oxidation was achieved by slow (!) addition of 66.0 mg (2.50 mmol, 10 eq.) *m*CPBA (70% moistened with water). The reaction mixture was diluted with EtOAc (60 mL) and washed twice with brine. The organic layer was dried over sodium sulfate, filtered and concentrated *in vacuo*. The mixture was not evaporated to dryness! After concentration to around 10 mL, TBME (70 mL) were added and the solution was stored at 4 °C for 1 hour. The precipitate was filtered and washed with cold TBME and then dried *in vacuo*. This procedure yielded material of reasonable purity for the next synthetic transformation with the major impurity being excess DCI. Further purification of the product by FC led to massive losses of product, although the material was obtained in slightly improved quality. Yield: 350 mg **67** as a colorless solid (0.25 mmol, 98%).

¹H-NMR (500 MHz, 298 K, CDCl₃, δ/ppm): 7.48 - 7.10 (m, 30H), 5.91 - 4.83 (m, 28H), 3.08 (dd, *J*=16.9, *J*=8.5, 1H), 2.96 (d, *J*=5.8, 2H), 2.77 (dd, *J*=16.9, *J*=1.9, 1H); **¹³C-NMR** (126 MHz, 298 K, CDCl₃, δ/ppm): 137.1 (d, *J*=4.6), 136.8 (d, *J*=2.7), 129.8 - 128.5 (m),

126.2, 126.0, 117.2, 116.1, 76.6 - 75.9 (m), 75.4 (d, $J=5.7$), 74.9 (d, $J=4.8$), 73.8-73.6 (m), 73.1 (d, $J=4.9$), 70.0 - 68.2 (m), 27.1 (d, $J=5.7$), 26.8 (d, $J=7.5$); $^{31}\text{P}\{^1\text{H}\}$ -NMR (202 MHz, 298 K, CDCl_3 , δ/ppm): -0.21, -2.93, -3.37, -3.57, -3.81, -4.38; **m.p.** 139-142 °C; **IR** (neat, cm^{-1}) 3395.1, 1289.2, 1049.1, 1021.1, 871.7, 858.2, 848.5, 761.7, 748.3, 735.7; **R_f** (SiO_2 , solvent EtOAc/MeOH 20:1) 0.3; **HRMS** (ESI) calcd for 1451.2016 ($\text{M}+\text{Na}$), 1474.1914 ($\text{M}+2\text{Na}$), found 1451.1991 (1+), 1474.1911 (2+); $[\alpha]_{\text{D}}^{20} = + 8.7$ (C 0.5, CHCl_3).

Synthesis of bis((*R*)-2-cyano-1-phenylethyl) ((1*R*,2*R*,3*R*,4*R*,5*R*,6*S*)-2,3,4,5,6-pentakis((3-oxido-1,5-dihydrobenzo[*e*][1,3,2]dioxaphosphepin-3-yl)oxy)cyclohexyl) phosphate **66**

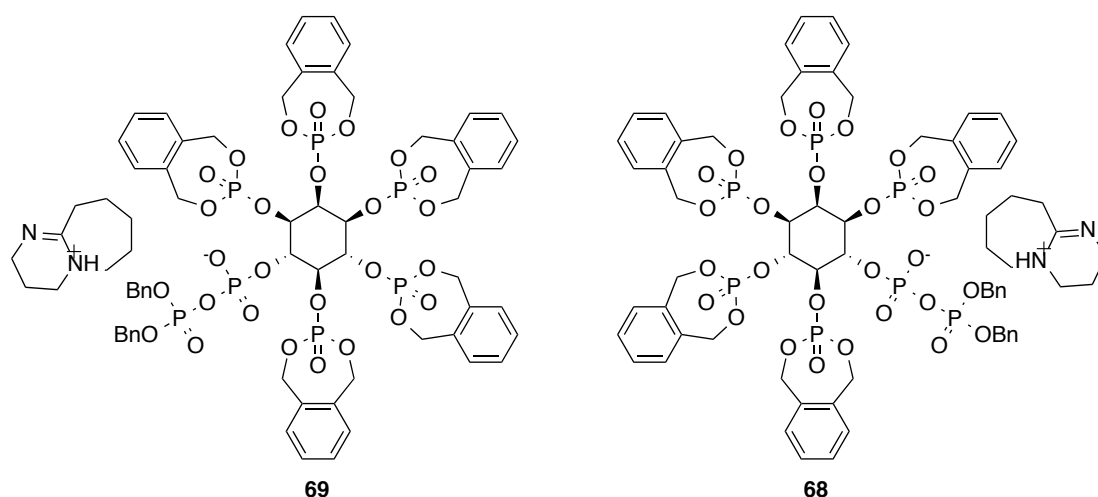


130 mg (0.25 mmol, 1.0 eq.) P-triester **64** and 738 mg (2.75 mmol, 11 eq.) *o*-xylylene *N,N*-diisopropylamino phosphoramidite were evaporated twice with dry acetonitrile (2 mL). The residue was dissolved in 10 mL dry MeCN and cooled down (-10 °C to -15 °C). To this solution 531 mg (4.5 mmol, 18 eq.) 4,5-dicyanoimidazole (DCI) were added. Progress of the reaction was monitored by ^{31}P -NMR. After completion of the reaction (20 min), the mixture was warmed to 0 °C. Oxidation was achieved by slow (!) addition of 66.0 mg (2.50 mmol, 10 eq.) *m*CPBA (70% moistened with water). The reaction mixture was diluted with EtOAc (60 mL) and washed twice with brine. The organic layer was dried over sodium sulfate, filtered and concentrated *in vacuo*. The mixture was not evaporated to dryness! After concentration to around 10 mL, TBME (70 mL) were added

and the solution was stored at 4 °C for 1 hour. The precipitate was filtered and washed with cold TBME and then dried *in vacuo*. This procedure yielded material of reasonable purity for the next synthetic transformation with the major impurity being excess DCI. Further purification of the product by FC led to massive losses of product, although the material was obtained in slightly improved quality. Yield: 342 mg **66** as a colorless solid (0.24 mmol, 96%).

¹H-NMR (500 MHz, 298 K, CDCl₃, δ/ppm): 7.51 - 7.35 (m, 28H), 7.29 - 7.24 (m, 2H), 5.87 - 5.58 (m, 11H), 5.45 - 4.86 (m, 17H), 3.34 - 3.17 (m, 2H), 3.10 (dd, *J*=16.9, 6.3, 1H), 2.89 (dd, *J*=16.9, 4.7, 1H); **¹³C-NMR** (101 MHz, 298 K, CDCl₃, δ/ppm): 137.0 (d, *J*=4.6), 136.8 (d, *J*=4.1), 135.8 - 135.13 (m), 134.7, 134.7, 130.0 - 128.8 (m), 128.7, 126.3, 126.0, 116.3, 116.02, 76.4 (m), 76.1 (d, *J*=4.5), 75.7 (d, *J*=6.5), 75.3 (m), 73.9 (m), 73.0 (m), 70.0 - 68.7 (m), 27.3 (d, *J*=5.8), 27.1 (d, *J*=6.7); **³¹P{¹H}-NMR** (202 MHz, 298 K, CDCl₃, δ/ppm): -0.44, -0.78, -0.84, -1.26, -1.61, -2.73; **m.p.** 138-142 °C; **IR** (neat, cm⁻¹) 3395.1, 1291.1, 1049.1, 1016.3, 862.0, 755.0, 734.8, 458.0; **R_f** (SiO₂, solvent EtOAc/MeOH 30:1) 0.5; **HRMS** (ESI) calcd for 1474.1914 (M+2Na), found 1474.1898 (2+); **[α]_D²⁰** = + 10.8 (C 0.4, CHCl₃).

Synthesis of 3,4,5,6,7,8,9,10-octahydro-2*H*-pyrimido[1,2-*a*]azepin-5-ium dibenzyl ((1*S*,2*R*,3*S*,4*S*,5*S*,6*S*)-2,3,4,5,6-pentakis((3-oxido-1,5-dihydrobenzo[*e*][1,3,2]dioxaphosphepin-3-yl)oxy)cyclohexyl)diphosphate **69** and its enantiomer 3,4,5,6,7,8,9,10-octahydro-2*H*-pyrimido[1,2-*a*]azepin-5-ium dibenzyl ((1*R*,2*R*,3*R*,4*R*,5*R*,6*S*)-2,3,4,5,6-pentakis((3-oxido-1,5-dihydrobenzo[*e*][1,3,2]dioxaphosphepin-3-yl)oxy) cyclohexyl) diphosphate **68**

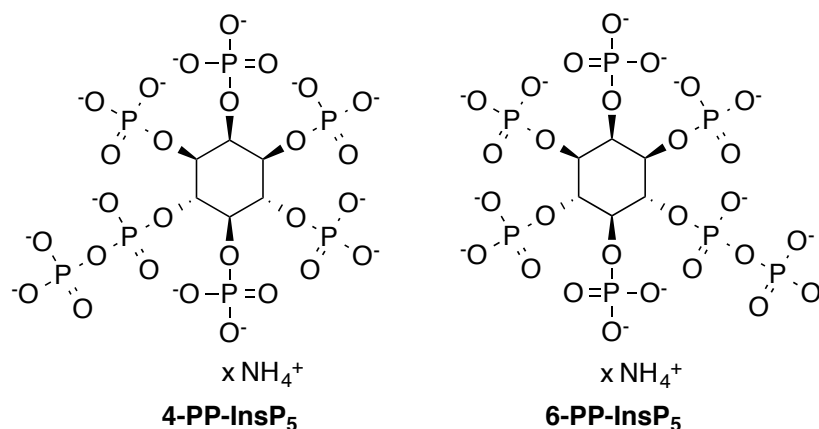


200 mg (0.14 mmol, 1.0 eq.) hexaphosphate **66** were dissolved in dry MeCN (4 mL). 84 μ L (85 mg, 0.56 mmol, 4.0 eq.) DBU were added followed by addition of 148 μ L (142 mg, 0.56 mmol, 4.0 eq.) BSTFA. The solution was stirred 10 minutes at room temperature. After completion of the deprotection (check by ^{31}P -NMR), a mixture of 140 μ L MeOH and 44 μ L (0.56 mmol, 4.0 eq.) TFA were added to the solution. The mixture was stirred for 5 min and then evaporated to dryness. The residue was taken up in 4 mL dry MeCN and 92 mg (0.28 mmol, 2.0 eq.) *bis*-benzyl *N,N*-diisopropylamino phosphoramidite and 600 μ L (0.27 mmol, 2.0 eq) 1*H*-tetrazole (0.45 M in MeCN) were added. The solution was stirred for 15 minutes at room temperature and then cooled down (0 $^{\circ}\text{C}$). Progress of the reaction was monitored by ^{31}P -NMR. After completion of the reaction, oxidation was achieved by slow (!) addition of 68.0 mg (0.28 mmol, 2.0 eq.) *m*CPBA (70% moistened with water). The reaction mixture was diluted with TBME (20 mL) and cooled to 0 $^{\circ}\text{C}$. The precipitate was filtered and washed with cold TBME and then dried *in vacuo*. The precipitate was purified by RP-18 chromatography (water/MeOH 3:1 – 1:2 v/v) and isolated by lyophilization. Yield: 152 mg **68** as a colorless solid (96.0 μ mol, 68%). The same procedure yielded the corresponding compound **69** starting from **67** in comparable

yield and purity.

¹H-NMR (400 MHz, 298 K, CDCl₃, δ/ppm): 10.95 (s, 1H), 7.50 - 7.01 (m, 30H), 5.97 - 4.72 (m, 30H), 3.42 - 3.34 (m, 2H), 3.33 - 3.19 (m, 4H), 2.85 - 2.66 (m, 2H), 1.90 - 1.80 (m, 2H), 1.69 - 1.43 (m, 6H); **¹³C-NMR** (126 MHz, 298 K, MeOD, δ/ppm): 138.1 - 136.7 (m), 135.7, 131.5 - 129.8 (m), 129.5, 129.5, 129.4, 129.1, 129.0, 115.7, 114.7, 78.8 - 18.4 (m), 75.4 - 75.2 (m), 75.0 - 74.8 (m), 74.8 - 74.6 (m), 71.7 - 70.4 (m), 70.2 - 70.0 (m), 55.9, 55.7, 55.4, 39.3, 33.7, 30.0, 27.5, 24.9, 20.4; **³¹P{¹H}-NMR** (162 MHz, 298 K, CDCl₃, δ/ppm): -1.87, -1.95, -2.29, -2.59, -3.11, -9.53 (d, *J*=12.9), -11.01 (d, *J*=12.9); **m.p.** 134- 137 °C; **IR** (neat, cm⁻¹) 2365.3, 2340.2, 2330.6, 1740.4, 1513.9, 1457.0, 1290.1, 1107.9, 1013.4, 735.7, 476.3; **R_f** (SiO₂, solvent DCM/MeOH 7:1) 0.4; **HRMS** (ESI) calcd for 1429.1491 (M⁺), found 1429.1492; **[α]_D²⁰** = + 8.2 (**69**, C 0.4, CHCl₃); - 8.8 (**68**, C 0.4, CHCl₃). The analytical data obtained for **69**, **68** were identical in all respects (besides minor concentration dependent shifts in the NMR spectra), except for the inverted optical rotations.

Synthesis of 4-diphosphoinositol-1,2,3,5,6-pentaphosphate and 6-diphosphoinositol-1,2,3,4,5- pentaphosphate



The reactions were either conducted in a stainless steel autoclave with a Teflon inlet at 80 bar H₂ (2 hours) or in a Parr apparatus at 4 bar H₂ (6 hours). The reaction is given as an example for compound **69** but was conducted the same way for compound **68**. 60.0 mg (37.9 μmol, 1.0 eq) P-anhydride **69** were dissolved in 4 mL *t*BuOH/H₂O 3:1 and mixed with 38.0 mg (0.45 mmol, 12 eq.) NaHCO₃ and 60 mg (0.56 mmol, 15 eq.) Pd

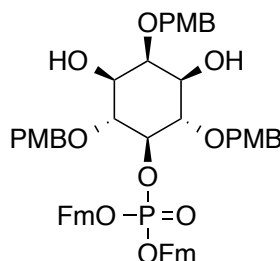
black. After 2 hours of hydrogenation (4 bar) with vigorous stirring, water was added (4 mL) and the reaction continued for another 4 hours. The catalyst was removed by centrifugation and rinsed with water (10 mL) twice. The combined aqueous fractions were extracted twice with EtOAc (10 mL) and the aqueous layer was freeze-dried. The residue was taken up in water (0.3 mL) and the product precipitated by addition of acetone (4 mL). After centrifugation, the product was purified by strong anion exchange (SAX, Q-Sepharose fast flow, Aldrich), eluting with ammonium formate from 0.5 M to 2 M. The product fractions were identified by ^{31}P -NMR, pooled and isolated by lyophilization. Yield: 22.0 mg **4-PP-InsP₅** as a colorless solid (29.7 μmol , < 78%, ammonium salt with unknown amount of counter ions. Maximal yield was calculated for completely protonated species $M = 740.01$; Minimal yield > 61% for 13 NH_4^+ ; $M = 961.41$). The same procedure yielded the corresponding **6-PP-InsP₅** starting from **68** in comparable yield and purity.

Analytical data for **4-PP-InsP₅**: ^1H -NMR (500 MHz, 298 K, D_2O , δ/ppm): 4.97 - 4.90 (m, 1H), 4.56 (ddd, $J=9.5$, $J=9.5$, $J=9.5$, 1H), 4.47 (ddd, $J=9.4$, $J=9.4$, $J=9.4$, 1H), 4.27 (ddd, $J=9.6$, $J=9.6$, $J=9.6$, 1H), 4.23 (ddd, $J=9.9$, $J=9.9$, $J=9.9$, 2H); ^{13}C -NMR (126 MHz, 298 K, D_2O , δ/ppm): 77.1 - 76.8 (m), 76.4 - 76.2 (m), 76.0 - 75.8 (m), 75.3 - 75.0 (m), 73.2 - 72.9 (m), 72.9 - 72.6 (m); $^{31}\text{P}\{^1\text{H}\}$ -NMR (202 MHz, 298 K, D_2O , δ/ppm): 1.33, 0.84, 0.75, 0.62, 0.52, -9.06 (d, $J=20.0$), -10.61 (d, $J=20.0$); ^{31}P -NMR (202 MHz, 298 K, D_2O , δ/ppm): 1.33 (d, $J=9.9$), 0.83 (d, $J=8.9$), 0.74 (d, $J=10.6$), 0.61 (d, $J=9.5$), 0.52 (d, $J=8.5$), -9.06 (d, $J=19.0$), -10.30 - (-)10.90 (m); HRMS (ESI) calcd for 379.8975 (M^{2-} , $\text{C}_6\text{H}_{16}\text{NaO}_{27}\text{P}_7^{2-}$), found 379.8978; calcd for 390.8885 (M^{2-} , $\text{C}_6\text{H}_{15}\text{Na}_2\text{O}_{27}\text{P}_7^{2-}$), found 390.8887; calcd for 412.8705 (M^{2-} , $\text{C}_6\text{H}_{13}\text{Na}_4\text{O}_{27}\text{P}_7^{2-}$), found 412.8709; $[\alpha]_{\text{D}}^{20} = +2.5$ (C 0.1, H_2O , adjusted to pH = 9 with NH_4OH), $^{33}\text{Lit.}$: $[\alpha]_{\text{D}}^{20} = +2.4$.

Analytical data for **6-PP-InsP₅**: ^1H -NMR (500 MHz, 298 K, D_2O , δ/ppm): 4.94 - 4.85 (m, 1H), 4.52 (ddd, $J=9.6$, $J=9.6$, $J=9.6$, 1H), 4.43 (ddd, $J=9.1$, $J=9.1$, $J=9.1$, 1H), 4.22 (ddd, $J=9.2$, $J=9.2$, $J=9.2$, 1H), 4.17 (ddd, $J=10.6$, $J=10.6$, $J=10.6$, 2H); ^{13}C -NMR (126 MHz, 298 K, D_2O , δ/ppm): 77.2 - 76.7 (m), 76.6 - 76.1 (m), 76.0 - 75.7 (m), 75.2 - 74.7 (m), 73.5 - 73.1 (m), 73.1 - 72.7 (m); $^{31}\text{P}\{^1\text{H}\}$ -NMR (202 MHz, 298 K, D_2O , δ/ppm): 1.47, 1.04, 0.98, 0.73, 0.54, -8.73 (d, $J=19.4$), -10.56 (d, $J=18.9$); ^{31}P -NMR (202 MHz, 298 K, D_2O , δ/ppm): 1.46 (d, $J=9.8$), 1.03 (d, $J=8.8$), 0.98 (d, $J=8.8$), 0.72 (d, $J=8.4$), 0.53 (d, $J=8.3$), -8.74 (d, $J=17.4$), -10.56 (dd, $J=17.7$, 10.9); HRMS (ESI) calcd for 245.6019 (M^{3-} , $\text{C}_6\text{H}_{16}\text{O}_{27}\text{P}_7^{3-}$), found 245.6016; $[\alpha]_{\text{D}}^{20} = -1.6$ (C 0.1, H_2O , adjusted to pH = 9 with NH_4OH), $^4\text{Lit.}$: $[\alpha]_{\text{D}}^{20} = -2.4$.

6.4 SYNTHESIS OF 1,5-(PP)₂-InsP₄ AND 3,5-(PP)₂-InsP₄

Synthesis of *meso* diol **72**



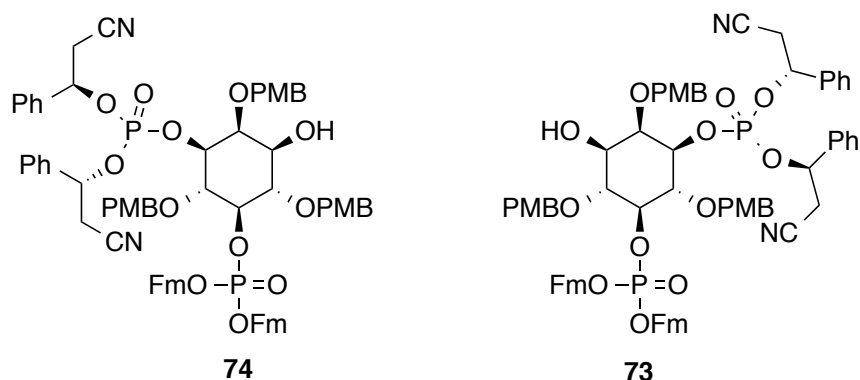
A) 5.1 g (8.2 mmol, 1.0 eq.) **14** and 5.1 g (9.8 mmol, 1.2 eq.) phosphoramidite **22** were evaporated twice with dry MeCN (5 mL) and then dissolved in dry MeCN (40 mL). After addition of 1.55 g (10.6 mmol, 1.3 eq) 5-phenyl-1*H*-tetrazole, the reaction mixture was stirred at room temperature for 2 h. The mixture was cooled down (0 °C) and 2.20 mL (12.2 mmol, 1.5 eq.) *tert*-butyl hydroperoxide solution (5.5 M in decane) were added. The mixture was stirred at this temperature for 20 min and half of the solvents were evaporated under high vacuum. The solution was diluted with ethyl acetate, washed with brine (3x), dried over MgSO₄ and the solvents were removed *in vacuo*. The crude material was directly used in the next step B).

B) The crude material (9.80 g, 9.20 mmol) was dissolved in MeOH (285 mL) and DCM (95 mL). 700 mg (3.68 mmol, 0.4 eq.) *p*TsOH were added and the solution was refluxed for 5 minutes and then again for another 5 min. The reaction was quenched by adding saturated aqueous NaHCO₃ and the mixture was extracted with Et₂O. After separation, the organic layer was washed with brine, dried over MgSO₄ and the solvents were removed *in vacuo*. Purification was achieved by gradient column chromatography (dichloromethane/ethyl acetate 8:2 until 4:6) yielding 5.23 g **72** as a sticky solid (5.35 mmol, 66%, over 2 steps).

¹H-NMR (500 MHz, 298 K, CDCl₃, δ/ppm): 7.70 – 7.64 (m, 4H), 7.45 - 7.15 (m, 18H), 6.95 - 6.92 (m, 2H), 6.83 - 6.80 (m, 4H), 4.73 - 4.70 (m, 4H), 4.59 – 4.56 (m, 2H), 4.28 - 4.18 (m, 5H), 3.96 - 3.93 (m, 3H), 3.86 - 3.85 (m, 3H), 3.77 - 3.72 (m, 8H), 3.52 - 3.49 (m, 2H); **¹³C-NMR** (126 MHz, 298 K, CDCl₃, δ/ppm): 159.4, 159.2, 143.2 (d, *J* = 8.5 Hz), 141.3, 130.6, 130.4, 129.6, 129.6, 127.7, 127.0, 125.2 (d, *J* = 5.1 Hz), 119.9 (d, *J* = 8.3 Hz), 113.9, 113.8, 80.70 (d, *J* = 7.5 Hz), 79.91 (d, *J* = 2.8 Hz), 78.4, 74.9, 73.9, 71.9, 69.2

(d, $J = 5.6$ Hz), 55.3, 55.2, 47.8 (d, $J = 8.4$ Hz); $^{31}\text{P}\{^1\text{H}\}$ -NMR (203 MHz, 298 K, CDCl_3 , δ/ppm): -2.12; IR (neat, cm^{-1}): 3384.5, 2946.7, 2906.2, 1612.2, 1513.9, 1450.2, 1247.7, 1015.3, 822.5, 741.5; R_f (SiO_2 , dichloromethane/ethyl acetate 4:6) 0.35; HRMS (ESI) calcd for $\text{C}_{58}\text{H}_{57}\text{NaO}_{12}\text{P}$ $[(\text{M}+\text{Na})^+]$ 999.3485, found 999.3483.

Synthesis of bis-phosphate triesters **73** and **74**

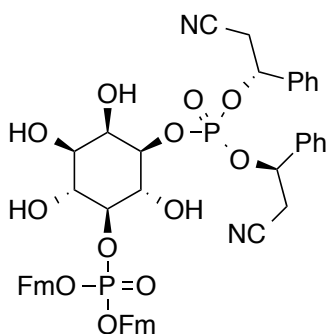


3.24 g (3.32 mmol, 3.5 eq.) PMB-protected diol **72** and 402 mg (0.95 mmol, 1.0 eq.) phosphoramidite **12** were evaporated twice with dry MeCN (3 mL) and then dissolved in dry MeCN (20 mL). After addition of 3.2 mL (1.43 mmol, 1.5 eq) 1*H*-tetrazole (0.45 M in MeCN) the reaction mixture was stirred at room temperature for 5 h. The mixture was cooled down (0 °C) and 197 mg (1.14 mmol, 1.2 eq.) *m*CPBA were added. The mixture was stirred for 10 min at this temperature and 10 min at room temperature. The solution was diluted with ethyl acetate, washed with brine (3x), dried over MgSO_4 and the solvents were removed *in vacuo*. The excess of starting material was recovered* by flash column chromatography (diethyl ether/*isopropanol* 100:1 until 9:1) yielding 874 mg of a mixture of both diastereomers (0.66 mmol, 69%, based on phosphoramidite **12**). The two diastereomers **73** and **74** were separated and purified by repeated flash column chromatographies (dichloromethane/ethyl acetate/methanol 50:50:1) and both were isolated as white solids.

*The recovered starting material **72** was again desymmetrized with phosphoramidite **12** several times, producing up to 2.7 g diastereomers **73** and **74** as a mixture, which, upon separation enabled the isolation of >1 g of each diastereomer in a purity of >90%.

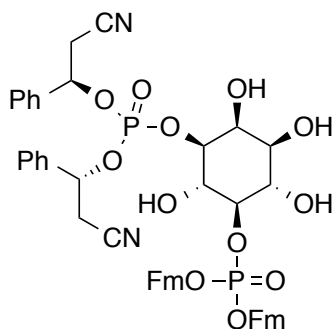
Analytical data for **73**: $^1\text{H-NMR}$ (500 MHz, 298 K, CDCl_3 , δ/ppm): 7.70 - 7.63 (m, 4H), 7.41 - 7.09 (m, 28H), 6.92 (d, $J=8.5$, 2H), 6.82 - 6.68 (m, 4H), 5.53 (ddd, $J=6.5$, $J=6.5$, $J=6.5$, 1H), 5.30 (m, 1H), 4.80 (d, $J=10.5$, 1H), 4.66 (d, $J=11.0$, 1H), 4.59 - 4.53 (m, 4H), 4.34 - 4.29 (m, 2H), 4.20 - 4.10 (m, 5H), 3.97 - 3.86 (m, 6H), 3.76 - 3.72 (m, 7H), 3.49 - 3.45 (m, 1H), 2.69 - 2.68 (m, 2H), 2.49 - 2.47 (m, 2H), 2.18 (d, $J=5.8$, 1H); $^{13}\text{C-NMR}$ (126 MHz, 298 K, CDCl_3 , δ/ppm): 159.3, 159.2, 159.1, 143.2 (d, $J = 4.9$ Hz), 143.1 (d, $J = 4.0$ Hz), 141.3 - 141.2 (m), 136.6 (d, $J = 3.1$ Hz), 136.5 (d, $J = 3.9$ Hz), 130.5, 130.4, 130.3, 129.7, 129.7, 129.6, 129.5, 129.0, 128.9, 127.7, 127.0, 127.0, 126.2, 125.9, 125.2 - 125.1 (m), 119.9, 119.8, 116.0, 115.4, 113.8, 113.8, 113.7, 80.1 (d, $J = 5.9$ Hz), 79.3 (d, $J = 2.8$ Hz), 78.7 (d, $J = 5.8$ Hz), 78.1 - 78.0 (m), 75.5 (d, $J = 4.7$ Hz), 75.1, 75.1, 74.0, 73.6, 71.0, 69.4 (d, $J = 5.6$ Hz), 55.3, 55.2 (d, $J = 3.8$ Hz), 47.8 - 47.7 (m), 26.9 (d, $J = 8.1$ Hz), 26.7 (d, $J = 6.6$ Hz); $^{31}\text{P}\{^1\text{H}\}\text{-NMR}$ (203 MHz, 298 K, CDCl_3 , δ/ppm): -2.08, -4.22; **m.p.** 81 °C; **IR** (neat, cm^{-1}): 2935.1, 1613.2, 1513.9, 1451.2, 1248.7, 1011.5, 823.5, 757.9, 741.5, 701.0, 419.4; **R_f** (SiO_2 , dichloromethane/ethyl acetate/meoh 5:5:0.1) 0.38; **HRMS** (ESI) calcd for $\text{C}_{76}\text{H}_{72}\text{N}_2\text{NaO}_{15}\text{P}_2$ $[(\text{M}+\text{Na})^+]$ 1337.4306, found 1337.4288; $[\alpha]_{\text{D}}^{20} = +11.2$ (C 0.6, CHCl_3).

Analytical data for **74**: $^1\text{H-NMR}$ (500 MHz, 298 K, CDCl_3 , δ/ppm): 7.74 - 7.62 (m, 4H), 7.42 - 7.24 (m, 21H), 7.20 - 7.14 (m, 5H), 7.10 - 7.08 (m, 2H), 6.97 - 6.96 (m, 2H), 6.84 - 6.80 (m, 4H), 5.52 (ddd, $J=6.2$, $J=6.2$, $J=6.2$, 1H), 5.27 (m, 1H), 4.76 - 4.67 (m, 4H), 4.56 - 4.48 (m, 2H), 4.22 - 4.10 (m, 6H), 3.95 - 3.90 (m, 2H), 3.87 - 3.83 (m, 5H), 3.79 - 3.75 (m, 7H), 3.46 - 3.42 (m, 1H), 2.89 (dd, $J=16.9$, 5.5, 1H), 2.66 (dd, $J=16.8$, 6.2, 1H), 2.48 (dd, $J=16.9$, 5.7, 1H), 2.35 (dd, $J=16.8$, 5.9, 1H), 2.16 (d, $J=5.5$, 1H); $^{13}\text{C-NMR}$ (126 MHz, 298 K, CDCl_3 , δ/ppm): 159.4, 159.2, 159.1, 143.2 - 143.0 (m), 141.3, 141.2, 136.6 (d, $J=3.5$), 136.5 (d, $J=2.9$), 130.6, 130.3 (d, $J=3.9$), 129.7 - 129.4 (m), 129.0 - 128.9 (m), 127.7, 127.7, 127.0 - 126.9 (m), 126.0, 126.0, 125.2 - 125.1 (m), 119.9, 119.8, 115.8, 115.6, 113.9, 113.8, 113.7, 80.2 (d, $J=6.6$), 79.2 (d, $J=2.9$), 78.1 (d, $J=6.5$), 77.8, 75.4 - 75.3 (m), 75.1, 74.2, 73.6, 71.1, 69.4 - 69.3 (m), 55.3 - 55.2 (m), 47.8 - 47.7 (m), 27.1 (d, $J=7.7$), 26.8 (d, $J=7.8$), 14.2; $^{31}\text{P}\{^1\text{H}\}\text{-NMR}$ (203 MHz, 298 K, CDCl_3 , δ/ppm): -2.08, -4.50; **m.p.** 70 °C; **IR** (neat, cm^{-1}): 3405.7, 2935.1, 2359.5, 1613.2, 1513.9, 1451.2, 1248.7, 1009.6, 821.5, 756.9, 701.0, 513.0; **R_f** (SiO_2 , dichloromethane/ethyl acetate/meoh 5:5:0.1) 0.45; **HRMS** (ESI) calcd for $\text{C}_{76}\text{H}_{72}\text{N}_2\text{NaO}_{15}\text{P}_2$ $[(\text{M}+\text{Na})^+]$ 1337.4306, found 1337.4291; $[\alpha]_{\text{D}}^{20} = +18.5$ (C 0.6, CHCl_3).

Synthesis of tetraol **75**

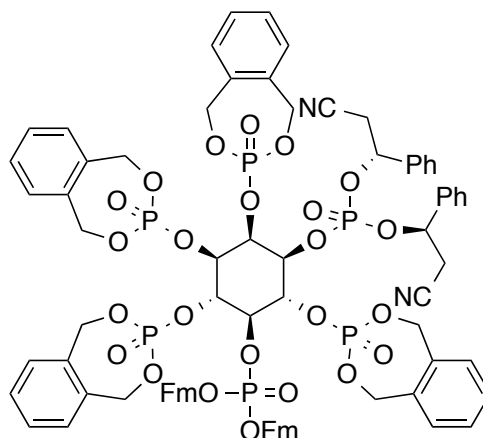
Diastereomer **73** (410 mg, 0.31 mmol) was dissolved in chloroform (20 mL) and trifluoroacetic acid (1.0 mL, 5% v/v) was added to the solution. After stirring for 4 h at room temperature, hexane (5 mL) was added and the solvents were removed *in vacuo*. The residue was dissolved in dichloromethane and methanol (5 mL) and crystallization by addition of diethyl ether and TBME (ca. 5 mL, until the solution becomes turbid, 0 °C, overnight) yielded compound **75** as a white solid (210 mg, 0.22 mmol, 71%).

¹H-NMR (500 MHz, 298 K, DMSO, δ /ppm): 7.87 - 7.85 (m, 4H), 7.62 - 7.56 (m, 4H), 7.41 - 7.26 (m, 18H), 5.75 - 5.71 (m, 1H), 5.67 - 5.63 (m, 1H), 4.34 - 4.18 (m, 8H), 4.06 - 4.01 (m, 2H), 3.90 - 3.86 (m, 2H), 3.77 - 3.65 (m, 3H), 3.29 - 3.18 (m, 5H); **¹³C-NMR** (126 MHz, 298 K, DMSO, δ /ppm): 143.9 - 143.8 (m), 141.3 - 141.2 (m), 138.1 (d, $J=4.3$), 138.0 (d, $J=4.8$), 129.2 (d, $J=7.8$), 128.9 (d, $J=8.1$), 128.1, 127.4, 126.7, 126.5, 125.7 - 125.6 (m), 120.5, 117.4, 82.7 (d, $J=6.5$), 79.8 (d, $J=6.0$), 74.8 (d, $J=5.7$), 74.4 (d, $J=4.6$), 71.3 - 71.1 (m), 70.0 - 69.9 (m), 68.8 - 68.7 (m), 49.2, 47.9 - 47.8 (m), 27.3, 26.6-26.4 (m); **³¹P{¹H}-NMR** (203 MHz, 298 K, DMSO, δ /ppm): -1.93, -4.46; **m.p.** 165 - 167 °C; **IR** (neat, cm^{-1}): 2361.4, 2174.4, 2163.7, 2010.4, 1974.8, 1025.0; **R_f** (SiO₂, ethyl acetate/methanol 10:1) 0.24; **HRMS** (ESI) calcd for C₅₂H₄₈N₂NaO₁₂P₂ [(M+Na)⁺] 977.2580, found 977.2568; **[α]_D²⁰** = +1.3 (C 0.45, DMSO).

Synthesis of tetraol **76**

Diastereomer **74** (490 mg, 0.37 mmol) were dissolved in chloroform (24 mL) and trifluoroacetic acid (1.2 mL, 5% v/v) was added to the solution. After stirring for 3.5 h at room temperature, hexane (5 mL) was added and the solvents were removed *in vacuo*. The residue was dissolved in dichloromethane and methanol (5 mL) and crystallization by addition of TBME (ca. 5 mL, until the solution becomes turbid, 0 °C, overnight) yielded compound **76** as a white solid (248 mg, 0.26 mmol, 70%).

¹H-NMR (500 MHz, 298 K, DMSO, δ /ppm): 7.88 - 7.85 (m, 4H), 7.61 - 7.57 (m, 4H), 7.42 - 7.26 (m, 18H), 5.74 (d, J =6.7, 1H), 5.71 - 5.65 (m, 2H), 5.32 (s, 1H), 5.20 (s, 1H), 5.00 (s, 1H), 4.35 - 4.15 (m, 7H), 4.10 - 4.04 (m, 2H), 3.92 - 3.86 (m, 1H), 3.69 - 3.65 (m, 1H), 3.40 - 3.25 (m, 3H), 3.22 - 3.16 (m, 2H); **¹³C-NMR** (126 MHz, 298 K, DMSO, δ /ppm): 143.9 - 143.8 (m), 141.3, 141.2, 138.1 (2xd, J =4.7), 129.2 (d, J =6.3), 128.9, 128.8, 128.1, 127.5, 127.5, 126.7, 126.4, 125.7, 125.7, 125.7, 120.5, 117.4, 82.6 - 82.5 (m), 79.7 (d, J =6.3), 74.9 (d, J =6.0), 74.3 (d, J =4.5), 71.3 (d, J =3.0), 71.0 (d, J =4.2), 70.0 - 69.9 (m), 68.8 - 68.7 (m), 47.9 - 47.8 (m), 26.7 - 26.5 (m); **³¹P{¹H}-NMR** (203 MHz, 298 K, DMSO, δ /ppm): -1.96, -4.57; **m.p.** 180 °C; **IR** (neat, cm^{-1}): 2358.5, 2341.2, 1698.0, 1558.2, 1507.1, 1260.3, 1014.4; **R_f** (SiO₂, ethyl acetate/methanol 10:1) 0.30; **HRMS (ESI)** calcd for C₅₂H₄₈N₂NaO₁₂P₂ [(M+Na)⁺] 977.2580, found 977.2562; **[α]_D²⁰** = +21.1 (C 0.46, DMSO).



- * long FC leads to decomposition

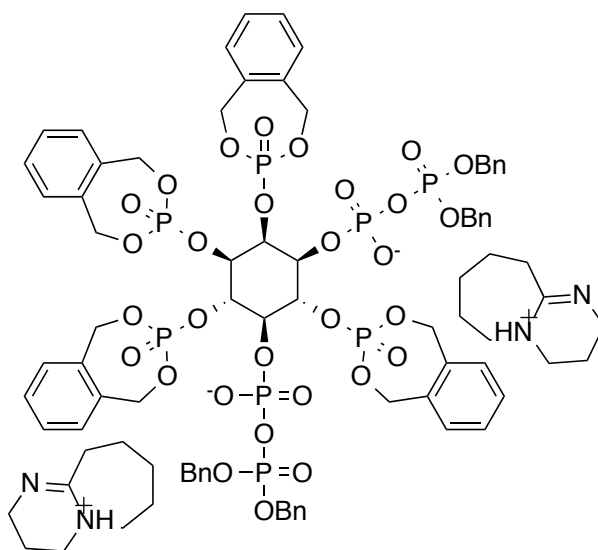
123

- * long FC leads to decomposition

124

143.2 (d, $J=8.2$), 142.8 (d, $J=3.1$), 141.4, 141.3, 140.4, 136.3 (d, $J=5.6$), 135.8 (d, $J=2.8$), 135.2 - 135.1 (m), 134.9 - 134.8 (m), 134.7, 134.5, 129.7 (d, $J=4.9$), 129.6, 129.5, 129.4 (d, $J=4.2$), 129.2 - 129.0 (m), 128.8 - 128.6 (m), 128.1 (d, $J=5.1$), 127.9 (d, $J=2.6$), 127.3 (d, $J=4.3$), 127.2 (d, $J=2.6$), 125.8 (d, $J=2.9$), 125.4 (d, $J=2.7$), 125.2, 125.1, 120.1, 120.1, 117.4, 115.9, 76.6, 76.5, 75.9 (d, $J=7.1$), 75.7, 75.6, 73.5 - 73.2 (m), 69.9 - 68.8 (m), 47.9 - 47.8 (m), 27.6 (d, $J=7.1$), 27.2 (d, $J=4.2$); $^{31}\text{P}\{^1\text{H}\}$ -NMR (203 MHz, 298 K, CDCl_3 , δ/ppm): -1.10, -1.42, -2.85, -3.20, -3.25, -4.81; **m.p.** 123 °C; **IR** (neat, cm^{-1}): 1292.1, 1049.1, 1022.1, 850.5, 757.9, 735.7, 456.1; **R_f** (SiO_2 , ethyl acetate) 0.53; **HRMS** (ESI) calcd for $\text{C}_{84}\text{H}_{76}\text{N}_2\text{NaO}_{24}\text{P}_6$ $[(\text{M}+\text{Na})^+]$ 1705.3111, found 1706.3150; $[\alpha]_{\text{D}}^{20} = +4.6$ (C 2.7, CHCl_3).

Synthesis of protected 1,5-IP₈ **79**

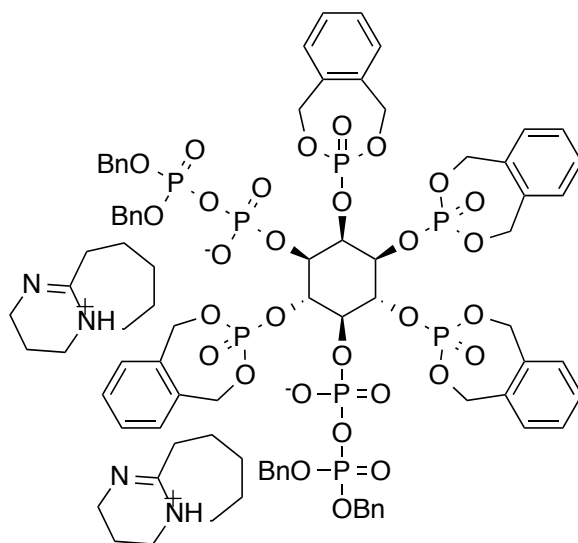


Hexakisphosphate derivative **77** (50 mg, 0.03 mmol, 1.0 eq.) was evaporated twice with dry MeCN (0.2 mL) and then dissolved in dry MeCN (1.5 mL). 36.0 μL (37.0 mg, 0.24 mmol, 8.0 eq.) DBU and 65 μL (62 mg, 0.24 mmol, 8.0 eq.) BSTFA were added. The solution was stirred 20 min at room temperature. After completion of the deprotection (checked by ^{31}P -NMR), 65 μL MeOH and 18.0 μL (27.0 mg, 0.24 mmol, 8.0 eq.) TFA were added simultaneously to the solution. The mixture was stirred for 30 min and then evaporated to dryness. The residue was dissolved again in dry MeCN (1.5 mL) and 40 μL (41 mg, 0.12 mmol, 4.0 eq.) *bis*-benzyl *N,N*-diisopropylamino phosphoramidite **20** and

0.27 mL (0.12 mmol, 4.0 eq.) 1*H*-tetrazole (0.45 M in MeCN) were added. The solution was stirred for 20 minutes at room temperature. Progress of the reaction was monitored by ³¹P-NMR. After completion of the reaction, oxidation was achieved by addition of 21 mg (0.12 mmol, 4.0 eq.) *m*CPBA at 0 °C. The mixture was stirred 10 min at this temperature and 10 min at room temperature. Solvents were removed *in vacuo* and the residue was dissolved in dichloromethane (1 mL). Crystallization by addition of diethyl ether (ca. 0.5 mL, added until the precipitate starts to form, 0 °C, overnight) yielded compound **79** (50 mg, 0.026 mmol, 87%) as a colorless hygroscopic solid.

¹H-NMR (500 MHz, 298 K, CDCl₃, δ/ppm): 10.77 (DBU), 8.93 (DBU), 7.37 - 6.98 (m, 36H), 5.86 - 4.73 (m, 30H), 3.36 - 3.29 (m, 16H, DBU), 2.71 - 2.69 (m, 5H, DBU), 1.87 - 1.85 (m, 5H, DBU), 1.60 - 1.57 (m, 16H, DBU), 1.29 - 1.25 (m, 5H, DBU); **¹³C-NMR** (126 MHz, 298 K, CDCl₃, δ/ppm): 166.4, 143.3, 136.2 - 135.6 (m), 135.0, 134.3, 132.7, 132.5, 129.9, 129.6, 129.3 - 128.7 (m), 128.5 - 128.1 (m), 127.9, 127.5, 74.3 - 74.2 (m), 72.5 - 72.4 (m), 69.7 - 69.0 (m), 54.4 (DBU), 48.6 (DBU), 38.2 (DBU), 32.5 (DBU), 28.9 (DBU), 26.7 (DBU), 23.8 (DBU), 19.4 (DBU);* **³¹P{¹H}-NMR** (162 MHz, 298 K, CDCl₃, δ/ppm): -0.68, -1.25, -1.95, -2.53, -9.77 (d, *J*=12.6), -9.83 (d, *J*=13.9), -11.65 (d, *J*=12.5), -12.01 (d, *J*=14.0); **IR** (neat, cm⁻¹): 3040.2, 2936.1, 1646.9, 1456.0, 1288.2, 1051.0, 1021.1, 848.5, 736.7; **R_f** (SiO₂, dichloromethane/methanol 8:1.5) 0.46; **HRMS** (ESI) calcd for C₆₆H₆₆NaO₃₀P₈⁻ [(M+Na)] 1609.1430, found 1609.1429; [α]_D²⁰ = +3.6 (C 2.0, CHCl₃).

* ¹H NMR and ¹³C NMR indicate the presence of TFA-DBU salt.

Synthesis of protected 3,5-IP₈ **80**

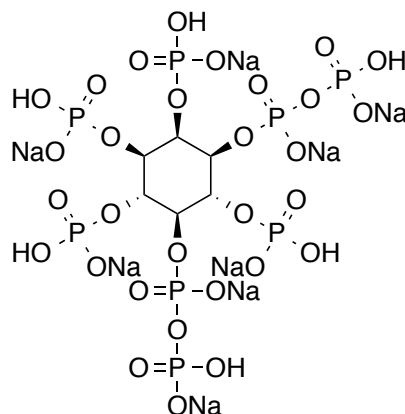
Hexakisphosphate derivative **78** (100 mg, 0.059 mmol, 1.0 eq.) was evaporated twice with dry MeCN (0.3 mL) and then dissolved in dry MeCN (2.5 mL). 71.0 μ L (72.0 mg, 0.47 mmol, 8.0 eq.) DBU and 126 μ L (121 mg, 0.47 mmol, 8.0 eq.) BSTFA were added. The solution was stirred 20 min at room temperature. After completion of the deprotection (checked by ^{31}P -NMR), 125 μ L MeOH and 36.0 μ L (54.0 mg, 0.47 mmol, 8.0 eq.) TFA were added simultaneously to the solution. The mixture was stirred for 30 min and then evaporated to dryness. The residue was dissolved again in dry MeCN (2.5 mL) and 80 μ L (82 mg, 0.24 mmol, 4.0 eq.) *bis*-benzyl *N,N*-diisopropylamino phosphoramidite **20** and 0.5 mL (0.24 mmol, 4.0 eq.) 1*H*-tetrazole (0.45 M in MeCN) were added. The solution was stirred for 20 minutes at room temperature. Progress of the reaction was monitored by ^{31}P -NMR. After completion of the reaction, oxidation was achieved by addition of 41.0 mg (0.24 mmol, 4.0 eq.) *m*CPBA at 0 °C. The mixture was stirred 10 min at this temperature and 10 min at room temperature. Solvents were removed *in vacuo* and the residue was dissolved in dichloromethane (2 mL). Crystallization from diethyl ether (ca. 1 mL, added until the precipitate starts to form, 0 °C, overnight) yielded compound **79** (110 mg, 0.058 mmol, 98%) as a colorless hygroscopic solid.

^1H -NMR (500 MHz, 298 K, CDCl_3 , δ /ppm): 11.03 (DBU), 8.84 (DBU), 7.36 - 6.97 (m, 36H), 5.87 - 4.73 (m, 30 H), 3.42 - 3.35 (m, 23H, DBU), 2.73 - 2.71 (m, 8H, DBU), 1.94 - 1.90 (m, 8H, DBU), 1.65 - 1.61 (m, 24H, DBU), 1.31 - 1.29 (m, 6H); ^{13}C -NMR (126 MHz, 298 K, CDCl_3 , δ /ppm): 166.4, 144.0, 136.1 - 135.9 (m), 135.7 - 135.6 (m), 135.4, 135.0,

134.9, 134.1, 131.8, 129.8, 129.4 - 128.7 (m), 128.5 - 128.4 (m), 128.3 - 128.2 (m), 128.1 - 128.0 (m), 127.9 - 127.8 (m), 127.6, 127.5, 74.3 - 74.1 (m), 73.3 - 73.2 (m), 72.5 - 72.4 (m), 69.8 - 69.0 (m), 68.29 (d, $J = 5.7$ Hz), 67.48 (d, $J = 5.7$ Hz), 54.4 (DBU), 48.6 (DBU), 47.2, 38.2 (DBU), 32.6 (DBU), 28.9 (DBU), 26.7 (DBU), 23.8 (DBU), 19.4 (DBU), 19.3 (d, $J = 3.5$); * $^{31}\text{P}\{^1\text{H}\}$ -NMR (162 MHz, 298 K, CDCl_3 , δ/ppm): -0.54, -0.95, -1.80, -2.33, -9.77 (d, $J = 12.3$), -9.83 (d, $J = 13.9$), -11.80 (d, $J = 12.3$), -12.12 (d, $J = 13.9$); IR (neat, cm^{-1}): 2931.3, 1646.0, 1456.0, 1289.2, 1051.0, 1021.1, 844.7, 810.9, 739.6; R_f (SiO_2 , dichloromethane/methanol 8:1.5) 0.44; HRMS (ESI) calcd for $\text{C}_{66}\text{H}_{67}\text{O}_{30}\text{P}_8^-$ [(M+H)] 1587.1624, found 1587.1625; $[\alpha]_D^{20} = -3.8$ (C 0.5, CHCl_3).

* ^1H NMR and ^{13}C NMR indicate the presence of TFA-DBU salt.

Synthesis of 1,5-InsP₈ (octasodium salt)



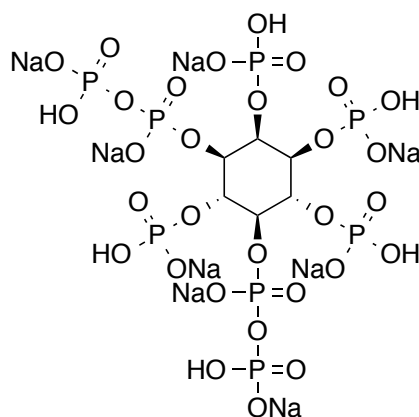
Protected bis-P-anhydride **79** (30 mg, 0.016 mmol, 1.0 eq.) was dissolved in *tert*-butanol/water 3:1 (1.0 mL). To this solution 11 mg (0.13 mmol, 8.0 eq.) NaHCO_3 and 100 mg (0.094 mmol, 6 eq.) Pd (10 wt. %, on carbon) were added. After 1 hour of hydrogenation at 180 bar in a steel autoclave, 0.4 mL water were added to the mixture and the hydrogenation was continued for another 2 hours. The mixture was centrifuged and the supernatant removed. The catalyst was washed with water (1 mL) and to this washing fraction, acetone (10 mL) was added. The precipitate was isolated by centrifugation yielding the octasodium salt of 1,5-InsP₈ (11 mg, 0.011 mmol, 69%) as a colorless solid.

^1H -NMR (500 MHz, 298 K, D_2O , water suppression, δ/ppm): 4.62 - 4.56 (m, 2H), 4.47 -

4.40 (m, 4H); **¹³C-NMR** (126 MHz, 298 K, D₂O, δ/ppm): 75.16 - 75.11 (m), 73.39 - 73.25 (m), 73.04 - 72.96 (m), 72.07 - 71.97 (m), 65.84 - 65.69 (m); **³¹P{¹H}-NMR** (203 MHz, 298 K, D₂O, δ/ppm): 4.59, 3.63, 3.27, 3.19, -4.33 – (-4.47) (m, 2P), -9.13 – (-9.21) (m, 1P), -9.74 – (-9.82) (m, 1P); **³¹P NMR** (203 MHz, 298 K, D₂O, δ/ppm): 4.59 (d, *J*=12.1), 3.63 (d, *J*=10.4), 3.30 – 3.16 (m), -4.33 - -4.48 (m, 2P), -9.19 – (-9.86) (m, 2P); **HRMS** (ESI) calcd for C₆H₁₇O₃₀P₈³⁻ 272.2574, found 272.2579; calcd for C₆H₁₈O₃₀P₈²⁻ 408.8897, found 408.8895.

Optical rotation data was inconclusive due to very small values that were distributed around 0. This data is therefore not reported.

Synthesis of 3,5-InsP₈ (octasodium salt)



Protected bis-P-anhydride **80** (30 mg, 0.016 mmol, 1.0 eq.) was dissolved in *tert*-butanol/water 3:1 (1.0 mL). To this solution 11 mg (0.128 mmol, 8.0 eq.) NaHCO₃ and 100 mg (0.094 mmol, 5.9 eq.) Pd (10 wt. %, on carbon) were added. After 1 hour of hydrogenation at 180 bar in a steel autoclave, 0.4 mL water were added to the mixture and the hydrogenation continued for another 2 hours. The mixture was centrifuged and the supernatant removed. The catalyst was washed with water (1 mL) and to this washing fraction, acetone (10 mL) was added. The precipitate was isolated by centrifugation yielding the octasodium salt of 3,5-InsP₈ (12 mg, 0.012 mmol, 75%) as a white solid.

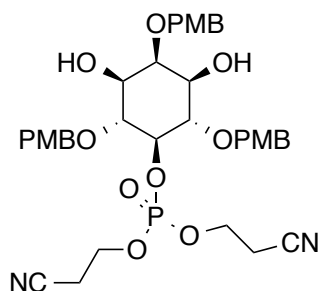
¹H-NMR (500 MHz, 298 K, D₂O, water suppression, δ/ppm): 4.59 - 4.53 (m, 2H), 4.43 (m, 4H); **¹³C NMR** (126 MHz, 298 K, D₂O, δ/ppm): 75.4 - 75.1 (m), 73.5 - 73.3 (m), 73.3 -

73.1 (m), 72.2 - 72.0 (m), 66.0 - 65.7 (m); $^{31}\text{P}\{^1\text{H}\}$ -NMR (203 MHz, 298 K, D_2O , δ/ppm): 4.56, 3.52, 3.17, 3.05, -4.62 – (-4.70) (m, 2P), -9.54 – (-9.62) (m, 1P), -9.87 – (-9.95) (m, 1P); ^{31}P -NMR (203 MHz, 298 K, D_2O , δ/ppm): 4.55 (d, $J=12.4$), 3.51 (d, $J=10.4$), 3.20 – 3.02 (m, 2P), -4.62 – (-4.71) (m, 2P), -9.54 – (-9.56) (m, 1P), -9.91 – (-9.96) (m, 1P); HRMS (ESI) calcd for $\text{C}_6\text{H}_{17}\text{O}_{30}\text{P}_8^{3-}$ 272.2574, found 272.2579; calcd for $\text{C}_6\text{H}_{16}\text{Na}_2\text{O}_{30}\text{P}_8^{2-}$ 430.8717, found 430.8711; calcd for $\text{C}_6\text{H}_{15}\text{Na}_3\text{O}_{30}\text{P}_8^{2-}$ 441.8627, found 441.8625; calcd for $\text{C}_6\text{H}_{14}\text{Na}_4\text{O}_{30}\text{P}_8^{2-}$ 452.8536, found 452.8535.

Optical rotation data was inconclusive due to very small values that were distributed around 0. This data is therefore not reported.

6.5 SYNTHESIS OF 5-PP-InsP₅ AND 5-PPP-InsP₅

Synthesis of **16**

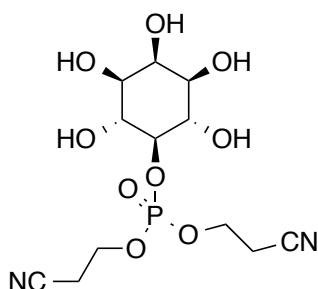


A) 2.10 g (3.34 mmol, 1.0 eq.) **14** and 1.09 g (4.01 mmol, 1.2 eq.) phosphoramidite **11** were evaporated twice with dry MeCN (2 mL) and then dissolved in dry MeCN (5 mL). After addition of 9.5 mL (4.34 mmol, 1.3 eq.) 1*H*-tetrazole (0.45 M in MeCN), the reaction mixture was stirred at room temperature for 1.5 h. The mixture was cooled down (0 °C) and 0.9 mL (5.01 mmol, 1.5 eq.) *tert*-butyl hydroperoxide solution (5.5 M in decane) were added. The mixture was stirred at this temperature for 5 minutes, then at room temperature for 20 min and half of the solvents were evaporated under high vacuum. The solution was diluted with ethyl acetate, washed with brine (3x), dried over MgSO_4 and the solvents were removed *in vacuo*. The crude material was directly used in the next step B). B) The crude material (3.34 g, 4.10 mmol) was dissolved in MeOH (105 mL) and DCM (35 mL). 282 mg (1.64 mmol, 0.4 eq.) *p*TsOH were added and the solution was refluxed for 5 minutes and then again for another 5 min. The reaction was diluted with ethyl

acetate and washed with saturated aqueous NaHCO_3 (3x). After separation, the organic layer was washed with brine, dried over MgSO_4 and the solvents were removed *in vacuo*. Purification was achieved by column chromatography (dichloromethane/methanol 50:1) yielding 1.40 g **16** as an oil (1.93 mmol, 58%, over 2 steps).

^1H -NMR (500 MHz, 298 K, CDCl_3 , δ/ppm): 7.36 – 7.32 (m, 4H), 7.27 – 7.23 (m, 2H), 6.93 – 6.87 (m, 6H), 4.80 – 4.72 (m, 6H), 4.34 – 4.27 (m, 1H), 4.15 – 4.07 (m, 2H), 4.04 – 3.94 (m, 3H), 3.83 – 3.75 (m, 11H), 3.60 – 3.57 (m, 2H), 2.49 – 2.34 (m, 4H); **^{13}C -NMR** (126 MHz, 298 K, CDCl_3 , δ/ppm): 159.5, 159.4, 130.3, 130.2, 129.7, 116.5, 114.0, 113.9, 79.9 (d, $J = 3.1$ Hz), 78.6, 75.1, 74.0, 72.1, 62.2 (d, $J = 4.8$ Hz), 55.3, 19.4, 19.3; **$^{31}\text{P}\{^1\text{H}\}$ -NMR** (162 MHz, 298 K, CDCl_3 , δ/ppm): -1.40; **IR** (neat, cm^{-1}): 3424.0, 2936.1, 2837.7, 1612.2, 1512.9, 1246.8, 1073.2, 1025.9, 821.5, 729.0; **R_f** (SiO_2 , dichloromethane/ethyl acetate 1:1) 0.24; **HRMS** (ESI) calcd for $\text{C}_{36}\text{H}_{43}\text{N}_2\text{NaO}_{12}\text{P}$ $[(\text{M}+\text{Na})^+]$ 749.2446, found 749.2441.

Synthesis of **17**

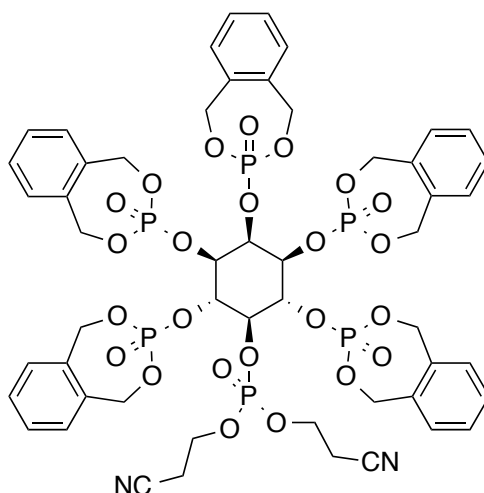


Meso compound **16** (650 mg, 0.89 mmol) was dissolved in chloroform (55 mL) and trifluoroacetic acid (2 mL, 3.6% v/v) was added to the solution. The reaction was stirred at room temperature with formation of a white precipitate. After stirring the solution for 4 h, hexane was added and the solvents were removed *in vacuo*. The residue was partially dissolved in dichloromethane and methanol and crystallization by addition of TBME and hexane (0 °C, overnight) yielded compound **17** as a white solid (280 mg, 0.76 mmol, 85%).

^1H -NMR (500 MHz, 298 K, DMSO, δ/ppm): 4.98 – 4.67 (m, 4H), 4.26 – 4.16 (m, 4H), 3.94 – 3.88 (m, 1H), 3.71 – 3.70 (m, 1H), 3.58 – 3.54 (m, 2H), 3.34 – 3.32 (m, 1H), 3.21 – 3.18 (m, 2H), 2.91 – 2.89 (m, 4H); **^{13}C -NMR** (126 MHz, 298 K, DMSO, δ/ppm): 118.8, 84.1 (d, $J = 7.1$ Hz), 72.9, 71.9, 71.6 (d, $J = 3.0$ Hz), 62.4 (d, $J = 5.0$ Hz), 19.4 (d, $J = 7.6$ Hz);

$^{31}\text{P}\{^1\text{H}\}$ -NMR (203 MHz, 298 K, DMSO, δ /ppm): -2.45; **IR** (neat, cm^{-1}): 3389.3, 3295.8, 2360.4, 1255.4, 1045.2; **HRMS** (ESI) calcd for $\text{C}_{12}\text{H}_{19}\text{N}_2\text{NaO}_9\text{P}$ $[(\text{M}+\text{Na})^+]$ 389.0720, found 389.0720.

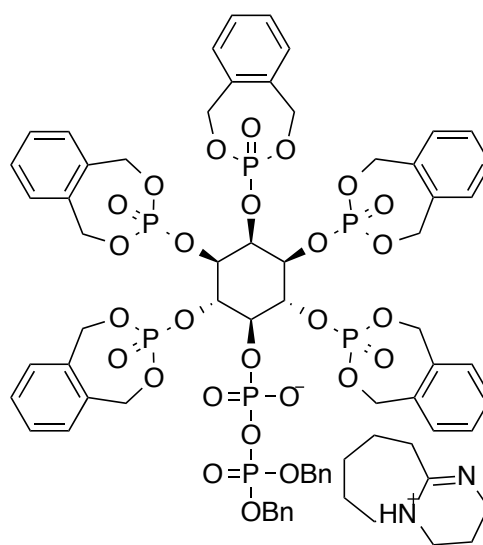
Synthesis of **19**



17 (280 mg, 0.76 mmol, 1.0 eq.) and *o*-xylene *N,N*-diisopropylamino phosphoramidite **18** (1.83 g, 6.84 mmol, 9.0 eq.) were evaporated twice with dry acetonitrile (3-5 mL). Dry MeCN (60 mL) was added and the mixture cooled down (0 °C). The residue was not completely soluble. To this mixture 1.62 g (13.7 mmol, 18.0 eq.) 4,5- dicyanoimidazole (DCI) were added and the residue started to dissolve. Progress of the reaction was monitored by ^{31}P -NMR. After completion of the reaction (4 h), oxidation was achieved by addition of 1.18 g (6.84 mmol, 9.0 eq.) *m*CPBA at 0 °C. The mixture was stirred for 10 min at this temperature and 10 min at room temperature. The reaction mixture was diluted with DCM, washed with brine, dried over MgSO_4 and the solvents were removed *in vacuo*. Crystallization from dichloromethane/diethyl ether (diethyl ether added until the solution becomes turbid, 0 °C, overnight) and purification by gradient column chromatography (ethyl acetate/methanol 1%-8%) yielded 580 mg **19** as a white solid (0.45 mmol, 59%).

^1H -NMR (500 MHz, 298 K, CDCl_3 , δ /ppm): 7.39 – 7.25 (m, 20H), 5.71 – 5.57 (m, 5H), 5.46 – 5.36 (m, 6H), 5.24 – 5.07 (m, 12H), 5.00 – 4.96 (m, 2H), 4.85 – 4.79 (m, 1H), 4.45 – 4.35 (m, 4H), 2.86 – 2.75 (m, 4H); **^{13}C -NMR** (126 MHz, 298 K, CDCl_3 , δ /ppm): 140.4,

135.3, 135.2, 135.2, 134.9, 134.5, 129.6 - 129.0 (m), 117.0, 110.8, 76.5, 73.6, 69.5 - 69.3 (m), 63.1 (d, $J = 5.4$ Hz), 21.1, 19.5, 19.4 (d, $J = 8.3$ Hz); $^{31}\text{P}\{^1\text{H}\}$ -NMR (203 MHz, 298 K, CDCl_3 , δ/ppm): -2.10 (2P), -3.14, -3.52 (2P), - 4.08; IR (neat, cm^{-1}): 1288.2, 1225.5, 1050.1, 1021.1, 878.4, 860.1, 731.9; R_f (SiO_2 , ethyl acetate/methanol 20:1) 0.22; HRMS (ESI) calcd for $\text{C}_{52}\text{H}_{54}\text{N}_2\text{NaO}_{24}\text{P}_6$ $[(\text{M}+\text{Na})^+]$ 1299.1384, found 1299.1383;

Synthesis of **21**

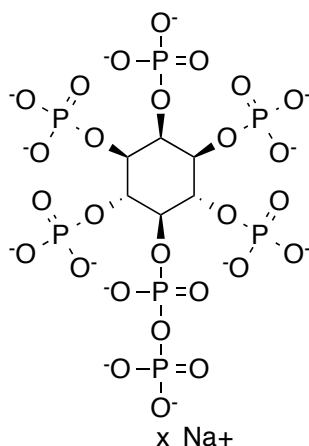
Hexakisphosphate derivative **19** (100 mg, 0.078 mmol, 1.0 eq.) was evaporated twice with dry MeCN (0.3 mL) and then dissolved in dry MeCN (3 mL). 46.0 μL (47.0 mg, 0.31 mmol, 4.0 eq.) DBU and 83 μL (80 mg, 0.31 mmol, 4.0 eq.) BSTFA were added. The solution was stirred 20 min at room temperature. After completion of the deprotection (checked by ^{31}P -NMR), 80 μL MeOH and 24.0 μL (36.0 mg, 0.31 mmol, 4.0 eq.) TFA were added simultaneously to the solution. The mixture was stirred for 30 min and then evaporated to dryness. The residue was dissolved again in dry MeCN (3 mL) slowly a precipitate was formed. DMF (3 mL) was added and the mixture was stirred until the residue dissolved. 52 μL (54 mg, 0.16 mmol, 2.0 eq.) *bis*-benzyl *N,N*-diisopropylamino phosphoramidite **20** and 0.35 mL (0.16 mmol, 2.0 eq.) 1*H*-tetrazole (0.45 M in MeCN) were added. The solution was stirred for 20 minutes at room temperature. Progress of the reaction was monitored by ^{31}P -NMR. After completion of the reaction, oxidation was achieved by addition of 27 mg (0.16 mmol, 2.0 eq.) *m*CPBA at 0 °C. The mixture was

stirred 10 min at this temperature and 10 min at room temperature. Crystallization by addition of diethyl ether (added until the precipitate starts to form, 0 °C, overnight) yielded compound **21** (85 mg, 0.054 mmol, 69%) as a colorless solid.

¹H-NMR (500 MHz, 298 K, CDCl₃, δ/ppm): 11.01 (DBU), 8.83 (DBU), 7.39 – 7.20 (m, 28H), 7.06 – 7.04 (m, 2H), 5.74 – 5.64 (m, 4H), 5.58 – 5.41 (m, 7H), 5.29 – 4.93 (m, 19H), 3.35 – 3.27 (m, 7H, DBU), 2.72 – 2.70 (m, 3H, DBU), 1.87 – 1.82 (m, 3H, DBU), 1.64 – 1.52 (m, 8H, DBU), 1.28 – 1.27 (m, 2H); **¹³C-NMR** (126 MHz, 298 K, CDCl₃, δ/ppm): 166.3, 162.6, 136.3 – 135.6 (m), 134.9, 129.4 – 128.8 (m), 128.4, 128.1, 127.9, 74.0, 69.4 – 69.1 (m), 54.3 (DBU), 48.6 (DBU), 47.3, 38.2 (DBU), 32.4 (DBU), 29.0 (DBU), 26.7 (DBU), 23.9 (DBU), 19.4 (DBU) 19.4;* **³¹P{¹H}-NMR** (162 MHz, 298 K, CDCl₃, δ/ppm): -2.60 (2P), -3.17, -3.59 (2P), -11.08 (d, J=12.8), -12.81 (d, J=13.0); **IR** (neat, cm⁻¹): 2936.1, 1646.9, 1457.0, 1288.2, 1224.6, 1049.1, 1020.2, 977.7, 846.6, 732.8; **HRMS** (ESI) calcd for C₆₀H₆₀O₂₇P₇⁻ 1429.1491, found 1429.1488.

* ¹H NMR and ¹³C NMR indicate the presence of TFA-DBU salt.

Synthesis of **5-PP-InsP₅**

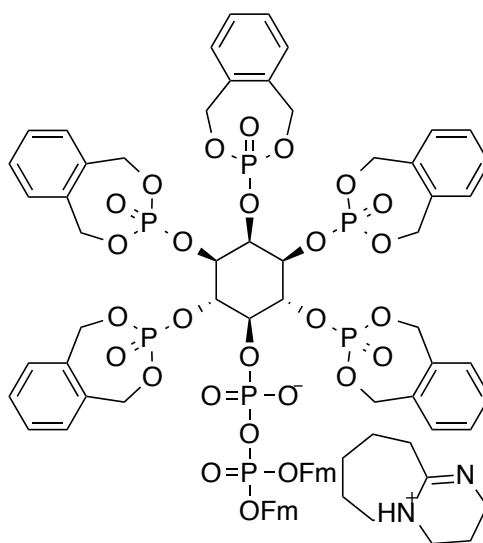


Protected P-anhydride **21** (20 mg, 0.013 mmol, 1.0 eq.) was dissolved in *tert*-butanol/water 3:1 (1.0 mL). To this solution 9 mg (0.104 mmol, 8.0 eq.) NaHCO₃ and 80 mg (0.078 mmol, 6 eq.) Pd (10 wt. %, on carbon) were added. After 1 hour of hydrogenation at 180 bar in a steel autoclave, 0.4 mL water were added to the mixture and the hydrogenation continued for another 2 hours. The mixture was centrifuged and

the supernatant removed. The catalyst was washed with water and to this washing fraction, acetone was added (ratio 1:8). The precipitate was isolated by centrifugation yielding **5-PP-InsP₅** (5.4 mg, 0.006 mmol, 46%) as a white solid.

³¹P{¹H}-NMR (203 MHz, 298 K, D₂O, δ/ppm): 1.68 (2P), 1.14, 0.79 (2P), -7.09, -9.84 – (-9.94) (m, 1P); **HRMS** (ESI) calcd for C₆H₁₇O₂₇P₇²⁻ 368.9066, found 368.9071.

Synthesis of **23**

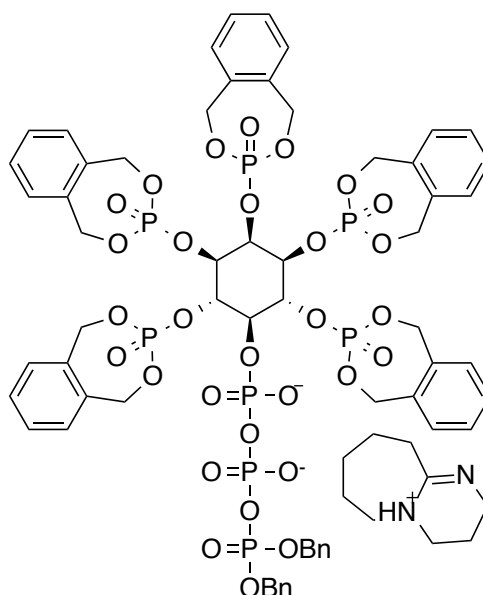


Hexakisphosphate derivative **19** (100 mg, 0.078 mmol, 1.0 eq.) was evaporated twice with dry MeCN (0.3 mL) and then dissolved in dry MeCN (3 mL). 46.0 μL (47.0 mg, 0.31 mmol, 4.0 eq.) DBU and 83 μL (80 mg, 0.31 mmol, 4.0 eq.) BSTFA were added. The solution was stirred 30 min at room temperature. After completion of the deprotection (checked by ³¹P-NMR), 80 μL MeOH and 24.0 μL (36.0 mg, 0.31 mmol, 4.0 eq.) TFA were added simultaneously to the solution. The mixture was stirred for 30 min and then evaporated to dryness. The residue was dissolved in dry DMF (1.5 mL) and the mixture was stirred until the residue dissolved completely. 1.4 mL (0.62 mmol, 8.0 eq.) 1*H*-tetrazole (0.45 M in MeCN) were added. Then a solution of 81 mg (0.16 mmol, 2.0 eq.) (FmO)₂PN(*i*Pr)₂ **22** in DMF (1.5 mL) previously coevaporated with acetonitrile (0.2 mL) was added. The solution was stirred for 40 minutes at room temperature. Progress of the reaction was monitored by ³¹P-NMR. After completion of the reaction, oxidation was achieved by addition of 27 mg (0.16 mmol, 2.0 eq.) *m*CPBA at 0 °C. The mixture was

¹H-NMR (500 MHz, 298 K, CDCl₃, δ/ppm): 10.78 (DBU), 8.81 (DBU), 7.63 – 7.57 (m, 8H), 7.36 – 7.06 (m, 28H), 5.74 – 5.27 (m, 13H), 5.16 – 4.96 (m, 13H), 4.39 – 4.30 (m, 4H), 4.16 – 4.14 (m, 2H), 3.25 - 3.17 (m, 7H, DBU), 2.60 - 2.58 (m, 2H, DBU), 1.74 – 1.72 (m, 2H, DBU), 1.48 - 1.46 (m, 7H, DBU); **¹³C-NMR** (126 MHz, 298 K, CDCl₃, δ/ppm): 166.1, 143.6, 143.4, 141.2, 141.1, 136.0 – 135.6 (m), 134.9, 129.4 – 128.8 (m), 127.6, 127.1, 127.0, 125.6 (d, *J* = 5.6 Hz), 119.7, 74.1, 69.5 – 69.0 (m), 54.2 (DBU), 48.5 (DBU), 47.9 (d, *J* = 8.1 Hz), 38.1 (DBU), 32.4 (DBU), 28.9 (DBU), 26.6 (DBU), 23.8 (DBU), 19.3 (DBU);* **³¹P{¹H}-NMR** (162 MHz, 298 K, CDCl₃, δ/ppm): -1.32 (2P), -2.07, -2.33 (2P), -10.27 (d, *J*=13.9), -11.70 (d, *J*=14.1); **IR** (neat, cm⁻¹): 2942.6, 1670.1, 1646.9, 1450.2, 1286.3, 1050.1, 1019.2, 972.9, 846.6, 732.8; **R_f** (SiO₂, dichloromethane/methanol 8:1) 0.24; **HRMS** (ESI) calcd for C₇₄H₆₈O₂₇P₇⁻ 1605.2117, found 1605.2098.

* ¹H NMR and ¹³C NMR indicate the presence of TFA-DBU salt.

Synthesis of **24**



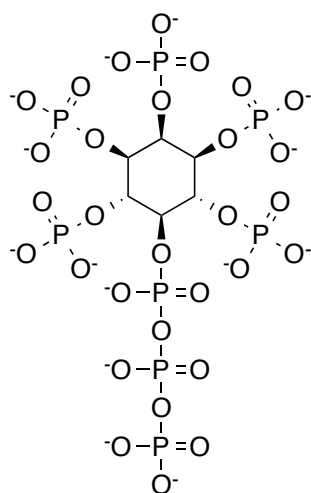
Pyrophosphorylated derivative **23** (40 mg, 0.022 mmol, 1.0 eq.) was evaporated twice with dry MeCN (0.2 mL) and then dissolved in dry DMF (2 mL). 13.0 μ L (13.0 mg, 0.088 mmol, 4.0 eq.) DBU were added and the solution was stirred 15 min at room temperature.

After completion of the deprotection (checked by ^{31}P -NMR), 0.30 mL (0.132 mmol, 6.0 eq.) 1*H*-tetrazole (0.45 M in MeCN) and 15 μL (15 mg, 0.044 mmol, 2.0 eq.) *bis*-benzyl *N,N*-diisopropylamino phosphoramidite **20** were added. The mixture was stirred for 45 min at room temperature and oxidation was achieved by addition of 8 mg (0.044 mmol, 2.0 eq.) *m*CPBA at 0 °C. The mixture was stirred 10 min at this temperature and 10 min at room temperature. Crystallization by addition of diethyl ether (added until the precipitate starts to form, 0 °C, overnight) yielded compound **24** (30mg, 0.017 mmol, 77%) as a sticky solid.

^1H -NMR (500 MHz, 298 K, CDCl_3 , δ/ppm): 10.98 (DBU), 8.98 (DBU), 7.37 – 7.18 (m, 30H), 5.77 – 4.94 (m, 30H), 3.31 – 3.22 (m, 14H, DBU), 2.69 (5H, DBU), 1.80 – 1.79 (m, 5H, DBU), 1.54 – 1.48 (m, 14H, DBU); ^{13}C -NMR (126 MHz, 298 K, CDCl_3 , δ/ppm): 166.2, 143.6, 138.7, 136.4 – 135.1 (m), 129.4 – 128.8 (m), 128.3 – 127.9 (m), 127.5, 127.3, 110.0, 74.1, 69.4 – 69.1 (m), 67.3 (d, $J = 5.4$ Hz), 54.2 (DBU), 48.5 (DBU), 46.8, 38.1 (DBU), 32.4 (DBU), 29.7, 28.9 (DBU), 26.7 (DBU), 23.8 (DBU), 19.3 (DBU), 19.3;* $^{31}\text{P}\{^1\text{H}\}$ -NMR (162 MHz, 298 K, CDCl_3 , δ/ppm): -1.47 (2P), -2.03, -2.56 (2P), -10.81 – (-11.22) (m, 2P), -21.09 – (-21.32) (m, 1P); IR (neat, cm^{-1}): 3487.6, 2930.3, 2860.9, 1713.4, 1667.2, 1573.6, 1496.5, 1437.7, 1386.6, 1285.3, 1255.4, 1092.5, 756.0, 705.8, 659.5.

* ^1H NMR and ^{13}C NMR indicate the presence of TFA-DBU salt.

Synthesis of 3-PPP-InsP₅



Protected P-anhydride **24** (10 mg, 0.006 mmol, 1.0 eq.) was dissolved in *tert*-butanol/water 3:1 (1.0 mL). To this solution 50 mg (0.047 mmol, 8 eq.) Pd (10 wt. %, on

carbon) were added. After 1 hour of hydrogenation at 80 bar in a steel autoclave, 0.5 mL water were added to the mixture and the hydrogenation continued for another 2 hours. The mixture was centrifuged and the supernatant removed. The catalyst was washed with water and to this washing fraction acetone was added (ratio 1:8). The precipitate was isolated by centrifugation yielding **5-PPP-InsP₅** (2.2 mg, 0.003 mmol, 50%) as a sticky solid.

6.6 GENERAL PROCEDURES FOR THE DESYMMETRIZATION OF *MYO*-INOSITOL

Desymmetrization of diol **43** (Scheme 4.14)

Phosphoramidite **12** (55 mg, 0.13 mmol, 1.0 eq.) was dissolved in DCM (2 mL) and 0.90 mL (0.39 mmol, 3.0 eq.) 1*H*-tetrazole (0.45 M in MeCN) were added. The mixture was stirred at room temperature for 45 min. In another flask, diol **43** was dissolved in DCM (1 mL). Both solutions were cooled to -78 °C. The solution containing phosphoramidite **12** was transferred to the solution containing diol **43** via cannula. The mixture was stirred at -78 °C and the progress of the reaction was monitored by ³¹P-NMR. After 1 h *m*CPBA was added and the reaction mixture was allowed to warm to room temperature. The mixture was diluted with ethyl acetate, washed with brine, dried over MgSO₂ and the solvents were removed *in vacuo*.

Desymmetrization of diol **49** (Scheme 4.16)

Phosphoramidite **12** (50 mg, 0.16 mmol, 1.5 eq.) was dissolved in acetonitrile (1.5 mL) and 60 µL (0.55 mmol, 5.0 eq.) pentafluorophenol were added. The mixture was stirred at room temperature for 1 h. After complete activation of phosphoramidite **12** (monitored by ³¹P-NMR), solvents were evaporated. The residue dissolved in DMF (1.0 mL) and the solution cooled to -40 °C. In another flask, diol **49** was dissolved in DMF (0.5 mL) and transferred to the mixture containing activated phosphoramidite **12**. The mixture was stirred at -40 °C and the progress of the reaction was monitored by ³¹P-NMR. 0.04 mL (0.22 mmol, 2 eq.) *tert*-butyl hydroperoxide solution (5.5 M in decane) was added and the reaction mixture was allowed to warm to room temperature. The mixture was diluted with ethyl acetate, washed with brine (3x), dried over MgSO₂ and the solvents were removed *in vacuo*.

LITERATURE

- (1) Potter, B. V. Recent advances in the chemistry and biochemistry of inositol phosphates of biological interest. *Nat. Prod. Rep.* **1990**, 7, 1–24.
- (2) Potter, B. V. L.; Lampe, D. Chemistry of inositol lipid mediated cellular signaling. *Angew. Chemie Int. Ed.* **1995**, 34, 1933–1972.
- (3) Sureshan, K. M.; Shashidhar, M. S.; Praveen, T.; Das, T. Regioselective protection and deprotection of inositol hydroxyl groups. *Chem. Rev.* **2003**, 103, 4477–4503.
- (4) Wang, W.; Safar, J.; Zopf, D. Analysis of inositol by high-performance liquid chromatography. *Anal. Biochem.* **1990**, 188, 432–435.
- (5) Kersting, M. C.; Boyette, M.; Massey, J. H.; Ryals, P. E. Identification of the inositol isomers present in *Tetrahymena*. *J. Eukaryot. Microbiol.* **2003**, 50, 164–168.
- (6) Scherer, J. Ueber eine neue, aus dem Muskelfleische gewonnene Zuckerart. *Annalen* **1850**, 73, 322–328.
- (7) Irvine, R. F.; Schell, M. J. Back in the water: the return of the inositol phosphates. *Nat. Rev. Mol. Cell Biol.* **2001**, 2, 327–338.
- (8) Agranoff, B. W. Cyclitol confusion. *Trends Biochem. Sci.* **1978**, 3, N283–N285.
- (9) Nomenclature Committee of the IUB. Numbering of atoms in *myo*-inositol. *Biochem. J.* **1989**, 258, 1–2.
- (10) Allison, J. H.; Stewart, M. A. Reduced brain inositol in lithium-treated rats. *Nat. New Biol.* **1971**, 233, 267–268.
- (11) Berridge, M. J.; Downes, C. P.; Hanley, M. R. Lithium amplifies agonist-dependent phosphatidylinositol responses in brain and salivary glands. *Biochem. J.* **1982**, 206, 587–595.
- (12) Alcázar-Román, A. R.; Wente, S. R. Inositol polyphosphates: a new frontier for regulating gene expression. *Chromosoma* **2008**, 117, 1–13.
- (13) Wilson, M. S. C.; Livermore, T. M.; Saiardi, A. Inositol pyrophosphates: between signalling and metabolism. *Biochem. J.* **2013**, 452, 369–379.
- (14) Shears, S. Diphosphoinositol polyphosphates: metabolic messengers? *Mol. Pharmacol.* **2009**, 76, 236–252.

- (15) Agranoff, B. W. Turtles all the way: reflections on *myo*-inositol. *J. Biol. Chem.* **2009**, *284*, 21121–21126.
- (16) Irvine, R. F. Inositide evolution - towards turtle domination? *J. Physiol.* **2005**, *566*, 295–300.
- (17) York, J. D. Regulation of nuclear processes by inositol polyphosphates. *Biochim. Biophys. Acta* **2006**, *1761*, 552–559.
- (18) Streb, H.; Irvine, R. F.; Berridge, M.; Schulz, I. Release of Ca^{2+} from a nonmitochondrial intracellular store in pancreatic acinar cells by inositol-1,4,5-trisphosphate. *Nature* **1983**, *306*, 67–69.
- (19) Berridge, M. Inositol trisphosphate and diacylglycerol: two interacting second messengers. *Annu. Rev. Biochem.* **1987**, *56*, 159–193.
- (20) Snyder, S. H.; Supattapone, S.; Danoff, S.; Worley, P. F.; Baraban, J. M. The inositol trisphosphate receptor: a potpourri of second-messenger regulation. *Cell. Mol. Neurobiol.* **1988**, *8*, 1–5.
- (21) Berridge, M. Inositol triphosphate and calcium signalling. *Nature* **1993**, *361*, 315–325.
- (22) Best, M. D.; Zhang, H.; Prestwich, G. D. Inositol polyphosphates, diphosphoinositol polyphosphates and phosphatidylinositol polyphosphate lipids: structure, synthesis, and development of probes for studying biological activity. *Nat. Prod. Rep.* **2010**, *27*, 1403–1430.
- (23) Lückhoff, A.; Clapham, D. E. Inositol 1,3,4,5-tetrakisphosphate activates an endothelial Ca^{2+} -permeable channel. *Nature* **1992**, *355*, 356–358.
- (24) Tsubokawa, H.; Oguro, K.; Robinson, H. P. C. T.; Masuzawa, T.; Kawai, N. Intracellular inositol 1,3,4,5-tetrakisphosphate enhances the calcium current in hippocampal CA1 neurones of the gerbil after ischaemia. *J. Physiol.* **1996**, 67–78.
- (25) Connolly, T. M.; Bansal, V. S.; Bross, T. E.; Imine, R. F.; Majeruse, P. W. The metabolism of tris- and tetraphosphates of inositol by 5-phosphomonoesterase and 3-kinase enzymes. *J. Biol. Chem.* **1987**, *267*, 2146–2149.
- (26) Kachintorn, U.; Vajanaphanich, M.; Barrett, K. E.; Traynor-kaplan, A. E. Elevation of inositol tetrakisphosphate parallels inhibition of Ca^{2+} -dependent Cl^- secretion in T84 cells. *Am. J. Physiol.* **1993**, *264*, C671–C676.
- (27) Stephens, L. R.; Hawkins, P. T.; Stanley, A. F.; Moore, T.; Poyner, D. R.; Morris, P. J.; Hanley, M. R.; Kay, R. R.; Irvine, R. F. *myo*-Inositol pentakisphosphates. *Biochem. J.* **1991**, *275*, 485–499.

- (28) Shears, S. B. Assessing the omnipotence of inositol hexakisphosphate. *Cell. Signal.* **2001**, *13*, 151–158.
- (29) Posternak, S. Sur la synthèse de l'ether hexaphosphorique de l'inosite avec le principe phosphoorganique de réserve des plantes vertes. *Compt. Rend. Acad. Sci.* **1919**, *169*, 130–140.
- (30) Menniti, F. S.; Miller, R. N.; Putney, J. W.; Shears, S. B. Turnover of inositol polyphosphate pyrophosphates in pancreatoma cells. *J. Biol. Chem.* **1993**, *268*, 3850–3856.
- (31) Stephens, L.; Radenberg, T.; Thiel, U.; Vogel, G.; Khoo, K. H.; Dell, A.; Jackson, T. R.; Hawkins, P. T.; Mayr, G. W. The detection, purification, structural characterization, and metabolism of diphosphoinositol pentakisphosphate(s) and bisdiphosphoinositol tetrakisphosphate(s). *J. Biol. Chem.* **1993**, *268*, 4009–4015.
- (32) Seeds, A. M.; Bastidas, R. J.; York, J. D. Molecular definition of a novel inositol polyphosphate metabolic pathway initiated by inositol 1,4,5-trisphosphate 3-kinase activity in *Saccharomyces cerevisiae*. *J. Biol. Chem.* **2005**, *280*, 27654–27661.
- (33) Albert, C.; Safrany, S. T.; Bembenek, M. E.; Reddy, K. M.; Reddy, K.; Falck, J.; Bröcker, M.; Shears, S. B.; Mayr, G. W. Biological variability in the structures of diphosphoinositol polyphosphates in *Dictyostelium discoideum* and mammalian cells. *Biochem. J.* **1997**, *327*, 553–560.
- (34) Wang, H.; Falck, J. R.; Hall, T. M. T.; Shears, S. B. Structural basis for an inositol pyrophosphate kinase surmounting phosphate crowding. *Nat. Chem. Biol.* **2012**, *8*, 111–116.
- (35) Wundenberg, T.; Mayr, G. W. Synthesis and biological actions of diphosphoinositol phosphates (inositol pyrophosphates), regulators of cell homeostasis. *Biol. Chem.* **2012**, *393*, 979–998.
- (36) Lee, Y.-S.; Mulugu, S.; York, J. D.; O'Shea, E. K. Regulation of a cyclin-CDK-CDK inhibitor complex by inositol pyrophosphates. *Science* **2007**, *316*, 109–112.
- (37) Mulugu, S.; Bai, W.; Fridy, P. C.; Bastidas, R. J.; Otto, J. C.; Dollins, D. E.; Haystead, T. A.; Ribeiro, A. A.; York, J. D. A conserved family of enzymes that phosphorylate inositol hexakisphosphate. *Science* **2007**, *316*, 106–109.
- (38) Lin, H.; Fridy, P. C.; Ribeiro, A. A.; Choi, J. H.; Barma, D. K.; Vogel, G.; Falck, J. R.; Shears, S. B.; York, J. D.; Mayr, G. W. Structural analysis and detection of biological inositol pyrophosphates reveal that the family of VIP/diphosphoinositol pentakisphosphate kinases are 1/3-kinases. *J. Biol. Chem.* **2009**, *284*, 1863–1872.

- (39) Laussmann, T.; Eujen, R.; Weissshuhn, C.; Thiel, U.; Vogel, G. Structures of diphospho-*myo*-inositol pentakisphosphate and bisdiphospho-*myo*-inositol tetrakisphosphate from *Dictyostelium* resolved by NMR analysis. *Biochem. J.* **1996**, *315*, 715–720.
- (40) Laussmann, T.; Hansen, A.; Reddy, K.; Reddy, K. K.; Falck, J. R.; Vogel, G. Diphospho-*myo*-inositol phosphates in *Dictyostelium* and *Polysphondylium*: identification of a new bisdiphospho-*myo*-inositol tetrakisphosphate. *FEBS Lett.* **1998**, *426*, 145–150.
- (41) Hatch, A. J.; York, J. D. Snapshot: inositol phosphates. *Cell* **2010**, *143*, 1030–1030.e1.
- (42) Saiardi, A.; Erdjument-Bromage, H.; Snowman, A. M.; Tempst, P.; Snyder, S. H. Synthesis of diphosphoinositol pentakisphosphate by a newly identified family of higher inositol polyphosphate kinases. *Curr. Biol.* **1999**, *9*, 1323–1326.
- (43) Saiardi, A.; Caffrey, J. J.; Snyder, S. H.; Shears, S. B. The inositol hexakisphosphate kinase family. Catalytic flexibility and function in yeast vacuole biogenesis. *J. Biol. Chem.* **2000**, *275*, 24686–24692.
- (44) Shears, S. B. How versatile are inositol phosphate kinases? *Biochem. J.* **2004**, *377*, 265–280.
- (45) Draskovic, P.; Saiardi, A.; Bhandari, R.; Burton, A.; Ilc, G.; Kovacevic, M.; Snyder, S. H.; Podobnik, M. Inositol hexakisphosphate kinase products contain diphosphate and triphosphate groups. *Chem. Biol.* **2008**, *15*, 274–286.
- (46) Losito, O.; Szijgyarto, Z.; Resnick, A. C.; Saiardi, A. Inositol pyrophosphates and their unique metabolic complexity: analysis by gel electrophoresis. *PLoS One* **2009**, *4*, e5580.
- (47) Fridy, P. C.; Otto, J. C.; Dollins, D. E.; York, J. D. Cloning and characterization of two human VIP1-like inositol hexakisphosphate and diphosphoinositol pentakisphosphate kinases. *J. Biol. Chem.* **2007**, *282*, 30754–30762.
- (48) Choi, J. H.; Williams, J.; Cho, J.; Falck, J. R.; Shears, S. B. Purification, sequencing, and molecular identification of a mammalian PP-InsP₅ kinase that is activated when cells are exposed to hyperosmotic stress. *J. Biol. Chem.* **2007**, *282*, 30763–30775.
- (49) Yang, X.; Safrany, S. T.; Shears, S. B. Site-directed mutagenesis of diphosphoinositol polyphosphate phosphohydrolase, a dual specificity NUDT enzyme that attacks diadenosine polyphosphates and diphosphoinositol polyphosphates. *J. Biol. Chem.* **1999**, *274*, 35434–35440.

- (50) Safrany, S.; Ingram, S.; Cartwright, J.; Falck, J. R.; McLennan, A. G.; Barnes, L.; Shears, S. B. Hydrolases from *Schizosaccharomyces pombe* and *Saccharomyces cerevisiae* are homologues of the human diphosphoinositol polyphosphate phosphohydrolase. *J. Biol. Chem.* **1999**, *274*, 21735–21740.
- (51) Caffrey, J. J.; Safrany, S. T.; Yang, X.; Shears, S. B. Discovery of molecular and catalytic diversity among human diphosphoinositol-polyphosphate phosphohydrolases. *J. Biol. Chem.* **2000**, *275*, 12730–12736.
- (52) Shears, S. B.; Ali, N.; Craxton, A.; Bembenek, M. E. Synthesis and metabolism of Bis-diphosphoinositol tetrakisphosphate *in vitro* and *in vivo*. *J. Biol. Chem.* **1995**, *270*, 10489–10497.
- (53) Ali, N.; Craxton, A.; Shears, S. B. Hepatic Ins(1,3,4,5)P₄ 3-phosphatase is compartmentalized inside endoplasmic reticulum. *J. Biol. Chem.* **1993**, *268*, 6161–6167.
- (54) Glennon, M. C.; Shears, S. B. Turnover of inositol pentakisphosphates, inositol hexakisphosphate and diphosphoinositol polyphosphates in primary cultured hepatocytes. *Biochem. J.* **1993**, *293*, 583–590.
- (55) Barker, C. J.; Illies, C.; Gaboardi, G. C.; Berggren, P.-O. Inositol pyrophosphates: structure, enzymology and function. *Cell. Mol. Life Sci.* **2009**, *66*, 3851–3871.
- (56) Bennett, M.; Onnebo, S. M. N.; Azevedo, C.; Saiardi, A. Inositol pyrophosphates: metabolism and signaling. *Cell. Mol. Life Sci.* **2006**, *63*, 552–564.
- (57) Burton, A.; Hu, X.; Saiardi, A. Are inositol pyrophosphates signalling molecules? *J. Cell. Physiol.* **2009**, *220*, 8–15.
- (58) Choi, K.; Mollapour, E.; Choi, J.; Shears, S. Cellular energetic status supervises the synthesis of bis-diphosphoinositol tetrakisphosphate independently of AMP-activated protein kinase. *Mol. Pharmacol.* **2008**, *74*, 527–536.
- (59) Choi, K.; Mollapour, E.; Shears, S. B. Signal transduction during environmental stress: InsP₈ operates within highly restricted contexts. *Cell. Signal.* **2005**, *17*, 1533–1541.
- (60) Pesesse, X.; Choi, K.; Zhang, T.; Shears, S. B. Signaling by higher inositol polyphosphates. Synthesis of bisdiphosphoinositol tetrakisphosphate (“InsP₈”) is selectively activated by hyperosmotic stress. *J. Biol. Chem.* **2004**, *279*, 43378–43381.
- (61) Szigyarto, Z.; Garedew, A.; Azevedo, C.; Saiardi, A. Influence of inositol pyrophosphates on cellular energy dynamics. *Science* **2011**, *334*, 802–805.

- (62) Saiardi, A.; Sciambi, C.; McCaffery, J. M.; Wendland, B.; Snyder, S. H. Inositol pyrophosphates regulate endocytic trafficking. *Proc. Natl. Acad. Sci. U. S. A.* **2002**, *99*, 14206–14211.
- (63) Ye, W.; Ali, N.; Bembenek, M. E.; Shears, S. B.; Lafer, E. M. Inhibition of clathrin assembly by high affinity binding of specific inositol polyphosphates to the synapse-specific clathrin assembly protein AP-3. *J. Biol. Chem.* **1995**, *270*, 1564–1568.
- (64) Ali, N.; Duden, R.; Bembenek, M. E.; Shears, S. B. The interaction of coatamer with inositol polyphosphates is conserved in *Saccharomyces cerevisiae*. *Biochem. J.* **1995**, *310*, 279–284.
- (65) Fleischer, B.; Xie, J.; Mayrleitner, M.; Shears, S. B.; Palmer, D. J.; Fleischer, S. Golgi coatamer binds, and forms K⁺-selective channels gated by, inositol polyphosphates. *J. Biol. Chem.* **1994**, *269*, 17826–17832.
- (66) Beck, K. A.; Keen, J. H. Interaction of phosphoinositide cycle intermediates with the plasma membrane-associated clathrin assembly protein AP-2. *J. Biol. Chem.* **1991**, *266*, 4442–4447.
- (67) Voglmaier, S. M.; Keen, J. H.; Murphy, J.-E.; Ferris, C. D.; Prestwich, G. D.; Snyder, S. H.; Theibert, A. B. Inositol hexakisphosphate receptor identified as the clathrin assembly protein AP-2. *Biochem. Biophys. Res. Commun.* **1992**, *187*, 158–163.
- (68) Illies, C.; Gromada, J.; Fiume, R.; Leibiger, B.; Yu, J.; Juhl, K.; Yang, S.-N.; Barma, D. K.; Falck, J. R.; Saiardi, A.; Barker, C. J.; Berggren, P.-O. Requirement of inositol pyrophosphates for full exocytotic capacity in pancreatic β cells. *Science* **2007**, *318*, 1299–1302.
- (69) Lemmon, M. A.; Ferguson, K. M. Signal-dependent membrane targeting by pleckstrin homology (PH) domains. *Biochem. J.* **2000**, *350*, 1–18.
- (70) Komander, D.; Fairservice, A.; Deak, M.; Kular, G. S.; Prescott, A. R.; Downes, P. C.; Safrany, S. T.; Alessi, D. R.; van Aalten, D. M. F. Structural insights into the regulation of PDK1 by phosphoinositides and inositol phosphates. *EMBO J.* **2004**, *23*, 3918–3928.
- (71) Jackson, S. G.; Al-Saigh, S.; Schultz, C.; Junop, M. S. Inositol pentakisphosphate isomers bind PH domains with varying specificity and inhibit phosphoinositide interactions. *BMC Struct. Biol.* **2011**, *11*, 11.
- (72) Jackson, S. G.; Zhang, Y.; Haslam, R. J.; Junop, M. S. Structural analysis of the carboxy terminal PH domain of pleckstrin bound to D-myoinositol 1,2,3,5,6-pentakisphosphate. *BMC Struct. Biol.* **2007**, *7*, 80.

- (73) Luo, H. R.; Huang, Y. E.; Chen, J. C.; Saiardi, A.; Iijima, M.; Ye, K.; Huang, Y.; Nagata, E.; Devreotes, P.; Snyder, S. H. Inositol pyrophosphates mediate chemotaxis in *Dictyostelium* via pleckstrin homology domain-PtdIns(3,4,5)P₃ interactions. *Cell* **2003**, *114*, 559–572.
- (74) Chakraborty, A.; Koldobskiy, M. a; Bello, N. T.; Maxwell, M.; Potter, J. J.; Juluri, K. R.; Maag, D.; Kim, S.; Huang, A. S.; Dailey, M. J.; Saleh, M.; Snowman, A. M.; Moran, T. H.; Mezey, E.; Snyder, S. H. Inositol pyrophosphates inhibit Akt signaling, thereby regulating insulin sensitivity and weight gain. *Cell* **2010**, *143*, 897–910.
- (75) Manning, B. D. Insulin signaling: inositol phosphates get into the Akt. *Cell* **2010**, *143*, 861–863.
- (76) Nagata, E.; Luo, H. R.; Saiardi, A.; Bae, B.-I.; Suzuki, N.; Snyder, S. H. Inositol hexakisphosphate kinase-2, a physiologic mediator of cell death. *J. Biol. Chem.* **2005**, *280*, 1634–1640.
- (77) Mather, K. A.; Jorm, A. F.; Parslow, R. A.; Christensen, H. Is telomere length a biomarker of aging? A review. *J. Gerontol. A. Biol. Sci. Med. Sci.* **2011**, *66*, 202–213.
- (78) Saiardi, A.; Resnick, A. C.; Snowman, A. M.; Wendland, B.; Snyder, S. H. Inositol pyrophosphates regulate cell death and telomere length through phosphoinositide 3-kinase-related protein kinases. *Proc. Natl. Acad. Sci. U. S. A.* **2005**, *102*, 1911–1914.
- (79) York, S. J.; Armbruster, B. N.; Greenwell, P.; Petes, T. D.; York, J. D. Inositol diphosphate signaling regulates telomere length. *J. Biol. Chem.* **2005**, *280*, 4264–4269.
- (80) Saiardi, A.; Bhandari, R.; Resnick, A. C.; Snowman, A. M.; Snyder, S. H. Phosphorylation of proteins by inositol pyrophosphates. *Science* **2004**, *306*, 2101–2105.
- (81) Shears, S. The long-awaited demonstration of protein pyrophosphorylation by IP₇ *in vivo*? *Proc. Natl. Acad. Sci. U. S. A.* **2010**, *107*, E17; author reply E18.
- (82) Bhandari, R.; Saiardi, A.; Ahmadibeni, Y.; Snowman, A. M.; Resnick, A. C.; Kristiansen, T. Z.; Molina, H.; Pandey, A.; Werner, J. K.; Juluri, K. R.; Xu, Y.; Prestwich, G. D.; Parang, K.; Snyder, S. H. Protein pyrophosphorylation by inositol pyrophosphates is a posttranslational event. *Proc. Natl. Acad. Sci.* **2007**, *104*, 15305–15310.
- (83) Barker, C. J. *Inositol Phosphates and Lipids. Methods and Protocols*. Springer Protocols. Methods in Molecular Biology, Vol. 645, 2010.

- (84) Westheimer, F. Why Nature Chose Phosphates. *Science* (80-.). **1987**, *235*, 1173–1178.
- (85) Teichert, J. F.; Feringa, B. L. Phosphoramidites: privileged ligands in asymmetric catalysis. *Angew. Chem. Int. Ed. Engl.* **2010**, *49*, 2486–2528.
- (86) Nifant'ev, E. E.; Grachev, M. K. Trivalent phosphorus acid amides as phosphorylating agents for alcohols and amines. *Russ. Chem. Rev.* **1994**, *63*, 575–609.
- (87) Nifant'ev, E. E.; Grachev, M. K.; Burmistrov, S. Y. Amides of trivalent phosphorus acids as phosphorylating reagents for proton-donating nucleophiles. *Chem. Rev.* **2000**, *100*, 3755–3799.
- (88) Nurminen, E.; Lönnberg, H. Mechanisms of the substitution reactions of phosphoramidites and their congeners. *J. Phys. Org. Chem.* **2004**, *17*, 1–17.
- (89) Beaucage, S.; Caruthers, M. Deoxynucleoside phosphoramidites-a new class of key intermediates for deoxypolynucleotide synthesis. *Tetrahedron Lett.* **1981**, *22*, 1859–1862.
- (90) Russell, M. A.; Laws, A. P.; Atherton, J. H.; Page, M. I. The mechanism of the phosphoramidite synthesis of polynucleotides. *Org. Biomol. Chem.* **2008**, *6*, 3270–3275.
- (91) Kamerlin, S. C. L.; Sharma, P. K.; Prasad, R. B.; Warshel, A. Why nature really chose phosphate. *Q. Rev. Biophys.* **2013**, *46*, 1–132.
- (92) Nurminen, E. J.; Mattinen, J. K.; Lönnberg, H. Protonation of phosphoramidites. The effect on nucleophilic displacement. *J. Chem. Soc. Perkin Trans. 2* **2000**, 2238–2240.
- (93) Wei, X. Coupling activators for the oligonucleotide synthesis via phosphoramidite approach. *Tetrahedron* **2013**, *69*, 3615–3637.
- (94) Dahl, B. H.; Nielsen, J.; Dahl, O. Mechanistic studies on the phosphoramidite coupling reaction in oligonucleotide synthesis. I. Evidence for nucleophilic catalysis by tetrazole and rate variations with the phosphorus substituents. *Nucleic Acid Res.* **1987**, *15*, 1729–1743.
- (95) Sabbagh, G.; Fettes, K. J.; Gosain, R.; O'Neil, I. A.; Cosstick, R. Synthesis of phosphorothioamidites derived from 3'-thio-3'-deoxythymidine and 3'-thio-2',3'-dideoxycytidine and the automated synthesis of oligodeoxynucleotides containing a 3'-S-phosphorothiolate linkage. *Nucleic Acids Res.* **2004**, *32*, 495–501.

- (96) Yoon, T. P.; Jacobsen, E. N. Privileged chiral catalysts. *Science* **2003**, *299*, 1691–1693.
- (97) Pfaltz, A.; Drury, W. J. Design of chiral ligands for asymmetric catalysis: from C_2 -symmetric P,P- and N,N-ligands to sterically and electronically nonsymmetrical P,N-ligands. *Proc. Natl. Acad. Sci.* **2004**, *101*, 5723–5726.
- (98) Dang, B. T. P.; Kagan, H. B. The asymmetric synthesis of hydratropic acid and amino-acids by homogeneous catalytic hydrogenation. *J. Chem. Soc. Chem. Commun.* **1971**, 481.
- (99) Estevez, V.; Prestwich, G. Synthesis of enantiomerically pure, P-1-tethered inositol tetrakis(phosphate) affinity labels via a Ferrier rearrangement. *J. Am. Chem. Soc.* **1991**, *113*, 9885–9887.
- (100) Bender, S.; Budhu, R. Biomimetic synthesis of enantiomerically pure D-*myo*-inositol derivatives. *J. Am. Chem. Soc.* **1991**, *113*, 9883–9885.
- (101) Nishikawa, A.; Saito, S.; Hashimoto, Y.; Koga, K.; Shirai, R. Synthesis of L- α -phosphatidyl-D-*myo*-inositol 3,5-bisphosphate from D-glucose. *Tetrahedron Lett.* **2001**, *42*, 9195–9198.
- (102) Ozaki, S.; Watanabe, Y.; Ogasawara, T.; Kondo, Y.; Shiotani, N.; Nishii, H.; Matsuki, T. Total synthesis of optically active *myo*-inositol 1,4,5-tris(phosphate). *Tetrahedron Lett.* **1986**, *27*, 3157–3160.
- (103) Bruzik, K. S.; Tsai, M. D. Efficient and systematic syntheses of enantiomerically pure and regiospecifically protected *myo*-inositols. *J. Am. Chem. Soc.* **1992**, *114*, 6361–6374.
- (104) Bruzik, K. S.; Salamonczyk, G. M. Synthesis of the enantiomeric 1,4,5,6-tetra-*O*-benzyl-*myo*-inositols. *Carbohydr. Res.* **1989**, *195*, 67–73.
- (105) Lee, H. W.; Kishi, Y. Synthesis of mono and unsymmetrical bis ortho esters of *scyllo*-inositol. *J. Org. Chem.* **1985**, *50*, 4402–4404.
- (106) Godage, H. Y.; Riley, A. M.; Woodman, T. J.; Potter, B. V. L. Regioselective hydrolysis of *myo*-inositol 1,3,5-orthobenzoate via a 1,2-bridged 2'-phenyl-1',3'-dioxolan-2'-ylium ion provides a rapid route to the anticancer agent Ins(1,3,4,5,6)P₅. *Chem. Commun.* **2006**, 2989–2991.
- (107) Riley, A. M.; Godage, H. Y.; Mahon, M. F.; Potter, B. V. L. Chiral desymmetrisation of *myo*-inositol 1,3,5-orthobenzoate gives rapid access to precursors for second messenger analogues. *Tetrahedron: Asymmetry* **2006**, *17*, 171–174.

- (108) Sureshan, K. M.; Watanabe, Y. An efficient route to optically active inositol derivatives via the resolution of *myo*-inositol 1,3,5-orthoformate: a short synthesis of D-*myo*-inositol-4-phosphate. *Tetrahedron: Asymmetry* **2004**, *15*, 1193–1198.
- (109) Han, F.; Hayashi, M.; Watanabe, Y. Chemical resolution of 1,2-*O*-cyclohexylidene-3,4-*O*-(tetraisopropylidisiloxane-1,3-diyl)-*myo*-inositol and synthesis of phosphatidyl-D-*myo*-inositol 3,5-bisphosphate from both L- and D-enantiomers. *European J. Org. Chem.* **2004**, *2004*, 558–566.
- (110) Mills, S. J.; Riley, A. M.; Liu, C.; Mahon, M. F.; Potter, B. V. L. A definitive synthesis of D-*myo*-inositol 1,4,5,6-tetrakisphosphate and its enantiomer D-*myo*-inositol 3,4,5,6-tetrakisphosphate from a novel butane-2,3-diacetal-protected inositol. *Chem. Eur. J.* **2003**, *9*, 6207–6214.
- (111) Downham, R.; Edwards, P. J.; Entwistle, D. A.; Hughes, A. B.; Kim, K. S.; Ley, S. V. Dispiroketal in synthesis (part 19): dispiroketal as enantioselective and regioselective protective agents for symmetric cyclic and acyclic polyols. *Tetrahedron: Asymmetry* **1995**, *6*, 2403–2440.
- (112) Sculimbrene, B. R.; Miller, S. J. Discovery of a catalytic asymmetric phosphorylation through selection of a minimal kinase mimic: a concise total synthesis of D-*myo*-inositol-1-phosphate. *J. Am. Chem. Soc.* **2001**, *123*, 10125–10126.
- (113) Sculimbrene, B. R.; Morgan, A. J.; Miller, S. J. Enantiodivergence in small-molecule catalysis of asymmetric phosphorylation: concise total syntheses of the enantiomeric D-*myo*-inositol-1-phosphate and D-*myo*-inositol-3-phosphate. *J. Am. Chem. Soc.* **2002**, *124*, 11653–11656.
- (114) Sculimbrene, B. R.; Morgan, A. J.; Miller, S. J. Nonenzymatic peptide-based catalytic asymmetric phosphorylation of inositol derivatives. *Chem. Commun.* **2003**, 1781–1785.
- (115) Morgan, A. J.; Komiya, S.; Xu, Y.; Miller, S. J. Unified total syntheses of the inositol polyphosphates: D-I-3,5,6P₃, D-I-3,4,5P₃, D-I-3,4,6P₃ and D-I-3,4,5,6P₄ via catalytic enantioselective and site-selective phosphorylation. *J. Org. Chem.* **2006**, *71*, 6923–6931.
- (116) Jordan, P. A.; Kayser-Bricker, K. J.; Miller, S. J. Asymmetric phosphorylation through catalytic P(III) phosphoramidite transfer: enantioselective synthesis of D-*myo*-inositol-6-phosphate. *Proc. Natl. Acad. Sci. U. S. A.* **2010**, *107*, 20620–20624.
- (117) Falck, J. R.; Reddy, K. K.; Ye, J.; Saady, M.; Mioskowski, C.; Shears, S. B.; Tan, Z.; Safranyg, S. Synthesis and structure of cellular mediators: inositol polyphosphate diphosphates. *J. Am. Chem. Soc.* **1995**, *117*, 12172–12175.

- (118) Reddy, K. M.; Reddy, K. K.; Falck, J. R. Synthesis of 2- and 5-diphospho-*myo*-inositol pentakisphosphate (2- and 5-PP-InsP₅), intracellular mediators. *Tetrahedron Lett.* **1997**, *38*, 4951–4952.
- (119) Watanabe, Y.; Mitani, M.; Morita, T.; Ozaki, S. Highly efficient protection by the tetraisopropylidisiloxane-1,3-diyl group in the synthesis of *myo*-inositol phosphates and inositol 1,3,4,6-tetrakisphosphate. *J. Chem. Soc. Chem. Commun.* **1989**, 482–483.
- (120) Zhang, H.; Thompson, J.; Prestwich, G. A scalable synthesis of the IP₇ isomer, 5-PP-Ins(1,2,3,4,6)P₅. *Org. Lett.* **2009**, *11*, 1551–1554.
- (121) A. Saiardi, Personal Communication.
- (122) Wu, M.; Dul, B. E.; Trevisan, A. J.; Fiedler, D. Synthesis and characterization of non-hydrolysable diphosphoinositol polyphosphate second messengers. *Chem. Sci.* **2013**, *4*, 405–410.
- (123) Murali, C.; Shashidhar, M. S.; Gopinath, C. S. Hydroxyl group deprotection reactions with Pd(OH)₂/C: a convenient alternative to hydrogenolysis of benzyl ethers and acid hydrolysis of ketals. *Tetrahedron* **2007**, *63*, 4149–4155.
- (124) Gilbert, I.; Holmes, A.; Pestchanker, M.; Young, R. Lewis acid-catalysed rearrangements of *myo*-inositol orthoformate derivatives. *Carbohydr. Res.* **1992**, *234*, 117–130.
- (125) Conway, S. J.; Gardiner, J.; Grove, S. J. A.; Johns, M. K.; Lim, Z.-Y.; Painter, G. F.; Robinson, D. E. J. E.; Schieber, C.; Thuring, J. W.; Wong, L. S.-M.; Yin, M.-X.; Burgess, A. W.; Catimel, B.; Hawkins, P. T.; Ktistakis, N. T.; Stephens, L. R.; Holmes, A. B. Synthesis and biological evaluation of phosphatidylinositol phosphate affinity probes. *Org. Biomol. Chem.* **2010**, *8*, 66–76.
- (126) Conway, S. J.; Miller, G. J. Biology-enabling inositol phosphates, phosphatidylinositol phosphates and derivatives. *Nat. Prod. Rep.* **2007**, *24*, 687–707.
- (127) Tener, G. M. 2-Cyanoethyl phosphate and its use in the synthesis of phosphate esters. *J. Am. Chem. Soc.* **1961**, *83*, 159–168.
- (128) Evans, D. A.; Gage, J. R.; Leighton, J. L. Asymmetric synthesis of calyculin A. 3. Assemblage of the calyculin skeleton and the introduction of a new phosphate monoester synthesis. *J. Org. Chem.* **1992**, *57*, 1964–1966.
- (129) Wang, H.; Godage, H. Y.; Riley, A. M.; Weaver, J. D.; Shears, S. B.; Potter, B. V. L. Synthetic inositol phosphate analogs reveal that PIP5K2 has a surface-

- mounted substrate capture site that is a target for drug discovery. *Chem. Biol.* **2014**, *21*, 689–699.
- (130) Cremosnik, G. S.; Hofer, A.; Jessen, H. J. Iterative synthesis of nucleoside oligophosphates with phosphoramidites. *Angew. Chem. Int. Ed. Engl.* **2014**, *53*, 286–289.
- (131) Roos, G. H. P.; Donovan, A. R. Synthesis of novel C_2 -symmetric ligands based on (R,R)- and (S,S)-diphenyl-1,3-propanediol. *Tetrahedron: Asymmetry* **1999**, *10*, 991–1000.
- (132) Kumar, P.; Upadhyay, R. K.; Pandey, R. K. Asymmetric dihydroxylation route to (R)-isoprenaline, (R)-norfluoxetine and (R)-fluoxetine. *Tetrahedron: Asymmetry* **2004**, *15*, 3955–3959.
- (133) Iuliano, A.; Pini, D.; Salvadori, P. Optically active N-1-phenylethyl derivatives of (1R)-2-amino-1-phenylethanol as chiral auxiliaries in the enantioselective addition of diethylzinc to arylaldehydes. *Tetrahedron: Asymmetry* **1995**, *6*, 739–744.
- (134) Duss, M. Novel applications of phosphoramidites: desymmetrization of *meso*-compounds and enrichment of phosphorylated proteins, Master Thesis, 2013.
- (135) Podeschwa, M. A. L.; Plettenburg, O.; Altenbach, H.-J. Flexible stereo- and regioselective synthesis of *myo*-inositol phosphates (part 1): via symmetrical conduritol B derivatives. *European J. Org. Chem.* **2005**, *2005*, 3101–3115.
- (136) Vibhute, A. M.; Vidyasagar, A.; Sarala, S.; Sureshan, K. M. Regioselectivity among six secondary hydroxyl groups: selective acylation of the least reactive hydroxyl groups of inositol. *Chem. Commun.* **2012**, *48*, 2448–2450.
- (137) Godage, H. Y.; Riley, A. M.; Woodman, T. J.; Thomas, M. P.; Mahon, M. F.; Potter, B. V. L. Regioselective opening of *myo*-inositol orthoesters: mechanism and synthetic utility. *J. Org. Chem.* **2013**, *78*, 2275–2288.
- (138) Capolicchio, S.; Wang, H.; Thakor, D. T.; Shears, S. B.; Jessen, H. J. Synthesis of densely phosphorylated bis-1,5-diphospho-*myo*-inositol tetrakisphosphate and its enantiomer by bidirectional P-anhydride formation. *Angew. Chem. Int. Ed. Engl.* **2014**, *53*, 9508–9511.
- (139) Capolicchio, S.; Thakor, D. T.; Linden, A.; Jessen, H. J. Synthesis of unsymmetric diphospho-inositol polyphosphates. *Angew. Chem. Int. Ed. Engl.* **2013**, *52*, 6912–6916.
- (140) Weaver, J. D.; Wang, H.; Shears, S. B. The kinetic properties of a human PPIP5K reveal that its kinase activities are protected against the consequences of a deteriorating cellular bioenergetic environment. *Biosci. Rep.* **2013**, *33*, e00022.

- (141) Wu, M.; Chong, L. S.; Capolicchio, S.; Jessen, H. J.; Resnick, A. C.; Fiedler, D. Elucidating diphosphoinositol polyphosphate function with nonhydrolyzable analogues. *Angew. Chem. Int. Ed. Engl.* **2014**, *53*, 7192–7197.
- (142) Meisterhans, C.; Linden, A.; Hesse, M. Stereoselective access to G-nitro carboxylates, precursors for highly functionalized G-lactams. *Helv. Chim. Acta* **2003**, *86*, 644–656.